The Synaptic Connections of Pyramidal Neurones and Interneurones in Rat and Cat Neocortex.

A thesis submitted to the University of London in part fulfilment of the requirements for the degree of Doctor of Philosophy in the Faculty of Life Sciences.

By

Anthony Peter Bannister.

Department of Physiology
University College London School of Medicine
Royal Free Campus
Rowland Hill Street
Hampstead
London
NW3 2PF

March 2004

ProQuest LLC
789 East Eisenhower Parkway
P.O. Box 1346
Ann Arbor, MI 48106-1346

DECLARATION.

I declare that this thesis, submitted for the degree of Doctor of Philosophy, is of my own composition and that the data presented herein is my own original work, unless otherwise stated. No part of this thesis has been submitted in any previous application for a higher degree.

A. Peter Bannister

ACKNOWLEDGEMENTS.

I would like to thank a number of people who have played parts in assisting me in the completion of this project.

Firstly, I would like to thank my supervisor, Professor Alex Thomson, who has been enthusiastic in her support and supervision, and for occasionally 'cracking the whip' as she describes it. Thanks must also go to Dr. Paul Herrling of Novartis Pharma in Basel for funding my PhD and to Dr. David West whose programming skills have proved to be invaluable.

I would also like to thank the rest of my colleagues both past and present including Drs Hughes and Bulmer for firm friendship and extended, occasionally surreal intellectual chats in the bar and Dr. Jim Deuchars for introducing me to neuroanatomical techniques. I also extend my appreciation to Dr. Oliver Morris and Audrey Mercer have been exceptional office mates and without whom my sanity would surely have suffered.

My friends, family and girlfriend have been a constant source of support and encouragement throughout the course of my studies. It has been much appreciated.

To all those people mentioned above I offer you, a very big, thank you.

ABSTRACT.

The layer 4 neurones of the mammalian primary sensory neocortex comprise diverse functional components for the first stage of cortical sensory processing. Dual intracellular recordings of synaptically connected pairs of neurones with biocytin-filling were used to study intra-laminar layer 4 connections in adult cat and rat slices.

Interestingly, all excitatory cells involved in intralaminar layer 4 connections were regular spiking despite burst firing cells comprising 37% of the population recorded. Neuronal morphology and synaptic properties were similar in both species, as were the probabilities of finding connections: 1 in 43 for pyramid to pyramid, 1 in 21 for pyramid to interneurone and 1 in 12 for interneurone to pyramid (cat and rat data combined).

Pyramid to pyramid connections generated EPSPs 1.33 ±0.9mV in amplitude (mean ±SD), with rise times of 1.71 ±0.83ms and half width 14.67 ±7.1ms. All EPSPs recorded in excitatory cells and in parvalbumin immuno-positive interneurones exhibited depression, the second and subsequent EPSPs in trains being smaller in amplitude than the first. Fluctuation analysis indicated that this depression was presynaptically mediated. The interneuronal EPSPs recorded in this study, were briefer (rise times 0.63 ±0.26ms and half width 5.25 ±2.85ms) than those recorded in pyramidal cells. Two interneurones that were immuno-negative for parvalbumin received EPSPs that were facilitating, second and subsequent EPSPs in trains being significantly larger than the first. Again, fluctuation analysis indicated that this facilitation was presynaptically mediated.

Possible branch point failure of axonal conduction, feed-forward inhibition and post-tetanic potentiation were observed at some excitatory connections in layer 4. In addition, novel evidence for electrical gap junctions between adult pyramidal cells was obtained in one dual recording in which current injections into an impaled layer 3 pyramidal cell elicited full action potentials and 'spikelets', both of which elicited EPSPs in a layer 5 pyramidal cell.

CONTENTS.

Page.

LIST OF FIGURES 8

LIST OF TABLES 11

ABBREVIATIONS 12

1.0 INTRODUCTION 14

1.1 Layer 4 activation and the cortical column 15
1.2 The subclassification of neocortical neurones 16
1.2.1 The postsynaptic targets 17
1.2.2 Neurochemistry 19
1.2.3 The firing patterns 20
1.3 The excitatory cells of the neocortex 25
1.4 The inhibitory interneurones of the neocortex 27
1.5 The excitatory cell to excitatory cell circuitry of layer 4 30
1.6 The interactions of excitatory and inhibitory cells in layer 4 32
1.7 The chemical synapse 34
1.7.1 Synaptic release 35
1.7.2 Short term plasticity of synaptic release 37
1.7.3 Chemical synapse properties in layer 4 39
1.8 The electrical synapse or gap junction 41
1.9 Aims of the project and thesis format 43

2.0 METHODS 45

2.1 Introduction to the techniques 45
2.2 Solutions 45
2.3 Animals and anaesthesia 46
2.4 Surgery 46
2.5 Slice preparation 47
2.6 *In-vitro* slice maintenance 48
2.7 Paired intracellular recordings with biocytin filling 48
2.7.1 Rig set up 48
2.7.2 Electrodes 52
2.7.3 Targeting and search strategy 52

2.8 Data acquisition 53
2.8.1 Data digitisation 53
2.8.2 Electrophysiological analysis 53
2.8.3 Coefficient of variation analysis 56
2.9 General histological techniques 56
2.10 Standard biocytin visualisation 60
2.11 Double immunofluorescence with biocytin localisation 62
2.12 Double peroxidase 66
2.13 Microscopy 69

RESULTS:

3.0 EXPERIMENT SUMMARY 70

4.0 THE EXCITATORY CONNECTIONS BETWEEN PYRAMIDAL CELLS IN LAYER 4. 75

5.0 THE INTERACTIONS OF PYRAMIDAL CELLS AND THE INTERNEURONES IN LAYER 4. 112

6.0 EVIDENCE FOR ELECTRICAL GAP JUNCTIONS BETWEEN PYRAMIDAL CELLS IN ADULT RAT NEOCORTEX. 146

7.0 POTENTIAL EXCITATORY CONNECTIONS FROM PYRAMIDAL CELLS TO IMMUNO-LABELLED INTERNEURONES. 157

8.0 DISCUSSION 175

8.1 Methodological considerations 175
8.2 The neurones of both cat and rat neocortex exhibit cross species conformity 177
8.2.1 The pyramidal cells 177
8.2.2 The interneurones 178
8.2.3 Summary 179
8.3 The probability of synaptic connection between the neurones of layer 4 179
8.3.1 All putative intralaminar synaptic contacts from layer 4 pyramidal cells were made onto the basal dendrites of their postsynaptic targets 180
8.3.2 Pyramidal cells frequently make putative autapses with their own dendrites 181
8.4 All layer 4 pyramidal neurones that were synaptically connected to other neurones in layer 4 were regular spiking 183

8.5 The synaptic properties of excitatory connections within layer 4 184
8.5.1 The EPSPs generated in excitatory and inhibitory neurones had different shapes 185
8.6 Frequency dependent EPSP properties 186
8.6.1 Paired pulse depression 187
8.6.2 Paired pulse facilitation 188
8.6.3 Functional implications of depression and facilitation 189
8.6.4 Post-tetanic potentiation 190
8.6.5 Branch point failure 191
8.6.6 Summary 192
8.7 Gap junction-mediated intercellular communication between adult pyramidal cells 192
8.7.1 The roles of gap junctions in adult cortex 194
8.8 Future studies/Personal research interests 196
8.9 Concluding remarks 197

9.0 REFERENCES 198

LIST OF FIGURES.

Figure.		Page.
1.1	Examples of interneuronal morphological diversity within the adult cat neocortex.	18
1.2	Examples of spike discharge patterns exhibited by rat neocortical neurones.	21
2.1	Photograph illustrating the main components of the interface chamber.	49
2.2	Schematic diagram summarising the wiring of the electrophysiology rig.	50
2.3	Diagram illustrating the measurement of PSP properties during post-hoc analysis.	55
2.4	Schematic of the reagent interactions used for permanent biocytin visualisation.	61
2.5	Schematic of the reagent interactions used in fluorescence immuno-cytochemistry.	63
2.6	Schematic of the reagent interactions used for the double peroxidase technique.	67
3.1	Diagram illustrating the connectivity tests and hit rates achieved in rat neocortex.	72
3.2	Diagram illustrating the connectivity tests and hit rates achieved in cat neocortex.	73
4.1	Typical firing patterns exhibited by layer 4 pyramidal neurones.	77
4.2	Typical dendritic and axonal morphology of layer 4 pyramidal cells in adult cat and rat neocortex.	79
4.3	Morphology of a reciprocally connected pair of cat pyramidal cells in layer 4 and physiological response to brief spike trains.	81
4.4	Morphology of a synaptically connected pair of cat pyramidal neurones in layer 4 and physiological responses of the same postsynaptic cell to action potentials evoked in two presynaptic excitatory neurones.	84
4.5	Morphology of a synaptically connected pair of rat pyramidal neurones and the postsynaptic response to spike doublets at increasing interspike intervals.	86
4.6	Morphology of a synaptically connected pair of rat pyramidal cells in deep layer 4 and the postsynaptic response to trains of 5 spikes and to spike doublets at a range of interspike intervals.	89
4.7	Morphology of a synaptically connected pair of rat pyramidal cells in superficial layer 4 and the postsynaptic response to trains of 3 spikes and spike doublets evoked at a range of interspike intervals.	91
4.8	Morphology of a reciprocally connected pair of rat pyramidal neurones in layer 4 and their postsynaptic responses to spike doublets and trains of 3 action potentials.	94
4.9	Recovery from depression at increasing interspike intervals of a rat layer 4 to layer 4 pyramid to pyramid connection and the pattern of use dependent depression.	100

4.10	Amplitude distributions for the first up to the fifth EPSPs for cat and rat layer 4 pyramid to pyramid connections	102
4.11	Normalised change in CV^{-2} plotted against normalised mean EPSP amplitude for depressing excitatory layer 4 pyramid to pyramid connections.	105
4.12	Possible axonal branch point failure at a pyramid to pyramid connection in layer 4 of cat neocortex.	107
4.13	Post tetanic potentiation exhibited by a layer 4 pyramid to pyramid connection in rat neocortex.	109
5.1	Morphology of a regular spiking PV and CB immuno-negative interneurone and two postsynaptic pyramidal neurones in layer 4 of cat neocortex and the IPSPs generated in response to interneuronal action potentials.	116
5.2	Morphology of a layer 4 regular spiking PV and CB immuno-negative interneurone from cat neocortex that was postsynaptic to a layer 4 pyramidal cell and presynaptic to another in layer 3. EPSPs generated in response to presynaptic trains of 3 spikes and IPSPs elicited in the postsynaptic pyramidal cell.	118
5.3	Morphology of a fast spiking PV positive and CB negative interneurone in layer 4 of cat neocortex that was reciprocally connected with a layer 4 pyramidal cell and the postsynaptic responses of both cells to presynaptic action potentials.	121
5.4	Morphology of a fast spiking PV positive and CB negative interneurone in layer 4 of rat neocortex that was postsynaptic to a layer 4 pyramidal cell and powerful depression exhibited by the synaptic connection.	123
5.5	Morphology of an irregular spiking PV and VIP immuno-negative interneurone in layer 4 of rat neocortex that was postsynaptic to a layer 4 pyramidal cell, presynaptic to another and the postsynaptic IPSPs and facilitating EPSPs in response to trains of action potentials.	125
5.6	Typical spikes superimposed from a regular spiking pyramidal cell and a regular spiking interneurone from cat layer 4 illustrating the rapid repolarisation of interneuronal spikes relative to those of pyramidal cells.	128
5.7	EPSPs generated in interneurones follow a different timecourse to those elicited in pyramidal cells.	133
5.8	Recovery from paired pulse depression for a cat pyramid to interneurone connection in layer 4.	134
5.9	Amplitude distributions for the first to fifth EPSPs generated by a depressing pyramid to interneurone connections in cat and rat neocortex.	136
5.10	EPSP amplitude distributions for a facilitating pyramid to interneurone connection in layer 4 of cat neocortex.	138
5.11	EPSP amplitude distributions for a facilitating pyramid to interneurone connection in layer 4 of rat neocortex.	139
5.12	Normalised change in CV^{-2} plotted against normalised mean EPSP amplitude for two facilitating layer 4 pyramid to interneurone connections in cat and rat neocortex.	140

5.13	Disynaptic IPSPs driven by one of two reciprocally connected pyramidal neurones in layer 4 of cat neocortex.	142
5.14	Spontaneous or disynaptic IPSPs generated in two reciprocally connected pyramidal cells.	144
6.1	Schematic diagram illustrating the sequence of events leading to double EPSP generation in a postsynaptic pyramidal cell resulting from gap junction mediated conductance of the injected current pulse to another presynaptic neurone.	147
6.2	Morphology and spike discharge characteristics of two directly recorded pyramidal cells in layers 3 and 5 of adult rat neocortex.	149
6.3	Raw data illustrating spikelet occurrence in a recording of a layer 3 pyramidal cell from adult rat neocortex and resultant double EPSPs generated in the postsynaptic layer 5 pyramidal cell.	152
6.4	Raw data illustrating spikelet induced changes to the normal firing pattern of a layer 3 pyramidal cell.	153
6.5	The combined effects of double EPSPs resulting from gap junction mediated communication, recorded in a postsynaptic layer 5 pyramidal cell.	155
7.1	Photomicrographs of typical immunopositive staining of interneurones labelled with antibodies for PV, VIP and CCK in layer 4 of adult rat neocortex.	160
7.2	Dendritic and axonal morphology of a layer 4 pyramidal cell from adult rat neocortex and the location of putative synaptic connections with interneurones labelled for PV (cell 1 of 3)	162
7.3	Dendritic and axonal morphology of a layer 4 pyramidal cell from adult rat neocortex and the location of putative synaptic connections with interneurones labelled for PV (cell 2 of 3)	163
7.4	Dendritic and axonal morphology of a layer 4 pyramidal cell from adult rat neocortex and the location of putative synaptic connections with interneurones labelled for PV (cell 3 of 3)	164
7.5	Dendritic and axonal morphology of a layer 4 pyramidal cell from adult rat neocortex and the location of putative synaptic connections with interneurones labelled for VIP (cell 1 of 3)	166
7.6	Dendritic and axonal morphology of a layer 4 pyramidal cell from adult rat neocortex and the location of putative synaptic connections with interneurones labelled for VIP (cell 2 of 3)	167
7.7	Dendritic and axonal morphology of a layer 4 pyramidal cell from adult rat neocortex and the location of putative synaptic connections with interneurones labelled for VIP (cell 3 of 3)	168
7.8	Dendritic and axonal morphology of a layer 4 pyramidal cell from adult rat neocortex and the location of putative synaptic connections with interneurones labelled for CCK (cell 1 of 2)	170
7.9	Dendritic and axonal morphology of a layer 4 pyramidal cell from adult rat neocortex and the location of putative synaptic connections with interneurones labelled for CCK (cell 1 of 2)	171

LIST OF TABLES.

		Page.
4.1	Properties of averaged EPSP elicited by single presynaptic action potentials for intralaminar layer 4 pyramid to pyramid connections.	98
5.1	Anatomical and neurochemical description of layer 4 interneurones in cat and rat neocortex and their interaction with pyramidal cells.	130
5.2	Properties of first EPSPs generated in layer 4 interneurones.	132
7.1	Total numbers of regular spiking layer 4 pyramidal cell axonal boutons and the location of putative synaptic contacts onto immuno-labelled interneurones.	173

ABBREVIATIONS.

ABC	Avidin biotin enzyme complex
ACSF	Artificial cerebrospinal fluid
AHP	After-hyperpolarisation
AMCA	Avidin-7-Amino-4-methylcoumarin-3-acetic acid
AMPA	α-amino-3-hydroxy-5-methyl-4-isoxazole proprionic acid
AP	Action potential
BC	Basket Cell
BF	Burst firing
cAMP	Cyclic adenosine mono phosphate
cGMP	Cyclic guanosine mono phosphate
CB	Calbindin D28k
Ca^{++}	Calcium ions
CA1	Cornu ammonis (area 1)
CCK	Cholecystokinin octapeptide
CFS	Classical fast spiking
Cl^-	Chloride ions
CNS	Central nervous system
CR	Calretinin
CV	Coefficient of variation
DAB	3,3 Diaminobenzidine tetrahydrochloride
DC	Direct current
EM	Electron microscopy
EPP	End plate potential
EPSP	Excitatory postsynaptic potential
fEPSP	Field excitatory postsynaptic potential
FITC	Fluorescein isothiocyanate
FS	Fast spiking
GABA	Gamma-amino butyric acid
GluR	Glutamate receptor
GluRB	A glutamate receptor subunit
GJIC	Gap junction intercellular communication
HRP	Horse radish peroxidase
HW	Width at half amplitude
I_A	Transient, rapidly inactivating current
IB	Intrinsically bursting
$I_{Ca(N)}$	High threshold transient calcium current
I_{DR}	Delayed rectifier potassium current

I_Q	Hyperpolarisation activated current
IP	Intra peritoneal
IP_3	Inositol triphosphate
IPSP	Inhibitory postsynaptic potential
IS	Irregular spiking
K^+	Potassium ions
kDa	Kilo-dalton
Kv3.1	Voltage gated potassium channel
LGN	Lateral geniculate nucleus
Mg^{++}	Magnesium ions
mGluR	Metabotropic glutamate receptor
mRNA	Messenger ribose nucleic acid
n	Number of synaptic release sites
Na^+	Sodium ions
NGS	Normal goat serum
NMDA	N-methyl-D-aspartate
NPY	Neuropeptide Y
mEPP	Miniature end plate potential
p	Probability of synaptic release
PB	Phosphate buffer
PBS	Phosphate buffered saline
PPD	Paired pulse depression
PPF	Paired pulse facilitation
PSP	Postsynaptic potential
PTP	Post tetanic potentiation
PV	Parvalbumin
q	Quantal amplitude
RS	Regular spiking
RT	Rise time
RT-PCR	Reverse transcriptase-polymerase chain reaction
SNAP-25	Synaptosomal associated protein (25 kDa)
SNARE	Soluble N-ethylmaleimide sensitive factor attachment protein receptor
SS	Somatostatin
ST	Spiny stellate
TR	Texas red
TRIS	Tris hydroxymethylaminoethane; Trisamine
TTP	Time to peak
VIP	Vasoactive intestinal polypeptide

1.0 INTRODUCTION.

General introduction.

Layer 4 of the six layer structure that forms the primary sensory regions of the mammalian cerebral cortex comprises the first stage of neocortical sensory information processing of input from the thalamic relay neurones that convey coded environmental information from the sense organs of the peripheral nervous system. The processing of this information depends upon the combined activity and flow of information though extraordinarily complex and exquisitely tuned interconnected networks of excitatory and inhibitory neurones that employ an enormous array of anatomical, physiological and dynamic synaptic properties to filter and distribute the neural code to regions that may effect an appropriate response.

Fundamental to our understanding of cortical function is the requirement for the experimental unveiling of precisely how the properties of neural networks combine to generate behaviourally relevant responses to sensory input. This represents an extraordinarily complex task, not least because the patterns and properties of individual connections between the enormous array of functionally distinct neurones is vast. To address these issues and to reveal how complete neural circuits operate we require precise information related to the types of neurones involved, their electrophysiological characteristics, the anatomical distribution of their synaptic connections, and the properties of those synapses within small circuits. In addition, as the cell types identified in rat cortex are largely conserved within the mammalian class, differing predominantly in number, size and complexity in each rather than in their functional properties, the potential correlation of information gathered in lower mammals with human brain function requires the comparison of circuit properties using animal tissue from similar regions of several species.

The studies presented here will attempt to describe and compare aspects of the microcircuitry of excitatory and inhibitory neurones in layer 4 of cat and rat cortex. The techniques used include paired intracellular recording with biocytin filling and histological demonstration of synaptically connected pairs to classify neurones according to their morphological and electrophysiological properties and to attempt to identify any selectivity of pre or postsynaptic

targeting within the circuits. In addition, the electrophysiological properties, efficacy, strength and dynamic properties of the synapses between cells of identified morphological and electrophysiological class from both species will be assessed and compared.

1.1 LAYER 4 ACTIVATION AND THE CORTICAL COLUMN.

In simplified terms the flow of thalamic input through the cortex is proposed to progress within vertically oriented functional processing units termed the 'cortical columns' (for review see Rockland, 1998) from layer 4 to layer 3 then from layer 3 to layers 5 and 6 through which the information is modified and distributed to other regions of the cortex (Gilbert & Wiesel, 1979) and to subcortical regions such as the potentially modulatory layer 6 projections from the primary visual cortex back to the LGN (Bourassa & Deschenes, 1995;Sherman, 2001). The relay pathways between the dorsal thalamic nuclei and layer 4 of the primary sensory cortices are thought to provide the primary route of sensory information to access the cortical processing power provided by these circuits.

The cellular targets of specific thalamic nucleus fibres include both the excitatory and inhibitory neurone classes within highly interconnected networks. The thalamic inputs to cortical neurones are relatively scarce; Of all the synapses made with layer 4 basket interneurones, thalamic inputs constitute only 13% (Ahmed *et al.*, 1997) and with spiny stellate cells (the primary excitatory recipient of thalamic input) only 6% (Ahmed *et al.*, 1994), the majority of contacts being supplied by other subcortical regions and particularly by other cortical neurones in layers 4 and 6 (Benshalom & White, 1986). However, despite the low numbers of thalamic afferent inputs the thalamocortical terminals are generally large when compared with those from cortico-cortical neurones (Ahmed *et al.*, 1994) which may account for the powerful and highly efficacious input (Castro-Alamancos & Connors, 1997;Gil *et al.*, 1999).

Comparisons of the physiological response properties of layer 4 neurones and those of layers 2 and 3 in primary visual cortex to simple and complex visual stimuli *in-vivo* reveal that the cells of layer 4 have similar response properties to the thalamic relay neurones that innervate them

and so reliably relay simple thalamic input to the superficial layers. In contrast, the cells of layers 2 and 3 that represent the second stage of cortical processing have more complex receptive fields (Gilbert & Wiesel, 1989) and will only respond to richer stimuli such as those involving movement, such that convergent inputs from layer 4 are required to ensure their activation. Thus, the layer 4 excitatory cells comprise an effective gate that relays topographically organised thalamic input to the superficial layers and the high levels of interconnectivity between the cells of layer 4 is thought to provide amplification of the thalamic signal (Ahmed *et al.*, 1994) while the inhibitory non-pyramidal neurones are proposed to control the gain of this amplification (Douglas & Martin, 1991).

A logical starting point therefore, for the comprehension of the early stages of cortical column function is to assess the interconnections of the excitatory and inhibitory neurones of layer 4. The anatomical demonstration of the dendritic and axonal geometry and the compartmental distribution of layer 4 cell synaptic connections reveals aspects of their role in columnar microcircuitry and descriptions of the efficacy, strength, frequency filtering characteristics of neuronal inputs and outputs will more precisely determine the nature of information flow through those cells and the mechanisms available for neuronal computation *in-vivo*.

1.2 THE SUBCLASSIFICATION OF NEOCORTICAL NEURONES.

The excitatory and inhibitory neocortical neurones comprise two very broad groups based upon their actions upon postsynaptic cells. Within each, a number of subclasses may be identified by their gross morphology: the size, shape and spatial distribution of their axonal and dendritic arbours at light microscopic level. Indeed the majority of major neuronal subclasses have been determined in this way, by pure anatomical techniques such as the non-specific Golgi technique and by intracellular dye loading and visualisation. However the morphologically defined neuronal classes can be further divided by a number of other features such as their specific target preferences for the dendrites, somata or axons of postsynaptic partners as revealed by the electron microscopic elucidation of synaptic contacts, by their electrophysiological properties (spike discharge characteristics) and by their neurochemical content. The application of techniques that identify such

features within the each of the anatomical neuronal groups reveals further subclasses that may have functionally distinct roles in cortical function.

1.2.1 The postsynaptic targets.

The excitatory neurones typically form synaptic contacts with the dendrites of their postsynaptic targets either on the dendritic spines or shafts of other excitatory neurones or the dendritic shafts (and the somata) of inhibitory neurones. The inhibitory neurones, however, comprise subclasses that may form synaptic contacts with specific subcellular compartments of their postsynaptic targets. In the hippocampus, postsynaptic targets can often be predicted by the location of axonal arbours relative to the highly ordered arrangement of a single layer of pyramidal neurones in stratum pyramidale. In neocortex however, the inference of the targets of synaptic contacts made by the interneurones is not so straight forward as the postsynaptic cells are much more widely distributed. The interneurones that target different regions of their postsynaptic partners do not always have axonal arbours that are readily distinguished in terms of structure or organisation at light microscope level (see figure 1.1). This difficulty in assessing the precise location of inhibitory synapses without multi-parameter classification of neurones and visualisation of their target distribution onto histologically identified postsynaptic targets has lead to considerable over-use of the term 'basket cell', implying that the majority of neocortical interneurones direct powerful inhibition to their postsynaptic cells by targeting the soma and most proximal dendrites. Studies utilising intracellular recording, filling and visualisation of synaptically connected pairs of neurones reveal how different classes, that may have many common anatomical features, exert their influences upon different postsynaptic sub-cellular compartments and may therefore have dramatically different effects upon the filtering of cortical information. In other words, the accurate anatomical definition of the interneuronal classes requires unambiguous identification of the cellular components that comprise their postsynaptic targets.

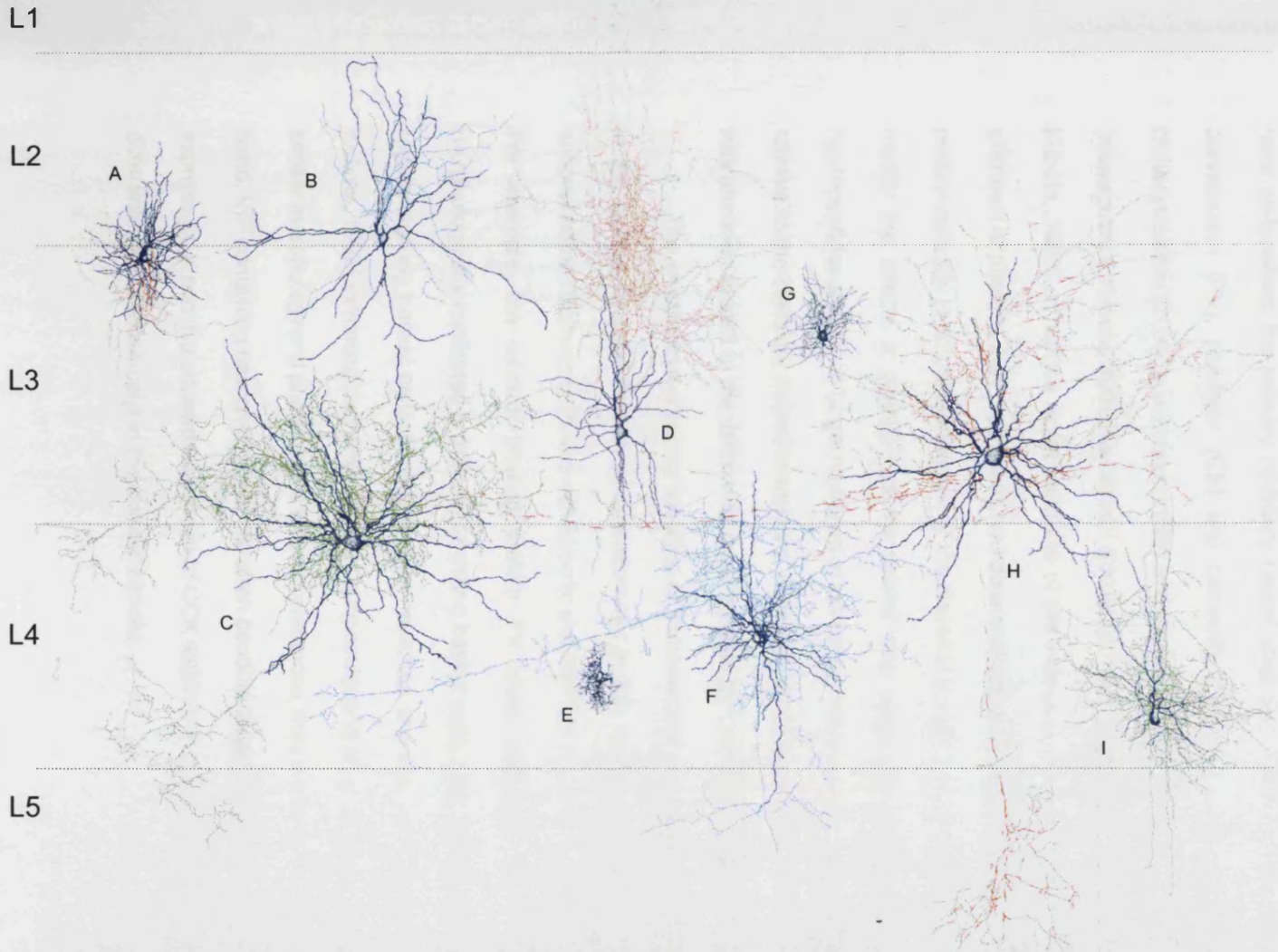

Figure 1.1. Examples of morphological diversity within the interneurone population of adult cat neocortex. All cells were reconstructed at x1000. Soma and dendrites are in black and axons in red green or blue. Apart from cells E and G which are neurogliaform and cell D which is Martinotti-like, all the other cells might be described as basket cells, their dendritic and axonal arbours fitting the general patterns of that class. However cell C was the only 'basket cell' who's proximal postsynaptic termination preferences were identified. Neurones postsynaptic to the other cells were either not recorded or not stained. Note that the diversity of axonal distribution patterns with different arbours from the same axon distributed in multiple layers. Modified from Thomson and Bannister, Interlaminar connections in the neocortex. *Cerebral Cortex*. 2003;**13**:pp 5-14. Also note that when referring to cat neocortex it is normal procedure to use arabic numerals to denote the layers, roman numerals for rat. These procedures will be used in all figures and text throughout except where both cat and rat neurones are discussed together in which case, for clarity, arabic numerals will be used.

1.2.2 Neurochemistry.

The inhibitory interneurones have specialised neurochemistry. Immunocytochemical studies have co-localised the primary inhibitory neurotransmitter GABA with Calcium binding proteins parvalbumin (PV), calbindin (CB) and calretinin (CR) and various neuropeptides including cholecystokinin (CCK), somatostatin (SS) and vasoactive intestinal polypeptide (VIP) (Kawaguchi & Kubota, 1993;Kawaguchi & Kubota, 1996;Kawaguchi & Kubota, 1997;Kawaguchi & Kubota, 1998). While the exact functions of the individual neuropeptides in the CNS are largely unknown at present, they may act as neurotransmitters or as neuromodulators acting either pre or postsynaptically to adjust the amount of the classical transmitter released at a given synapse or to modify the effects a quantum of transmitter has upon the postsynaptic cell. Typically the neuropeptides affect their target neurones at low concentrations and the effect is ordinarily prolonged relative to the classical neurotransmitters. Different affinities of the calcium binding proteins may indicate roles related to the differential requirements for calcium buffering of neurone subclasses.

The immunocytochemical labelling of interneuronal peptides is proving to be a useful tool in the further subclassification of interneurones in this complex group by revealing numerous subpopulations that can correlate with specific electrophysiological or anatomically defined groups. For example, the calcium binding protein PV often correlates with the fast spiking and morphologically confirmed proximally targeting basket cells, and CCK sometimes correlates with regular spiking basket cells. No basket interneurones express both PV and CCK (Kawaguchi & Kubota, 1997) indicating that while different subpopulations of basket neurones may have strikingly similar morphology and postsynaptic target preferences, they may have different roles. On the other hand, VIP containing neurones which are often dendrite targeting may occasionally be seen to also express CCK and this occasional overlap of CCK within VIP labelled populations may also indicate different roles of those cells in the cortical circuits.

1.2.3 The firing patterns.

Four basic spike discharge patterns are observed in adult neocortical neurones: Regular Spiking (RS), Burst Firing (BF), Fast Spiking (FS) and Irregular Spiking (IS). The differences are determined by expression and orchestrated activity of specific membrane ion channels with differential permeabilities to K^+, Na^+ and Ca^{++} and different activation (or opening) requirements, in the various neuronal classes. The firing characteristics observed in different classes of neurones are of fundamental importance to their function within cortical circuits and also allow for electrophysiological identification of broad neurone classes. Examples of the RS, BF, FS and IS firing patterns are given in figure 1.2.

1.2.3.1 Regular Spiking Neurones:

The regular spiking neurones found in layers 2-6 of neocortex respond to sustained depolarising current pulses with repetitive discharges at an initial rate of around 200-300 spikes per second and slow to a steady rate of 50-100 spikes per second. Some RS cells slow their spike frequency to zero and these are termed RS-2 cells. The frequency adaptation observed in these cells is the result of Na^+ spike inactivation and the activation of calcium dependent K^+ currents by sustained depolarisation resulting in a gradual hyperpolarisation of the cell (Colino & Halliwell, 1993). So, in addition to the fast transient I_A and delayed rectifier $I_{K(DR)}$, calcium dependent K^+ currents are responsible for variations in the AHP (Schwindt *et al.*, 1988) in RS pyramidal cells.

The RS discharge pattern is recorded from a large proportion of neocortical pyramidal cells and from some interneurones. Interneurones that display RS type firing properties are however often distinguishable from the pyramidal population during recordings because they have short duration action potentials.

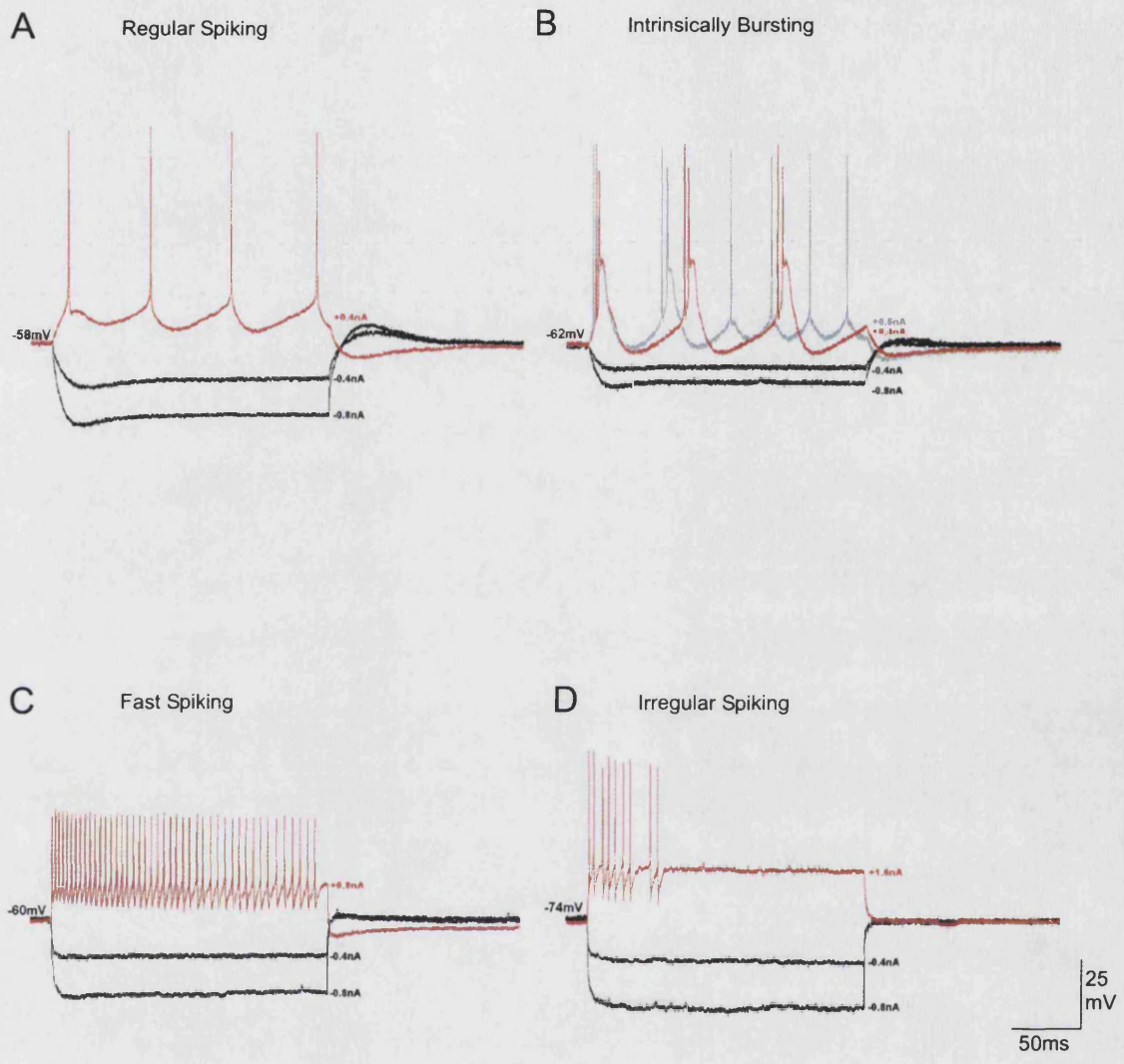

Figure 1.2. Examples of firing patterns typically exhibited by cortical neurones in rat somatosensory and visual areas. Red and grey traces represent responses to square wave depolarising current pulses and black traces represent responses to hyperpolarising current. A, Regular spiking (RS) firing pattern of a layer IV pyramidal cell. B, Intrinsically bursting (IB) firing pattern of a layer IV pyramidal cell and its adaptation to the RS-like pattern in response to increasingly powerful depolarising current injection, in grey. C, Classical fast spiking (FS) of a layer V interneurone. D, Interrupting (irregular) spiking (IS) of a layer IV interneurone. Note that for the interneurones C and D the electrodes are not perfectly balanced; the firing characteristics are not affected.

1.2.3.2 Burst Firing Neurones:

In contrast to the RS cells BF cells fire rapid bursts of 3 to 5 action potentials in response to short depolarising current pulse injections. Sustained application of depolarising current reveals a further subclass of BF neurones based upon the patterns of burst generation termed intrinsically bursting (IB). The non-IB BF cells typically fire one burst of spikes followed by single spikes that show similar spike frequency adaptation as seen in RS cells. However, the (IB) neurones respond to sustained depolarisation with repetitive trains of 5-15 bursts of 3 to 5 spikes per second. Increased strength of depolarising pulses in IB cells often evoke 1 or 2 bursts of APs followed by trains of single spikes.

The IB firing pattern results from the activation of voltage gated Ca^{++} conductances and low threshold, broad and refractory Ca^{++} spikes (Llinas & Yarom, 1981) that are thought to be primed at hyperpolarised membrane potential for activation by back propagation of Na^{+} spikes, particularly in pyramidal cells with prominent apical dendrites. During repetitive burst firing the elevated intracellular Ca^{++} concentration activates Ca^{++} dependent hyperpolarising K^{+} currents which contribute to the silent phase between bursts (Schwindt *et al.*, 1988). The refractory nature of the calcium spikes in part accounts for the regularly spaced bursts of action potentials and the requirement for hyperpolarisation of the membrane to prime the Ca^{++} channels account for the adaptation of the IB pattern to that similar to RS in response to increased strength depolarising current pulses (or by the artificial depolarisation of the membrane potential prior to the current pulse).

The BF discharge patterns are found in both excitatory and inhibitory cortical neurones most typically in the deeper layers. Neocortical interneurones exhibiting BF behaviour are typically dendrite targeting and immunopositive for the calcium binding protein calbindin (Kawaguchi & Kubota, 1993). The IB firing pattern is correlated with spiny excitatory neocortical neurones that are typically located in layer 5 (and rarely in layer 4), are generally large with many basal dendrites and a distal terminal tuft of the apical dendrite in layer 1 (Connors *et al.*, 1982).

1.2.3.3 Fast Spiking Neurones:

The FS discharge pattern is characterised by trains of high frequency spikes (in excess of 200 spikes per second) in response to large sustained depolarising current pulses, that show little or no frequency adaptation or spike accommodation. The discharge frequencies attained by the FS cells are attributed to short duration action potentials that repolarise rapidly, before the inactivation of Na^+ channels therefore allowing repeated spike generation without attenuation of spike or frequency. These fast AHPs result from activation of fast K^+ delayed rectifier ($I_{K(DR)}$) and transient currents (and $I_{K(A)}$) and by the calcium activated K^+ ($I_{K(Ca)}$) conductances (I_C and I_{AHP}). The fast AHPs have been associated with the specific K^+ channel subunit Kv3.1 by RT-PCR studies (Massengill *et al.*, 1997) which is expressed by FS cells in greater concentrations than on RS cells indicating that Kv3.1 may be at least in part responsible for FS discharge characteristics.

The Fast Spiking discharge pattern correlates exclusively with non-spiny, nonpyramidal inhibitory interneurones found in all layers of the neocortex. Hence, as no excitatory pyramidal neurones have been identified with FS properties they are considered concomitant with inhibitory neurone recordings. Of the interneurone classes, FS properties have been observed in recordings of several morphologically distinct inhibitory neurone subclasses including the chandelier cells (axo-axonic), basket cells and a number of dendrite targeting neurones (Buhl *et al.*, 1994;Buhl *et al.*, 1996;Pawelzik *et al.*, 2002). These morphological correlations with firing pattern have most often been made in hippocampal preparations where the regular arrangement of postsynaptic cellular target neurones within the laminae allows the targets of the interneurones to be derived from the distribution of axon terminals at light microscopic level. In cortex the paired recording of synaptically connected electrophysiologically classified interneurones and their targets with biocytin filling (or electron microscopic examination of axon terminals from individually filled cells) is required to permit the unambiguous correlation of interneurone electrophysiological characteristics with morphology, particularly when in combination with the immunocytochemical localisation of interneurone markers including the calcium binding proteins and neuropeptides.

The FS cells of the neocortex often express the calcium binding protein parvalbumin (Kawaguchi & Kubota, 1993) which may have roles in the control of increased intracellular Ca^{++}

transients resulting from FS behaviour. In hippocampus some dendrite targeting FS interneurones express the neuropeptide CCK that may have a roles in modulation of interneurone activity. Co-expression of both CCK and PV in the same neurone is rarely seen (Pawelzik *et al.*, 2002).

1.2.2.4 Irregular spiking neurones.

The Irregular spiking (IS) pattern is defined by bursts of short duration action potentials followed by a series of spike bursts with similar interspike intervals emitted at an irregular frequency resulting from subthreshold membrane potential oscillations. Pharmacological studies on a population of VIPergic bipolar interneurones (peptide cells) found in all layers of rat neocortex have indicated that the IS discharge pattern is due to the involvement of $I_{K(D)}$ type current as blocking of specific Kv1.1 K^+ ion channels promotes sustained discharge (Porter *et al.*, 1998) in such cells.

The IS discharge pattern is also exclusively observed in recordings of inhibitory neurones in this case correlated with dendrite targeting interneurones such as the bipolar cells (Kawaguchi, 1995) and of interneurones that express mRNA for the calcium binding protein calretinin (Cauli *et al.*, 1997).

The role of the IS pattern in interneurone function is as yet unclear but it has been suggested by Porter *et al* that the $I_{K(D)}$ type current which is active at subthreshold voltages and slowly inactivates with depolarisation may be involved in the temporal integration of multiple subthreshold, depressing excitatory inputs as is seen in hippocampal CA1 pyramidal neurones (Storm, 1988) therefore detecting increases in local activity. Also, the release of VIP is thought to be frequency dependent requiring multiple action potentials (Lundberg *et al.*, 1981) so the inactivation of the $I_{K(D)}$ current by the integration of multiple excitatory inputs may be a mechanism for enhancing blood flow through the release of VIP during periods of increased activity.

1.3 THE EXCITATORY CELLS OF THE NEOCORTEX.

The neocortical excitatory neurones comprise two main groups, the pyramidal cells and the spiny stellates whose role is to excite their postsynaptic partners in response to appropriate integrated inputs. Whilst the relative proportions of these neurones varies across the depth of the cortex both classes share a number of features in common. Both make local connections with other cortical neurones, have a similar range of electrophysiological properties responding to sustained depolarising current pulse injections with either burst firing or regular spiking discharge patterns, utilise glutamate as their primary neurotransmitter and have spiny dendrites.

1.3.1 The Pyramidal Cells.

Pyramidal cells make up 70-80% of the neurones in the mammalian cortex (Feldman, 1984) and are present in all cortical layers except layer 1. They comprise a cell body of variable size, a number of bifurcating basal dendrites emerging close to and largely confined within the same layer as the cell body and a single large apical dendrite ordinarily oriented towards and perpendicular to the pial surface, the distal portion of which may branch into a 'tuft' in the superficial layers the tips of which may terminate in layer 1. The size and shape of pyramidal dendritic arbours is heterogeneous (largely related to position and orientation) through the depth of the cortex with typically smaller cells in the superficial layers compared with those in layer 4 and particularly layer 5. The often myelinated axon issues from the base of the cell body towards the deeper layers producing horizontal or obliquely oriented collaterals as it projects towards the white matter where it may exit the cortex to activate subcortical areas and/or reenter and activate other cortical regions.

Pyramidal cells receive both excitatory and inhibitory inputs. The synaptic contacts onto the cell body and axon initial segment are almost exclusively symmetrical, GABAergic and, by definition inhibitory, corresponding with the connections from local circuit interneurones such as the basket and chandelier cells described below (see section 1.4). The dendritic shafts and spines receive mostly (though not exclusively) glutamatergic excitatory input from other excitatory cells in the vicinity as well

as from other cortical areas. The extrinsic afferent inputs to cortical pyramidal cells form asymmetric, presumed excitatory synapses with the dendrites, that originate from numerous subcortical loci including thalamocortical projections from principal and general thalamic nuclei (Gil *et al.*, 1999) to visual cortex and from numerous other subcortical regions supplying context specific input depending upon the region of cortex the pyramidal cells occupy.

1.3.2 The spiny stellate cells.

Spiny stellate cells account for less than 3 percent of the cortical neurones, are typically located in layer 4 and share many features in common with the pyramidal cells including similar spine density covering the dendritic tree, the same glutamatergic type synapses and similar patterns of excitatory and inhibitory synaptic inputs (Ahmed *et al.*, 1994). The most apparent difference at first observation is the absence of an apical dendrite. Spiny stellate dendrites project in all directions from the cell body (hence the term 'stellate') and are generally confined to the layer occupied by the soma. Axons project horizontally within layer 4 and in narrow vertical bundles through all layers of the cortex excluding layer 1 contacting the spines and dendritic shafts of other spiny stellates and pyramidal cells and the dendritic shafts of non spiny interneurones (Anderson *et al.*, 1994). The axon is sometimes seen to exit the cortex via the white matter though the supposed contacts of these subcortical projections are unclear. These cells constitute a major recipient of thalamocortical inputs to the cortex and due to their high levels of interconnection with other spiny stellates as well as pyramidal cells in the vicinity are expected to play a major role in layer 4 excitation in response to thalamic relay activity (Ahmed *et al.*, 1994).

Spiny non-pyramidal cells are often referred to as the cortex's 'Excitatory Interneurones' based on their glutamatergic, intracortical axonal projection pattern. For the purposes of this thesis, these cells will only be referred to as 'Spiny Stellates' to avoid confusion with their inhibitory counterparts.

1.4 THE INHIBITORY INTERNEURONES OF THE NEOCORTEX.

There are several classes of non spiny nonpyramidal inhibitory cells (interneurones) in the neocortex, constituting about 20 percent of the neuropil (Gabbott & Somogyi, 1986) that are essential for normal function of the CNS. These cells influence the activity of excitatory cell networks as well as other inhibitory cells and certain features are common to all. For example, the majority of interneurones have smooth aspiny dendrites in adult tissue (and those that do harbour dendritic spines typically have significantly fewer than are observed upon excitatory cells). Their axons generally do not project to subcortical regions, instead making intrinsic projections terminating with symmetrical synapses on other interneurones or pyramidal cells in the vicinity (hence the term 'interneurones') and primarily utilise the inhibitory transmitter gamma-aminobutyric acid (GABA).

1.4.1 The proximally targeting interneurones (Basket Cells).

The large basket cells of the neocortex are found in all laminae though most abundantly in layers 3 - 5 of motor, visual and somatosensory areas. The dendritic arbours are generally stellate in appearance radiating in all directions from the cell body. The dendrites are smooth, aspiny, often beaded, bifurcate infrequently and, being particularly long, can extend through multiple layers of the cortex. Basket cells often have large quantities of thick, myelinated axon that arborises close to the soma and in smaller nests at distances of up to 2mm away (in cat cortex) and are reported to be densely interconnected (Kisvarday, 1992). The term 'basket cell' refers to the appearance of axonal baskets formed when these cells envelope the cell bodies and proximal dendrites of their postsynaptic cells to provide strong inhibition at these targets (S.Ramón Y Cajal, 1911). Cortical basket cells frequently express the Ca^{2+} binding protein parvalbumin (PV) or the neuropeptide cholecystokinin (CCK) (DeFelipe, 1997;Kawaguchi & Kondo, 2002).

There is also a population of cells identified as 'small basket cells' sometimes referred to as clutch cells (in layer 4) which are essentially miniature replicas of the large basket cells. These cells are preferentially located in layers2 and 3 where they innervate the somata and proximal dendrites

of neurones within their own or adjacent cortical columns (Budd & Kisvarday, 2001).

Basket cells are diverse in terms of morphological properties (Kisvarday, 1992), immuno-reactivities for calcium binding proteins and neuropeptides (Kawaguchi & Kubota, 1998) and electrophysiology (they often exhibit fast spiking (FS) or regular spiking (RS) discharge properties) (Kawaguchi & Kubota, 1997;Thomson *et al.*, 1996), and the functional significance of this diversity is unknown. But, based on the strategic placement of their dendrites and their axonal projections onto the somata and proximal dendrites of their targets, the layer 4 basket cells are proposed to be involved in the generation of powerful inhibition of pyramidal cells which may be initiated by monosynaptic input from extrinsic thalamocortical afferents (Ahmed *et al.*, 1997) and therefore control the gain of summed synaptic potentials and so the action potential discharge of their postsynaptic neurones (Miles *et al.*, 1996).

1.4.2 The Axo-axonic interneurones (Chandelier cells).

The chandelier cells are relatively rare in occurrence and are most frequently found in layers 2 and 3 though they are also present in the infra-granular layers. They have striking axonal morphology that makes them one of the few cortical interneuronal classes readily identifiable by simple light level microscopy as their terminals are arranged in distinctive 'cartridges' giving the appearance of the candlesticks of a chandelier. The axons appear to be highly selective for the initial segment of pyramidal cell axons; hence their alias 'axo-axonic neurones' (Somogyi, 1977). Each cell has the potential to contact between 100 and 400 local pyramidal cells providing strong inhibition that can block the generation of an action potential. The chandelier cells typically express FS discharge characteristics (though they may also be RS, BF or IS) in hippocampus (Pawelzik *et al.*, 2003) and some but not all express parvalbumin (DeFelipe *et al.*, 1989b;Williams *et al.*, 1992).

1.4.3 The dendrite targeting interneurones.

The interneurones whose axons target the dendrites of their postsynaptic cells comprise many subtypes defined by their general dendritic/axonal morphology. Whilst the dendritic targets of these interneurones are the same, their differential size, location and the distribution of their processes suggest that they have different roles in cortical circuitry. For example, the neurogliaform cells, the smallest non-spiny cells of the neocortex are suggested to be involved in the local modulation of cortical excitability. They are present in all layers of the motor, somatosensory and visual areas and in layer 4 have been shown to target specifically the dendritic spines of adjacent spiny neurones (Tamas *et al.*, 2003). Another dendrite targeting class, the Martinotti cells are also found in all areas of the cortex, primarily in the deeper layers and project their axon vertically into layer 1 where their targets appear to be the distal apical dendritic tufts of pyramidal cells (Wahle, 1993). The Double Bouquet cells, whose name derives from the shape of their dendritic arbour, are found in all layers of the cortex (most concentrated in layers 2 and 3) and have axons that produce short ascending branches and long tightly bundled descending branches that reach into all laminae targeting the dendritic shafts of other interneurones and the spines or small dendritic shafts of excitatory neurones. The distribution of double bouquet cell processes suggest a role in the channelling of neuronal activity within cortical columns (DeFelipe *et al.*, 1989a).

1.4.4 Summary of the Neuronal Subclasses in Relation to Layer 4.

All of the above morphological classes of excitatory and inhibitory cells are present (in different proportions) in layer 4. The electrophysiological and neurochemical subclasses that divide them equate to enormous variability of circuit properties provided by each. At present it is still unknown which specific cell subclasses are involved in which circuits in layer 4, and therefore we cannot assess their roles definitively. For example, we can assume from the different output properties of the BF and RS excitatory cells that they perform significantly different roles in the activation of their postsynaptic targets, but still we don't know which cell subclasses they contact

within layer 4. Put more simply, we do not know whether the RS pyramidal cells provide selective activation of specific postsynaptic targets or just randomly contact anything within range of their axon. And more specifically still, we do not know if there is any correlation between the specific firing patterns of anatomically identified neurones and their connections with other cells that may comprise specific circuit pathways. If such patterns do exist, are they consistent and conserved in both the cat and rat cortex?

1.5 THE EXCITATORY CELL TO EXCITATORY CELL CIRCUITRY OF LAYER 4.

The networks of pyramidal and spiny stellate cells in layer 4, have extensive axonal arbours within layer 4 as well as focussed axonal projections to layer 3 and less dense projections to the deeper layers 5 and 6 (Anderson *et al.*, 1994; Burkhalter, 1989) indicating that in addition to their role feeding excitation to layer 3 they are responsible for the amplification of input received in layer 4. Naturally this amplification is dependent on the level of interconnectivity between excitatory cells. Recent studies using electron microscopic examination of dye filled axonal boutons from single cells have shown that the outputs of excitatory layer 4 cells of juvenile rat barrel cortex tend not to make contact with the GABAergic interneurones and instead make synaptic contact with the small calibre dendrites and dendritic spines of other spiny neurones (Lubke *et al.*, 2000) presumably also originating in layer 4 though these methods cannot exclude contacts with the apical or apical oblique dendrites of deeper layer pyramidal cells as they ascend towards the superficial layers. The filling of synaptically connected excitatory layer 4 neurones from the same EM study indicated that the preferred sites of synaptic contacts onto confirmed layer 4 postsynaptic cells are the tertiary dendrites, close to the postsynaptic cell body. The level of connectivity between excitatory cells in layer 4 is estimated to be high at 1 in 5.7 in adult cat (Thomson *et al.*, 2002)and corresponding levels have also been observed in immature rat (Feldmeyer *et al.*, 1999).

Electrophysiological studies directed at assessing the large scale characteristics of layer 4 excitatory networks to which the high level of interconnectivity contributes have revealed some interesting properties. For example, field excitatory postsynaptic potential(fEPSP) recordings using

a stimulating electrode positioned at the centre of a layer 4 barrel and simultaneous systematic whole cell recordings at increasing distance from the barrel centre and across barrel borders indicate that the strength of EPSPs is highly dependent on the distance of the recorded neurones from the stimulating electrode (Petersen & Sakmann, 2000) and that amplitude of the EPSP drops significantly at the edge of the corresponding cortical column. This effect might perhaps be explained by the preferential orientation of layer 4 spiny neurone dendrites towards the centre of the barrel and the vertical orientation of their axons. However, this observation has also been made using paired intracellular recordings from layer 4 of the striate cortex in young cats where no such dendritic orientation is observed and in which recordings the lateral separation of synaptically connected pairs of neurones also indicated that the EPSP amplitude decreases with increasing distance between the connected cells (Tarczy-Hornoch *et al.*, 1999). These observation are most probably explained by a model of axonal bouton 'clouds' that overlap with the dendritic arbours of the postsynaptic cells, the implication being that assuming random connectivity the number of release sites decreases as a function of the distance between the connected neurones (Douglas *et al.*, 1995). However, the random distribution of intracortical neurone connectivity is a matter of considerable controversy. Mounting evidence suggests that the postsynaptic targets may have specific criteria for the quality and origin of the inputs they receive (see Thomson & Morris, 2002 for review) though any selectivity of connectivity between electrophysiological subclasses of neurones in layer 4 has so far not been identified.

The majority of published studies relating to the excitatory networks of layer 4 are directed at the barrel cortex, particularly of juvenile animals. Studies based entirely upon morphological characterisation of the excitatory cells in layer 4 at light microscopic level reveal the locations from which those cells receive input (the location of their dendrites) and the distribution of their outputs (the location of their axonal boutons). Electrophysiological studies reveal aspects of circuit properties. But alone these studies reveal nothing conclusive related to the specific cell types making inputs to or receiving outputs from them. There is evidence of selective, high probability connectivity between the excitatory neurones of other layers within cortical columns such as the targeting of large BF layer 5 pyramids by layer 3 pyramidal axons (Thomson & Bannister, 1998) which may represent an

important route for the activation of corticofugal pathways but to date the selectivity of layer 4 excitatory connections between specific neuronal subpopulations in layer 4 has received little attention.

1.6 THE INTERACTIONS OF EXCITATORY AND INHIBITORY CELLS IN LAYER 4.

The interneurones of layer 4 receive intracortical input from other excitatory and inhibitory cells (Douglas & Martin, 1991) and direct thalamocortical input. In terms of the timing facilitated by the generation of fast and depressing EPSPs within them, the fast spiking interneurones may be the first layer 4 cells activated by thalamic input (Swadlow, 1994) promoting inhibition of networks immediately following novel thalamic input. The potential roles for early inhibition through fast interneuronal activation are many and varied. For example, depending on the strength and duration of inhibitory input to the excitatory cells, the period of electrical silence created may allow at least partial recovery from short term depression within excitatory networks that will promote more powerful and/or more synchronised activity in response to a subsequent novel thalamic input and may also promote the establishment of oscillations thought responsible for the coordinated activity of neuronal networks via interconnections through chemical and possibly electrical synapses (Gibson *et al.*, 1999;Tamas *et al.*, 1998;Tarczy-Hornoch *et al.*, 1998). Precisely how these interactions might coordinate cellular activity to generate properties such as the direction selectivity observed within the excitatory neurones of layer 4 visual cortex for example, are as yet unknown. But as these properties are not exhibited by the thalamic afferents themselves it would seem plausible that the interneuronal interactions provide the most likely explanation (Sillito, 1975). In order to reveal how such properties are generated, the specific interactions of well defined neuronal subclasses is required.

Studies by Tarczy-Hornoch *et al* have been able to indicate that the 'basket cells' of layer 4 in cat visual cortex are monosynaptically excited by the local spiny neurones and in turn monosynaptically inhibit neighbouring spiny and smooth neurones (Tarczy-Hornoch *et al.*, 1998). As with the excitatory to excitatory connections, the estimated level of interconnectivity between excitatory and inhibitory cells in cat layer 4 is high at 1 in 5 for excitatory connections and 1 in 10 for

inhibitory (Thomson *et al.*, 2002) and reciprocal connections are often observed (Tarczy-Hornoch *et al.*, 1998;Thomson *et al.*, 2002). No such estimates of synaptic connectivity are available for similar connections in rat and there is limited precise information related to the morphology or the sites of interneuronal synaptic contacts that would allow more accurate classification of the cells involved in these connections from either species. Also, little information is available that allows the possible correlation of connection specificity between cells of identified electrophysiological subclass. There are indications that such selectivity of excitatory to inhibitory cell interaction does occur, primarily through studies in the hippocampus (Ali *et al.*, 1998; Ali & Thomson, 1998) where differences in the ratios of connectivity and in the excitatory postsynaptic potential (EPSPs) amplitude are observed at excitatory connections to different interneurone classes.

The variety of interneurones and their subclasses indicate that these cells must be of great importance to cortical function. Models in which cortical inhibition is described as a single homogenous event probably stem, at least in part from our lack of understanding of the physiological variability of the interneurones. The anatomy of cortical interneurones has received a great deal of attention over recent decades and has led to many anatomically derived assumptions as to their roles in cortical microcircuitry, but very little evidence of their specific inputs and outputs within layer 4 and the nature of these connections has been presented to date. Layer 4 Interneurones, particularly the parvalbumin immunopositive thalamorecipient interneurones that include the basket cells may have potentially huge importance in the control of excitation both within layer 4 and other layers, due to their multiple 'clouds' of axonal boutons distributed within layer 4, often crossing column borders and/or with multiple arbours situated in different layers (see figure 1.1). Aside from increasing the database of classified interneuronal subtypes it would be interesting to know whether the frequency dependent properties displayed by the excitatory connections seen in cat cortex are consistent or if they vary between connections involving different neuronal subclasses and to find out whether these properties are expressed by similar connections in rat. Also, it would be advantageous to know if there is any pattern of selective connectivity, be it electrophysiological, morphological or both, of the presynaptic or the postsynaptic cells involved. To these ends, accurate subclassification of morphologically determined layer 4 cell classes is required.

1.7 THE CHEMICAL SYNAPSE.

The direction of information flow within cortical circuits is quite apparent in terms of wiring through the conformity of dendritic and axonal arbours within groups of excitatory neurones. The contribution made to those circuits by the complex groups of interneurones and the different firing patterns exhibited by all groups of neurones allude to an enormous capability of the cortex to generate highly tuned patterns of action potential generation capable of manipulating the neural code. Electrophysiological studies of the synaptic connections between neurones reveal further capacity for information filtering via the extensive and differentially distributed synaptic connections that may utilise the cable properties of cellular processes, the time locked interactions of excitatory and inhibitory neurones. But these factors are only half of the story as far as cortical tuning is concerned. An enormous amount of variation in the potency of cortical signals is generated by a huge array of frequency and use dependent modulatory mechanisms employed at each synapse (see Thomson, 2003 for review), all of which may combine to govern the generation of stimulus specific temporal and spatially dependent patterns of action potentials.

The synapses that make use of chemical transmitters are by far the most common type of synapse employed by the neocortex. They are characterised in electron micrographs by the presence of a presynaptic element (usually an axonal bouton) containing synaptic vesicles and an opposing postsynaptic element separated by a smooth and uniform cleft 10-20nm wide (Gray, 1959). In the majority of synapses, the postsynaptic membrane has a characteristic electron dense structure which in the absence of a similar density on the presynaptic element defines them as asymmetric synapses. The vesicles of asymmetric synapses have been shown to contain glutamate (an excitatory amino acid), indicating an excitatory role and the vesicles of symmetric synapses that have both pre and postsynaptic densities most frequently contain GABA, the primary inhibitory neurotransmitter of the neocortex (Storm-Mathisen *et al.*, 1983).

1.7.1 Synaptic release.

At the chemical synapse, the vesicular release of neurotransmitter into the synaptic cleft for detection by the postsynaptic receptors was first muted in the 1950's (Fatt & Katz, 1952) based on evidence from recordings of postsynaptic muscle fibres at the neuromuscular junction. The results of these studies led to the theory that the end plate potentials (EPPs) are brought about by the actions of individual quanta of transmitter whose release is initiated by an action potential. This release of transmitter occurs via a probabilistic process. The vesicle hypothesis also applies at central synapses which have remarkably similarity in structure when compared with the neuromuscular junction at the electron microscope.

The release of the contents of a vesicle into the synaptic cleft has been shown to be calcium dependent. An action potential propagates down the axon to the terminal where voltage gated calcium channels open for a limited period allowing calcium ions from the extracellular space to enter and trigger fusion of the vesicle membrane with the plasma membrane and the release of transmitter to the cleft. Transmitter release is tightly controlled by presynaptic protein interactions. In order for release to occur a vesicle must first be docked onto the membrane at the active zone, become fusion competent and be able to sense calcium entry long before the arrival of the action potential.

Docking, the action of holding the vesicle in position at the active zone, allows the complex interactions of synaptic proteins identified as Synaptobrevin, SNAP-25 and Syntaxin, collectively called SNARE proteins (soluble N-ethylmaleimide sensitive factor attachment protein receptor) which form the fusion core complex (see Seagar *et al.*, 1999 for review). Once the docking process is complete the fusion core complexes incorporate a calcium sensor capable of detecting calcium influx during the action potential, the activation of which initiates fusion and release of vesicle contents into the cleft. The most likely candidates for this sensor protein are synaptotagmin I and II (Davis *et al.*, 1999), proteins bound into the vesicle membrane that incorporate two large calcium binding domains. Interestingly, synaptotagmin is required to bind at least 4 calcium ions based on evidence of a 4^{th} power relation between extracellular Ca^{++} and release (Carlson & Jacklet, 1986;Dodge & Rahamimoff, 1967;Reid *et al.*, 1998) which may have implications in short term synaptic plasticity. The docked and fusion competent vesicle is now capable of releasing its contents into the synaptic

cleft extremely rapidly in response to local calcium influx during the action potential ensuring near synchronous release of transmitter at the multiple release sites of a single axon.

As the vesicular proteins are very different from those in the plasma membrane it is suggested that the fused vesicles are recycled and refilled with transmitter within the axon terminal (Bittner & Kennedy, 1970;Betz & Wu, 1995). Recycling of vesicle membranes and associated proteins thus removes the need for energetically demanding and time consuming resynthesis. However the refilling of transmitter vesicles inevitably takes time and as such this process is considered an important factor in the determination of the rate of transmitter release possible at each synapse to successive action potentials and therefore has implications in synaptic plasticity. The ability of synapses to release the contents of transmitter vesicles at high frequencies over extended periods of time is thought to be more reasonably explained by the integration of different 'pools' of vesicles in the presynaptic terminal that are proposed to cooperate in the provision of releasable vesicles at times of high frequency activity.

The collection of docked and fusion competent vesicles described above has been termed the 'immediately available pool' of transmitter quanta reflecting their availability to release transmitter immediately an action potential occurs. As each vesicle fuses and begins the process of endocytosis and recycling, it is replaced from a much larger pool to maintain the equilibrium of releasable vesicles. This larger pool comprises vesicles that are fusion competent but are held in check by protein interactions at the release site, some that are docked but not yet fusion competent and others that are available for docking but as yet undocked. This constitutes the 'readily releasable pool' which makes up 0.5-15% of all vesicles in each terminal (Benfenati *et al.*, 1999). When the demand upon the immediately and readily releasable pools is high, depletion of transmitter filled vesicles is prevented by liberation of a 'reserve pool' constituting roughly 85-99% of all vesicles present in the terminal, bound to microfilaments of the cytoskeleton. The sizes and rates at which each of these pools can be replenished by each other are factors that govern the frequency of release a particular synapse can maintain. As such, the depletion of the immediately releasable pool has implications in short term plasticity phenomena exhibited at synapses.

1.7.2 Short term plasticity of synaptic release.

Synaptic events that achieve successful transmitter release are characterised by shifts in membrane potential in a postsynaptic neurone in response to a presynaptic action potential. These potential shifts have been observed to vary in amplitude in response to multiple APs leading to the attractive hypothesis that postsynaptic responses are governed by a quantal framework whereby the amplitude of the postsynaptic events depends on the probabilistic release of neurotransmitter from a number of release sites. Experimental elucidation of the variability of these characteristics is fundamental to the understanding of short term synaptic plasticity.

Experiments utilising post recording visualisation of coupled neurones and electron microscopy have begun to provide physical data on the numbers of potential transmitter release sites (n) with certain connections utilising multiple release sites while others use only one. Paired recordings at connections that appear to utilise only one release site suggest that the quantal size (q) is subject to variations in the order of 20 - 40% thought to be the result of variability in the size of transmitter vesicles (Karunanithi *et al.*, 2002), which is intrinsic to each release site (Liu & Tsien, 1995), and/or the stochastic opening of postsynaptic ion channels which may also contribute to the variance of the postsynaptic response as the channels have opening probabilities of less than 1 (~0.7) (Hestrin, 1992).

Synaptic plasticity is defined as the activity dependent changes in the strength of connections between neurones. In other words, the prior history of activity within a given cortical network has lasting implications for the future processing of information within it. The time over which these plasticities exert their effect varies depending on the mechanisms involved in their activation.

To date, eight independent mechanisms have been discovered that contribute to the paired pulse modulation of axon terminal output properties (see Thomson, 2000;Thomson, 2003 for review). Five are involved in frequency dependent depression and three in the facilitation of synaptic strength during repeated activity.

1.7.2.1 Depression of postsynaptic potential amplitude.

The reduction in the amplitude of a postsynaptic potential can occur during conditions of repetitive stimulation, particularly in cases of increased rate of release. This depression has been shown to comprise slow and fast components in adult pyramid to pyramid excitatory connections which may act as band pass filters for repetitive inputs at specific frequencies.

The proposed mechanisms of depression vary from the decrease in the probability of vesicle release from a given release site for a time period following preceding release (release site refractoriness) even when docked and fusion competent vesicles are present, to the depletion of vesicle pools under conditions of high frequency activity (frequency (or use) dependent depression). More than one form of depression (as well as facilitation) may be expressed at the same synapses and as the time courses of each overlap, multiple mechanisms of depression at a single release site further enhance the ability of a particular synapse to reliably convey information at specific frequencies whilst filtering out others. Release site refractoriness for example is a fast component of paired pulse depression (PPD) proposed to prevent the release of transmitter close to sites of recent release which may prevent release onto potentially partially desensitised postsynaptic receptors is most potent at short interspike intervals and therefore acts as a low pass filter during repeated high frequency activity. Another component termed 'slowly decaying', as its name suggests, has a slower timecourse whereby 2nd EPSPs require 2-3 seconds between successful releases to recover to an amplitude corresponding with the 1st EPSP (Thomson & West, 2003). The contribution of this component of depression is typically small at about 15% at intervals of around 100ms and decreases in strength with increasing interval duration.

1.7.2.2 Short term enhancement of postsynaptic potential amplitude.

To date, three main mechanisms that enhance the release of neurotransmitter during paired pulse and repetitive activity have been described. Facilitation, augmentation and post tetanic potentiation (PTP). The mechanisms responsible and the timecourses of each differ greatly but all

have the same outcome: the promotion of synaptic strength over and above control values when under the influence of specific stimulus parameters.

The short duration enhancement (or facilitation) of PSP efficacy is found at all connections (though often masked by depression) and the most probable mechanism proposed to explain it is 'the residual calcium hypothesis' first proposed at the frog neuromuscular junction (Katz & Miledi, 1968). In this model it is proposed that a single action potential may not allow enough Ca^{++} ions to enter the terminal to meet the requirement for 4 Ca^{++} ions to bind to the Ca^{++} sensor for release to occur, therefore resulting in transmission failure. However Ca^{++} influx in response to successive action potentials is more likely to promote release due to residual calcium already having partially primed the Ca^{++} sensor. Facilitation decays rapidly (within 60ms), follows an exponential curve with a time constant of around 13ms (Thomson, 1997).

PTP and augmentation decay more slowly than facilitation and result in longer lasting enhancement of PSP amplitude resulting from an increased probability of transmitter release. Both mechanisms are perceived to be calcium dependent and whilst the manner in which augmentation is initiated is as yet unclear the elevation of calcium entry into the terminal during the periods of prolonged high frequency action potentials that activate PTP is suggested to increase the probability of release by increasing the size of the releasable pool of vesicles (and therefore increasing the number potentially docked and release competent) via the liberation of the reserve pool by phosphorylation of synapsin molecules that bind the reserve vesicles to an actin anchor (see Doussau & Augustine, 2000 for review).

1.7.3 Chemical synapse properties in layer 4.

The excitatory cell interconnections thus far studied between pyramidal cells express significant variability of their dynamic synaptic properties that appears to be dependent on the location of the postsynaptic cells they innervate. For example, pyramid to pyramid connections typically exhibit paired pulse depression (Markram & Tsodyks, 1996; Thomson & West, 1993) but have also been shown to express paired pulse facilitation in excitatory connection recordings from

layers 3 and 5 (Thomson, 1997). Strong facilitation has not been demonstrated between excitatory cells in layer 4. In rat barrel cortex the short term dynamics of excitatory networks in layer 4 have been shown to exhibit variable levels of paired pulse depression between individual connections and the strongest depression correlated with the shortest interspike intervals. The further examination of these phenomena and the identification of potentially specific synaptic properties (see section 1.7.2) within circuits of the spiny cells represents a major task in terms of the understanding of layer 4 excitatory network activity.

The EPSPs generated at spiny cell connections to smooth cells show many features in common with those between the spiny cells. For example, aspects of short term synaptic plasticity imparted to connections by specific mechanisms at the synapse are common to both types of connection. Interneuronal EPSPs in cat often exhibit paired pulse or frequency dependent depression (Tarczy-Hornoch *et al.*, 1998) and less frequently may show facilitation upon repeated activation depending on the type of interneurone innervated, as identified by their postsynaptic target preferences (Beierlein *et al.*, 2003;Reyes *et al.*, 1998). The inputs from RS pyramidal cells in rat barrel cortex to FS layer 4 interneurones also exhibit short term depression from highly reliable synapses (Beierlein *et al.*, 2003) but again, unfortunately, these studies did not permit the correlation of these synaptic properties with the morphological class of interneurones, any of which may express the stated electrophysiological properties.

In addition to the complexity of layer 4 microcircuits and the variations imparted to them by the subclasses of neurones they comprise, the wealth of frequency dependent mechanisms at the disposal of their individual synapses and the presence of many at the same connections provide enormous depth to the tuning of cortical circuitry above and beyond that provided by the 'wiring' of neuronal elements. The frequency dependent properties used in these circuits are therefore of prime importance and require accurate correlation with the subclasses of neurones comprising each circuit. To date, while the properties of synapses and the levels of connectivity between broad neuronal classes have been studied and attempts have been made to model the synaptic properties of neuronal networks, particularly between excitatory cells (Petersen, 2002), we still know relatively little of which specific subclasses or which dynamic synaptic mechanisms are involved and for what

purpose (in the cortex as whole let alone in layer 4). A number of important questions remain. For example, are the observations made using neonatal or juvenile rat tissue comparable with similar connections in the adult? And are there any features of cat connections that do not correlate with similar recordings in rat? And, what are the fundamental frequency dependent properties of excitatory connections utilised by these connections and which electrophysiological subtypes are involved?

1.8 THE ELECTRICAL SYNAPSE OR GAP JUNCTION.

Historically the electrical or gap junction synapses have been considered to be the more primitive relations of the chemical synapse prevalent in invertebrate and lower vertebrate systems (Bennett, 1997) believed to serve only to pass current from one cell to another without any refinement of the information those currents may convey. More recently however, the gap junction has been observed as a highly specialised protein array capable of opening and closing in response to external stimuli in such a way as to modulate the synchronisation of adjacent neurones of the same class and to allow the passage of small molecules of less than 1000 Da (Kumar & Gilula, 1996).

Gap junction connections can form between the dendrites (Kosaka & Hama, 1985), or between axons and soma/dendrites (Pappas & Bennett, 1966) by an array of 6 connexin subunits which combine to create a connexon capable of docking with a similar unit on an adjacent cell to form a direct transport conduit. The connections are not indiscriminate electrical contacts between the cells; they are specialisations in the surface membranes which provide a high speed, low resistance pathway useful in the coordination and synchronisation of specific nerve cells. Moreover it has become apparent that the gap junction channels can be formed by a variety of different connexins which may lead to differential permeabilities that will permit the transfer of inorganic ions including Na^+, K^+ and Ca^{++} and specific second messengers such as cAMP, cGMP, or IP_3 from cell to cell by passive diffusion but prevent the passage of proteins or nucleic acids (see Loewenstein, 1981 for review). The differential expression of connexin subunits and the gap junction coupling of

specific cell classes may allow specific population-wide regulation effected by changes in concentration of metabolites and second messengers.

The presence of gap junction connected cells in the cortex is most apparent during development and most often between glia or between glia and neurones indicating a role in homeostasis during cortical development. Neurone to neurone gap junction communication during development and within interneurone populations in adult tissue is also well documented (Chang *et al.*, 1999;Tamas *et al.*, 2000). Their presence is often revealed by the transfer of small dye molecules such as neurobiotin and certain fluorescent probes and the consequent demonstration of co-stained neurones when individual neurones were filled, which is considered indicative of gap junctions and has also allowed estimation of the channels' pore size (Loewenstein, 1981). Interestingly, dye-coupling is most apparent between neurones of similar class at embryonic level and at postnatal days 1-4 is common (Naus & Bani-Yaghoub, 1998;Peinado *et al.*, 1993) but occurs progressively less frequently into adulthood indicating that the pore size or pore properties change during postnatal development (preventing dye transfer), or that they are simply lost with maturation. The possible changes in gap junction properties with postnatal age are backed up by differential expression of certain mRNA molecules coding for connexin subunits that correspond with developmental events including cell proliferation and migration as well as the establishment of cortical circuits (Nadarajah & Parnavelas, 1999). However, gap junction communication is not totally absent in the adult brain, and certain gap junction protein subunits persist particularly between parvalbumin containing interneurones (Freund, 2003;Fukuda & Kosaka, 2003), though the observation of dye-coupling declines rapidly with postnatal age.

To date the evidence for gap junction connectivity between pyramidal cells in adult tissue has largely been based on predictions made with computer simulations of cortical activity indicating a role in the generation of network oscillations (Traub & Bibbig, 2000; Traub *et al.*, 2003) as well as some experimental evidence of the retained expression of connexin mRNA in layer 5 pyramidal cells (Simburger *et al.*, 1997). No direct physiological evidence for neocortical pyramid to pyramid electrical coupling has been presented.

1.9 AIMS OF THE PROJECT AND THESIS FORMAT.

The aims of the project presented here are essentially centred around the study of microcircuitry, specificity and the properties of intercellular communication employed in layer 4 of the adult cat and rat neocortex. Firstly, to study the frequency and strength of connections between layer 4 excitatory neurones of the adult rat and compare these with similar connections previously described in immature rat and mature cat and more directly with new data from adult cat layer 4. To identify the frequency dependent synaptic properties of the excitatory to excitatory connections, compare them with the pyramidal connections published previously and attempt to correlate neuronal properties such as morphology and spike discharge patterns with any specific connections that they might form. Secondly, to study the frequency and strength of interactions between excitatory and inhibitory neurones in adult rat cortex and compare these with similar connections in cat, and with those previously described in other layers and in layer 4 of immature rat and adult cat, again attempting to identify any novel specificity of connection patterns between neuronal subclasses, and also to assess the morphological diversity of the interneurones involved. To determine whether the properties of excitatory inputs to interneurones correlate with their physiological, morphological and immunocytochemical properties as has been suggested for similar connections in other layers. In addition, to test for possible electrical junctions between pairs of recorded neurones.

The thesis format will proceed with a description of the techniques employed in the recording and dye filling of synaptically connected pairs of neurones and the histological and immunocytochemical techniques used to allow anatomical identification of each.

A summary of the electrophysiological classification of all neurones recorded from all cortical layers during the course of these projects and their likelihood of connectivity with other neurones will precede four main studies. The first will highlight major properties of intralaminar connections between excitatory neurones. The second, will present data illustrating the interactions of excitatory cells and identified interneurones. Thirdly, evidence will be presented for the existence of gap junction mediated intercellular connectivity between pyramidal cells of adult neocortex. And fourth, an assessment of the technique devised to judge potential connectivity between permanently

visualised pyramidal cells and immunocytochemically labelled interneurones

Finally, a discussion of the data gathered throughout these studies and their relation to other studies in the field will be presented.

2.0 METHODS AND MATERIALS.

2.1 INTRODUCTION TO THE TECHNIQUES.

Electrophysiological and histological techniques were employed to allow the recording of pairs of synaptically connected neurones in adult cat and rat neocortex using sharp intracellular electrodes with biocytin filling, and to subsequently reveal the morphology of those cells.

The histological and immunocytochemical techniques described below were devised to demonstrate the anatomy of filled neurones, to reveal aspects of their neurochemistry and also to retain as much of the neuronal fine structure as possible.

2.2 SOLUTIONS

2.2.1 Artificial Cerebro-Spinal Fluid (ACSF):

NaCl 124mM

$NaHCO_3$ 25.5mM

KCl 3.3mM

KH_2PO_4 1.2mM

$MgSO_4$ 1.0mM

$CaCl_2$ 2.5mM

D-Glucose 15mM

Equilibrated with 95% O_2 and 5% CO_2.

ACSF for perfusion was made in the same way but substituting 248mM Sucrose for NaCl.

2.2.2 Electrode-filling Solution:

2% Biocytin (w/v)(Sigma) in 2M Potassium Methylsulphate.

2.3 ANIMALS AND ANAESTHESIA

All procedures carried out on the rats and cats used throughout this study complied with British Home Office regulations for animal use.

2.3.1 Rat: Male Sprague Dawley rats 116 - 230g were anaesthetised in a gas jar containing a saturated atmosphere of Fluothane (ICI Pharmaceuticals, UK) until the righting reflexes had ceased and then by intra-peritoneal injection of Sodium Pentobarbitone (Sagatal, Rhone Merieux, 60mg kg^{-1}). The animal was judged to be sufficiently deeply anaesthetised using the cessation of the withdrawal reflex following paw pinch as an indicator.

2.3.2 Cat: Young adult male cats (2.5-3.4kg) (tissue obtained following acute experiments described elsewhere (Wang & Ramage, 2001) were anaesthetised with a mixture of α-chloralose (70mg kg^{-1}) and sodium pentobarbitone (Sagatal, Rhone Merieux, 6mg kg^{-1}) injected i.v. The level of anaesthesia was judged by the absence of a withdrawal reflex and/or the cardiovascular response to paw-pinch and by the stability of resting cardiovascular and respiratory variables as well as pupil size. After the acute experiment the right carotid artery was cannulated and the skull overlying the occipital lobes removed. The animal was then overdosed with an intra-venous injection of sodium pentobarbitone (100mg kg^{-1}), prior to perfusion via the right carotid with ice cold sucrose ACSF (see below).

2.4 SURGERY

2.4.1 Rat: A large incision was made in to the peritoneum below the sternum. Spencer Wells forceps were clamped to the base of the sternum and the diaphragm was cut deflating the lungs. The ribs on either side of the chest were cut to produce a large flap of tissue which was raised clear of the heart. A needle was then inserted into the left ventricle of the heart and the peristaltic pump (Watson-Marlow 502s, Cornwall, UK) charged with O_2/CO_2 equilibrated, ice cold Sucrose ACSF

(with added sodium pentobarbitone 60mg l^{-1}) was switched on. The right atrium was snipped with scissors to allow free flow of blood and perfusion medium from the body. Once the liquid flowing from the right atrium had become clear, indicating complete exsanguination, the animal was decapitated.

An incision of the scalp was made to expose the skull and flat nosed pliers were used to remove the skull plates exposing the brain. After careful removal of the dura a scalpel was used to cut through the frontal lobe and a spatula was inserted to scoop the brain out of the skull and into a beaker containing fresh ice cold sucrose ACSF whilst simultaneously severing the cranial nerves.

2.4.2 Cat: The right carotid artery was cannulated and the occipital portion of the skull removed to reveal the brain. After overdosing the animal with an intra-venous injection of sodium pentobarbitone (100mg kg^{-1}), the left carotid artery clamped and both jugular veins cut prior to perfusion with 200ml of ice cold sucrose ACSF through the right carotid. The dura covering the visual cortex was removed and a block of brain tissue containing areas 17, 18 and 19 of visual cortex was taken for slice preparation.

2.5 SLICE PREPARATION

Both rat and cat material was trimmed into a block approximately 1-2 cm^3 containing the primary sensory regions of cortex which was glued using cyanoacrylate adhesive (Loctite Superglue), onto the chuck of a Vibroslice (Campden Instruments, Loughborough, UK). 450-500µm coronal slices were cut and placed temporarily in a petri dish of ice cold O_2/CO_2 equilibrated Sucrose ACSF before being transferred to the interface chamber. Slices were then maintained with Sucrose ACSF at a flow rate of approximately 1ml $minute^{-1}$ supplied by a peristaltic pump (Gilson Minipulse3, France) and warm, humidified 95% O_2/5% CO_2 at 34-35°C for one hour. The Sucrose ACSF was then replaced with standard ACSF and equilibrated for a further hour prior to electrophysiological recording.

2.6 IN-VITRO SLICE MAINTENANCE

2.6.1 The recording chamber and perfusion system:

The interface/recording chamber consisted of a heated Perspex water jacket used to warm a coil of perfusion tubing containing aerated ACSF to 34-35°C, and to warm moist 95% O_2/5% CO_2 gas prior to delivery to cortical slices held within a small holding chamber above the water jacket (see figure 2.1). A peristaltic pump (Gilson Minipuls 3, Wisconsin, USA) was used to maintain a perfusion rate of approximately 1ml min^{-1} and the temperature was monitored throughout the experiment using a thermocouple.

2.7 PAIRED INTRACELLULAR RECORDINGS WITH BIOCYTIN FILLING

2.7.1 Rig set up:

The Electrophysiology rig consisted of an interface chamber which kept neurones viable by warming, oxygenating and perfusing tissue slices as described above (section 2.6.1). A low power dissecting microscope with a long working distance was required to visualise the gross anatomy of the slices and to aid the alignment of glass microelectrodes using micro-manipulators (Prior, UK). A low noise AXOPROBE 1 amplifier (Axon Instruments, Burlingame, USA), was used to record cells, oscilloscopes enabled visualisation of their activity and a tape recorder (Racal, Southampton, UK) recorded their responses. The wiring of the rig is summarised in figure 2.2.

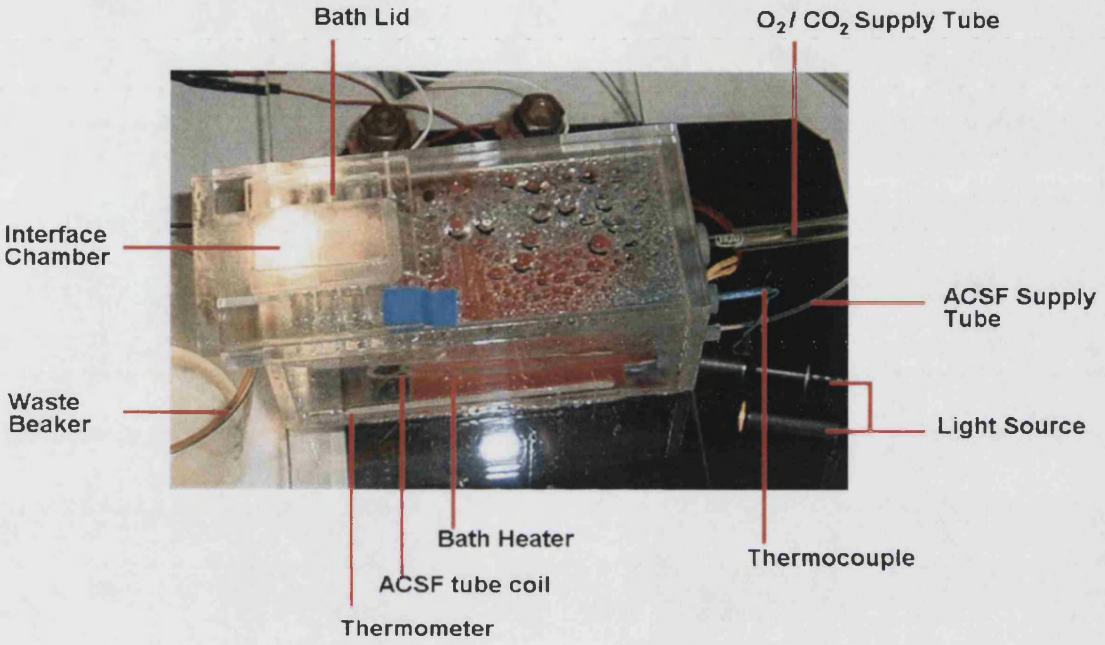

Figure 2.1. Photograph illustrating the main components of the interface chamber used to maintain the slices. The heated water jacket is used to warm the ACSF and to warm and moisten the O_2/CO_2 supply prior to delivery onto the slices.

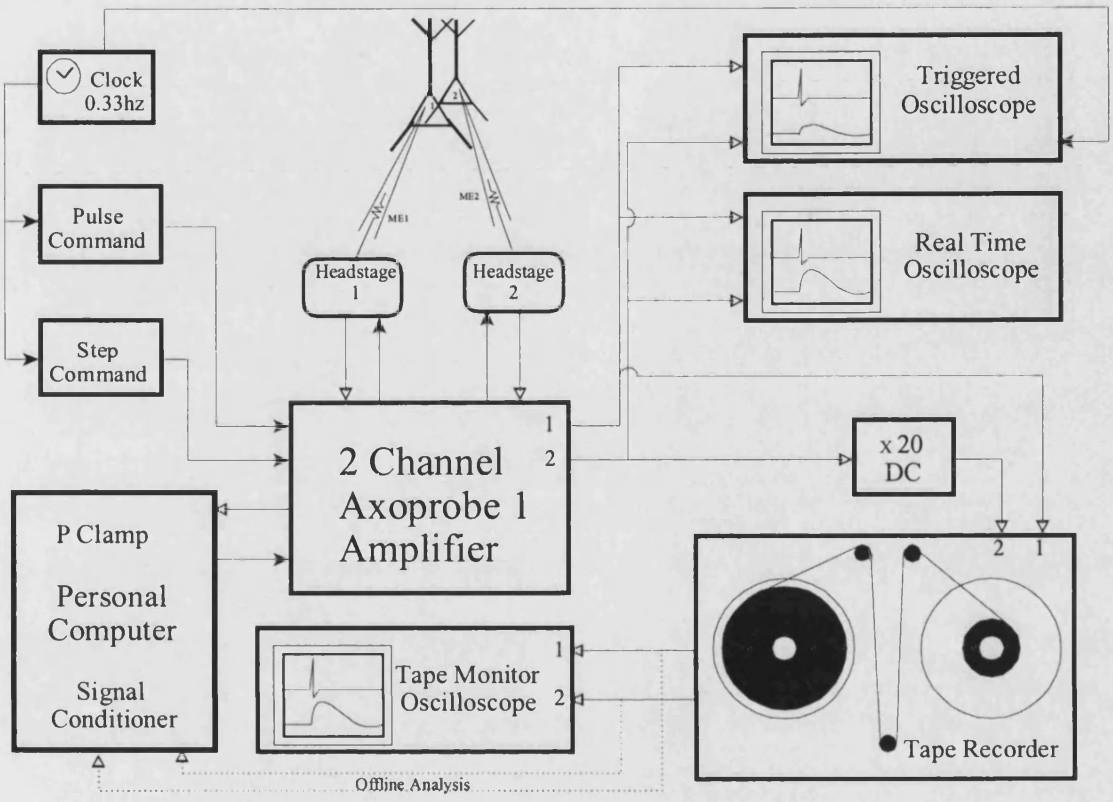

Figure 2.2. Schematic diagram summarising the wiring of the electrophysiology rig.

2.7.1.1 The Amplifier

At the heart of the rig set up was the amplifier model Axoprobe-1 (Axon Instruments, Burlingame, USA), utilising two multipurpose low-noise microelectrode amplifiers used independently for intracellular voltage recording with simultaneous current passing. The amplifier was used to facilitate the impaling of neurones, measure membrane potential against a reference electrode which was housed in the interface chamber, to drive voltage dependent cell activity by passing current directly into impaled neurones and to monitor voltage fluctuations in real time using a frequency modulated loudspeaker.

2.7.1.2 The Oscilloscopes, x20 DC and Timing Device

The peripheral devices used in the rig included a clock to establish regular triggers for current injection and recording (0.33Hz), a x20 DC amplifier connected to the postsynaptic channel to boost potentially tiny postsynaptic responses relative to tape noise. Two digital oscilloscopes were used to monitor neuronal activity in both triggered and continuous real time modes. The triggered storage oscilloscope generated a visual representation of the presynaptic cell's responses for the duration of the current injection and the postsynaptic cell's responses to presynaptic action potentials in a sweep by sweep mode.

The oscilloscopes allowed membrane potentials to be monitored throughout the recording to assess baseline activity and to assess the condition of the recorded neurones. A third oscilloscope was used to monitor the gains used for recordings made onto magnetic tape to ensure signals did not saturate.

2.7.2 Electrodes:

Conventional sharp microelectrodes (resistance 90-170MΩ) filled with a solution of 2% Biocytin in Potassium Methylsulphate (w/v) (see section 2.2.2) were used for all paired intracellular recording experiments. These were produced from borosilicate glass capillaries (Clark electromedical, GC120F-10, 1.2mm O.D x 0.69mm I.D) using a Flaming/Brown micropipette puller (Sutter Instruments, Co, USA). Cells were filled either by passive diffusion of Biocytin (372.48 Molecular Weight), from the recording electrode into the impaled neurones or by deliberate iontophoresis by passing positive current in a half duty cycle (0.5nA, 500ms, 1 pulse second^{-1}).

2.7.3 Targeting/Search Strategy:

In general, the first microelectrode was inserted into the region of cortical layer 4 and a neurone was impaled. Once the cell had stabilised and a suitable high quality/resolution recording of its baseline activity and satisfactory responses to square wave current pulse injections were observed, a second electrode was inserted into the same layer or column as the first. Neurones were then impaled with the second electrode sequentially and tested in both directions for presynaptic and/or postsynaptic connectivity with the first cell. If connectivity was observed the cells were allowed to stabilise before positive square wave and/or ramp current injections were delivered to the presynaptic cell to elicit action potentials. Both pre and postsynaptic activity was recorded onto tape for subsequent offline analysis. If connectivity was not observed, the second cell was abandoned, the electrode was moved and another cell was impaled and tested.

Neurones within layers 2 - 6 were sampled by the second microelectrode in both medio-lateral (same layer) and dorso-ventral (same column) planes until a connection was identified or until the number of non-connected cells sampled (and therefore potentially filled with biocytin) was deemed to be likely to compromise the subsequent identification of connected neurones during morphological analysis. If no synaptic connections were identified, both electrodes were withdrawn and moved to another region of layer 4 sufficiently far away from the first search area to avoid excessive overlapping of filled neuronal processes.

2.8 DATA ACQUISITION

Pre and postsynaptic membrane potential recordings of synaptically connected pairs of neurones were stored on analogue magnetic tape (Quantegy Inc, Alabama, USA) using a Racal Store 4 DS tape recorder (Racal, Southampton, UK). As the characteristics of postsynaptic responses are affected by spontaneous changes in membrane potential, the cells were held within ±1mV of the resting membrane potential by continuous manual current clamp. The postsynaptic electrode balance was monitored by applying small (0.05nA) and brief (5ms) current pulse injections prior to the presynaptic current pulse.

2.8.1 Data digitisation:

Analogue tape recordings were digitised by passing the data through a CED 1401 analogue to digital converter (CED, Cambridge, UK). A sample rate of 10kHz (voltage resolution 0.005-0.01mV) was chosen to produce a high resolution image of the original signal. Data were stored on optical disc for subsequent offline analysis using Spike2 software and were converted to a data format compatible with in-house software used for sweep selection, averaging and waveform component measurements.

2.8.2 Electrophysiological analysis:

In-house software designed to allow the simultaneous visualisation of pre and postsynaptic electrophysiological waveforms over a predefined time course of 300ms (termed a 'sweep'), was used for detailed analysis. The quality of recordings and the properties of the neuronal responses to current pulse injection were observed and sweeps were selected according to criteria including the number of action potentials generated, the postsynaptic responses to spike-induced neurotransmitter release and the levels of spontaneous synaptic activity.

Data subsets were used to generate sweep averages of PSPs from multiple records triggered on the rising phase of presynaptic action potentials to allow accurate measurement of mean PSP properties in the absence of noise. The mean PSP shape characteristics of peak amplitude, 10-90% rise time (the time required for an event to rise from 10% to 90% of the peak amplitude, RT) and width at half amplitude (the time difference between the rising and falling phase of the PSP at 50% of peak amplitude, HW) were assessed using these averaged data (see figure 2.3a). Where PSPs within a train of spikes were averaged, a narrow time window (<1ms) was used to select records with similar interspike intervals to allow accurate analysis of any time dependent properties affecting subsequent spikes. Numbers given in the text are means ± standard deviation.

Where single sweep measurements of all PSPs in each sweep were performed, the amplitude of the first PSP in a train was taken as the difference between the peak and the baseline measured just prior to the spike artefact on the postsynaptic trace. Where the second (third.....) PSP was sufficiently separated in time for the preceding event to have decayed fully, measurements were made in the same way (figure 2.3b). However, if the subsequent PSPs were found to sum at shorter interspike intervals, measurements were made from the peak of the PSP to equivalent point in time on the decay phase of an averaged 1^{st} PSP superimposed and scaled to fit the preceding event (figure 2.3c). This process was under manual control and was repeated for all subsequent PSPs in a train and for all selected sweeps in each data set analysed. Sweeps and/or events containing large spontaneous events were excluded from measurement and where no postsynaptic response was observed a value of 0mV was included to represent apparent transmission failures.

In figures, artefacts corresponding to the onset and end of current pulse injection and spike artefacts present on the postsynaptic recordings were removed graphically after the generation of averages responses.

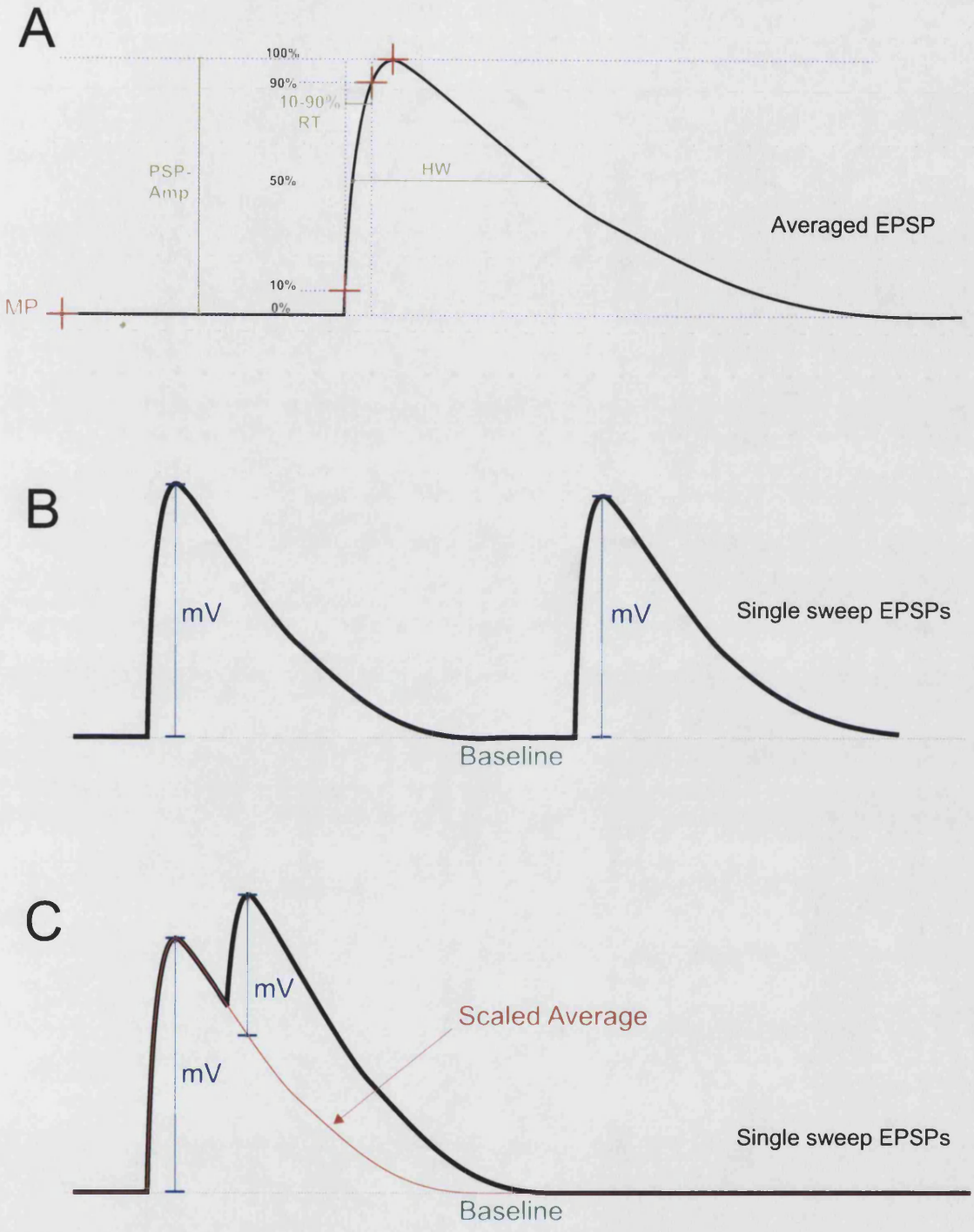

Figure 2.3. Diagram illustrating the measurement of PSP properties during post-hoc electrophysiological analysis. A, Measurement of PSP amplitude, 10-90% rise time and width at half amplitude from an averaged first EPSP. B, Single sweep measurement of two EPSPs at intervals sufficiently long for the first to decay completely. Measurements for both are taken to baseline. C, Measurement of two EPSPs separated by a short interval with the second arriving before the first has decayed. The first EPSP is measured to baseline and the second against the decay phase of a superimposed scaled average of the first.

2.8.3 Coefficient of Variation analysis:

Coefficient of variation (CV) analysis allows identification of the pre- and postsynaptic loci that underlie synaptic plasticity (Faber & Korn, 1991). In a simple binomial model applied to synaptic connections it is assumed that a constant number of release sites (n) contribute, the probability (p) of neurotransmitter release is equal to or less than 1 (ie. release does not occur in response to every spike) and the same at all release sites, and the quantal amplitude (q) (ie. the size of postsynaptic events occurring in response to a single quantum of transmitter) remains constant.

Mean EPSP amplitudes and CVs were calculated from single sweeps measurements of the 1st, 2nd and 3rd EPSPs in response to trains of presynaptic action potentials and plotted as normalised CV^{-2} versus normalised mean EPSP amplitude. Expressed mathematically the mean EPSP amplitude (M) is equivalent to M=npq and CV^{-2} is np/(1-p). As CV^{-2} is independent of q, plots of the CV^{-2} versus M for 2nd and 3rd EPSPs normalised to the 1st EPSP indicate whether changes in synaptic efficacy were due to pre- or postsynaptic mechanisms. If a change in mean EPSP was postsynaptically mediated (Δq) this would be demonstrated by a slope of zero. Presynaptic change (Δp) is represented by a slope of >1. If the change in the mean amplitude was directly proportional to the change in CV^{-2} then a slope of 1 would correspond to a change in n (or both p and q).

2.9 GENERAL HISTOLOGICAL TECHNIQUES

The histological procedures used to demonstrate double immunofluorescence, peroxidase labelling and ultrastructural analysis of neurones throughout this study have been published (Hughes *et al.*, 2000).

2.9.1 Fixation:

Slices were trimmed while in the recording chamber to isolate the area of tissue containing the recorded neurones. This portion of the slice was then placed between two pieces of moistened

micropore filter paper to keep the tissue flat and submerged in an aldehyde containing fixative solution whose composition was determined by the histological procedures to be carried out. Fixation was allowed to occur overnight at 4°C prior to the replacement of fixative with 0.1M Phosphate Buffer.

The double fixation technique (Sabatini *et al.,* 1963) was used for all slices. This involved the submersion of slices in a solution of buffered paraformaldehyde and glutaraldehyde and followed after histochemical and immunohistochemical processing by post fixation in buffered Osmium Tetroxide. The aldehydes act upon tissue proteins by cross linkage (Habeeb & Hiramoto, 1968) and the Osmium Tetroxide reacts strongly with the unsaturated lipids of cell membranes (Hess, 1959) whilst also staining the tissue to provide enhanced contrast for both light and electron microscopy. Slices that were to be processed for immunocytochemistry were initially immersed in glutaraldehyde -free fixative solution containing only 4% paraformaldehyde in 0.1M Phosphate buffer but, while this proved optimal for immunolabelling of the tissue the preservation of peroxidase labelled neurones proved to be poor. As a result, a small amount of Glutaraldehyde (0.025%) was added to improve the preservation of the tissue and a small amount of saturated picric acid solution was added (0.2%) to preserve the immunogenicity in the light of glutaraldehyde fixation and to enhance further the fine structural detail (Somogyi & Takagi, 1982).

2.9.2 Sectioning:

While both vibrating microtome (Vibratome) and Frozen sections are suitable for visualisation of recorded neurones and immunocytochemistry, the production of 60μm thick Vibratome sections was preferred for all slices as this technique allows significantly better preservation of ultrastructural detail. In brief, tissue slices were embedded in a warm 12% aqueous gelatine solution which was subsequently cooled to 4°C and hardened in the same fixative solution as the tissue slice for 1 hour. The gelatine embedded slices were glued onto the stage of the Vibratome (Agar Scientific, Stanstead, UK) using cyanoacrylate adhesive (Loctite Superglue), and sectioned using a razor blade set to advance through the tissue whilst vibrating at 90° to the direction of advance. All sections were sketched and counted carefully before being transferred to 0.1M Phosphate Buffer in glass scintillation vials using a sable paintbrush.

2.9.3 Tissue Processing:

Gelatine was carefully removed under close observation using a stereoscopic dissecting microscope and a sharp scalpel. In all subsequent incubations, sections were free-floating within the glass scintillation vials and subject to constant gentle agitation on a Titramax 100 rotary shaker (Heidolph Instruments, Schwabach, Germany)

2.9.4 Permeabilisation:

To preserve the ultrastructure of cellular components the freeze/thaw technique was favoured over the use of detergents such as Triton X-100 and Saponin that enable penetration of large molecules such as antibodies to the cell interior by dissolving portions of the cellular membranes. The freeze/thaw technique also enhances penetration but by rupturing the membranes via the rapid formation of ice crystals.

Sections were cryoprotected in graded 0.1M PB-based solutions containing 10% sucrose (w/v) for 2x10 minutes, 20% sucrose with 6% glycerol for 2x20 minutes and then 30% sucrose with 12% glycerol for 2x30 minute changes. Sections were then placed flat onto aluminium foil, frozen over the surface of liquid nitrogen and thawed to room temperature. This process was repeated three times and the sections returned to 0.1M PB in glass vials. At this stage the three main processing paths divide for those slices requiring only standard Biocytin visualisation, those destined for double immunofluorescence with subsequent peroxidase labelling or immunoperoxidase so at this point the reader is referred to individual sections.

STANDARD BIOCYTIN VISUALISATION TECHNIQUE	2.10
IMMUNOFLUORESCENCE	2.11
IMMUNOPEROXIDASE	2.12

2.9.5 Post Fixation:

Once the labelling and staining procedures were complete, sections were subjected to post fixation in Osmium Tetroxide to fix cell membranes prior to dehydration and to provide contrast at both light and electron microscopy. Using an artists paintbrush, sections were rolled flat onto, and sandwiched between, two pieces of filter paper. 8-10 drops of 1% Osmium Tetroxide in 0.1M PB were applied and left to act for 30 minutes in a fume hood.

2.9.6 Dehydration:

As the epoxy resin used to embed tissue sections is not miscible with water it was necessary to dehydrate the tissue through graded ethanols. Sections were placed on a clean microscope slide and held flat by a coverglass. Graded alcohols (50, 70, 95 and 100%) were applied sequentially, each for at least 15 minutes with gentle agitation to ensure gentle and complete dehydration of the sections whilst minimising shrinkage artefacts and retaining shape.

2.9.7 Clearing, Embedding and Curing:

Alcohol was removed from the tissue sections by the application 2 x 10 minute washes in Propylene Oxide (C_3H_6O) (BDH, Poole, UK) followed by propylene oxide mixed with Durcupan epoxy resin (Fluka, Steinheim, Switzerland) (1:1) for 30 minutes. Sections were then carefully transferred to a small aluminium planchette containing neat unpolymerised resin for a minimum of 3 hours to allow evaporation of the linking agent and infiltration of resin into the tissue spaces. Sections were then mounted onto glass slides, coverslipped and cured at 56°C for 48hrs. At this point the sections can be stored indefinitely.

2.10 STANDARD BIOCYTIN VISUALISATION TECHNIQUE

The visualisation of biocytin fixed within the recorded neurones relies upon the Avidin Biotin-HRP Complex (ABC peroxidase) technique. This protocol utilises the binding of biocytin by an Avidin/Horse Radish Peroxidase (HRP) complex. The HRP is then used to catalyse the reduction of H_20_2 to facilitate the oxidation of 3,3 Diaminobenzidine tetrahydrochloride (DAB), generating a coloured pigment visible at both light and electron microscopic levels.

The cellular tracer Biocytin used to fill cells is a derivative of the water soluble vitamin biotin (also commonly referred to as Vitamin B7 or H). It has a low molecular weight of 372.48 Daltons and an effectively irreversible, extraordinarily high affinity with the glycoprotein Avidin. The egg white derived protein Avidin (MW 68 KDa), comprises four identical subunits each capable of binding biocytin. In the ABC peroxidase solutions used in this study (Vector Laboratories, Peterborough, UK), one of the biotin binding sites is occupied by a molecule of biotinylated HRP. HRP is a 40KDa MW detection molecule which, when activated by the presence of low concentrations of H_2O_2 (0.01%) catalyses its breakdown into H_2O. The oxygen liberated by this reaction is then available to oxidise the substrate DAB which polymerises to form a non-soluble, stable, brown/black coloured precipitate which may be intensified to dark blue/black in the presence of nickel or cobalt chloride. The sequential binding of reagents in the ABC technique is summarised in figure 2.4.

Permeabilised sections were washed in 0.1M Phosphate Buffered Saline (PBS) and incubated in a solution of ABC peroxidase in PBS overnight at 4°C on a shaker. After washing, a 15 minute incubation in 3,3 Diaminobenzidine (DAB) (Sigma-Aldrich, St. Louis, USA) containing 1 drop of 8% Nickel Chloride ($NiCl_2$) was performed prior to initiation of the peroxidase reaction by the application of 1% Hydrogen Peroxide giving a final concentration of 0.01% H_2O_2 in DAB+$NiCl_2$. The reaction was allowed to proceed for 3-5 minutes or until positively stained neurones were clearly visible with the aid of a stereoscopic dissecting microscope.

Sections were then post fixed in osmium tetroxide, dehydrated in graded ethanol, embedded in Durcupan epoxy resin, mounted onto microscope slides and cured as described above (see sections 2.9.5 - 2.9.7).

Biocytin Visualisation

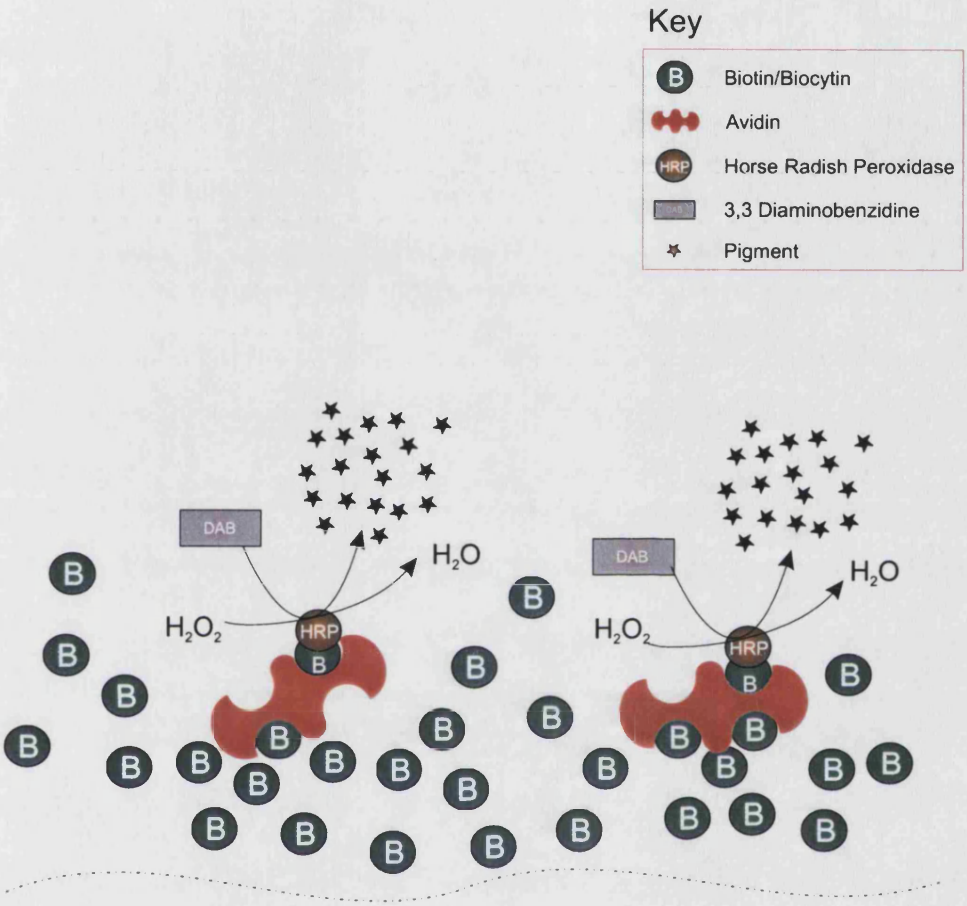

Figure 2.4. Schematic diagram of reagent interactions used for standard permanent biocytin visualisation.

2.11 DOUBLE IMMUNOFLUORESCENCE WITH BIOCYTIN LOCALISATION

The immunofluorescence technique was used for the demonstration of calcium binding proteins and neuropeptides present within specific populations of neurones. Secondary antibodies conjugated to fluorescent probes were used to label primary antibodies raised against specific antigens. The general principles involved are summarised in figure 2.5.

Permeabilised sections were washed in 0.1M PB then incubated for 30 minutes in an uncapped vial containing a solution of 1% Sodium Borohydride ($NaBH_4$)(Sigma, St. Louis, USA) in 0.1M PB. The hydrogen ions liberated by this solution act to reduce the general background fluorescence and non-specific staining experienced as a result of aldehyde fixation by the reduction of excess aldehyde groups (Kosaka *et al.*, 1987). Sections were then washed thoroughly in multiple changes of PB and PBS prior to incubation in 10% normal goat serum (NGS) in PBS for 30 minutes. This blocking serum was used to prevent binding of antibody to inappropriate sites and goat serum chosen as both of the fluorescent-tagged secondary antibodies used in these protocols were raised in goat.

2.11.1 Primary Antibody Incubations:

Combinations of primary antibodies were chosen based on the correlated electrophysiology and neurochemistry of interneurones demonstrated in previous studies (Kawaguchi & Kubota, 1993;Kawaguchi & Kubota, 1996;Kawaguchi & Kubota, 1997;Kawaguchi & Kubota, 1998). In a previous study performed by this research group (Pawelzik *et al.*, 2002) it was shown that the distributions of immunopositive cells in slices did not change with incubation time in the interface chamber. Slices from the same animal were fixed 30 minutes after slicing and after 12 hours in the interface chamber. All slices were processed simultaneously with identical protocols and were observed to display indistinguishable immunopositive cell distributions.

The possible combinations of primary antibodies used was restricted in that they must be raised in different species to allow the labelling of each primary antibody with a different secondary antibody carrying a fluorescent marker (see below for the choice and working dilutions of available

Triple Fluorescence with Biocytin Visualisation

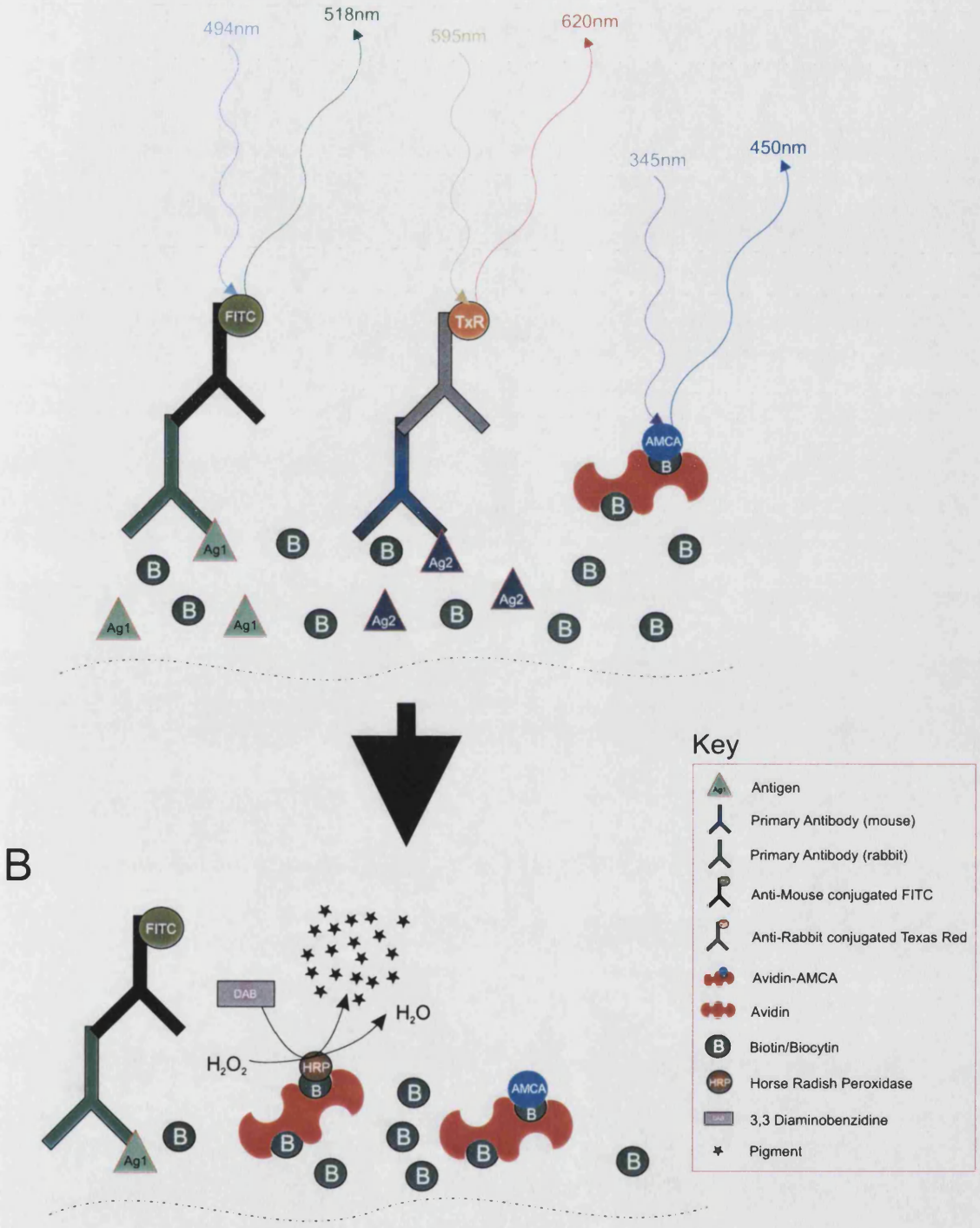

Figure 2.5. Schematic diagram summarising the reagent interactions used in fluorescence immunocytochemistry for two antibodies raised against specific proteins and permanent biocytin visualisation. A, The attachment of fluorescent probes, their excitation and resulting emission of visible light. B, Permanent visualisation of biocytin by the ABC peroxidase technique.

antibodies). All antibody mixtures were made up using ABC peroxidase in PBS as the diluent and incubations were carried out overnight at 4°C on a shaker. ABC solution was chosen as the diluent at this stage in the protocol to label Biocytin filled neurones with HRP for subsequent visualisation as in the standard Biocytin visualisation technique described above. An overnight incubation was required for adequate penetration of ABC into the tissue sections and it did not cause significant interference with the binding of the fluorescent Biocytin marker avidin-AMCA.

2.11.2 Dilutions of primary antibodies for immunofluorescence:

Primary Antibody	Source	Working Dilution
Mouse anti Parvalbumin (clone PA-235)	Sigma	1:1000
Rabbit anti Parvalbumin (R301)	Prof K. Baimbridge	1:1000
Rabbit anti Calbindin (R9501)	Prof K. Baimbridge	1:1000
Rabbit anti Calbindin (R8701)	Prof K. Baimbridge	1:1000
Mouse anti Gastrin/CCK (MAb #9303)	Cure, UCLA	1:3000
Rabbit anti VIP (Ab #698)	DiaSorin	1:250

2.11.3 Secondary Antibody Incubation:

Sections were washed thoroughly in five changes of PBS before incubation in a mixture of fluorescent markers for 2-3 hours. The secondary antibody and fluorescent marker mixture comprised 15µl Avidin-7-Amino-4-methylcoumarin-3-acetic acid (Avidin-AMCA)(1:240), 22.5µl goat anti-mouse fluorescein isothiocyanate (FITC)(1:160) and 6µl goat anti-rabbit Texas Red (TR)(1:600) in 3.6ml of PBS.

2.11.4 Fluorescence microscopy and digital imaging:

Sections were washed thoroughly and mounted using 50% glycerol in PBS onto clean microscope slides. Sections were then studied using a Leica DMR microscope with a mercury vapour light source and filters suitable for the differential visualisation of AMCA (excitation wavelength 345 - 355nm, emission wavelength 448 - 454nm), FITC (excitation wavelength 470 - 490nm, emission wavelength 515 - 550nm), and Texas Red (excitation wavelength 595 - 604nm, emission wavelength 606 - 615nm). After identification of positively AMCA labelled neurones (ie. those cells filled with biocytin), digital images of all three fluorochrome channels were taken at the same focal plane using a JVC 3 CCD colour digital camera at x40 magnification. Images were manipulated and overlaid using Photopaint software (Corel Corporation, Ontario, Canada) to demonstrate any colocalisation of fluorochrome labelling. Sections were then carefully lifted from the slides and incubated in a solution of ABC peroxidase in PBS for at least 1 hour to boost levels of bound HRP, as the free radicals emitted during UV stimulation of the fluorescent probes were suspected to cause bleaching of neurones subjected to the prolonged UV exposures required for digital imaging. Sections were then subjected to peroxidase/DAB staining, osmication, dehydration and resin mounting as described above (see sections 2.10 then 2.9.5 - 2.9.7).

2.12 DOUBLE PEROXIDASE

The immunoperoxidase technique was used to assess the potential intra-cortical connections made by identified pyramidal axons with interneurones expressing Parvalbumin, CCK or VIP. The technique used two separate peroxidase reactions to locate cells labelled with the parvalbumin antibody and biocytin filled pyramidal cell processes. The interactions of reagents is summarised in figure 2.6.

Permeabilised sections were washed in 0.1M PB then incubated in a solution of 1% Hydrogen Peroxide (H_2O_2) for 30 minutes to block endogenous peroxidase activity. After gentle washing in 0.1M PB the sections were incubated in an uncapped vial containing a solution of 1% Sodium Borohydride ($NaBH_4$)(Sigma, St. Louis, USA) in 0.1M PB for 30 minutes to reduce non-specific background staining resulting from aldehyde fixation. Sections were then washed thoroughly in multiple changes of PB and PBS prior to incubation in 10% normal goat serum (NGS) in PBS for 30 minutes.

2.12.1 Antibody dilutions for Immunoperoxidase:

Primary Antibody	Source	Working Dilution
Mouse anti Parvalbumin (clone PA-235)	Sigma	1:10000
Mouse anti Gastrin/CCK (MAb #9303)	Cure, UCLA	1:3000
Rabbit anti VIP (Ab #698)	DiaSorin	1:10000

Antibodies were made up in ABC peroxidase (Vector) and incubated for 12 - 48 hours at 4°C with constant agitation on a shaker to promote adequate penetration of reagents into the tissue.

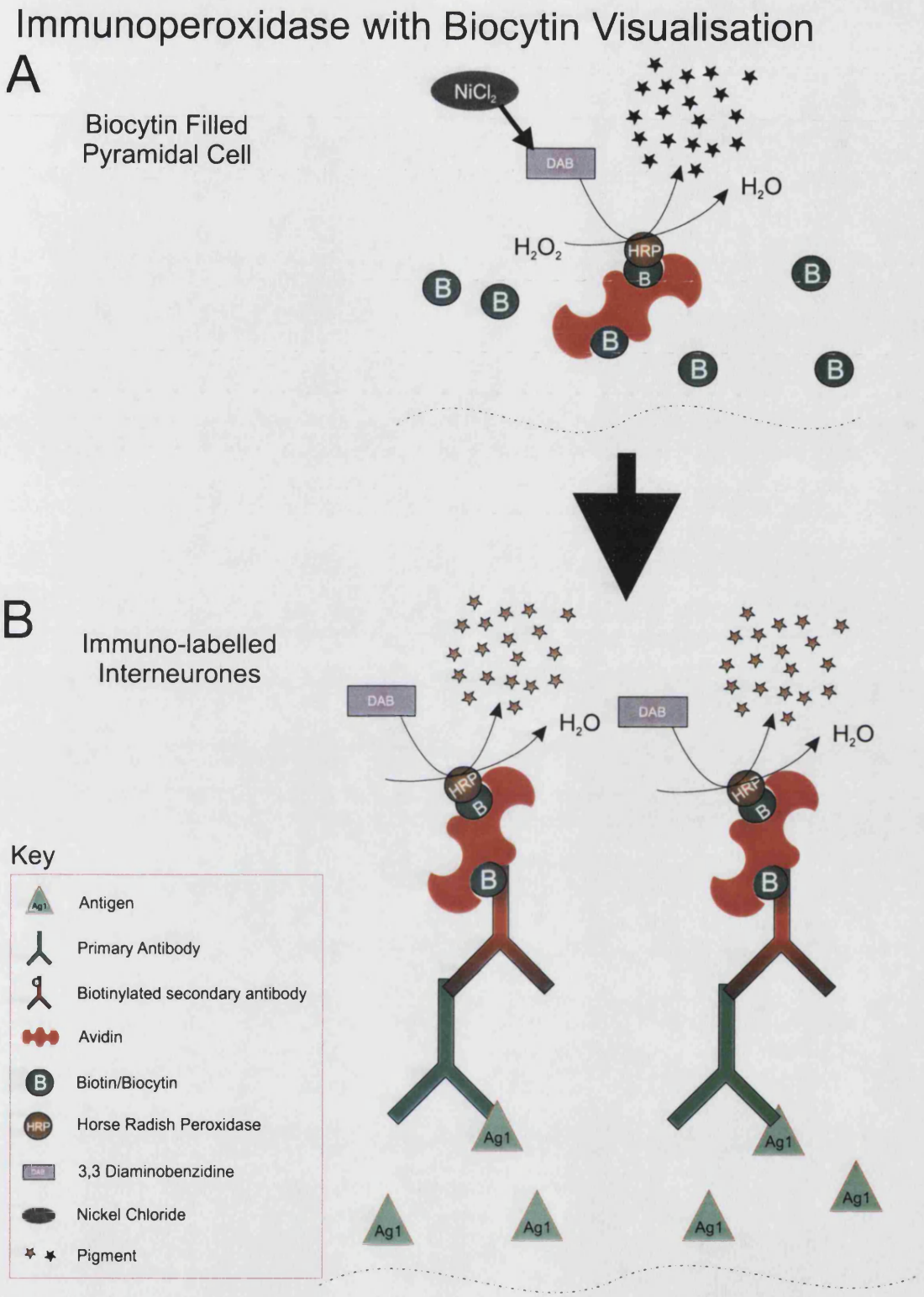

Figure 2.6. Schematic diagram summarising the reagent interactions used for biocytin and immunoperoxidase visualisation. A, Cells filled with biocytin were visualised by the ABC peroxidase technique. B, Immunolabelled neurones were also permanently visualised using the ABC peroxidase reaction but differential staining for the two reactions is achieved by omitting Nickel Chloride from the DAB mixture for the second reaction creating different coloured reaction products for each.

2.12.2 Peroxidase reaction to visualise Biocytin filled neurones:

After washing in PBS and TRIS buffer, sections were incubated in 5ml of DAB with 1 drop of 8% aqueous Nickel Chloride ($NiCl_2$) for 15 minutes. The peroxidase reaction was initiated by the application of 1% Hydrogen Peroxide giving a final concentration of 0.01% H_2O_2 in DAB+$NiCl_2$. The reaction was allowed to proceed for 3-5 minutes or until positively stained neurones were clearly visible with the aid of a stereoscopic dissecting microscope. The reaction was stopped in TRIS buffer and a second incubation in 1% buffered H_2O_2 was performed to block ABC peroxidase activity.

2.12.3 Secondary Antibody incubation:

After thorough washing in PBS, sections were incubated in PBS containing biotinylated secondary antibody raised in goat against the primary antibody species (eg. for mouse anti-Parvalbumin primary antibody the secondary required would be biotinylated goat anti-mouse). The diluted secondary antibody was made up in PBS at 1:500 and incubations were allowed to continue for 12 - 48 hours at 4°C. Sections were then washed in PBS and incubated once more in ABC peroxidase (Vector Laboratories Ltd., Peterborough, UK).

2.12.4 Peroxidase reaction to visualise antibody labelled neurones:

The DAB reaction was performed again as described above with a slight modification in the omission of $NiCl_2$ from the DAB solution. This was done to produce a brown coloured end product to contrast with the blue/black of the previous reaction to allow visual differentiation of filled neurones from those immunopositive for the chosen antibody. The reaction was allowed to proceed on ice and under close observation using a stereoscopic dissecting microscope and stopped in TRIS when positively stained neurones were clearly visible.

Sections were then osmicated, dehydrated, resin impregnated and mounted onto glass microscope slides as described above (see sections 2.9.5 - 2.9.7).

2.13 MICROSCOPY

Tissue sections were viewed using a x100 oil immersion objective on a Leitz DMR microscope (Leica Microsystems, Wetzlar, Germany), equipped with a drawing tube and x10 magnification eyepieces. All dendritic and axonal processes were drawn in fine detail with a total magnification of x1000. The microscopic plane of focus was systematically adjusted to cover the full thickness of the specimen and processes observed exiting the sections were marked, matched up with the adjacent sections and drawings continued to the natural point of termination or the point at which they left the plane of the slice. Where filled axon and filled/immuno-labelled dendrite could not be resolved at the light microscope as separate components, marks were placed on the drawings to represent sites of putative synaptic and/or autaptic contact. Drawings were then carefully traced, photocopied and digitised using an optical scanner prior to manipulation with Corel Photopaint bitmap editing software (Corel Corporation, Ontario, Canada).

3.0 EXPERIMENT SUMMARY.

3.1 General properties of tested neurones.

Rat Experiments: Thirty seven experiments were performed on adult rat neocortical slices. In total 2407 pairs of neurones were recorded and tested for synaptic connections indicated by PSPs in response to evoked presynaptic action potentials. In total 376 neurones were impaled with the first sharp microelectrode, held and tested for connections with 2031 other neurones recorded with a second electrode.

Of the 376 neurones impaled and held with the first electrode 341 were electrophysiologically classified according to their action potential shape/duration, intrinsic firing pattern and the postsynaptic potentials they generated in coupled cells. 312 were predicted or confirmed by the EPSPs they generated to be excitatory cells in layers II to VI. Of those 312, 137 displayed regular spiking (RS) characteristics (1 in Layer II, 6 in Layer III, 93 in Layer IV, 6 in Layer V, 3 in Layer VI and a further 28 in unconfirmed layers). Thirty six cells displayed burst firing (BF) patterns (5 in Layer III, 18 in Layer IV, 7 in Layer V and 6 in unconfirmed layers). Three cells in layer IV would only generate single spikes and 136 were not classified. None of these 312 excitatory cells displayed fast spiking (FS) discharge characteristics.

Twenty nine electrophysiologically characterised neurones were predicted by their FS discharge patterns, or confirmed by the IPSPs they generated to be inhibitory cells, in layers III to VI. One cell displayed a RS firing pattern (Layer IV), 1 cell was BF (Layer IV) and 22 cells exhibited FS characteristics (6 in Layer IV, 1 in Layer V, 1 in Layer VI and 14 from unconfirmed layers). Three inhibitory cells generated only single spikes.

Cat Experiments: Eight experiments were performed on adult cat neocortical slices. In total 464 pairs of neurones were recorded and tested for synaptic connections. Ninety one neurones were impaled with the first sharp microelectrode, held and tested for synaptic connections with 373 other neurones recorded with a second electrode. Of the 91 cells impaled with the first electrode 62 were electrophysiologically classified during the experiments.

Of the 62 neurones classified 51 were predicted by the shape of their action potentials and intrinsic firing patterns or confirmed by the EPSPs they generated to be excitatory cells from layers 3 to 5. Forty nine excitatory neurones displayed RS firing characteristics (9 in layer 3 and 40 in layer 4). Two cells in layer 4 would only generate single action potentials and none of the excitatory neurones tested displayed BF or FS firing patterns.

Eleven electrophysiologically characterised neurones were confirmed as inhibitory cells from layers 3 and 4. Two inhibitory neurones from layer 4 exhibited RS firing characteristics, 5 showed the FS pattern (1 in layer 3 and 4 in layer 4). Four cells in layer 4 would only generate single action potentials. None of the inhibitory neurones tested was BF or IS.

3.2 Connections and Hit rates:

The simultaneous recording of pairs of neurones and testing for synaptic connection in both directions allowed estimation of the level of connectivity (hit rate) between broadly classified neurones in different layers for each species.

Rat: From a total of 2407 pairs of neurones recorded, 53 were synaptically connected giving a general average hit rate for the experiment series of 1 connection for every 45 tests. Of these, 47 were excitatory connections of which 41 were to other excitatory cells and 6 were to inhibitory cells. Six inhibitory connections to excitatory cells were seen. The number of individual layer to layer tests and the hit rates for positively identified synaptically connected pairs in rat cortex are summarized in figure 3.1.

Cat: From a total of 464 pairs of neurones tested for synaptic connections, 36 generated PSPs giving a general average hit rate for the series of experiments of 1 connection observed for every 13 tests. Twenty six excitatory connections were seen of which 21 were with other excitatory cells and 5 with inhibitory neurones. Ten inhibitory connections were seen with excitatory neurones. No inhibitory to inhibitory neurone connections were observed from 11 tests. Figure 3.2 summarises the number of layer to layer tests performed and the hit rates for synaptically connected pairs.

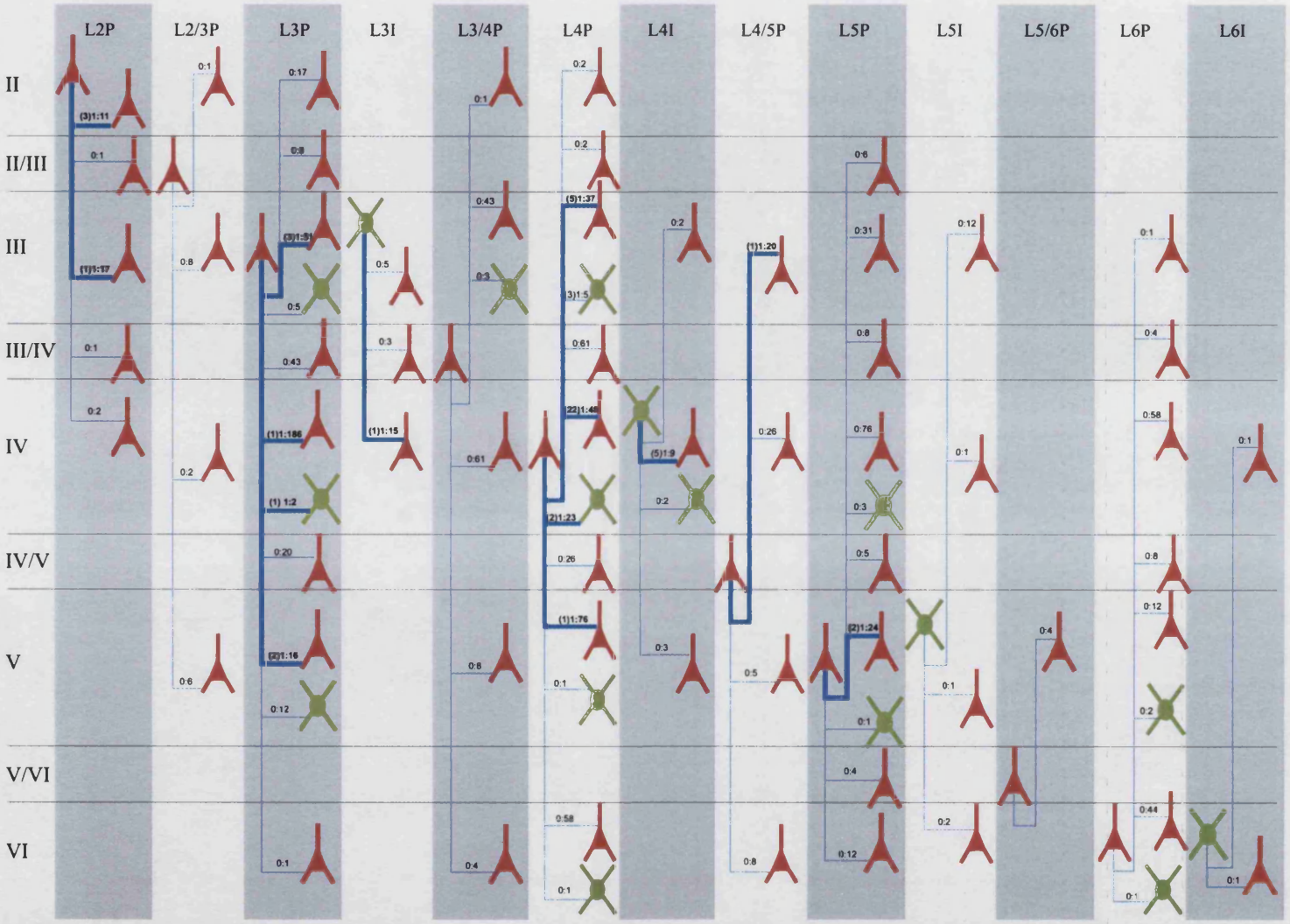

Figure 3.1. Diagrammatic representation of connectivity tests achieved in the different layers of rat neocortex. The blue lines represent the connections tested and bold blue lines indicate positively identified connections. Excitatory cells are represented in red and inhibitory cells in green. The hit rate is expressed as a ratio and the actual number of recorded pairs is in parenthesis.

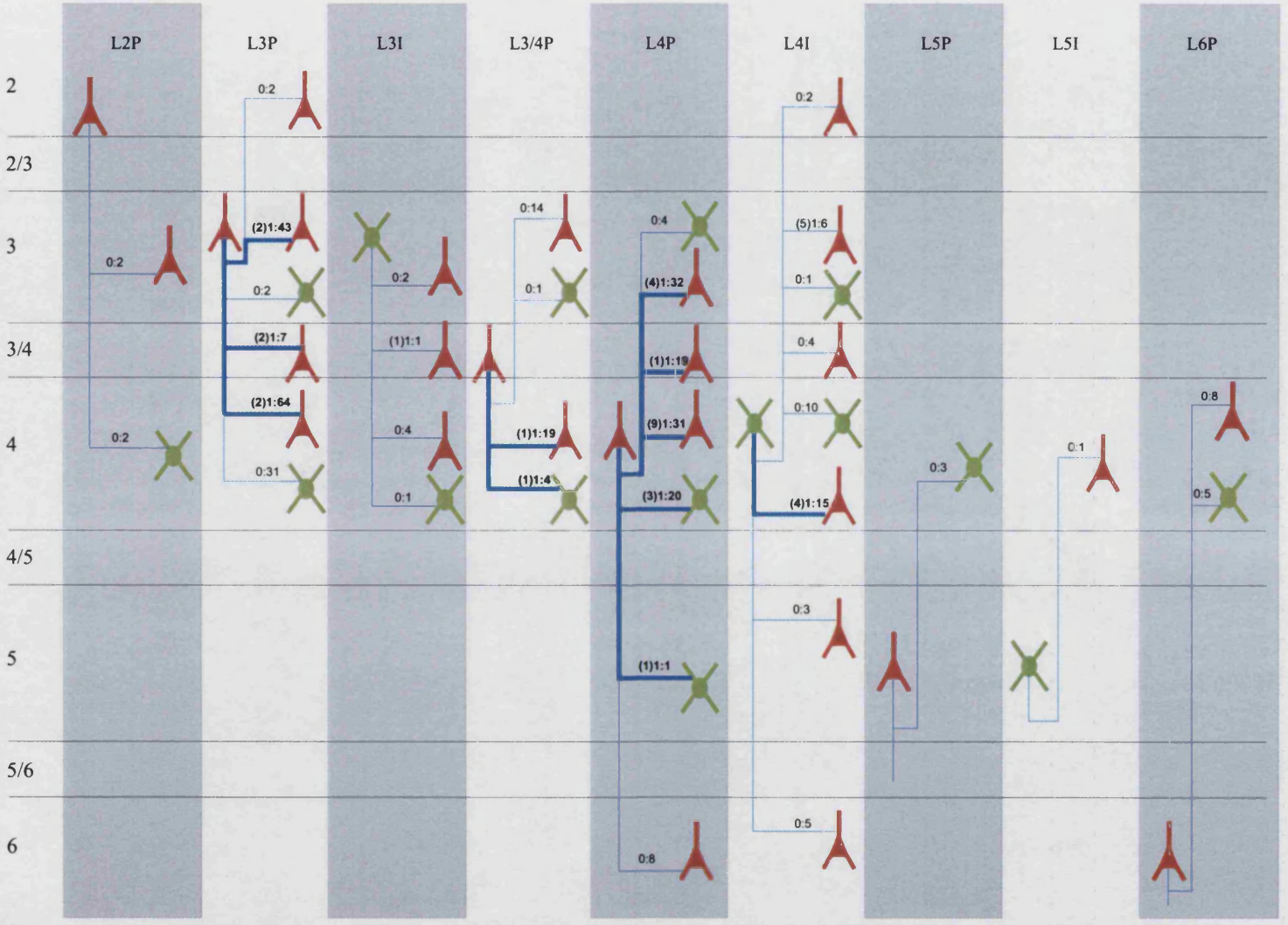

Figure 3.2. Diagrammatic representation of connectivity tests achieved in the different layers of cat neocortex. The blue lines represent the connections tested and bold blue lines indicate positively identified connections. Excitatory cells are represented in red and inhibitory cells in green. The hit rate is expressed as a ratio and the actual number of recorded pairs is in parenthesis.

3.3 Histologically recovered Neurones.

Slices were cut in the interface chamber to select regions containing filled neurones that were processed histologically according to the procedures described in section 2 to reveal cell morphology and to confirm the layer of origin. A total of 57 rat and 14 cat slices were processed from which 275 rat and 63 cat neurones were successfully stained. Fifty one rat and 38 cat cells that were pre- or post-synaptically connected were suitable for morphological reconstruction.

Rat: Ten cells were recovered from layer II (9 pyramids and 1 interneurone), 51 from layer III (50 pyramids, 1 interneurone), 127 from layer IV (118 pyramids (3 star pyramids), 2 spiny stellates, 7 interneurones), 76 from layer V (74 pyramids, 2 interneurones), and 11 from layer VI (9 pyramids, 2 interneurones).

Of the synaptically connected cells 2 pyramidal cells were recovered from layer II, 12 pyramids from layer III, 31 pyramids and 3 interneurones were recovered form layer IV and 3 pyramids from layer V.

Cat: One pyramidal cell was recovered from layer 2, 18 cells from layer 3 (17 pyramids, 1 interneurone), 44 from layer 4 (38 pyramids (7 star pyramids) and 6 interneurones).

Of the synaptically connected neurones from cat slices 12 pyramidal cells and 1 interneurone were recovered from layer 3, 20 pyramidal cells and 5 interneurones were recovered from layer 4.

4.0 THE EXCITATORY CONNECTIONS BETWEEN PYRAMIDAL CELLS IN LAYER 4.

Paired intracellular recordings with biocytin filling of pyramidal cells was performed to investigate synaptic connectivity within layer 4 of adult cat and rat primary visual and somatosensory cortex. Visualisation of connected pairs was performed to compare the neurones of both species, putatively identify the targets of synaptic connections and to attempt to identify any differences in the patterns or probability of connections between electrophysiologically and morphologically classified neurones. Analysis of electrophysiological recordings was performed to compare the EPSP properties between the species and to identify paired pulse and frequency dependent properties employed at their synaptic connections.

4.1 Probability of synaptic connection between excitatory cells in layer 4.

In 45 experiments using both rat and cat cortical slices 799 paired intracellular recordings were made where both cells' somata were within layer 4. All pairs of neurones were tested in both directions for synaptic connections identified by postsynaptic voltage responses to spikes induced in the presynaptic cells by square wave and/or ramped current pulse injections. A total of 32 layer 4 cells (confirmed by light microscopy of stained pairs) generated excitatory postsynaptic potentials (EPSPs) in other excitatory neurones of the same layer (10 in cat and 22 in rat slices). The probability of finding synaptically connected pairs of excitatory cells in layer 4 was 1 in 31 for cat and 1in 48 for rat material. In cat cortex, 4 of the 10 connections found were from 2 reciprocally connected pairs of neurones with both cells of each pair generating EPSPs in the other. One pair of reciprocally connected layer 4 excitatory cells was observed in a rat slice.

4.2 General Electrophysiological Properties of Layer 4 Pyramidal Cells.

Layer 4 pyramidal cells of both species typically exhibited one of two main firing characteristics, 63% were regular spiking (RS) and the remaining 37% were burst firing (BF). A population (62%) of RS cells sampled in this study showed rapid spike frequency adaptation to zero within the first 50ms of a 500ms pulse and as such can be classified further as the phasic type RS-2 cells. The BF cells typically produced short bursts of 3-5 action potentials followed by single spikes that progressively slowed in frequency as is seen in the RS cells. Intrinsically bursting (IB) cells similar to those described in layer 5 (Connors *et al.*, 1982;McCormick *et al.*, 1985) were rarely seen in layer 4. Typical examples of layer 4 pyramidal firing characteristics observed in both cat and rat are given in figure 4.1.

4.3 General Morphology of Layer 4 Pyramidal Cells.

A total of twenty layer 4 pyramidal cells from all studies were reconstructed in their entirety from both cat and rat cortical slices. All fitted the general patterns of pyramidal cell anatomy described earlier (section 1.3.1).

Cell somata and the most proximal portions of between 4 and 7 primary dendrites were smooth and aspiny. From 5-20μm from the cell body to the dendritic extremities all were spiny. Basal dendrites bifurcated up to 7 times to terminate with between 11 and 33 last order branches. Apical dendrites extended towards and perpendicular to the pial surface and terminated in layers 1 or 2 producing between 2 and 10 oblique branches en route to the superficial layers. All but one rat pyramidal apical dendrite bifurcated at least once in the most superficial layer reached to form an apical tuft. No spiny stellate cells that were demonstrably connected to other layer 4 excitatory cells were recovered in this study. No obvious differences in dendritic morphology were observed between layer 4 cells involved in connections with other layer 4 cells compared with those contacting cells in other layers.

The axons originated from an initial segment situated at the base of all pyramidal cell bodies from where a partially myelinated primary axon projected towards the white matter. At nodes

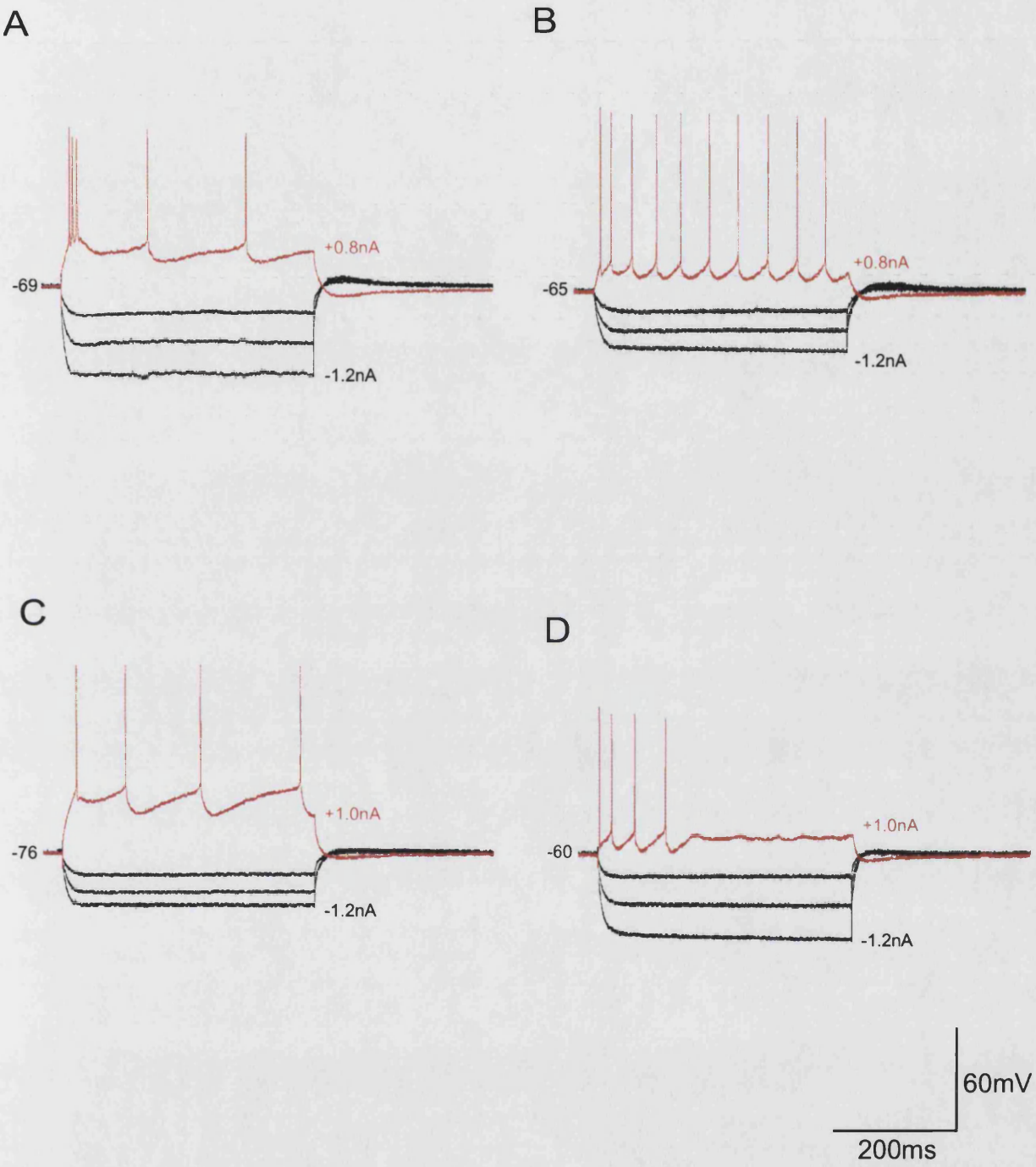

Figure 4.1. Typical firing patterns exhibited by layer 4 pyramidal neurones in both cat and rat material. All examples given here are from rat cortex. Responses to depolarising current pulses are in red and hyperpolarising pulses in black. A, Burst firing pattern most typical in layer 4 with an initial burst of action potentials followed by single spikes. The intrinsically bursting (IB) firing pattern was most typically found in layer 5 and only very rarely in layer 4, so is not illustrated. B and C, Regular spiking (RS) with different rates of spike frequency adaptation. D, RS-2 phasic firing pattern. Only cells of types RS and RS-2 were found to be presynaptic in layer 4 pyramid to pyramid or pyramid to interneurone connections in this study whereas both RS and BF pyramidal cells were seen to make connections to and from the neighbouring layers.

between myelinated portions, axon collaterals projected horizontally or at oblique angles towards the superficial layers. No axonal profiles were seen to project further into the superficial layers than the cells' apical dendrite and indeed where large quantities of axon were reconstructable the majority terminated within a column of a radius comparable with 1 or occasionally 2 times the span of basal dendrites with processes reaching into layer 3 and rarely into layer 2. A minority of long horizontal axonal processes extending laterally up to 750μm were observed in 2 reconstructed axons and in non-reconstructed neurones from both species.

Despite the increased depth of cat neocortex relative to that of rat, no significant difference in the average size of drawn pyramidal neurones was observed between the species though the cat cells sampled did have a greater range of both vertical and horizontal dendritic spans. Eight cat layer 4 pyramidal cells had an average soma diameter of 15.7μm (SD=5.1), average horizontal dendritic span parallel with the pial surface of 305μm (SD=70), vertical span perpendicular to the pial surface 616μm (SD=174). Twelve rat layer 4 pyramids had an average soma diameter of 14.9μm (SD=5.1), horizontal dendritic span of 307μm (SD=49) and vertical span of 658μm (SD=80). See figure 4.2 for a comparison of typical layer 4 pyramidal cells from both species.

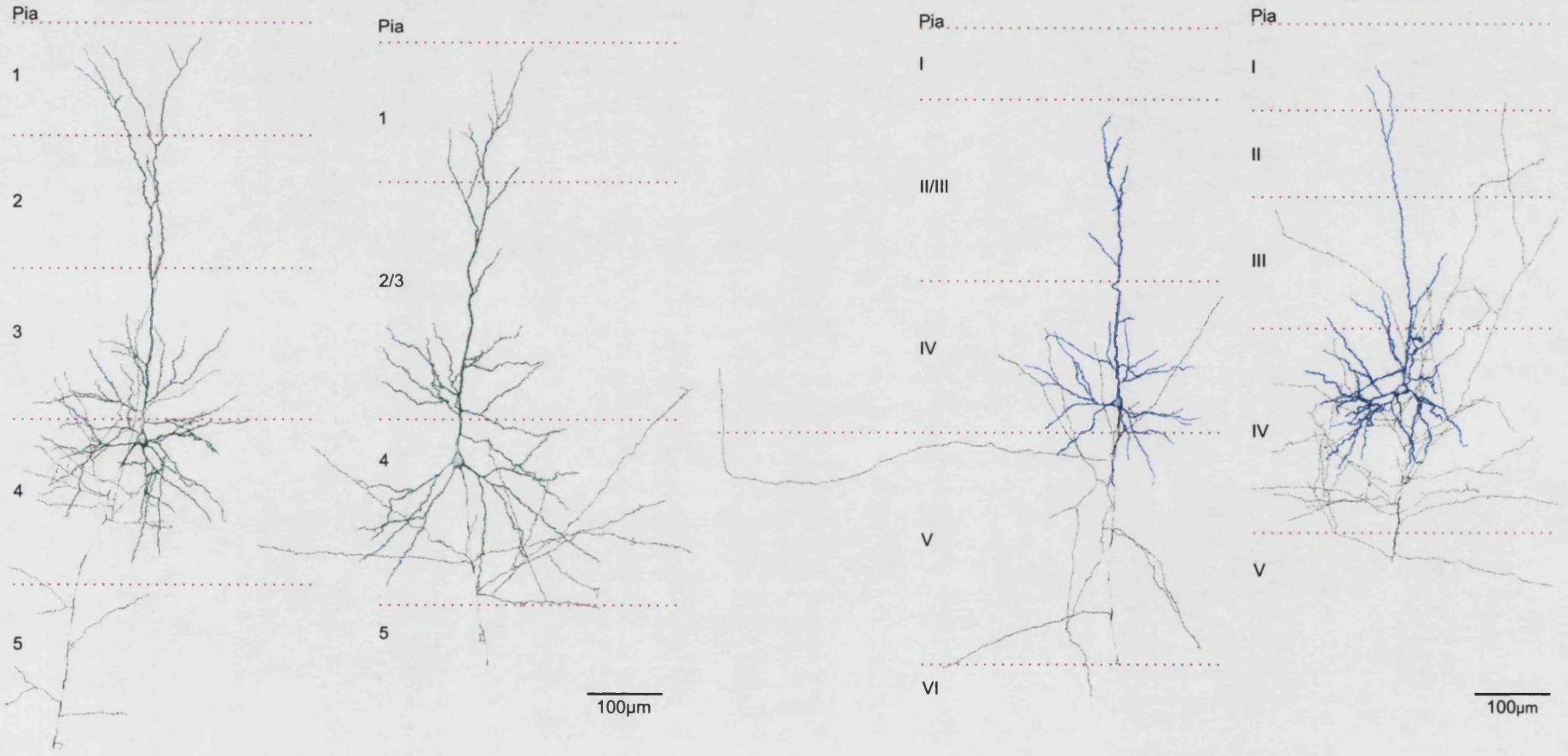

Figure 4.2. Typical dendritic and axonal morphology of pyramidal cells in layer 4 of adult cat and rat neocortex. The somata and dendritic arbours of cat cells (green) and axon (black), rat cells somata and dendrites (dark blue) and axons (black) reconstructed at x1000. All have RS discharge characteristics and all are displayed at the same scale. Note that many layer 4 pyramidal cells may project long lateral axonal collaterals as seen in the 3rd cell but these may frequently be cut during the slicing process.

4.4 Electrophysiological and Morphological Characteristics of Synaptically Connected Pairs of Layer 4 Pyramidal Cells.

4.4.1 Spike discharge characteristics.

All of the layer 4 excitatory cells tested for connections with other cells in layer 4 had either RS or BF spike discharge characteristics. Interestingly, in all cases where synaptic connections between layer 4 cells were identified from both species all of the presynaptic cells were RS. None of 240 tests involving BF Layer 4 pyramidal cells in rat resulted in a synaptic connection though layer 4 cells involved in connections with other layers (recorded throughout the same series of experiments) exhibited either RS or BF discharge patterns. In addition, where the spike discharge properties of postsynaptic layer 4 pyramids from both species were identified, they were also RS. These data suggest that (in rat at least) the probability of synaptic connections involving the BF cells within layer 4 is very low and that they may be involved in connections with the other layers.

4.4.2 Morphology, putative sites of synaptic contact and general EPSP properties.

Figure 4.3 illustrates a reciprocally connected pair of cat pyramidal cells. Both cells were situated in superficial layer 4 and had similar dendritic radiations spanning the entire depth of layer 4 and extending basal dendritic and apical oblique branches into layer 3. The basal dendritic lateral span was 295 and 355μm and both had apical bifurcations that began in layer 2 to produce tufts that spanned 170 and 275μm respectively in layer 1. Both cells had partially myelinated primary axonal trunks passing down though layer 4 to layer 5 from which the most dense branching of unmyelinated axon laden with small synaptic boutons was found in layer 4. The smaller of the two cells (illustrated in red) made 7 putative synaptic contacts with the spiny dendrites of the other cell and generated large EPSPs (mean 1st amplitude 3.23mV) in the other cell. This cell also made 3 potential autapses with its own dendrites. One putative contact was found from the larger of the two presynaptic cells (black) and generated smaller (0.92mV) EPSPs in the other. The EPSPs generated in both cells exhibited paired pulse depression.

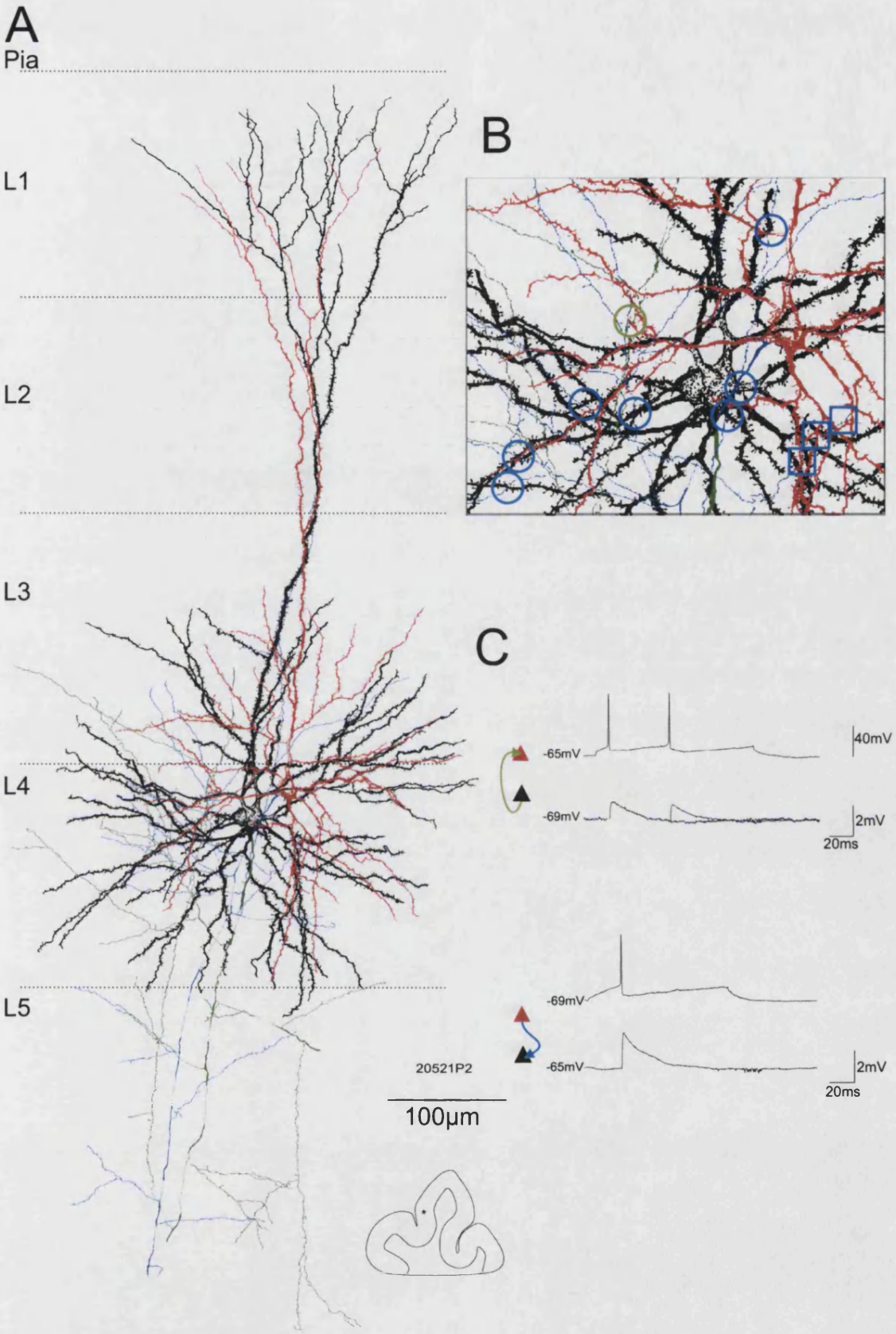

Figure 4.3a. Morphology of a reciprocal cat layer 4 to layer 4 pyramid - pyramid pair (20521p2a/b). A, The upper cell dendrites (red) and axon (blue) and lower cell dendrites (black) and axon (green) reconstructed at x1000. The dendrites of both cells were spiny, both had partially myelinated primary axons from which collaterals ramified in layers 4 and 5. Both cells have axon extending into layer 3. B, An enlarged portion of A indicating the locations of 7 axo-dendritic close appositions from the red cell to the black cell in blue circles and 3 potential autapses onto itself in blue squares. One axo-dendritic apposition from the black cell to the red cell is indicated by a green circle. C, Example of presynaptic spikes and corresponding average EPSPs in both directions.

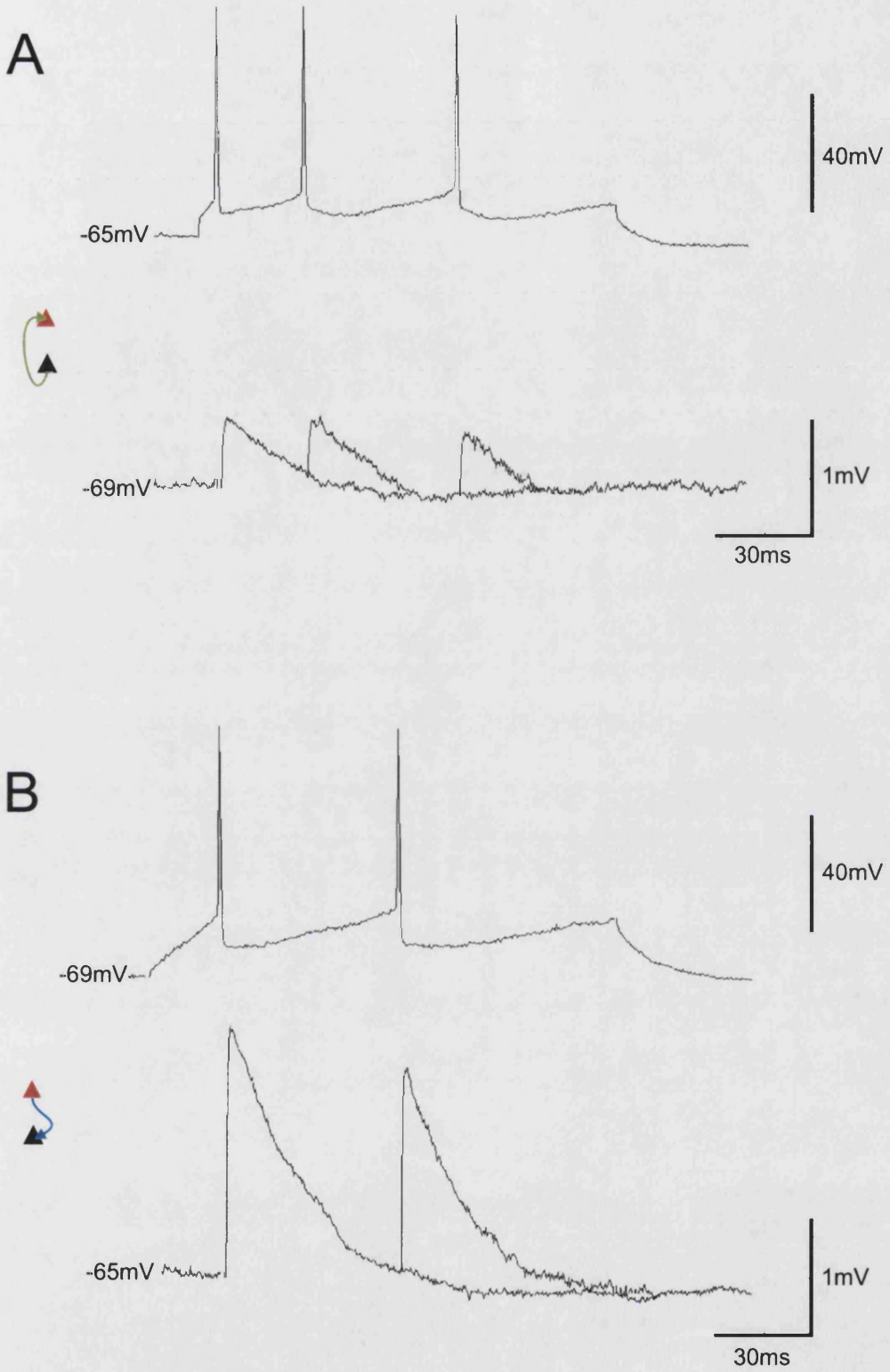

Figure 4.3b. (20521p2a/b) Averaged EPSPs of the reciprocally connected cat layer 4 to layer 4 pyramid pair illustrated in figure 4.3a. A, Averaged 1st EPSP and 2nd and 3rd EPSPs at interspike intervals 25 and 36±1ms respectively. 1st, 2nd and 3rd EPSP averages were made from 57, 16 and 26 sweeps respectively and show depression of EPSP amplitude in response to each spike in the trains. B, Averaged 1st (23 sweeps) and 2nd (14 sweeps) at 51 ±2ms for the reverse connection again showing depression. These cells were contacted by an unidentified interneurone generating spontaneous IPSPs in both that were also disynaptically driven by the red pyramidal cell. These connections will be described in section 5.

Figure 4.4 illustrates a large superficial layer 4 pyramidal cell from cat cortex that received two unidirectional, depressing connections of different amplitudes (3.06 and 1.83mV respectively) but with very similar timecourses, from two other layer 4 pyramidal cells. One of the two presynaptic cells generated large (3.06mV) EPSPs in the postsynaptic cell (see figure 4.4b) that showed unusual patterns of total synaptic transmission failure that may be due to branch point failure of action potential propagation (see section 4.9 and figure 4.12), but was not adequately filled with biocytin for reconstruction. The other presynaptic cell soma was situated deep within layer 4 and had fine dendrites. The basal arbour was confined mostly to layer 4 with a few non-branching dendrites reaching into superficial layer 5. Apical oblique dendrites were produced in layer 4, 3 of which reached into deep layer 3. This cell had a poorly developed apical tuft beginning in layer 2 and terminating with two dendrites in layer 1. The main axon trunk was partially myelinated with unmyelinated branches in layer 4 but was not well stained and no close membrane appositions with the postsynaptic cell were observed. The postsynaptic cell was situated close to the layer 3 border and had basal dendrites confined largely to layer 4, apical oblique dendrites projecting in layer 3 and reaching into layer 2 and a well developed apical tuft spanning 240μm in layer 1. The primary axon of the postsynaptic cell was also partially myelinated, branched most densely in layer 4 and made 3 potential autaptic contacts with 2 basal dendrites in layer 4 and one apical oblique dendrite in layer 3.

The pre- and post-synaptic layer IV pyramidal cells from rat cortex shown in figure 4.5 had very similar dendritic and axonal arbourisations. The basal dendrites of both were entirely confined to layer 4 with a maximal lateral span of 373 and 380μm respectively, produced few apical oblique dendrites and neither had a tuft in layer I, instead terminating within layer II. Both cells had partially myelinated primary axon trunks that projected into layer VI and had bouton laden branches within layers IV, V and one innervated layer VI. Both cells had long lateral branches and neither had any close axonal membrane appositions with their own dendrites. The presynaptic cell was the most superficial and made 5 putative synaptic contacts onto the basal dendrites of the postsynaptic cell within layer IV. The average 1st EPSP was 2.06mV in amplitude and 2nd EPSPs exhibited paired pulse depression.

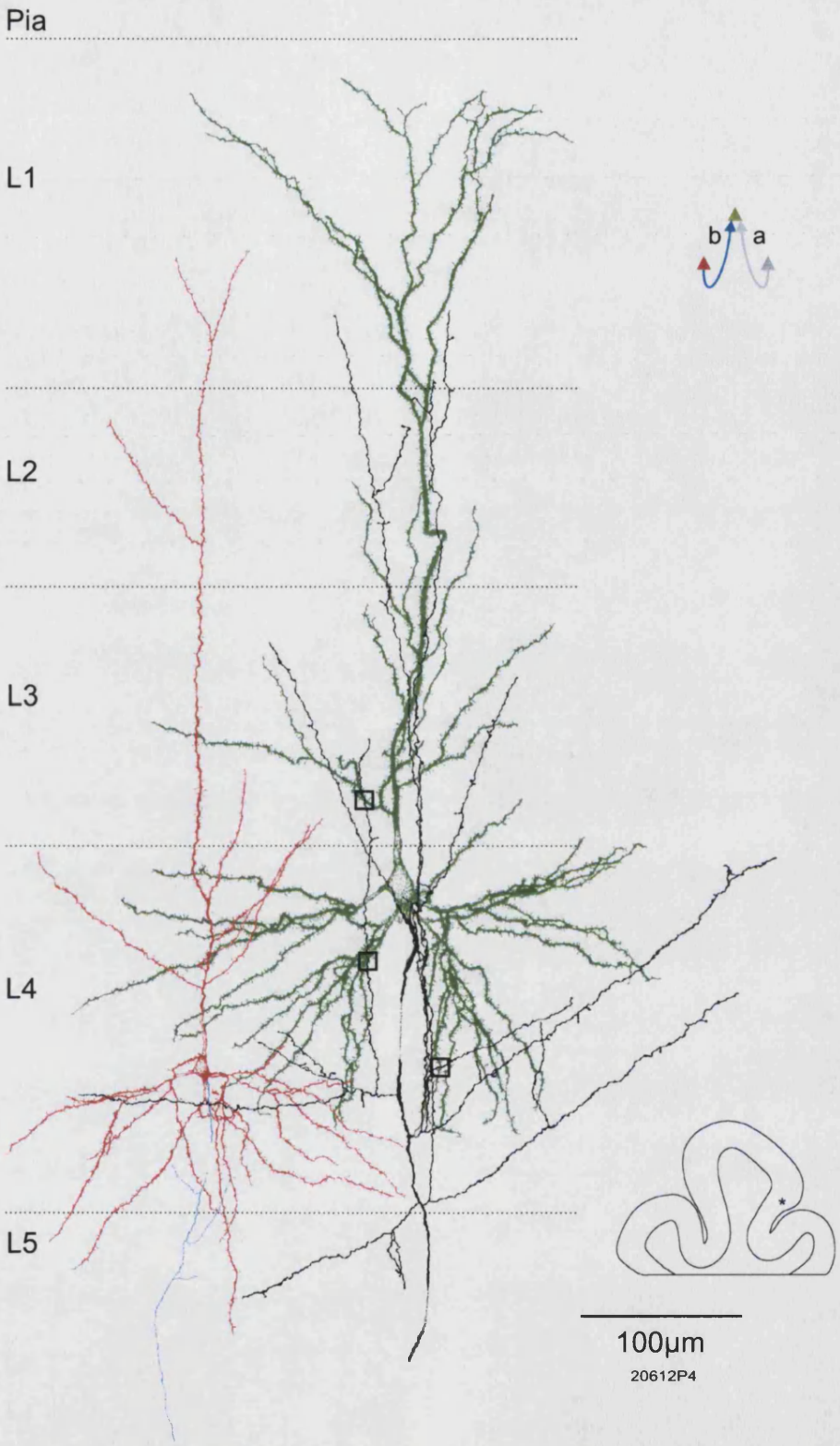

Figure 4.4a. Morphology of a cat layer 4 to layer 4 pyramid - pyramid pair (20612p4). The presynaptic cell dendrites (red) and axon (blue) and postsynaptic dendrites (green) and axon (black) are reconstructed at x1000. The dendrites of both cells were spiny. The green cell was situated close to the layer 3 border and the dendrites show characteristics of layer 3 pyramids whilst its axonal arbour, being most dense in layer 4 is more typical of layer 4 pyramids. No putative synaptic appositions were apparent as the presynaptic axon was poorly labelled histologically. Three potential autapses on the postsynaptic cell are marked by black squares. The green cell was also postsynaptic to another pyramidal cell, also in layer IV that was not sufficiently stained for reconstruction.

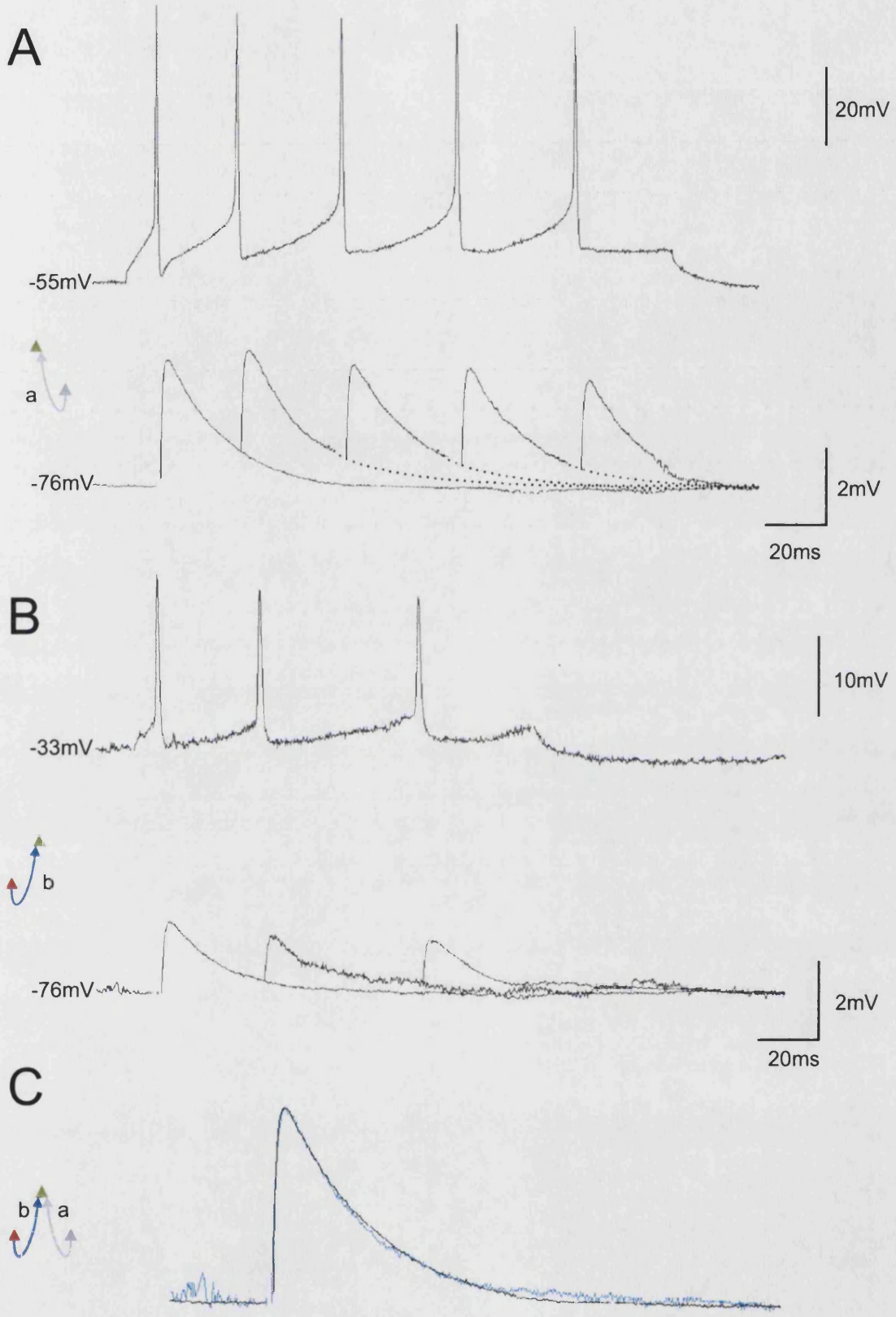

Figure 4.4b. (20612p4a/b) Averaged EPSPs for 2 excitatory connections from layer 4 cells to the same postsynaptic pyramidal cell in layer 4 of cat cortex. A, Averaged 1st to 5th EPSPs (21 sweeps each) from consecutive sweeps at near consistent interspike intervals. B, 1st, 2nd and 3rd EPSPs averages (50, 8 and 12 sweeps respectively) for the connection illustrated in figure 4.4a The 2nd EPSP is 33 ±2ms from the 1st and the 3rd is 54 ±3ms from the 2nd. Both EPSPs exhibit depression of average amplitude within trains. C, The average 1st EPSPs from both connections superimposed, scaled to match and enlarged to illustrate the similar time courses of both EPSPs in the postsynaptic cell.

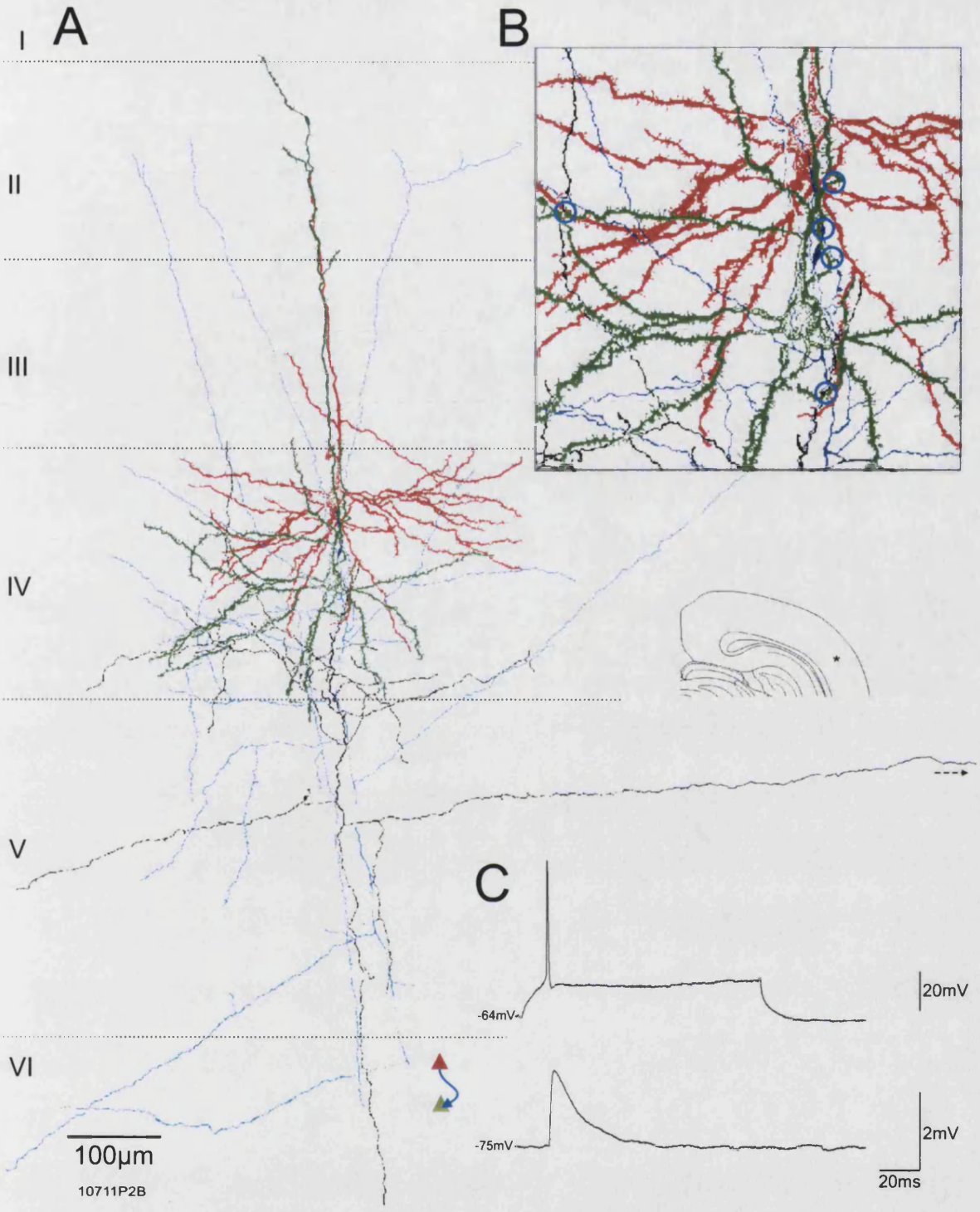

Figure 4.5a. Morphology of a rat layer IV to layer IV pyramid - pyramid pair (10711p2b). A, The presynaptic cell dendrites (red) and axon (blue) and postsynaptic dendrites (green) and axon (black) reconstructed at x1000. The dendrites of both cells were spiny, both had partially myelinated primary axons from which collaterals ramified most densely in layer IV. The postsynaptic cell has a long lateral axonal projection within layer V. The presynaptic cell has sparse projections into deep layer II. Both cells have axon extending into layer VI but neither was seen to exit cortex via the white matter. B, an enlarged portion of A indicating the locations of 5 axo-dendritic close appositions in blue circles. C, example of a presynaptic spike and corresponding average first EPSP.

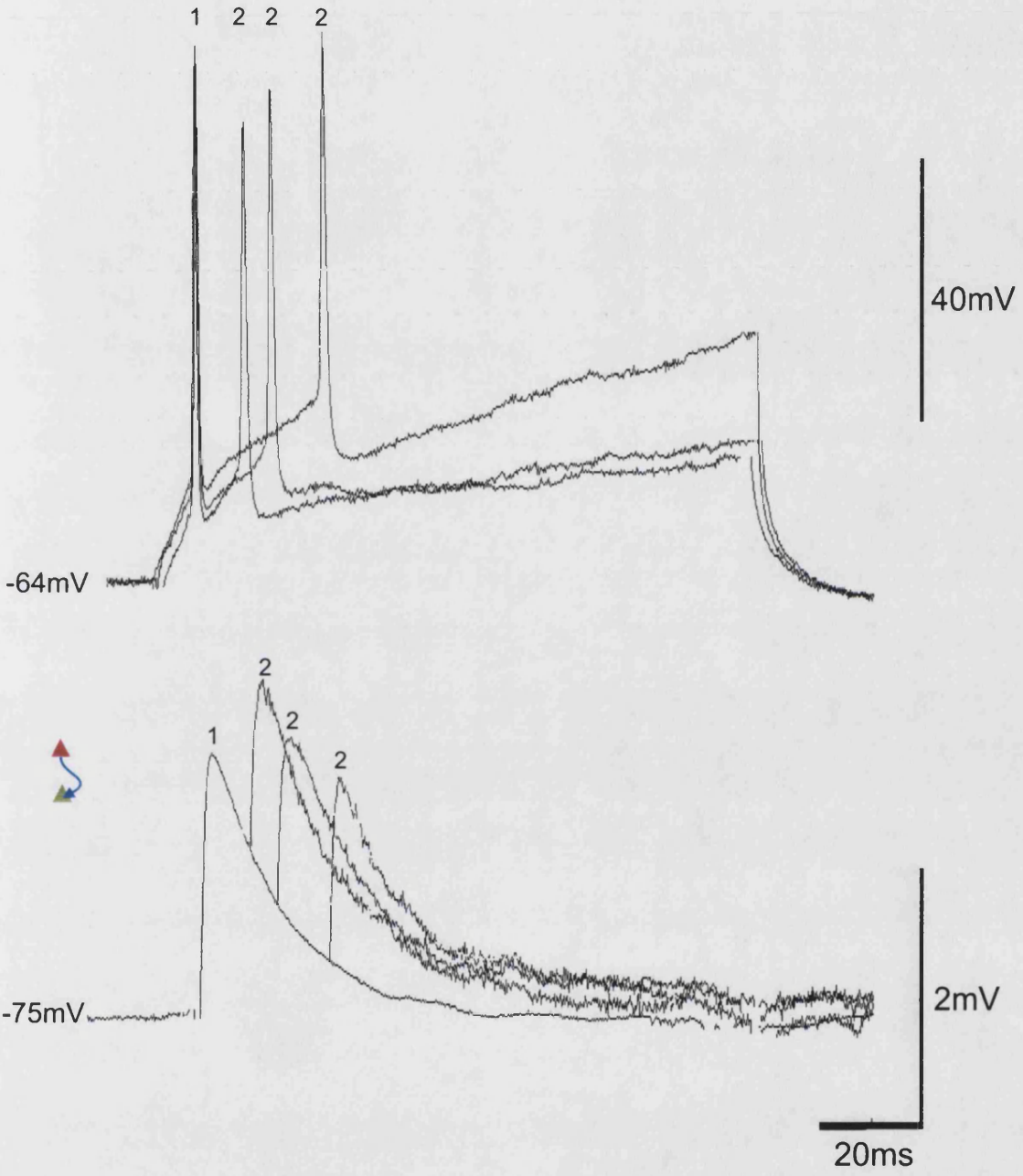

Figure 4.5b. (10711p2b) Average 1st EPSP amplitude (216 sweeps) and averaged 2nd EPSP amplitude at 10, 15 and 25 ±1.5ms interspike intervals (12, 25 and 9 sweeps respectively) from the layer IV to layer IV pyramid - pyramid connection in rat neocortex illustrated in figure 4.5a. 2nd EPSPs are depressed in amplitude relative to the mean 1st EPSP.

Figure 4.6 illustrates a unidirectional connection between two deep layer IV pyramidal cells from rat. The presynaptic cell was situated close to the border with layer V and into which it extended the majority of its basal dendrites. The apical dendrite was slender, produced few oblique branches in deep layer IV and terminated after a single bifurcation in layer III. The postsynaptic cell had a dense dendritic arbour in layer IV, some of which extended without branching into layer V. The apical dendrite produced numerous oblique branches through layer IV and branched in layers III, II and I to terminate with a wide tuft in layer II and I spanning 386µm. Both the pre- and post-synaptic cells had similar maximal basal dendritic spans of 393 and 406µm respectively. The primary axons of both cells were partially myelinated and ramified most densely in the 200µm below their cell bodies in layer V. Two putative synaptic contacts were observed. The average 1st EPSP was 1.67mV in amplitude, exhibited paired pulse, frequency dependent depression and demonstrable post-tetanic potentiation (see section 4.10 and figure 4.13)

A superficial layer IV pyramid to pyramid connection is shown in figure 4.7. The presynaptic cell soma was located close to the border of layer III. The basal dendrites spanned 287µm in layer IV and extended into (but did not branch within) layer III. Three apical oblique dendrites terminated in layer III and a small apical tuft terminated in layer I. The primary axon was partially myelinated and projected down into layer V before exiting the slice. Axonal collateral branches were poorly stained so no axo-dendritic appositions were observed. The postsynaptic cells' basal dendrites were confined entirely within layer IV and three of five apical oblique branches originating from layer IV terminated in deep layer III. A small apical tuft was situated in layer I. The mean 1st EPSP amplitude was 0.55mV and subsequent EPSPs in trains exhibited powerful paired pulse depression that recovered slowly at increasing interspike intervals.

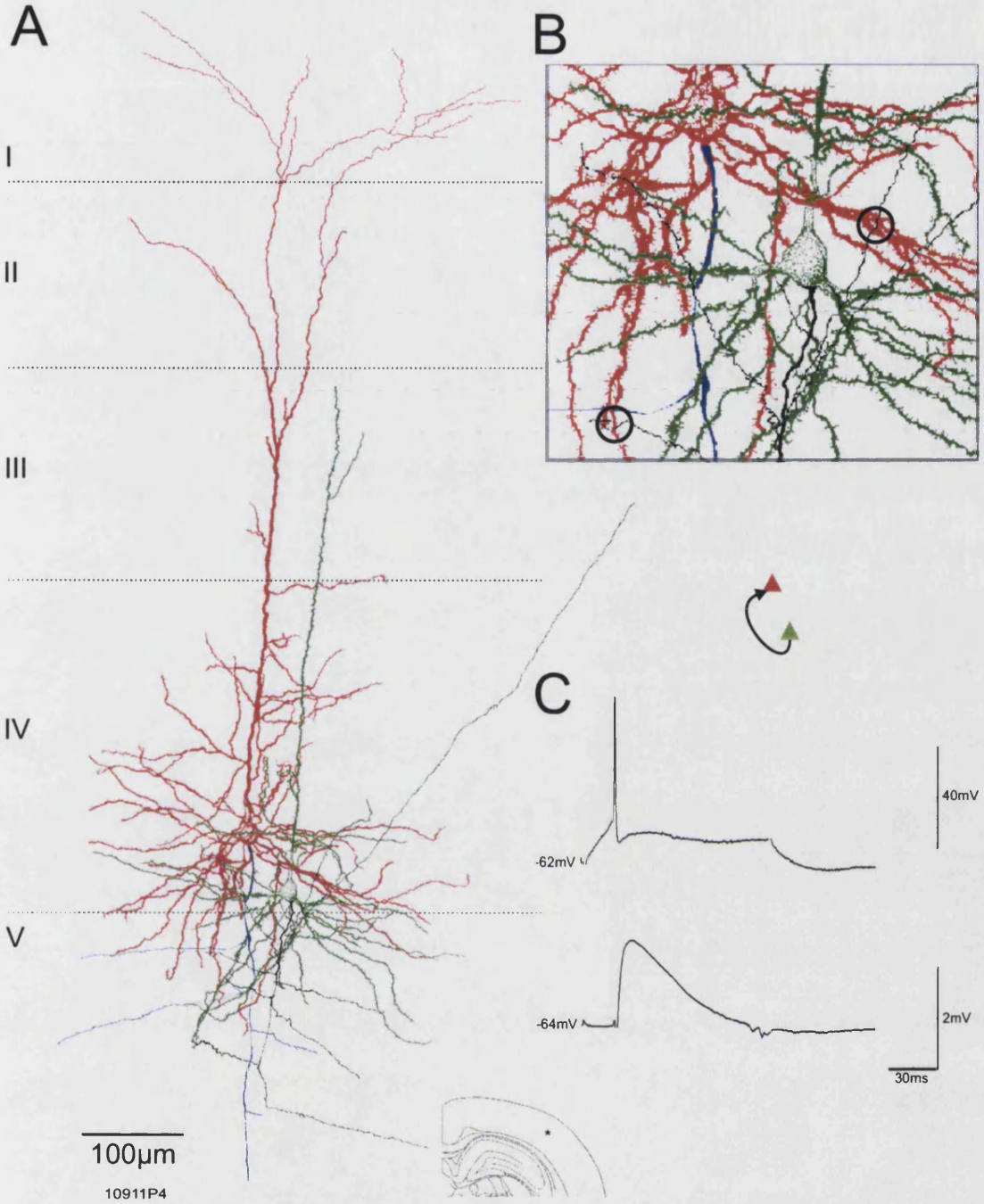

Figure 4.6a. Morphology of a deep layer IV to layer IV pyramid - pyramid pair from rat cortex (10911p4). A, The presynaptic cell dendrites (green) and axon (black) and postsynaptic dendrites (red) and axon (blue) reconstructed at x1000. The dendrites of both cells were spiny. The axons of both cells ramify most extensively in layer V and the presynaptic cell extends one branch into layer III. Neither axon was seen to reach white matter. B, An enlarged portion of figure A with 2 axo-dendritic appositions highlighted by black circles. C, An example of a presynaptic spike and corresponding average first EPSP.

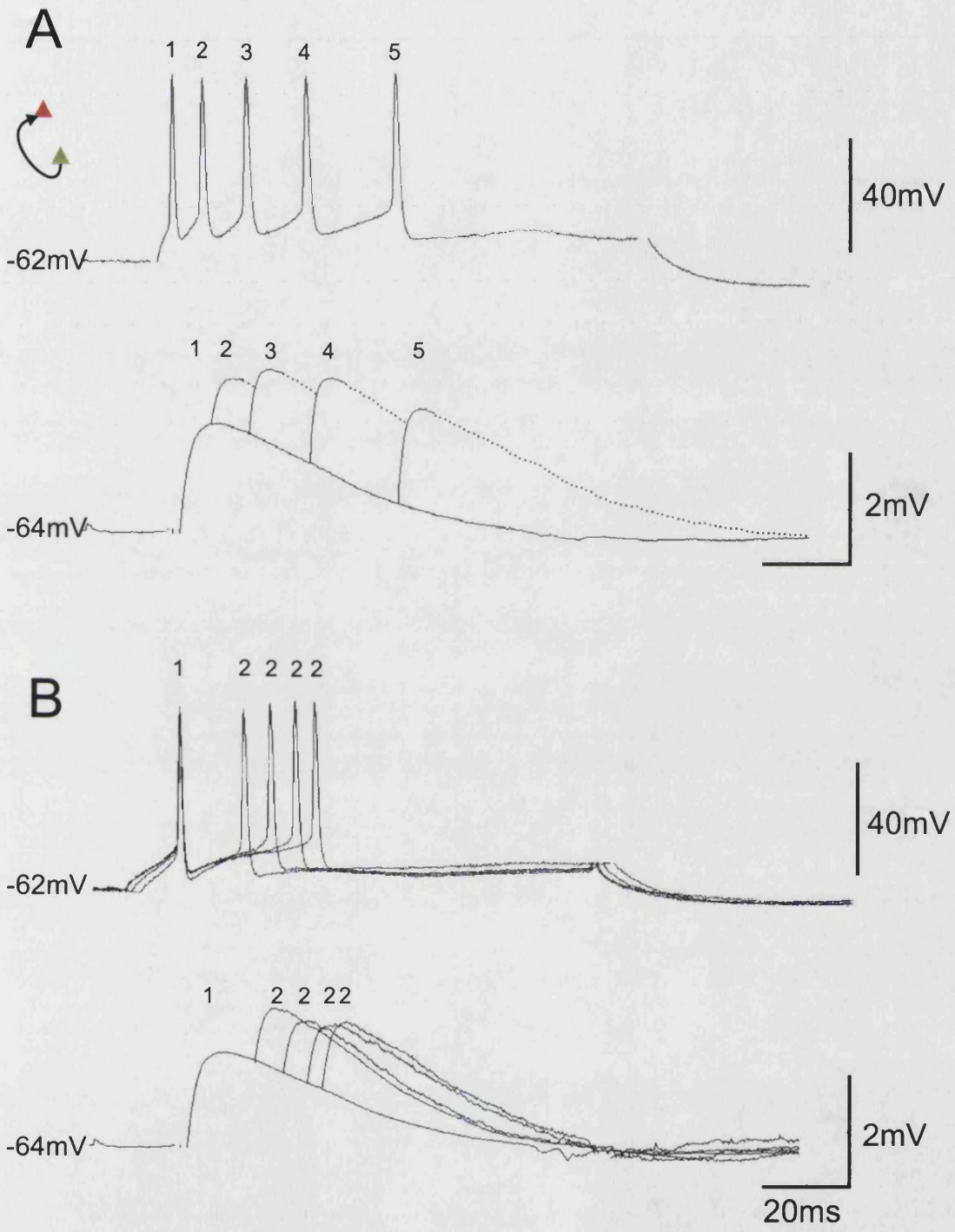

Figure 4.6b. (10911p4) EPSP properties for the rat layer IV to layer IV pyramid - pyramid connection illustrated in figure 4.6a. A, Depression of average EPSP amplitude generated by trains of 5 action potentials. Averages were made from 64 consecutive sweeps with a consistent firing pattern. B, Depression of averaged second EPSPs at a range of interspike intervals. Each average was made from >20 sweeps triggered by the rising phase of the second spike 15, 21, 27 and 31.5 ±1ms from the first. Note that due to post tetanic potentiation at this connection (see section 4.10) the average 1st EPSPs in figures A and B are different sizes.

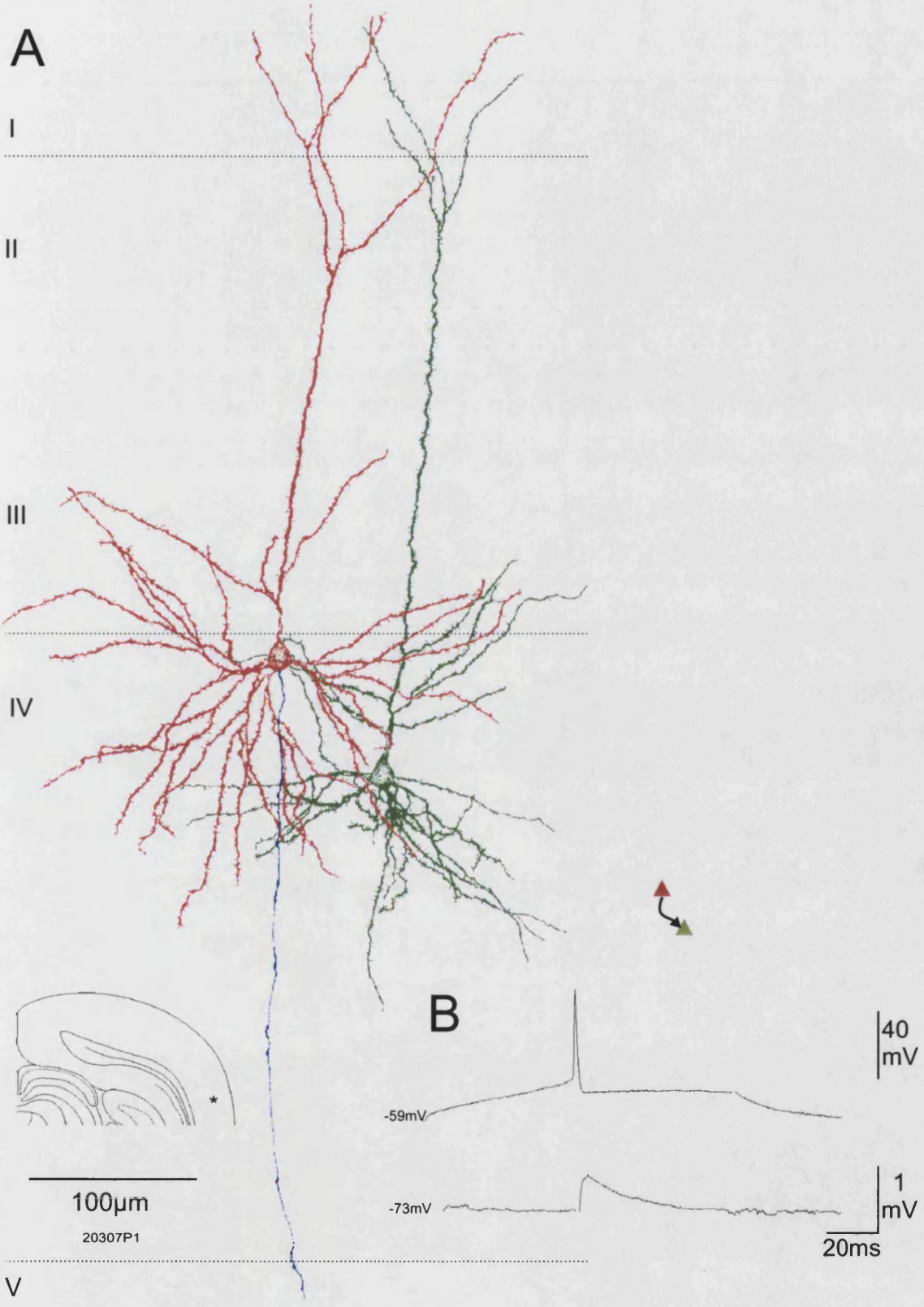

Figure 4.7a. Morphology of a rat layer IV to layer IV pyramid - pyramid pair (20307p1). A, The presynaptic cell dendrites (red) and axon (blue) and postsynaptic dendrites (green) reconstructed at x1000. The axon of the postsynaptic cell is not shown. The dendrites of both cells were spiny. No axo-dendritic appositions were apparent. B, Example of a presynaptic spike and corresponding average first EPSP (252 sweeps).

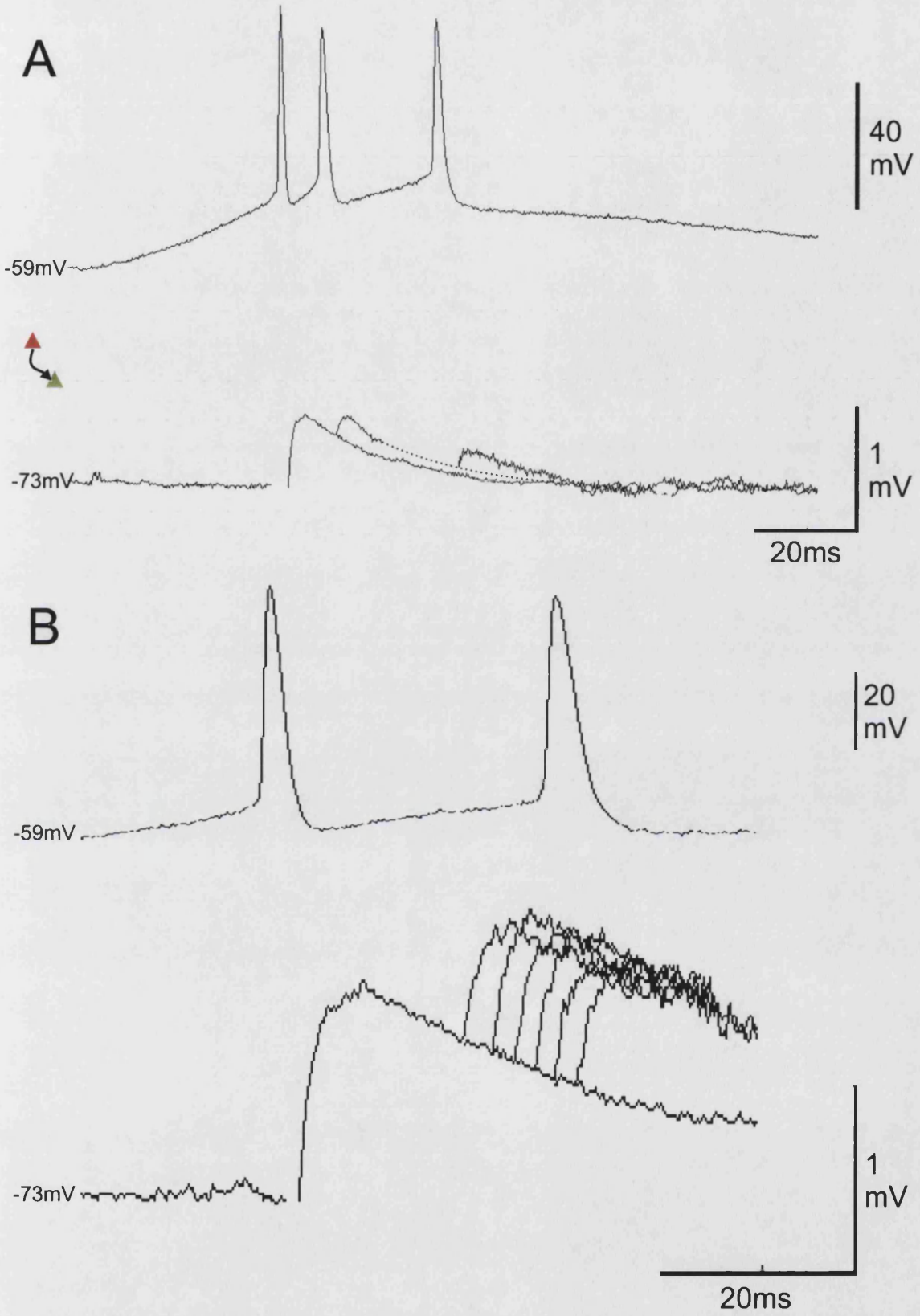

Figure 4.7b. (20307p1) Layer IV to layer IV pyramid - pyramid connection in rat neocortex illustrated in figure 4.7a. A, Averaged 1st, 2nd and 3rd EPSPs showing depression of EPSP amplitude in response to each successive spike. The averaged 2nd EPSPs were 9 ±1ms from the 1st (98 sweeps) and 3rd EPSPs were 25 ±1ms from the 2nd (31sweeps). B, Average 1st EPSP amplitude (252 sweeps) and averaged second EPSP amplitude at intervals of 8, 9, 10, 11,12 and 13 ±0.5ms from the first (>20 sweeps for each). Second EPSP amplitude is depressed relative to the 1st. The presynaptic trace illustrates the longest interspike interval used.

A reciprocally connected pair of rat layer IV pyramidal cells situated either side of the middle of layer IV is illustrated in figure 4.8. The dendritic morphology of the most superficial cell (shown in green) differed in size and shape from its recorded partner. The basal dendrites were mostly confined to layer IV with a maximal lateral span of 234µm. The tips of two basal and two apical oblique dendrites reached into deep layer III. The apical dendrite produced a single apical oblique dendrite that originated and terminated in layer IIi, and bifurcated once in layer II to terminate with two branches in deep layer I. The deeper cells' basal dendrites were also mostly confined to layer IV (the tips of 5 just crossing the layer V border) spanning 335µm laterally. The apical dendrite produced a single branching oblique dendrite in layer IV and another non-branching dendrite spanning most of layer III. The distal apical tuft was formed through multiple bifurcations beginning in layer II and terminating in layer I with a lateral span of 234µm. The primary axonal trunks of both cells were partially myelinated, at nodes between which numerous unmyelinated and bouton laden branches ramified extensively within layer IV and projected up into the layer III. One axon reached into layer II. The more superficial cell made two putative synapses with the deeper cell (mean 1^{st} EPSP amplitude 0.86mV) and 4 potential autapses with its own dendrites. The deeper cell made one potential synapse with the superficial cell (mean 1^{st} EPSP amplitude 0.46mV) and 2 potential autapses with basal dendrites. All sites of potential synaptic contact were onto the spiny dendrites. The EPSPs generated at both connections exhibited depression in amplitude in response to each successive action potential in the trains.

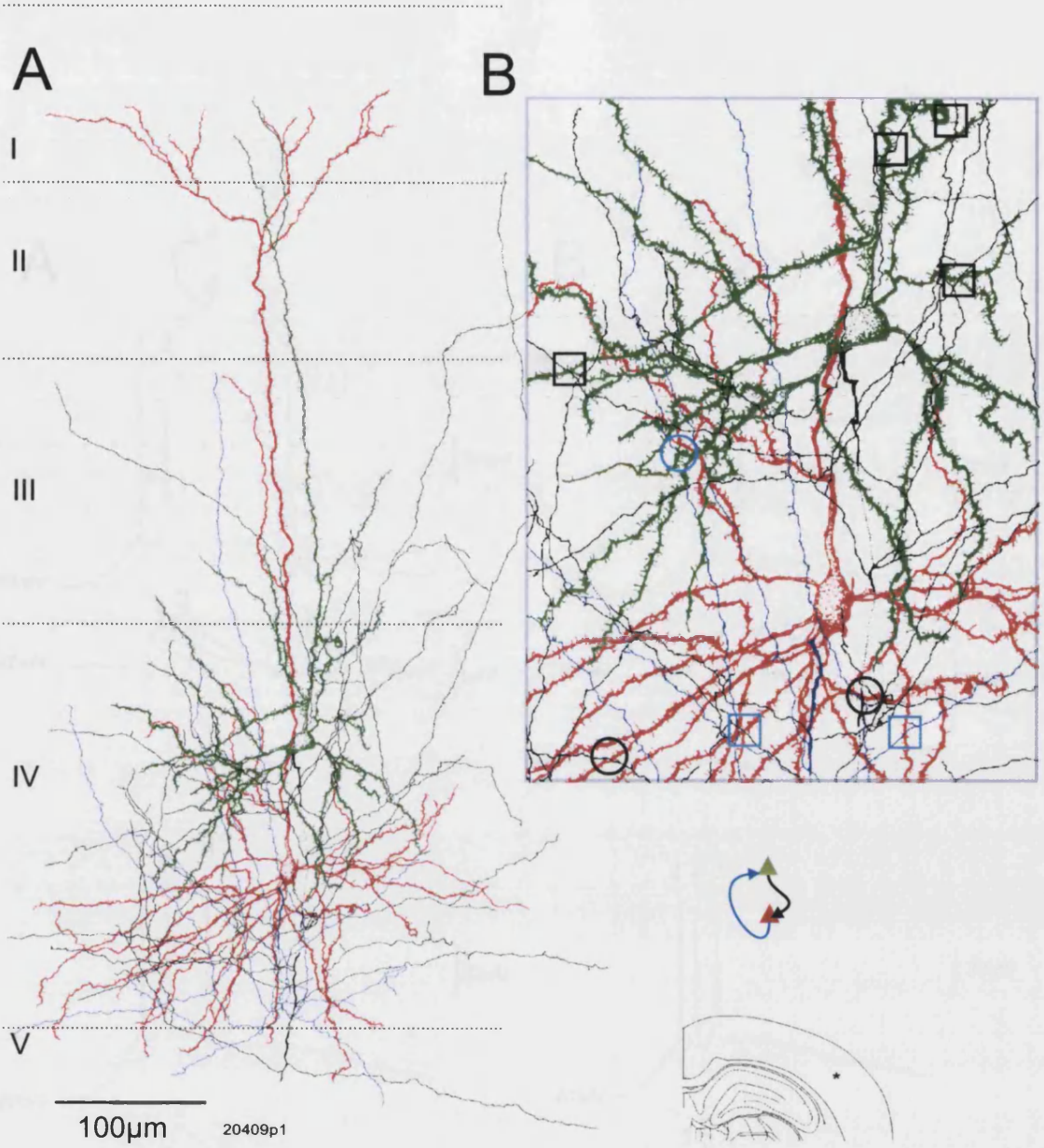

Figure 4.8a. Morphology of a reciprocal rat layer IV to layer IV pyramid - pyramid pair (20409p1a/b). A, The upper cell dendrites (green) and axon (black) and lower cell dendrites (red) and axon (blue) reconstructed at x1000. The dendrites of both cells were spiny, both had partially myelinated primary axons from which collaterals ramified most densely in layer IV. Both cells have a small amount of axon extending into layer III. Neither was seen to exit cortex via the white matter. B, An enlarged portion of A indicating the locations of 2 axo-dendritic close appositions from the green cell to the red cell in black circles and 4 potential autapses in black squares. One axo-dendritic apposition from the red cell to the green cell is indicated by a blue circle and 2 potential autapses are marked by blue squares.

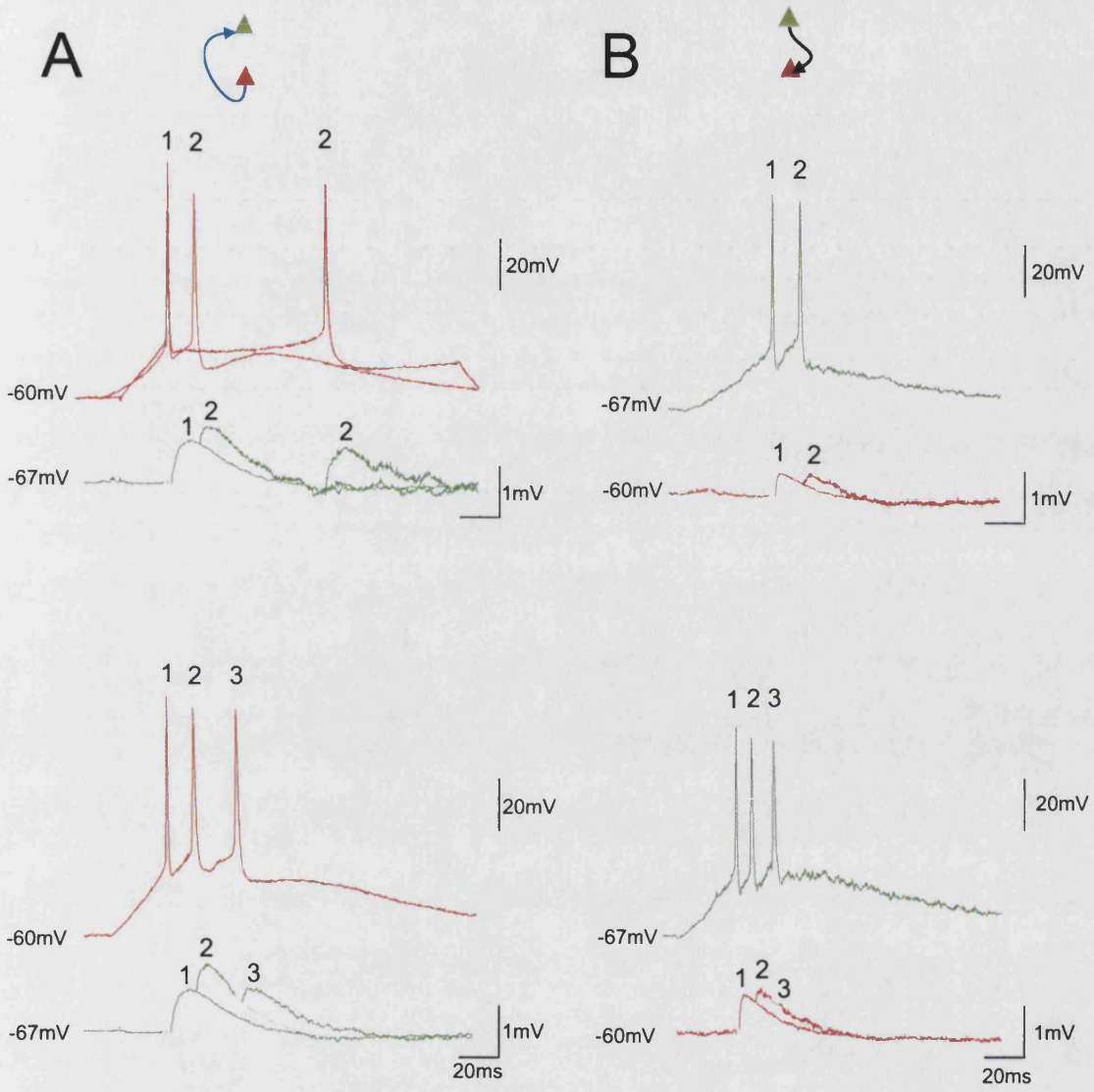

Figure 4.8b. (20409p1a/b) EPSP properties for a reciprocally connected layer IV to layer IV pyramid - pyramid connection in rat cortex. Red and green traces relate to the colour of the cell bodies from which they were recorded that are illustrated in figure 4.8a. A, Upper, the average 1st EPSP (186 sweeps) and averaged 2nd EPSP at 12 ms and 74 ±1ms. The second EPSP is depressed relative to the first and recovers in amplitude at the longer interspike interval. Lower, Averaged 1st, 2nd and 3rd EPSP taken from 69 consecutive sweeps. The average EPSP amplitude decreases with each AP in the trains. B, Upper, the average 1st EPSP (146 sweeps) and average 2nd EPSP at 14 ±2ms from the 1st (22 sweeps). Lower, averaged 1st, 2nd and 3rd EPSPs taken from 38 consecutive sweeps with a consistent firing pattern. Again the average EPSP amplitude decreases with each AP in the train.

4.4.3 Summary of connected layer 4 excitatory cell pair properties.

In cat, the distance between synaptically connected pairs of pyramidal cell somata (calculated in 3 dimensions) within layer 4 ranged between 50 and 171µm (mean 107 ±SD 61µm). Lateral separation was between 0 and 123µm (mean 50 ±SD 43µm). In rat cortex the total distance between connected layer 4 pyramidal cells was 5 to 158µm (mean 87±SD 43µm). Lateral separation was between 0 and 86µm (mean 35 ±SD 33µm).

The general morphology of the cat and rat pyramidal cells in these samples was similar with the exception that the apical tufts of the cat cells were typically larger and more dense than those of the rat cells. The basal dendritic trees of cells from both species typically radiated in all directions from the cell bodies and spanned comparable distances through layer 4. The dendrites of cells situated superficially or deep within layer 4 crossed the borders and could potentially receive input within these neighbouring layers.

The amplitude of the EPSPs recorded at these connections did not show any direct correlation with either the positions of the cells relative to each other or with the size of the cells recorded. All exhibited demonstrable paired pulse depression of mean EPSP amplitudes in response to each successive spike in trains.

In paired recordings where the cells were adequately filled, reconstructed and putative sites of synaptic contact were identified, the majority of contacts were made onto the spiny portions of basal dendrites and the number of contacts observed appeared to correlate with the size of the average 1st EPSP (range 0.46mV for 1 contact to 3.23mV for 7 contacts). Potential autaptic contacts were observed on cells from both species.

4.5 Properties of EPSPs exhibited at Layer 4 pyramidal cell connections.

In order to analyse characteristics of EPSPs such as recovery from depression in detail a number of requirements must first be met by the recordings. Firstly, recordings were selected if adequate numbers sweeps for first, second (third..) EPSPs were available for the generation of PSP averages necessary to overcome sweep to sweep fluctuations in EPSP amplitude. The required number of sweeps was determined by comparing the averaged 1st EPSP triggered from the rising phase of the second spike with the mean 1st EPSP amplitude triggered on the first spike and ensuring the amplitudes matched (typically >20 sweeps were required). Secondly, sufficient numbers of sweeps must be available to generate averages for EPSPs in brief trains for a range of interspike intervals. Thirdly, datasets were selected where the average 1st EPSP did not vary dramatically (>10%) from the mean to avoid erroneous measurements affected by negative correlations of 1st and 2nd EPSP amplitudes. Fourthly, all of the above criteria must be met in portions of the recording where the membrane potential was stable throughout. Recordings with insufficient sweeps available for analysis were discarded though it should be noted that in all, data appeared to be consistent with the recordings illustrated here.

The measurements of EPSP shape characteristics given below were taken from averages (>40 sweeps each, including apparent transmission failures) triggered by the rising phase of the presynaptic action potential in sweeps with only single spikes obtained from portions of the recordings in which the membrane potential remained stable. The measurements of EPSP amplitude and time course for each layer 4 to layer 4 pyramid to pyramid connection for both species are given in table 4.1.

Species	Pair ID	Postsynaptic MP (mV)	Mean Amp (mV)	10-90% Rise Time (ms)	Half Width (ms)	%1st failure	1st EPSP CV
CAT	20521p1a	-67	3.23	1.4	12.9	0	0.08
	20521p1b	-67	0.92	1.6	13.4	0	0.21
	20521p2a	-64	0.73	0.9	15.1	23	0.54
	20521p2b	-59	2.13	1.9	6.7	0	-
	20522p2	-66	1.72	1.4	11.7	0	0.13
	20523p2	-60	1.08	0.9	11.4	0	0.21
	20611p2a	-58	2.08	0.6	8.8	0	0.16
	20612p3	-60	1.46	1.1	9.6	17.9	0.16
	20612p4a	-71	3.06	1.1	15.2	36.4	0.77
	20612p4b	-76	1.83	1.5	14	0	0.09
	Mean	-64.8	1.82	1.24	11.88	-	0.26
	±SD	5.79	0.84	0.39	2.81	-	0.23
RAT	10711p2	-74	2.06	1.2	12.7	0	0.13
	10911p4	-64	1.67	3.6	34.1	0	0.21
	20116p1	-65	0.77	1.8	18.9	0	0.29
	20206p4	-48	0.32	1.1	7.7	19.8	-
	20307p1	-73	0.55	1.8	13.8	0	0.33
	20307p2	-42	0.75	1.7	23.3		-
	20312p1	-72	1.24	2.9	14.5	0	0.21
	20409p1a	-68	0.86	3.9	24.9	0	0.29
	20409p1b	-70	0.46	1.4	14.2	11.3	0.54
	20411p1a	-43	0.6	1.3	5.8		-
	20417p1	-68	0.51	1.5	15.1	6.5	0.47
	21024p1	-69	3.01	2.4	27.9	0	0.11
	30520p3a	-62	0.27	-	-	0	-
	30520p4	-53	0.51	2.4	5.7	12.7	-
	Mean	-62.2	0.97	2.07	16.81	-	0.28
	±SD	11.09	0.78	0.91	8.67	-	0.14

Table 4.1. Properties of average EPSPs elicited by single presynaptic action potentials for intralaminar layer 4 pyramid to pyramid connections, the percentage of 1st spike transmission failures and the coefficient of variation (CV). The pair IDs represent the code number for each recording made.

4.6 Paired Pulse Depression

All recordings of layer 4 to layer 4 pyramid to pyramid connections in both cat and rat demonstrated variable degrees of paired pulse depression and progressive use dependent depression in trains of EPSPs. At 5-100ms interspike intervals the average amplitude of all second and all subsequent EPSPs were depressed relative to the first. All EPSPs recovered from depression over time such that the shorter the interval between spikes the more powerful the depression observed and as the interspike interval for 2nd EPSP averages lengthened the more they recovered to approach the amplitude of the mean 1st EPSP (figure 4.9).

4.7 Transmission Failures and EPSP Amplitude distribution.

A straightforward method of judging the mechanism involved in depression at these synapses is to count the numbers of apparent transmission failures for each spike in trains as the number of failures has an inverse correlation with the probability of release or the number of release sites.

Of all the recordings with more than one hundred sweeps (ie. recordings longer than 5 minutes with sweeps taken at intervals of 3 seconds), 5 of 8 cat and 6 of 10 rat layer 4 pyramid to pyramid connections showed no apparent failures of synaptic transmission in response to the 1st action potential. Of the remaining 7 recordings (3 cat and 4 rat) the mean 1st AP failure rate was 25.76% for cat and 12.53% for rat. For all connections the failure rate (if any) tended to increase with each successive action potential in trains of up to 10 spikes.

Plots of EPSP amplitude distributions were made for recordings where adequate numbers of sweeps (>30) each with up to 5 EPSPs are shown in figure 4.10. Except where large numbers of transmission failures skewed the plots, the amplitude distributions of the 1st to 5th EPSPs were all relatively evenly distributed around the mean (ie. they appeared to fit a binomial distribution). The peak distributions of EPSP amplitude shifted to the left in response to each successive AP in 3 of 5 cat and 6 of 7 rat recordings (the remaining 2 cat and 1 rat recordings exhibited only slight depression).

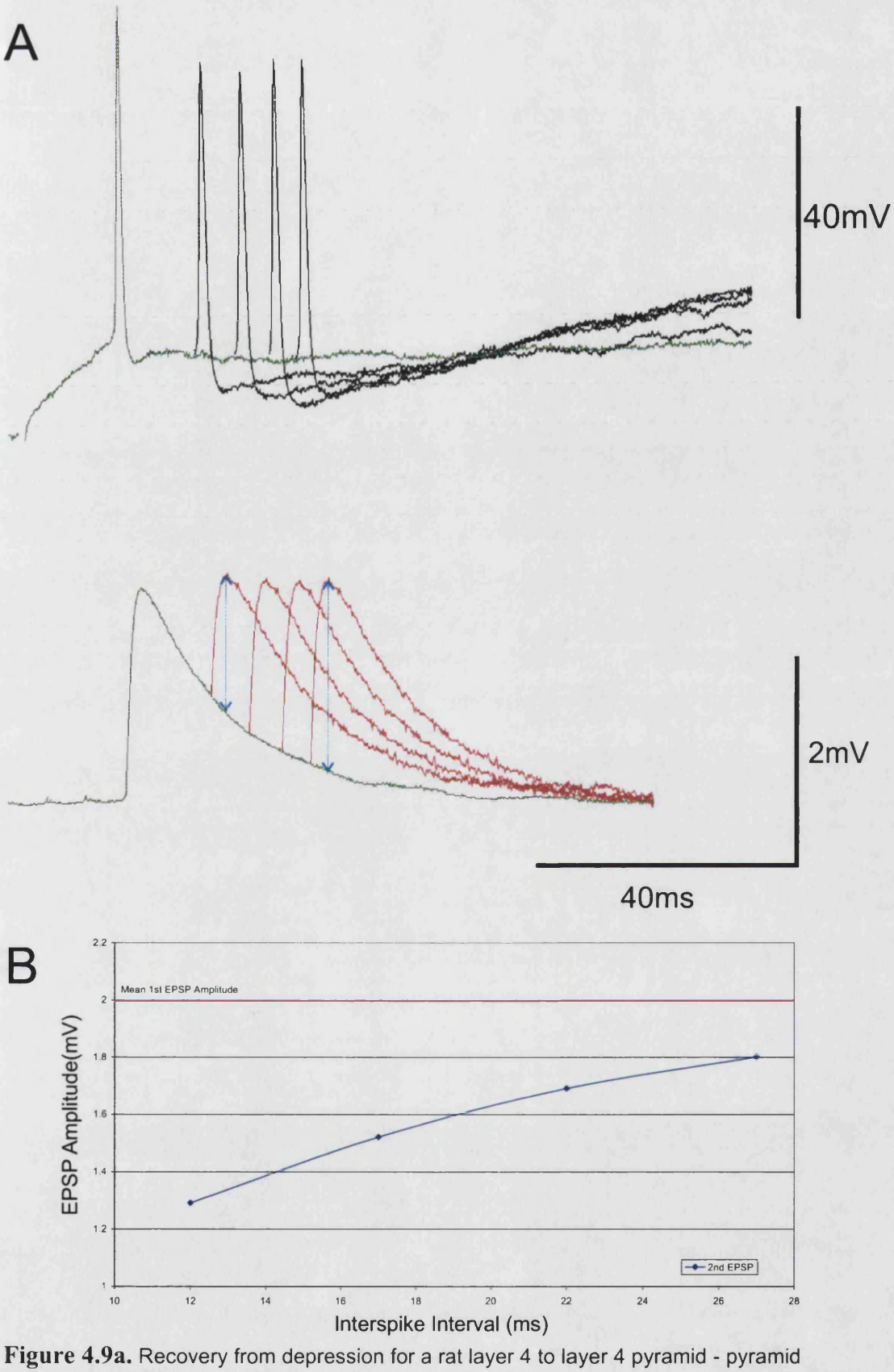

Figure 4.9a. Recovery from depression for a rat layer 4 to layer 4 pyramid - pyramid connection (10711p2). A, The first action potential and its corresponding postsynaptic EPSP (green), second action potentials at intervals from the first (black) and corresponding EPSPs in red. EPSP averages are made from >10 sweeps and show a progressive recovery from depression with increasing interspike interval. B, Plot of recovery. Each data point is measured from the peak of the EPSP to the decay phase of the average 1st EPSP. The red line indicates the mean 1st EPSP amplitude.

A

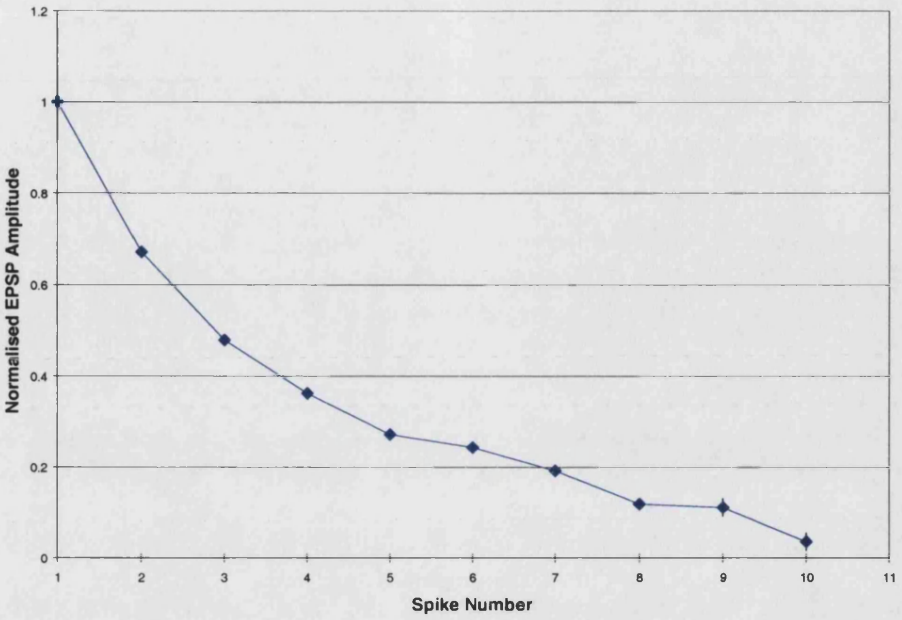

B

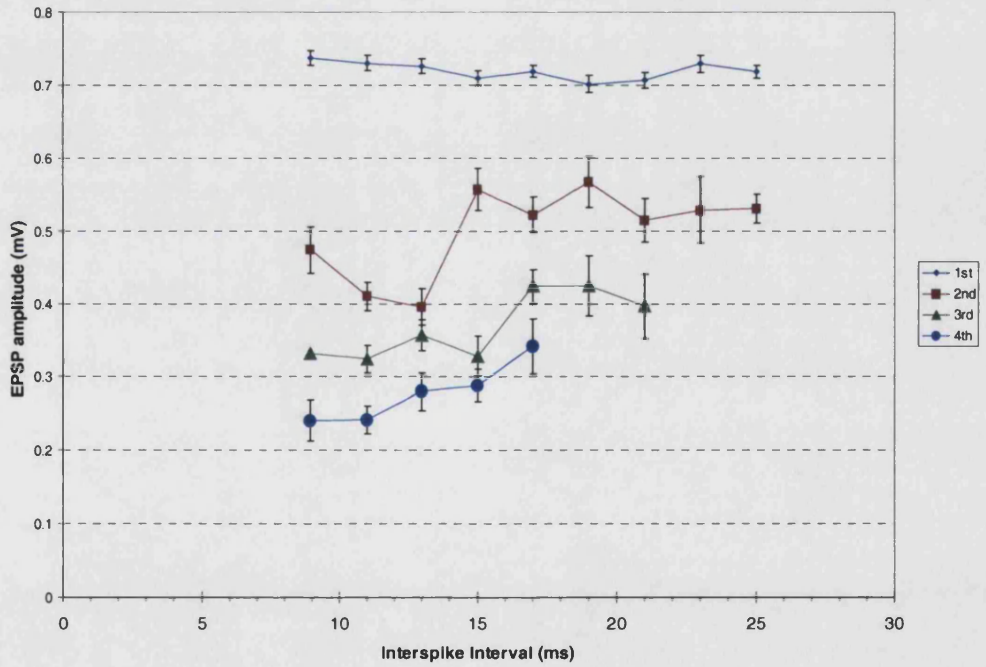

Figure 4.9b. The pattern of use dependent depression for a rat layer 4 to layer 4 pyramid to pyramid connection (20116p1). A, Progressive depression in average EPSP amplitude in trains of 1 to 10 EPSPs irrespective of interspike intervals (SE bars included). B, Recovery from depression of 2nd, 3rd and 4th EPSPs over time from the preceding spike. Each consecutive EPSP is more depressed then the last and all show a trend to increase in amplitude as the interval from the preceding spike lengthens. Data subsets were selected in which the average 1st EPSP amplitude was within 10% of the mean, data were binned at 2ms intervals, were plotted with standard error bars and all data point averages contain a minimum of 17 sweeps (maximum 54). Blue diamonds represent the average 1st EPSP corresponding with the, 2nd 3rd and 4th EPSP averages (red squares, green triangles and blue circles respectively).

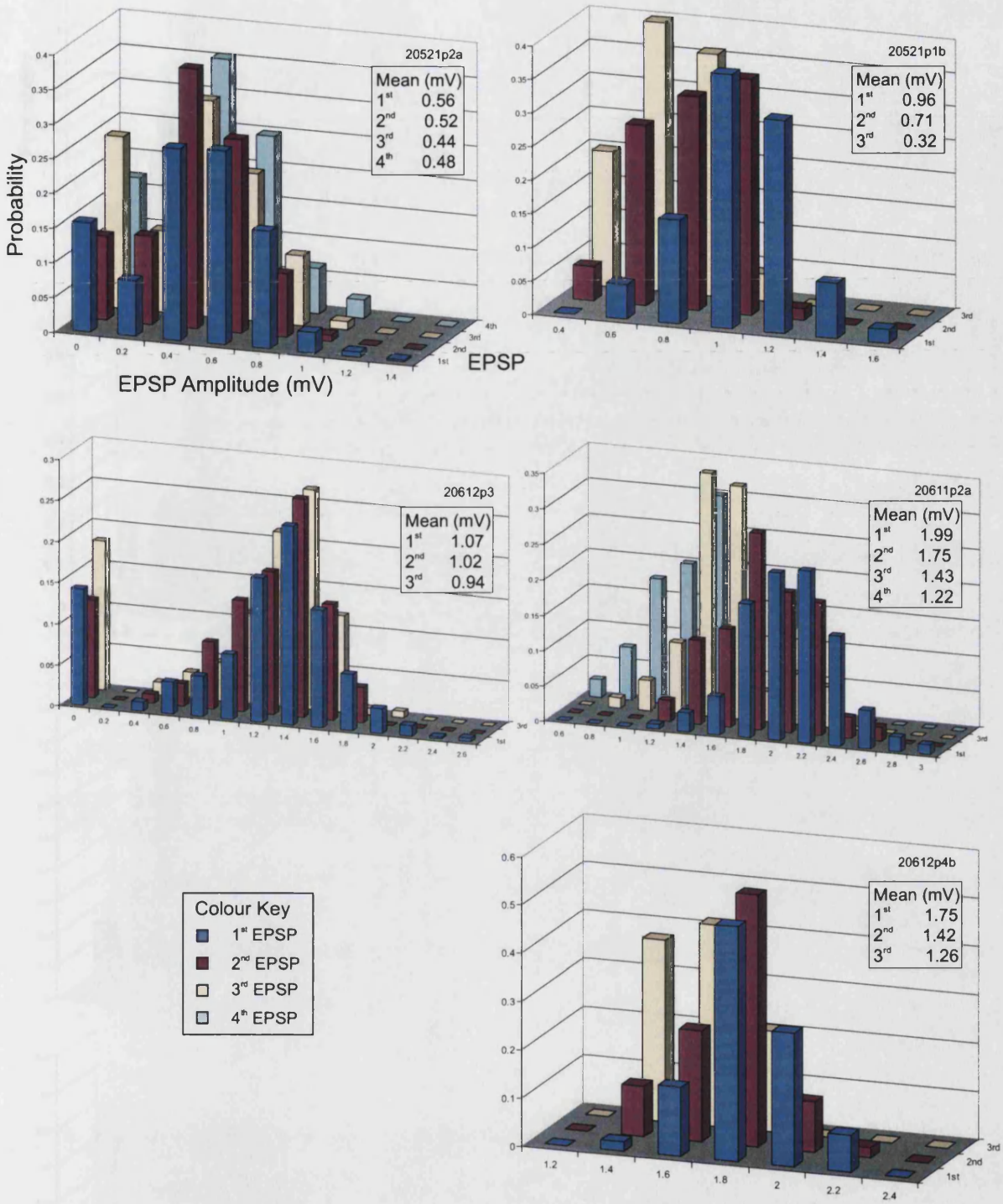

Figure 4.10a. Amplitude distribution histograms for 1st, 2nd, 3rd (4th) EPSPs for cat layer 4 pyramid to pyramid connections. Data were binned in sets of 0.2mV (since relatively small numbers of events were available for each plot and no attempt was made to distinguish peaks) with a value of zero representing apparent failures of synaptic transmission. Interval ranges for each bin did not exceed 48ms for 2nd, 53ms for 3rd and 54ms for 4th EPSPs. Note that in the 3 recordings on the right the peak amplitude distribution shifts to the left of preceding EPSPs. In the 2 recordings on the left that depressed only slightly on average, no such shift was apparent. In 2 recordings, no apparent transmission failures were seen for the first 3 spikes.

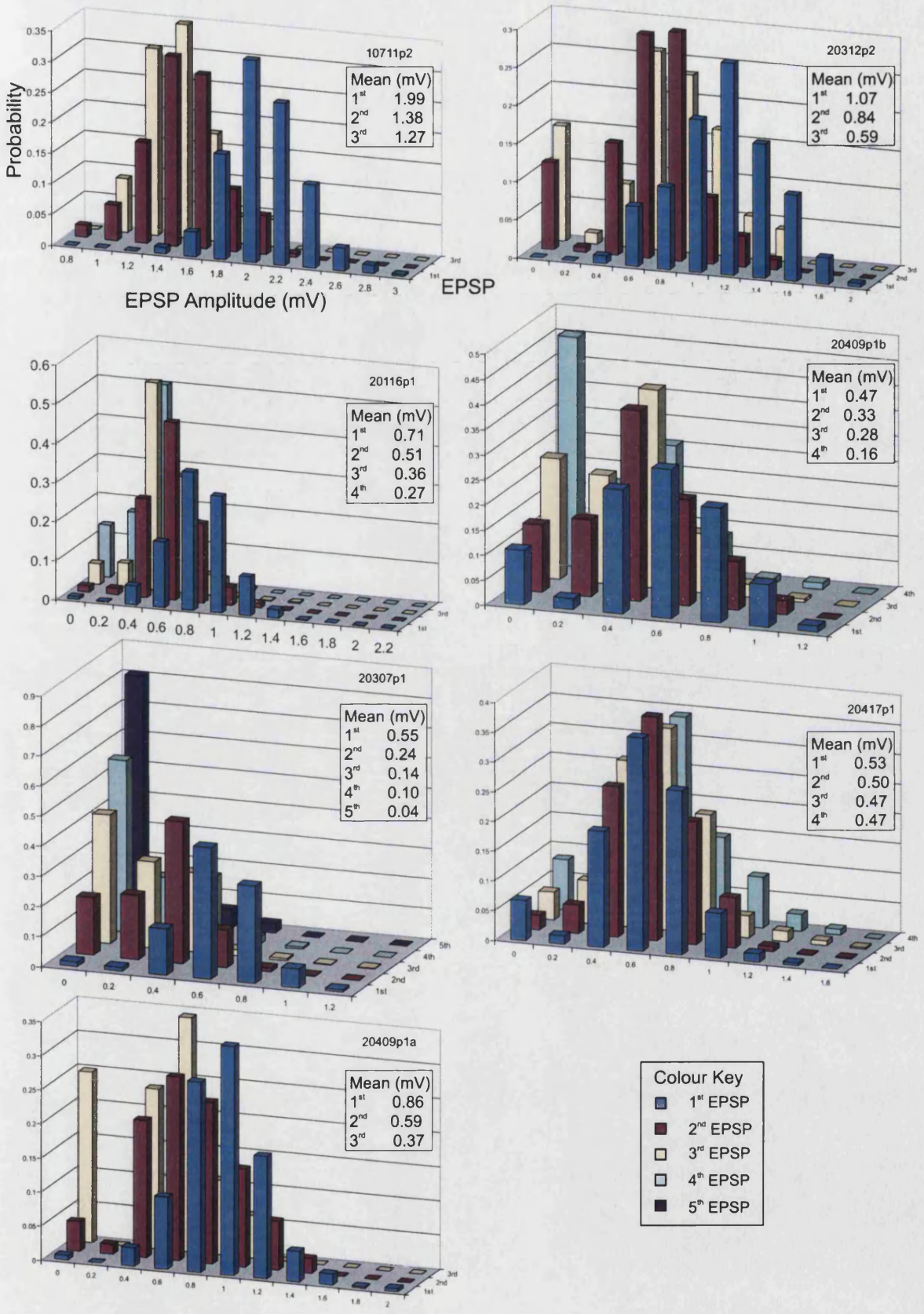

Figure 4.10b. Amplitude distribution histograms for 1st, 2nd, 3rd (4th and 5th) EPSPs for rat layer 4 pyramid to pyramid connections. Data were binned in sets of 0.2mV with a value of zero representing apparent failures of synaptic transmission. Note that in all but one recording (20417p1) the peak amplitude distribution shifts to the left of preceding EPSPs. In all but one recording (10711p2) transmission failures occurred with increasing probability in response to each successive spike.

For all paired recordings where it was possible to measure the amplitudes of sufficient single sweep events, the mean amplitudes and CVs for 1st, 2nd and 3rd EPSPs occurring within narrow interspike interval ranges were calculated. The CV for each 1st EPSP was typically small (0.26 ±0.23 for cat and 0.28 ±0.14 for rat). Despite a decrease in mean amplitude the CVs for 2nd and 3rd EPSPs were larger (0.36 ±0.11 and 0.42 ±0.17 for cat 2nd and 3rd EPSPs and 0.46 ±0.19 and 0.65 ±0.35 for rat) than that of the 1st EPSP.

4.8 Depression of Layer 4 Pyramid to Pyramid EPSPs Appears to be Presynaptically Mediated.

The EPSP amplitude histograms given above showed an even distribution about the mean that appeared to match a binomial distribution, suggesting that comparisons of the changes in EPSP CV^{-2} and mean amplitude may indicate whether the depression observed was of pre- or post-synaptic origin.

For all recordings where suitable sweeps containing multiple spikes were available according to the criteria described above, plots were made of the normalised inverse square of the coefficient of variation (CV^{-2}) versus normalised mean EPSP peak amplitude (M) for second and third EPSPs in trains to assess whether the depression exhibited at these synapses was of pre- or post-synaptic origin. In a binomial distribution CV^{-2} is equivalent to np/(1-p) and M = npq. As the coefficient of variation is independent of q a plot of second and third EPSP CV^{-2} against M gives an indication as to whether the changes in EPSP amplitude are due to pre or postsynaptic mechanisms (ie. The number of release sites (n) and the probability of release (p) are presynaptically determined while the quantal amplitude (q) is largely determined postsynaptically). Points resulting from a change in q will fall on a slope of zero, proportional changes in M and CV^{-2} give a slope of 1 indicating a change in n. A slope of >1 demonstrates a disproportionately larger change in CV^{-2} than in M indicating that variations are the result of a change in p.

Figure 4.11 shows a plot of normalised CV^{-2} against normalised EPSP amplitude for layer 4 pyramid to pyramid connections analysed from both species. In all connections analysed the depression appears to be the result of a decrease in the probability of release and therefore is interpreted as depression of presynaptic origin.

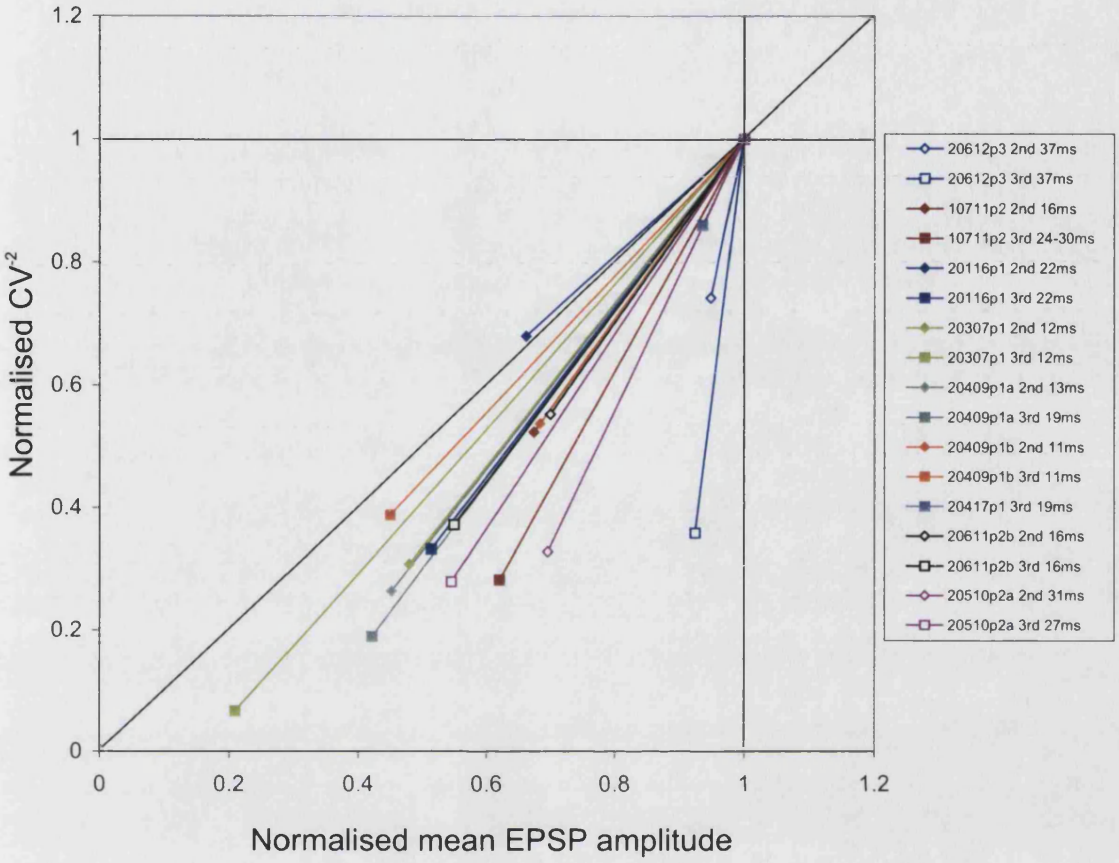

Figure 4.11. Normalised change in CV^{-2} (np/(1-p)) plotted against normalised mean EPSP amplitude (npq) for depressing excitatory layer 4 to layer 4 pyramid - pyramid connections in cat and rat. Most of the points fall with a slope >1 indicating that the depression in EPSP amplitude is presynaptic in origin involving a decrease in the probability of release (p) and/or the number of available release sites (n). Filled points relate to rat and open points to cat connections. Diamonds represent the 2nd EPSP and squares represent 3rd EPSPs at a known intervals ±1ms unless otherwise stated.

4.9 Branch Point Failure.

Another potential cause of failure of synaptic transmission could be the failure of action potential propagation. Axonal conduction failure has been described in pyramidal cells in hippocampal slice cultures in which the voltage dependent activation of A-type K^+ channels was revealed by the application of 4-aminopyridine (a K^+ channel blocker) to be involved in curtailing AP propagation at individual axonal branch points (Debanne *et al.*, 1997). In sequential recordings from pairs of pyramidal cells they also found that the propagation of action potentials failed at some but not all connections from the same axon, suggesting that the physiological activation of the K^+ channels may allow the time dependent integration of membrane potential changes at individual axonal branch points, thereby altering their ability to transmit action potentials.

One layer 4 to layer 4 pyramid to pyramid recording from cat neocortex exhibited an unusual pattern of EPSP generation that may be explained by branch point failure (BPF) (see figure 4.12). The postsynaptic neurone generated powerful EPSPs in response to action potentials evoked in the presynaptic cell and an unusual pattern of total transmission failures. Observations at the time of the experiment suggest that the number of transmission failures was directly related to the strength of the current pulse injected into the presynaptic cell. Where more powerful stimuli were applied, the postsynaptic EPSP was less likely to fail.

EPSP amplitude distribution plots revealed the depression of peak EPSP amplitude with each successive spike in trains of up to 5. However, large numbers of transmission failures occurred in response to each spike in these trains despite the peak amplitude distribution remaining around 3mV (see figure 4.12a/b) suggesting that the failures are not the result of progressive reduction in the probability of synaptic release from multiple release sites. Unfortunately, the number of potential synapses could not be assessed as (despite 28 minutes of continuous recording) the presynaptic cell was not filled and therefore remained unstained in the histological preparation.

Averages of second presynaptic spikes did not show evidence of spikelets in the presynaptic recording that would suggest that another, electrically coupled neurone was responsible for EPSP generation in the postsynaptic cell as the averaged spikes that resulted in successful transmission did not vary in shape from those that did not (ie. there was no apparent spike fractionation in either case), see figure 4.12d.

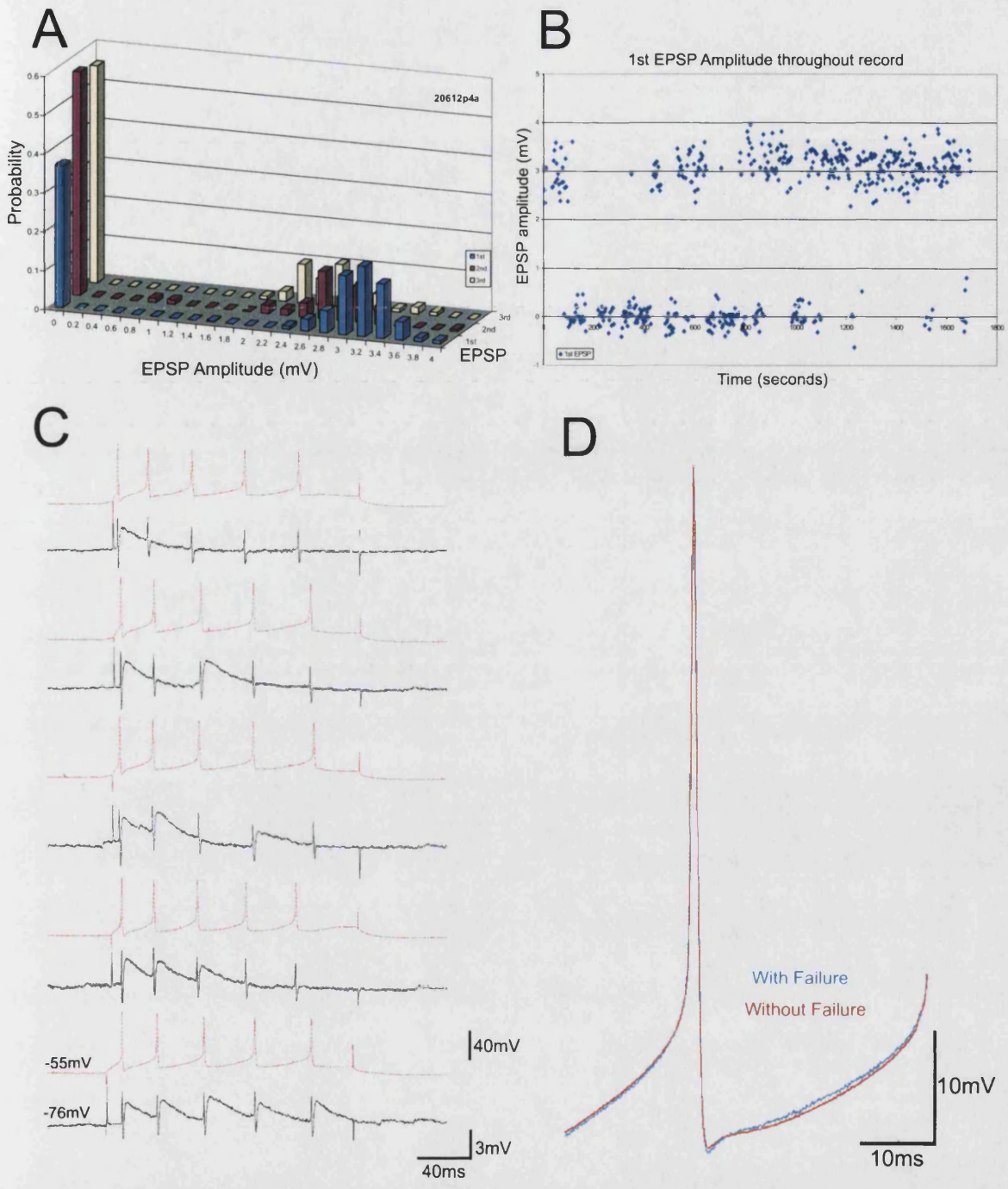

Figure 4.12. Possible axonal branch point failure at a pyramid to pyramid connection in layer 4 of cat neocortex. A, Unusually skewed EPSP amplitude distribution in response to the 1st, 2nd and 3rd presynaptic action potentials. The distribution of peak EPSP amplitude shifts towards the left for each successive spike in the trains. B, Single sweep measurements of 1st EPSP amplitude throughout the recording. The mean amplitude of successful 1st EPSPs is around 3mV with a range of 2.4 to 3.9mV. Total transmission failures occur frequently. C, Raw data illustrating the unusual pattern of EPSP generation. The observation at the time of the experiment was that synaptic efficacy improved when current pulse strength was increased. D, Ten sweep averages triggered on the rising phase of second spikes that either succeeded or failed to generate EPSPs in the postsynaptic cell. Second spikes that achieved successful transmission did not differ in shape when compared with those that did not, indicating that a gap junction coupled cell is not likely to be generating the EPSPs as would be detected by the presence of spikelets, the timing of which would affect the time course of the averaged spike (unless the gap junction was powerfully rectifying). The morphology of the postsynaptic cell from this connection can be seen in figure 4.4a.

4.10 Post-Tetanic Potentiation.

In one recording containing sweeps where the presynaptic pyramidal cell was driven to produce between 1 and 10 spikes in response to current pulses of different intensities, measurement of EPSP amplitude evoked by the 1st spike in sweeps preceded by sweeps containing different numbers of spikes revealed an enhancement of 1st EPSP amplitude consistent with post-tetanic potentiation (PTP) Figure 4.13 illustrates an example of PTP exhibited at a layer 4 pyramid to pyramid connection in rat cortex.

Data subsets were used to calculate the mean EPSP amplitude in response to the 1st action potential from sweeps preceded by 1, 2 or 3 pulses (at intervals of 1 every 3 seconds) that generated between 1 and 8 spikes. The mean 1st EPSP amplitude calculated from records preceded by a sweep containing only a single spike was 1.62 ±SD 0.34mV. The mean 1st EPSP amplitude calculated from sweeps following trains of 3, 4, 5...or 8 spikes progressively increased to 2.19 ±SD 0.25mV for those preceded by 8 spikes trains (see figure 4.13a). All subsequent EPSPs elicited by successive APs in the trains were depressed in amplitude relative to the preceding response.

Plots of sequential 1st EPSP amplitude for a section of the recording containing consistent numbers of spikes in the preceding trains with a series of sweeps containing 2 spikes followed by a series of trains containing 8 to 10 spikes showed a progressive increase in 1st EPSP amplitude over time with increased presynaptic activity (figure 4.13c). When the injected current was reduced to evoke a series of single spike sweeps following the series of 8 to 10 spikes per sweep, the 1st EPSP amplitude decreased to below the mean of 1st EPSPs following sweeps with the same selection criteria (1.14 ±SD 0.22mV compared to 1.62 ±SD 0.34mV).

These data suggest that synaptic connections that exhibit PTP have the potential to retain information relating to previous spike frequency over a period of seconds. The potentiation of EPSP amplitude following periods of increased activity may have important implications in information processing such that the postsynaptic cells are rendered more likely to reach action potential threshold (and for longer) in response to coincident inputs following periods of high frequency spike activity.

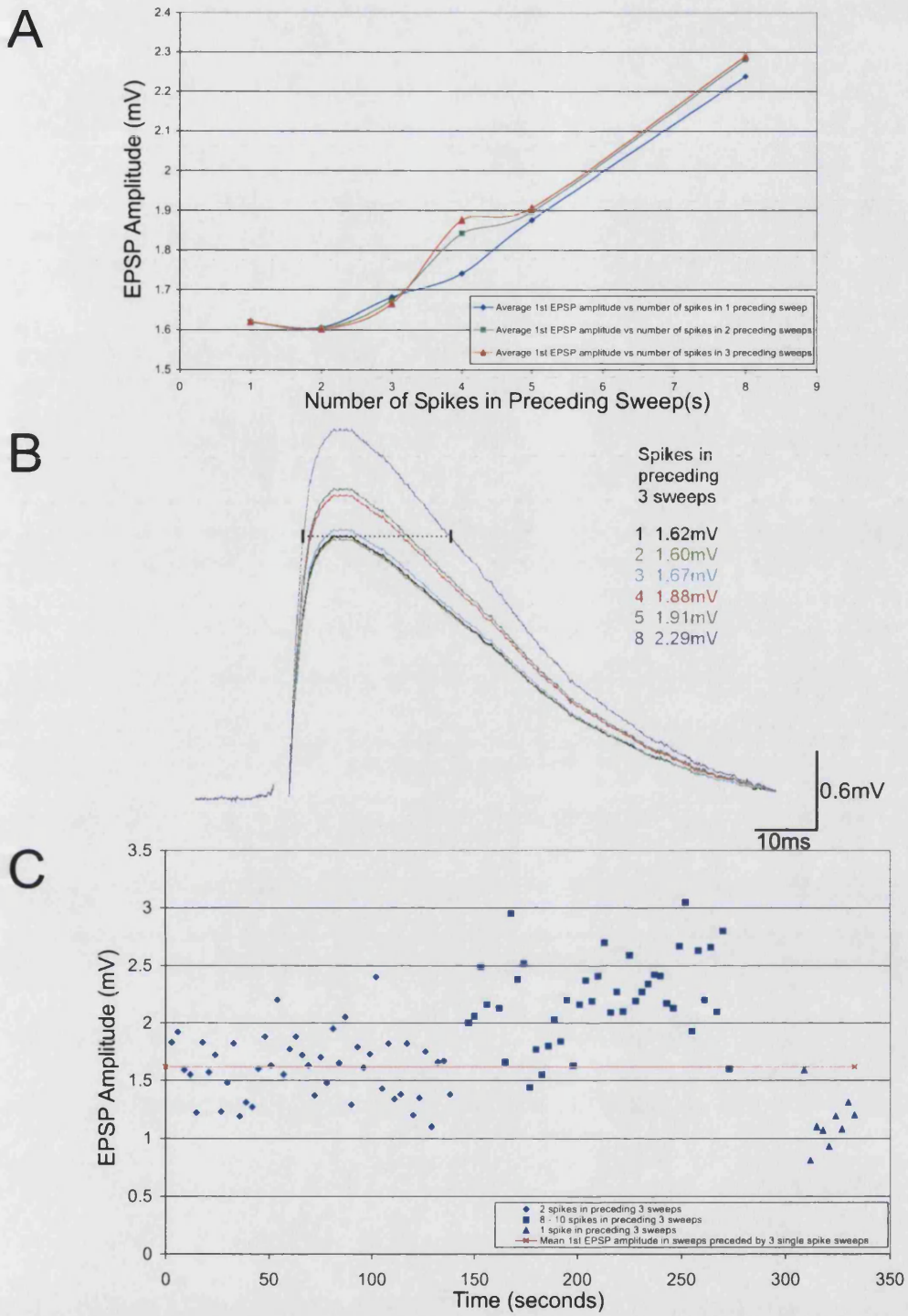

Figure 4.13. Post tetanic potentiation (PTP) exhibited in a layer IV to layer IV pyramid to pyramid connection in rat neocortex. A, Plot of the average 1st EPSP amplitude (27 - 252 sweeps per average) from sweeps with between 1 and 8 spikes in the preceding 1,2 or 3 sweeps. The average EPSP amplitude is potentiated as the number of spikes in the preceding trains increases. B, Scaled 1st EPSP averages illustrating the level of potentiation of the 1st EPSP when preceded by 3 sweeps containing 1 to 8 spikes. Note that in the most potentiated EPSP (purple) the cell remains more depolarised than the peak of unpotentiated EPSPs (or 1st EPSPs resulting from sweeps preceded by 3 sweeps containing single spikes - black) for ~23ms. C, Single sweep amplitude measurements of 110 consecutive first EPSPs. Diamonds correspond to EPSPs preceded by 3 sweeps containing 2 spikes, Squares relate to EPSPs preceded by 3 sweeps containing between 8 and 10 spikes and triangles to EPSPs preceded by sweeps containing 1 spike. First EPSP amplitude is progressively potentiated over time when the presynaptic cell is driven to generate 8 - 10 spikes. Following potentiation, the first EPSP amplitude decreases to below the mean 1st EPSP amplitude measured from similar records preceded by 3 sweeps containing single spikes recorded before potentiation. The anatomy of the cells involved in this connection is illustrated in figure 4.6a.

4.12 Conclusions.

The gross anatomy of the cortical pyramidal cells from both species show similar patterns of dendritic and axonal distribution though the cat cells did appear to have larger or more developed apical dendritic tufts. The majority of the basal dendrites from both species were located within layer 4 as would be predicted by the location of the targeted somata. The majority of non-myelinated axon was located in layers 4 and also in layer 3. These findings concur with the hypothesis that the layer 4 pyramidal cells receive the majority of their input (including that from the specific thalamic nuclei) in layer 4, amplify the signal and feed it forward to layer 3 within the columns to which they contribute.

No significant differences in the anatomy of the layer 4 pyramidal cells involved in excitatory connections with other layer 4 pyramids was observed between the species and the probability of such connections was also similar (1:31 for cat and 1:48 for rat). Perhaps the most striking observation was that of the physiological subclasses of pyramidal cells present in layer 4, all cells that were presynaptic to other layer 4 pyramids were RS. Paired recordings of layer 4 cells connected with neurones in the neighbouring layers in rat were not necessarily RS (no tests with BF cells of other layers were performed in cat) so these data indicate a level of specificity between different electrophysiological subclasses of pyramidal cells and raise some interesting questions for further study. For example, what cells are the BF pyramids of layer 4 receiving synaptic input from? To where and to which cells do they distribute their outputs? And is there any correlation between the cells with different firing patterns and their axonal morphology?

The numbers and locations of observed putative synaptic contacts onto the spiny dendrites of their postsynaptic partners was similar in both species and both appeared to make significant numbers of autapses with their own dendrites.

The EPSPs generated exhibited a wide and overlapping range of EPSP amplitudes and time courses and no correlation between cell morphology and EPSP amplitude could be identified in either species. All of the connections exhibited paired pulse depression that was apparently presynaptically mediated by a reduction in the probability of synaptic release from multiple release sites. Frequency and use dependent depression was also demonstrable at layer 4 to 4 excitatory connections. PTP was observed in one rat connection. The probability of total transmission failure

in response to the 1st action potentials was generally low (7 of 10 cat and 8 of 11 rat connections did not fail) and no evidence of facilitation of mean EPSP amplitudes was observed in recordings of connections between layer 4 excitatory cells in either species.

The identification of these features indicate that the cat and rat excitatory networks of layer 4 operate with similar input and output distributions, are tuned to convey novel input with the greatest efficacy via depressing synapses that reliably release transmitter in response to regular spiking discharge properties and that some layer 4 cells are capable of retaining information of recent network activity.

5.0 THE INTERACTIONS OF PYRAMIDAL CELLS AND THE INTERNEURONES IN LAYER 4.

Introduction.

Simultaneous intracellular recordings were performed to investigate and compare the properties of excitatory and inhibitory synaptic connections in small circuits of pyramidal cells and interneurones in layer 4 of cat and rat neocortex and to compare them with the excitatory connections between pairs of pyramidal cells described in section 4. Subsequent visualisation of biocytin injected into synaptically connected cells and immunocytochemical localisation of interneuronal calcium binding proteins and neuropeptide content was used to classify the cells involved further, extend the database of known interneurone subtypes present in layer 4 and to attempt the correlation of interneuronal firing pattern, neurochemistry and gross anatomy with the connections they made. The synaptic strength, efficacy and frequency dependent properties of excitatory connections to anatomically determined classes of interneurones were studied to identify the properties utilised by connections in layer 4 and to find any characteristics that may differ between the species or may be specific to neuronal subclass.

In 45 experiments a total of 22 layer 4 interneurones (12 cat and 10 rat) were tested with 57 (cat) and 32 (rat) cells simultaneously recorded in layers 3,4 and 5, for synaptic connections. A total of 8 excitatory layer 4 pyramid to layer 4 interneurone connections were found (5 in cat, 3 in rat) where the presynaptic cell generated EPSPs in a postsynaptic interneurone. One layer 3 to layer 4 excitatory connection was seen in rat. Eight inhibitory connections were seen where both the presynaptic interneurone and the postsynaptic pyramid were in layer 4. Four inhibitory connections from layer 4 interneurones onto pyramidal cells in layer 3 were found in cat and none in rat. One reciprocally connected layer 4 interneurone to layer 4 pyramidal cell pair was found in cat. In 15 tests (12 cat and 3 rat) of simultaneously recorded inhibitory cells, no interneurone to interneurone connections were identified in either species. Hit rates for connections involving layer 4 interneurones are illustrated in figures 3.1 and 3.2 in section 3.

5.1 Characteristics of pyramidal cells connected to or by layer 4 interneurones.

The electrophysiological and morphological characteristics of layer 4 pyramidal cells from both species have been described in detail in previous sections. No morphological differences were observed between the layer 4 pyramids involved in excitatory connections with other excitatory cells in layer 4 and those involved in the interactions with the layer 4 interneurones described here so the reader is referred to section 4.3 for description of their anatomy.

Layer 3 pyramidal cells fit the general patterns of pyramidal cell morphology described in section 1.3.1. Of the rat layer III pyramidal cells reconstructed in their entirety all had spiny dendrites and partially myelinated axon. Between 4 and 6 primary basal dendrites emerged from the soma and bifurcated to form between 17 and 27 last order branches. The main apical trunks extended perpendicular to the pial surface, bifurcated in layer II and extended dendritic tips of their sparse apical tufts into deep layer I. The mean horizontal span parallel to the pial surface was 230 ±68µm and vertical span perpendicular to the pia was 396 ±99µm. One layer 3 pyramid from cat tissue typical of many observed at light level was reconstructed in its entirety (see figure 5.2a). Dendrites were spiny with 7 primary basal dendrites bifurcating to terminate in 20 last order branches. The apical dendrite of this cell bifurcated early in layer 3 within 50µm of the soma and again in layer 2 extending 6 dendritic tuft tips into layer 1. Horizontal dendritic span was 304µm and vertical span 590µm. Axonal ramification of layer 3 pyramids from both species was most prominent in layer 3 within the first 200µm below the cell body and in layer 5, typically passing through layer 4 without ramifying there.

Electrophysiological characterisation of pre and postsynaptic pyramidal cells at the time of the experiment or during post hoc offline analysis showed that, interestingly, all cells synaptically coupled with interneurones in layer 4 from both species, from both layers 3 and 4, were regular spiking despite burst firing cells comprising 37% of the layer 4 excitatory neurones tested.

5.2 Characteristics of Layer 4 Interneurones

Morphology.

The family of inhibitory interneurones comprise a number of morphologically defined subgroups. Certain features were common to all the interneurones reconstructed; all had oval cell bodies between 10 and 20μm in diameter and smooth, aspiny dendrites. Beyond this, morphological similarities were more difficult to identify. A great deal of variation in dendritic tree shape was apparent indicating that the cells had significantly different preferences for the laminar locations at which they receive input, and in particular a very different distribution of their axonal arbours (and therefore their outputs) within the layers. One rat and three cat interneurones were multipolar (stellate) in appearance with dendrites extending from the cell bodies in all directions. Of these, 2 cat cells were regular spiking, 1 fast spiking and the multipolar rat cell was fast spiking. The remaining rat interneurone had a bitufted appearance with dendrites projecting only from the top and bottom of the cell body and had irregular spiking characteristics.

Cat interneurones.

Figure 5.1 (20430p1) illustrates a layer 4 interneurone from cat cortex. The interneurone's cell body was oval, with 3 primary dendrites bifurcating within layer 4 to produce 12 last order branches. All dendrites were short (<130μm)and confined to layer 4. The axon was fine with few myelinated portions and formed 3 distinct arbours. The first and largest arbour most extensively ramified within layer 4 with small varicosites situated throughout. Four long and straight unmyelinated axonal profiles extended through layers 2 and 3 to terminate in a small arbour in layer 1. Six long and straight unmyelinated axons projected down through layer 5 to form a discreet arbour in layer 6 and another, smaller output 300μm laterally. Synaptic boutons are distributed throughout all layers of the cortex. The axonal arborisation in layers 1 and 6 may have been more extensive *in-vivo* as the slicing procedure appears to have curtailed these long distance projections. These patterns of dendritic and axonal arborisation indicate that the cell received input only in layer

4 and then distributed a powerful inhibition to its vicinity in layer 4 and less powerfully through all layers within a narrow column perpendicular to the pial surface.

This interneurone was presynaptic to 2 layer 4 pyramidal cells (figure 5.1) generating IPSPs. In one postsynaptic cell the average 1st IPSP was -1.53mV in amplitude and in the other -0.53mV though differences in the postsynaptic membrane potentials of the two cells do not allow comparison of amplitude (-45 and -61mV respectively). Nine Axo-dendritic close appositions onto the pyramidal cells were all located on 3rd to 5th order basal dendritic branches indicating that the interneurone is of a dendrite targeting class. The cell had fast action potentials with regular spiking firing characteristics and was immunonegative for both parvalbumin and calbindin.

Figure 5.2a (20501p2) illustrates another cat layer 4 interneurone with similarities to the cell in figure 5.1. This cell also had regular spiking firing characteristics, was also immunonegative for antibodies raised against parvalbumin and calbindin; and appeared to contact pyramidal cell dendrites making 6 close axo-dendritic appositions in this case, again on 3rd to 5th order dendrites (2 basal and 4 apical oblique). This cell differed in gross morphology however. Seven primary dendrites projected in all directions from the smooth oval cell body, with multiple bifurcations to produce 24 beaded, aspiny last order branches in both layers 4 and 3. The axon was primarily non-myelinated bar the primary axon projecting from the top of the cell body and a long partially myelinated projection extending obliquely into layer 5 the destination of which could not be confirmed since it exited the plane of the slice. The primary axonal arbour was uniform in density through superficial layer 4, and throughout layers 3 and 2 with several short portions reaching into layer 1. Four axonal profiles extended into layer 5 and exited the plane of the slice. Synaptic boutons were distributed evenly throughout.

This cell generated -0.42mV average amplitude IPSPs in a short (poorly stabilised) recording from a layer 3 pyramidal cell (MP approximately -46mV) and received facilitating EPSPs from a layer 4 pyramidal cell (figure 5.2b).

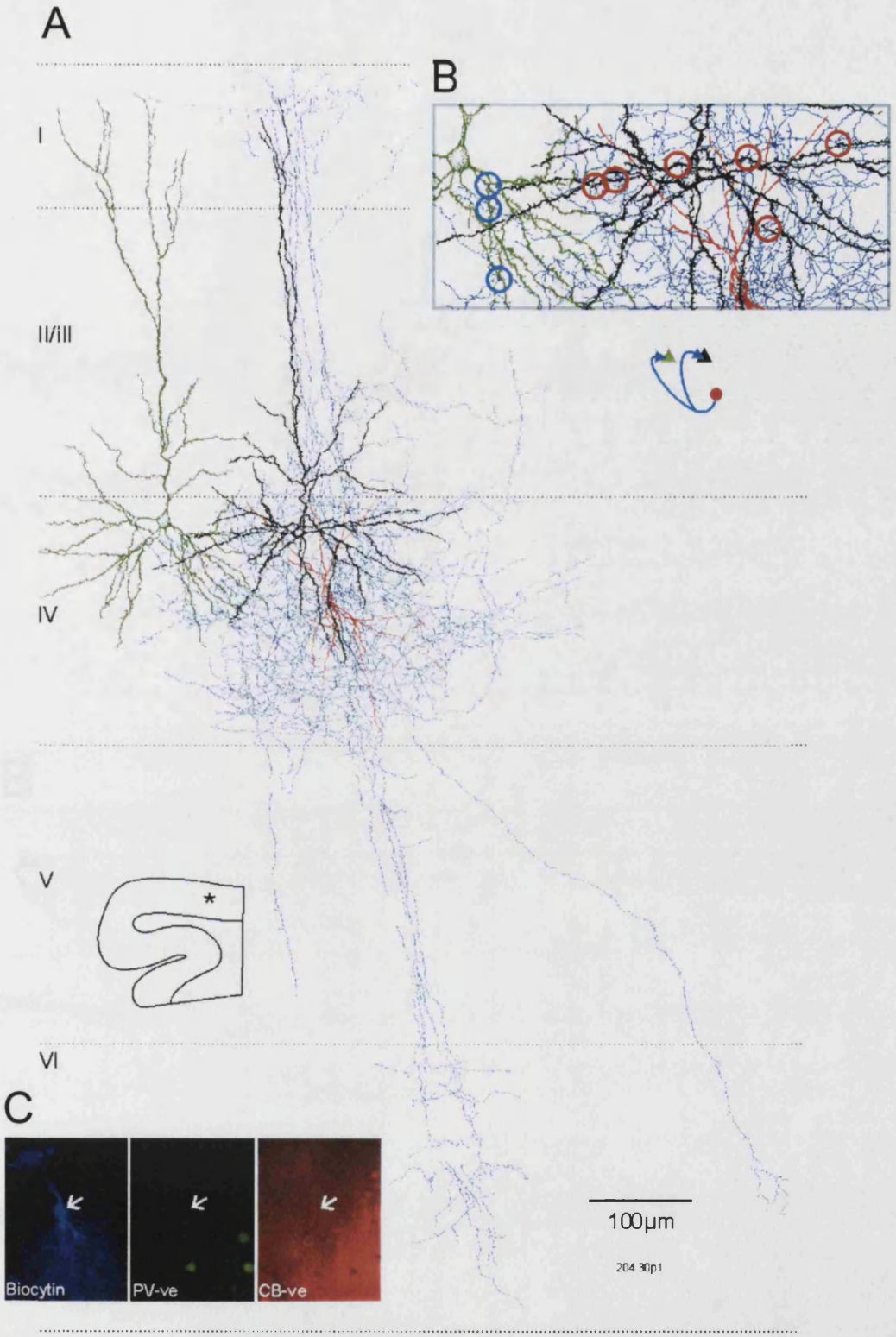

Figure 5.1a. Morphology of a cat layer 4 RS interneurone that was presynaptic to two layer 4 pyramidal cells (20430p1) reconstructed at x1000. A, The presynaptic interneurone dendrites (red) and axon (blue) and the two postsynaptic pyramidal cell dendrites (green and black). For clarity the axonal arbours of the two pyramids are not illustrated. B, Enlarged portion of A showing the location of 3 axo-dendritic appositions with the green pyramid (blue circles) and 6 with the black cell (red circles) C, Immunofluorescence photomicrographs of biocytin labelling with AMCA (blue) Parvalbumin with FITC (green) and Calbindin with Texas red. The cell was immunonegative for both PV and CB. The electrophysiological characteristics of these connections are described in figure 5.1b.

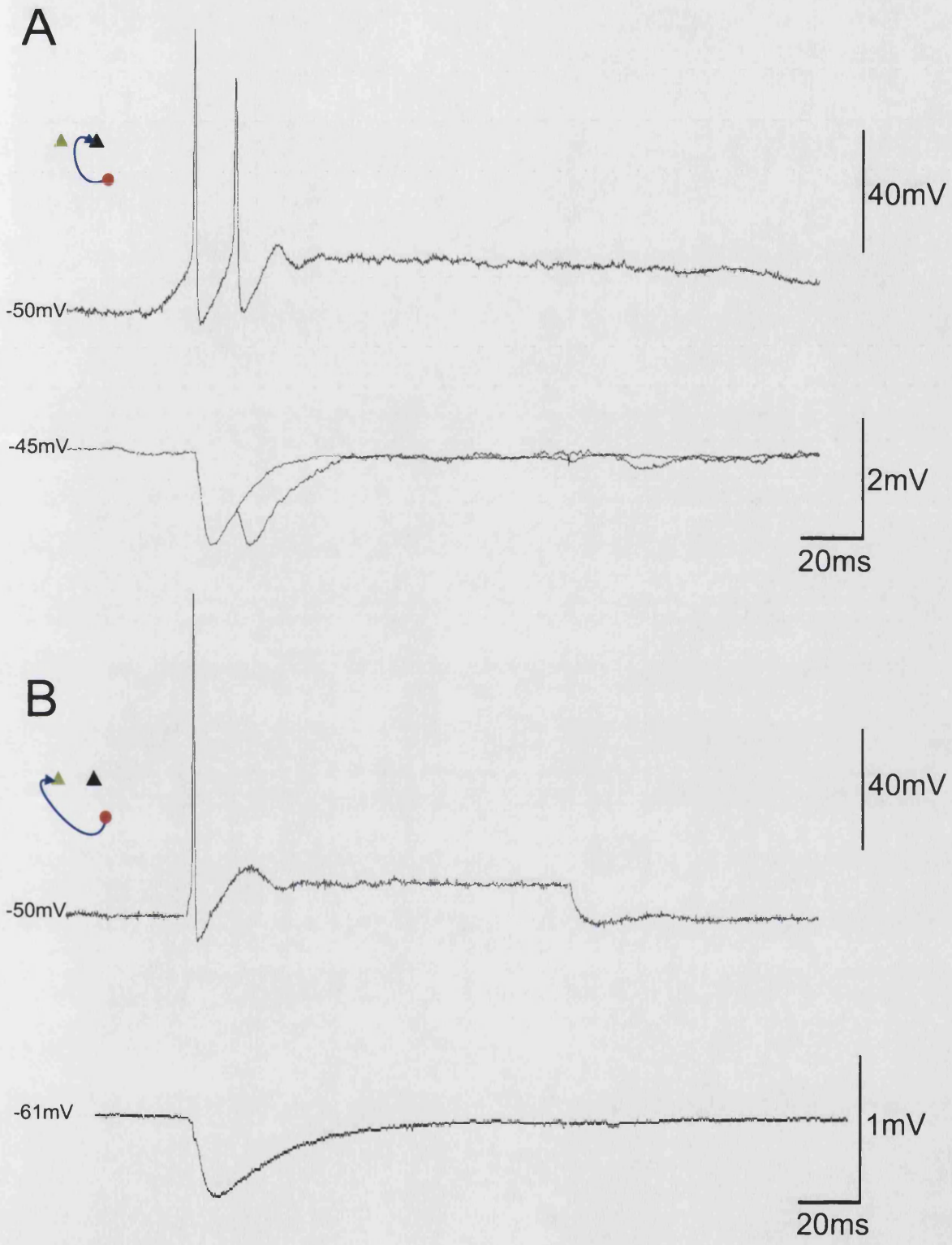

Figure 5.1b. (20430p1b/c) IPSPs elicited in 2 layer 4 pyramidal cells by the same RS layer 4 interneurone in cat cortex. The interneurone was negative for PV and CB. A, Recording (b) shows a depressing IPSP with the second IPSP amplitude measured against the decay phase of the 1st. The average 1st IPSP was made from 56 sweeps and the average 2nd from 17 sweeps 13ms ±1ms after the 1st. B, Recording (c) shows an IPSP in the second postsynaptic pyramidal cell (233 sweeps). The interneurone only fired single action potentials in the second recording. The anatomy of these cells is illustrated in figure 5.1a.

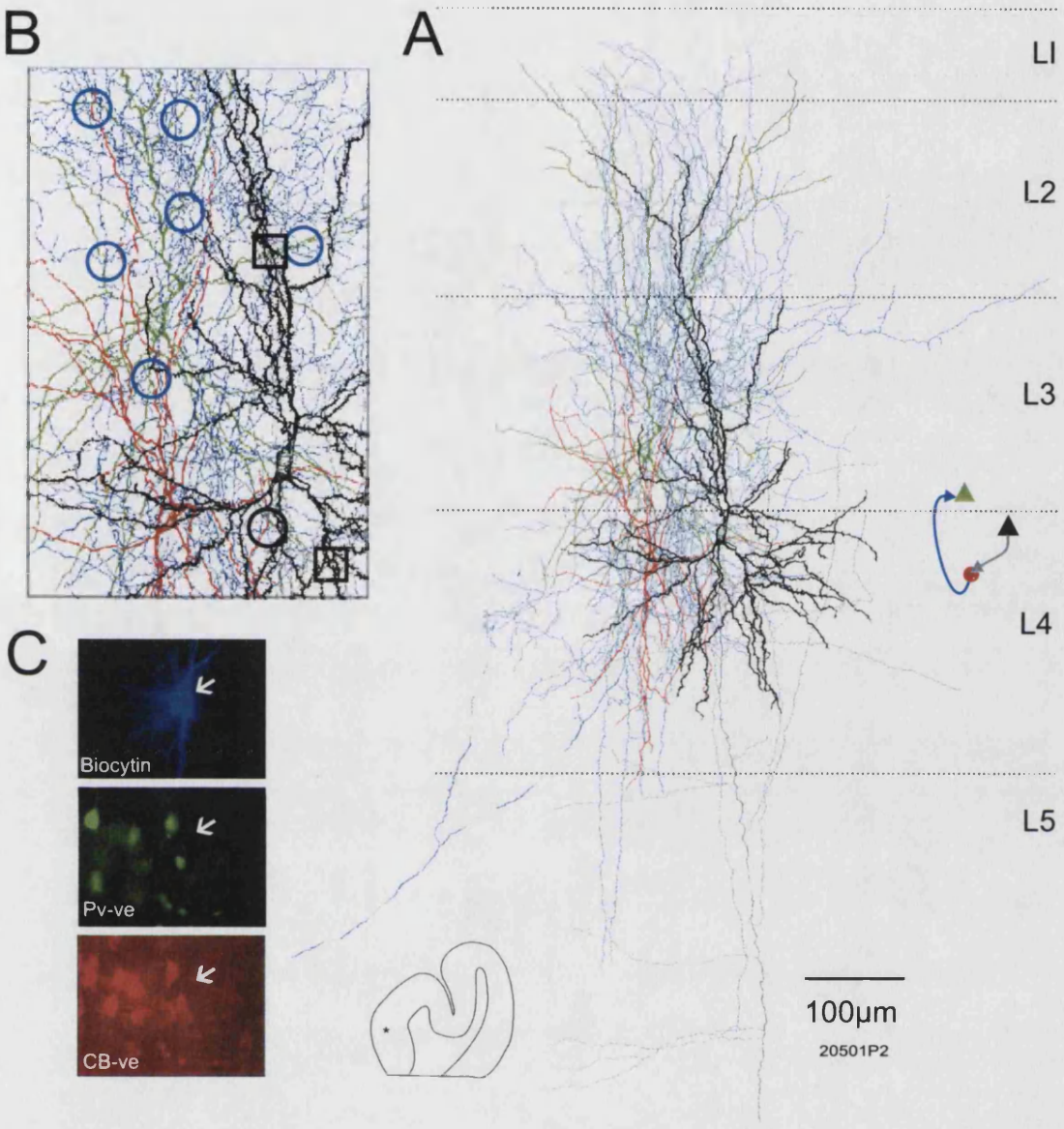

Figure 5.2a. (20501p2) Morphology of a cat layer 4 RS interneurone that was presynaptic to a layer 3 pyramidal cell and postsynaptic to a layer 4 pyramidal cell reconstructed at x1000. A, The interneurone is illustrated with red soma and dendrites and blue axon. The presynaptic pyramidal cell soma and dendrites are in black and the axon grey, the postsynaptic pyramidal cell dendrites are green. B, enlarged portion of A indicating 1 axo-dendritic contact from the presynaptic pyramidal cell to the interneurone (black circle) and two potential autapses (black squares). Six axo-dendritic contacts from the interneurone to the postsynaptic pyramid are also indicated (blue circles) C, Immunofluorescence photomicrographs of biocytin labelling with AMCA (blue), Parvalbumin with FITC (green) and CB with Texas red. The cell was immunonegative for both PV and CB. The facilitating EPSP and the IPSP exhibited in these connections are described in more detail in figure 5.2b.

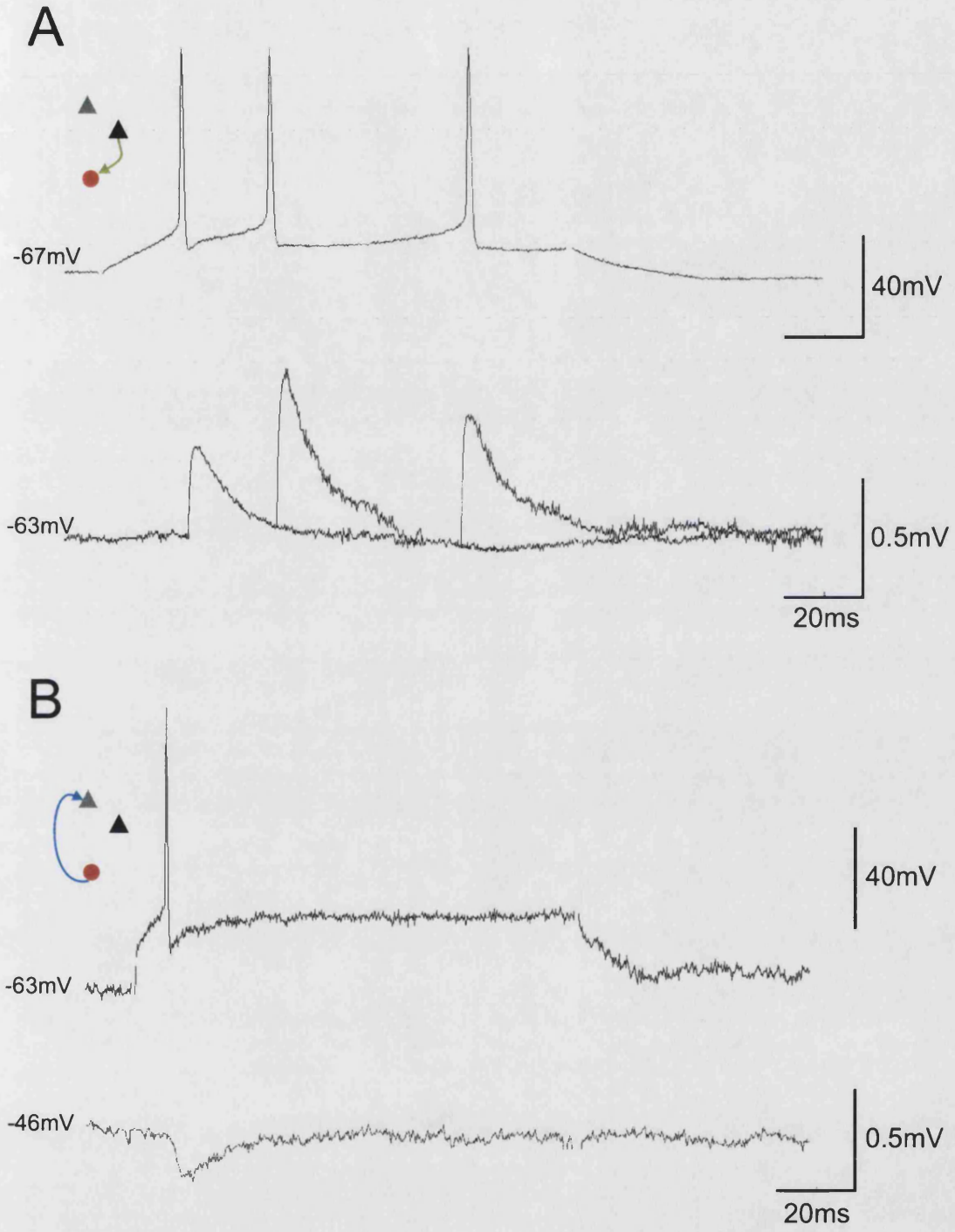

Figure 5.2b. (20501p2b/c) EPSPs elicited in a RS layer 4 interneurone by a layer 4 pyramidal cell in cat neocortex and IPSPs elicited by the interneurone in a layer 3 pyramid. The interneurone was negative for PV and CB. A, Average 1st 2nd and 3rd EPSPs illustrating facilitation. The second EPSP is 21±1ms from the 1st and the 3rd 47±1ms from the 2nd (244, 37 and 45 sweep averages respectively). B, Raw data illustrating a IPSP elicited by the interneurone in a layer 3 pyramid. The anatomy of these cells is illustrated in figure 5.2a.

The cat layer 4 interneurone in figure 5.3a (20521p1) was reciprocally connected with a layer 4 pyramidal cell. The dendritic arbour was stellate with 7 smooth aspiny primary dendrites bifurcating to form 27 last order branches which were beaded at their extremities in layers 2 to 5. The axonal arbour was sparse, ramifying most densely within 250µm of the cell body throughout layer 4 with evenly distributed synaptic boutons. Few axonal branches extended into layers 2 and 3. Numerous straight axon branches projected into layer 5 and 6 with short (5-40µm) offshoots laden with synaptic boutons.

The anatomy of this neurone suggests that it received inputs in layers 3, 4 and 5 and distributed its outputs in layers 2 to 6, but most densely within the span of its inputs in layer 4. A single close membrane apposition with a 2nd order basal dendrite of a layer 4 pyramidal cell was found. First IPSPs were -0.2mV in amplitude at -65mV. The EPSPs generated by the reciprocally connected pyramid were slightly depressing with peak first amplitude of 0.77mV (figure 5.3b). The cell was immunopositive for parvalbumin and negative for calbindin.

Rat interneurones.

One layer IV interneurone from rat cortex (figure 5.4) that was fast spiking, immunopositive for parvalbumin, negative for CCK and received a strongly depressing EPSP from a layer IV pyramidal cell had unusual patterns of dendritic and axonal arborisation. Seven primary dendrites projected from the 14µm diameter cell body with all but one extending at oblique angles to produce 19 last order branches with a lateral span of 443µm in superficial layer IV and also into layer III. One primary dendrite extended directly down into layer V where it bifurcated to produce 8 last order branches, 3 of which terminated in layer VI. The axon initial segment emerged from the top (most superficial) surface of the cell body from which heavily myelinated sections projected through layers III to VI from which unmyelinated bouton laden axons ramified most extensively in layers IV,III. Myelinated axon passed down through layer V without extensive ramification there and produced an arbour situated in layer VI. Boutons were most densely distributed in layer IV then III then VI with relatively few in layer V. This anatomy would suggest that the cell received most inputs in layer IV and less so in layers III, V and VI. Its output distribution appears to be similar to that of its inputs but is significantly greater in extent through those layers spanning 538µm in layer II/III, 730µm in layer IV, 230µm in layer V and 515µm in layer VI .

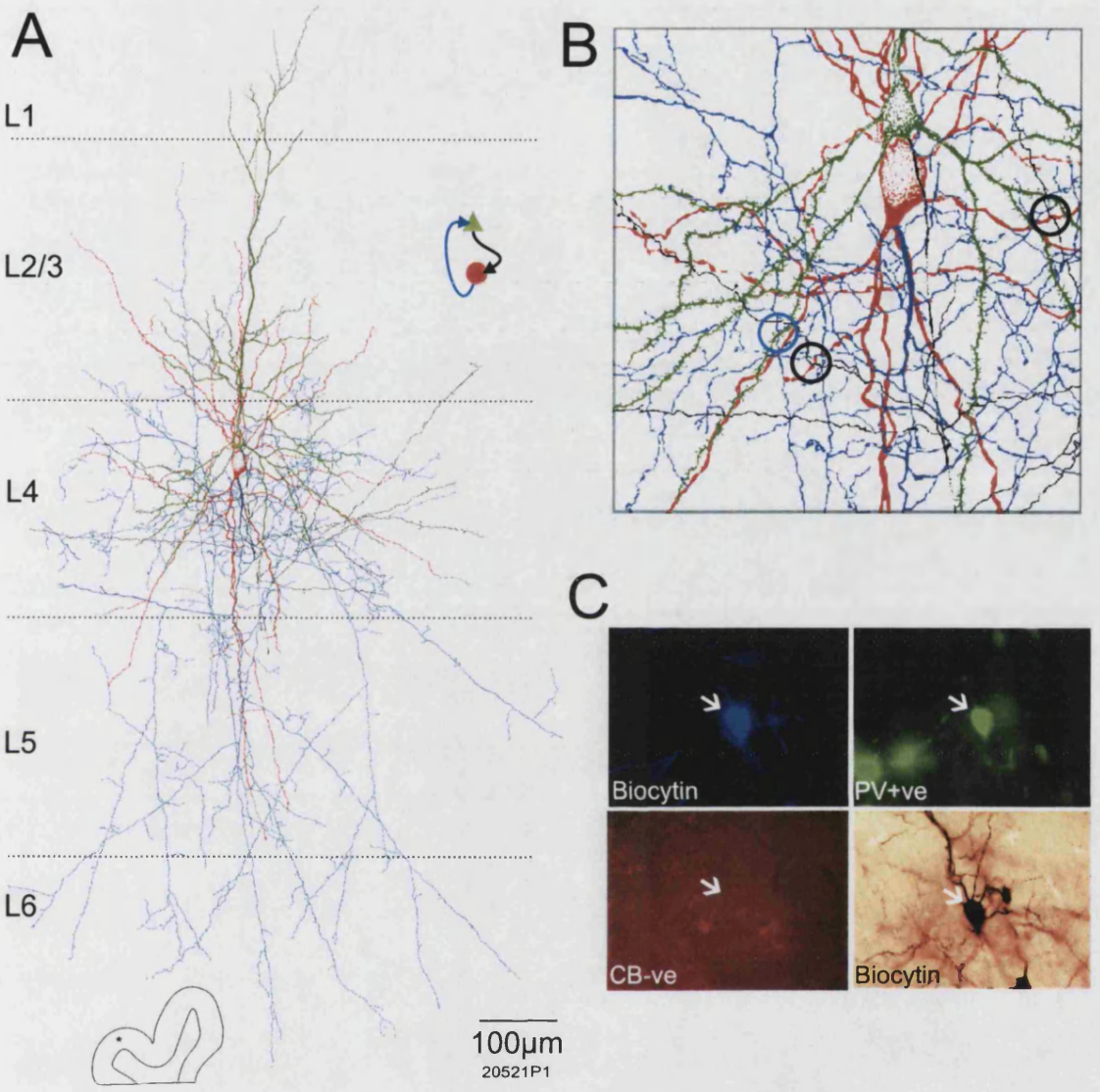

Figure 5.3a. (20521p1c/d) Morphology of a reciprocally connected layer 4 FS interneurone and layer 4 pyramidal cell from cat neocortex reconstructed at x1000. A, The interneurone is illustrated with red soma and dendrites and blue axon. The pyramidal soma and dendrites are in green and axon in black. B, enlarged portion of A indicating 2 axo-dendritic contacts from the pyramidal cell to the interneurone (black circles) and one axo-dendritic contact from the interneurone to the pyramidal cell (blue circle). C, Immunofluorescence photomicrographs of biocytin labelling with both AMCA (blue) and permanent DAB labelling, Parvalbumin with FITC (green) and Calbindin with Texas red. The cell was immunopositive for PV and negative for CB. The EPSPs and IPSPs exhibited at these connections are illustrated in figure 5.3b.

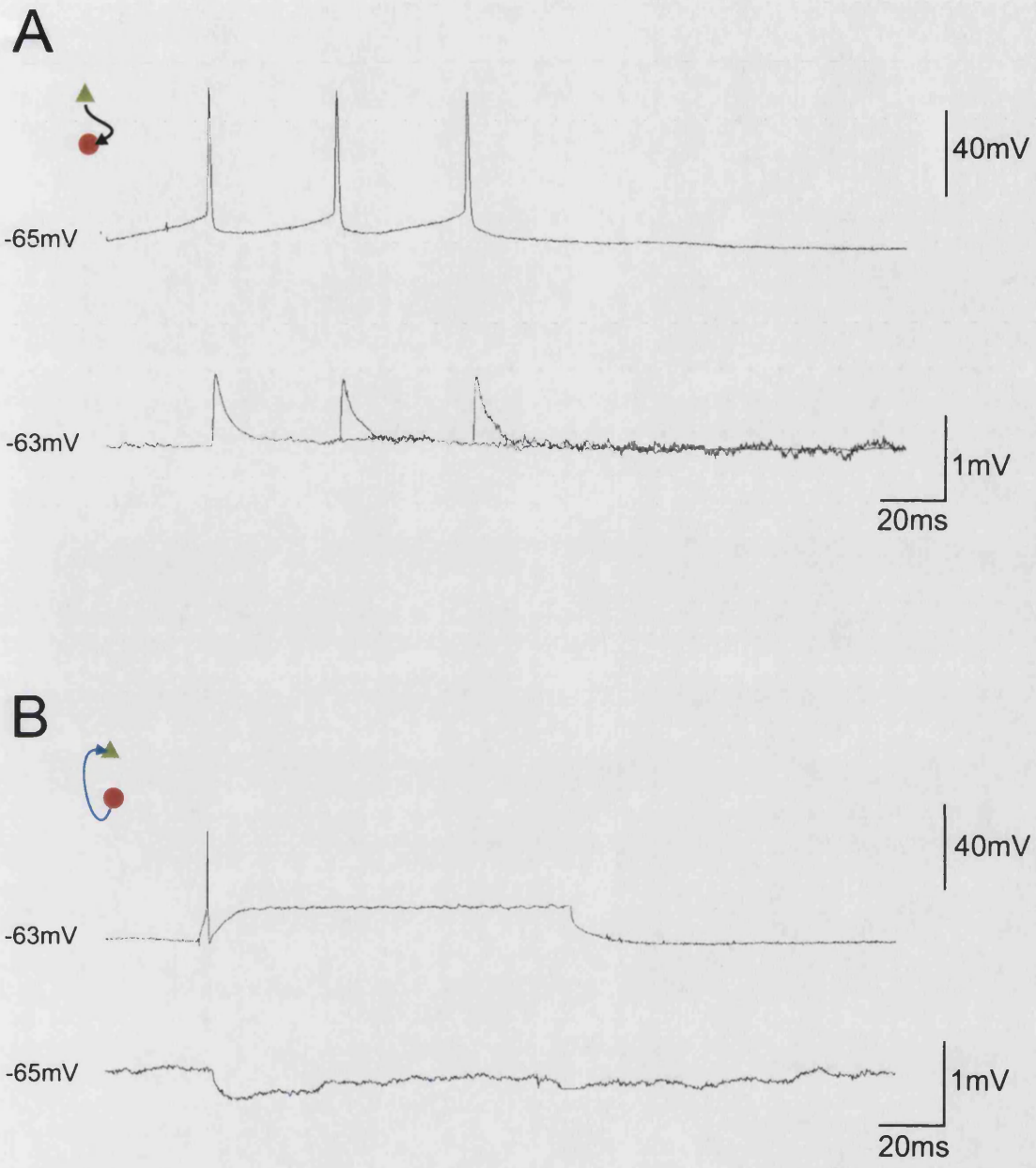

Figure 5.3b. (20521p1c/d) Reciprocally connected FS interneurone and pyramidal cell in layer 4 of cat cortex. A, Averages of 1st (583 sweeps), 2nd (38 ±1ms from 1st, 14 sweeps) and 3rd (40 ±1ms from 2nd, 13 sweeps) EPSPs elicited in the interneurone show little depression at these intervals. The interneurone was parvalbumin positive and CB negative. B, average 1st IPSP (39 sweeps). The anatomy of these cells is illustrated in figure 5.3a.

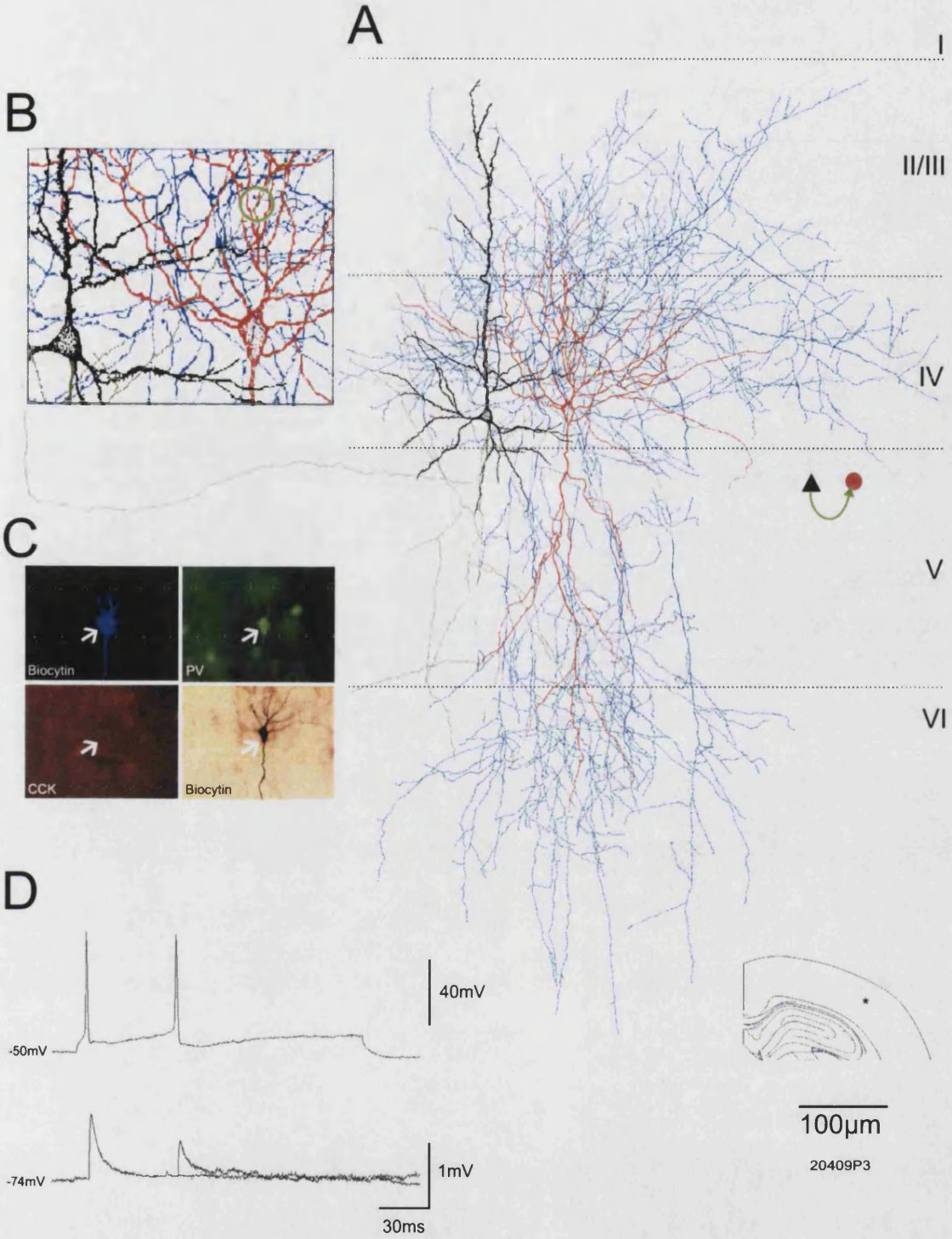

Figure 5.4. (20409p3) Morphology of a rat layer IV FS interneurone that was postsynaptic to a layer IV pyramidal cell reconstructed at x1000. A, The interneurone is illustrated with red soma and dendrites and blue axon. The presynaptic pyramidal cell soma and dendrites are in black and the axon green. B, enlarged portion of A indicating 1 axo-dendritic contact from the presynaptic pyramidal cell to the interneurone (green circle). C, Photomicrographs of permanent biocytin labelling with DAB and Immunofluorescence of biocytin labelling with AMCA (blue), Parvalbumin with FITC (green) and CCK with Texas red. The cell was immunopositive for PV and negative for CCK. D, Average EPSPs illustrating the strongly depressing connection. The average 1st EPSP is made from 429 sweeps, the 2nd EPSP average is made from 86 sweeps 35±1ms from the 1st.

Figure 5.5a illustrates the dendritic arbour of an irregular spiking layer IV interneurone that received a 0.13mV average first EPSP that facilitated with subsequent presynaptic action potentials in trains of up to 7. One potential synaptic contact was observed on a tertiary basal dendrite from a layer IV pyramidal cell. This interneurone also made an inhibitory connection with another layer IV pyramidal cell (IPSP -1.45mV in amplitude at MP -57mV) (see figure 5.5b). Immunofluorescence for parvalbumin and VIP was negative. The cell body was situated deep in layer IV from which 1 primary dendrite emerged from the top and terminated without branching in superficial layer IV. Two primary dendrites emerged from the bottom and branched to produce 11 last order branches that terminated in layer IV or upper layer V. The cell was poorly labelled with no axon staining at all, perhaps due to the electrode being inserted into the nucleus which was well filled with biocytin when observed with fluorescence microscopy. The dendrites were fine, pale and may not represent the complete arbour but do indicate the cell received the majority of its inputs close to the layer IV/V border.

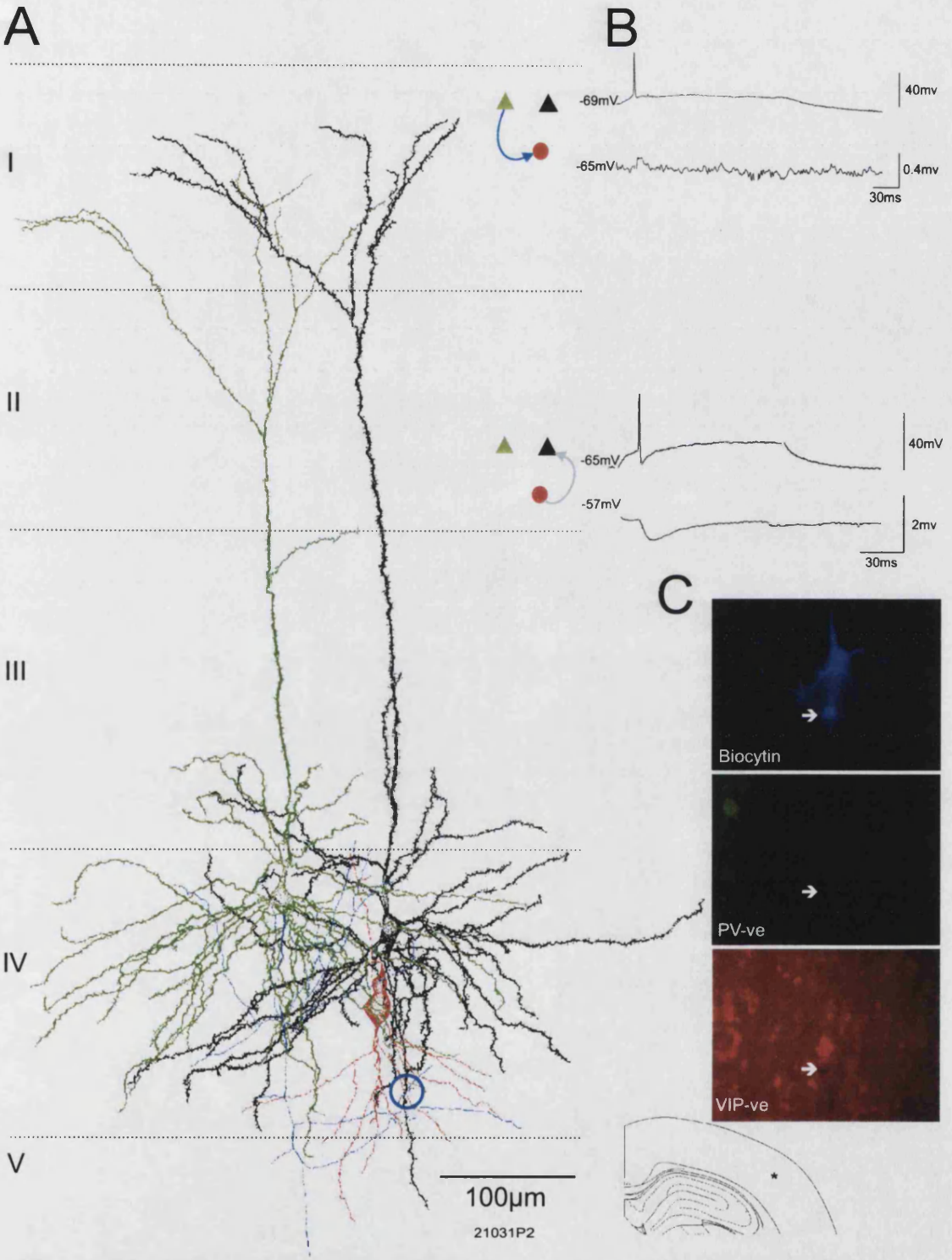

Figure 5.5a. Morphology of a rat layer IV IS interneurone that was presynaptic to one layer IV pyramid and postsynaptic to another (21031p2) reconstructed at x1000. A, The presynaptic pyramidal cell dendrites (green) and axon (blue) and the postsynaptic cell dendrites (black). The interneurone dendrites are in red (the axon was not filled). The interneurone receives one dendritic close apposition (blue circle). B, examples of electrophysiological recordings of both a facilitating EPSP from the green layer IV pyramid to the interneurone and an IPSP elicited in the black postsynaptic pyramid. C, Immunofluorescence photomicrographs of biocytin labelling with AMCA (blue) Parvalbumin with FITC (green) and VIP with Texas red. The cell was immunonegative for both PV and VIP. The electrophysiological characteristics of these connection is described in more detail in figure 5.5b

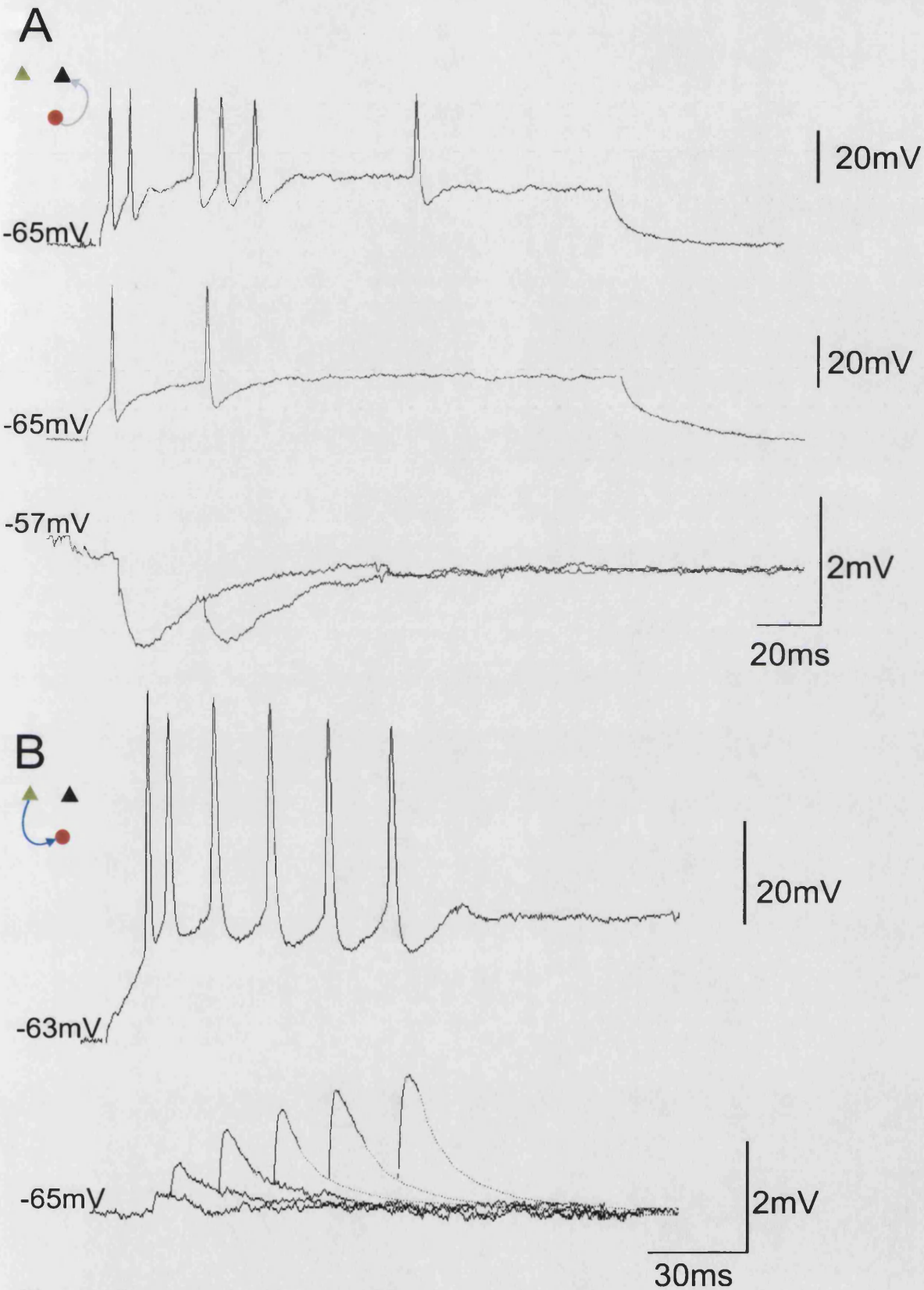

Figure 5.5b. (21031p2a/b) PSPs generated in and by a layer IV rat irregular spiking interneurone immunonegative for PV and VIP. A, An example of the presynaptic firing pattern and depressing IPSPs elicited in a RS layer IV pyramidal neurone from 2 spikes. B, Facilitating EPSPs elicited in the interneurone by another RS layer IV pyramid. Averages were triggered on the rising phase of spikes at intervals ±1ms of the preceding spike (17-59 sweeps per average). In B, the averages of the 1st four EPSPs were made using sweeps containing 1 to 4 spikes respectively, the 5th and 6th EPSP averages were made from sweeps containing up to 9 spikes. The anatomy of the cells involved in these connections is illustrated in figure 5.5a.

5.4 Electrophysiology.

A total of 9 cat and 6 rat layer 4 interneurones including all of those described and illustrated above were pre and/or postsynaptic to pyramidal cells in the vicinity were recorded during the course of these studies. At the time of the experiments their firing patterns were noted and exhibited a range including regular spiking (RS), fast spiking (FS) and irregular spiking (IS). No burst firing (BF) interneurones were recorded.

The RS interneurones had a firing pattern similar to that of the pyramidal cells with spike frequency adaptation over the duration of the square wave current pulse injections such that discrimination of pyramidal cells and this class of interneurones is more difficult to achieve in the absence of inhibitory potentials in postsynaptic cells. However, the interneurones of all firing patterns including the RS cells typically had action potentials that were shorter in duration than those of pyramidal cells (see figure 5.6).

The FS interneurones were characterised by rapid repetitive action potentials when depolarised that showed little or no spike frequency adaptation. Four of 6 FS interneurones from layer 4 (3 cat, 1 rat) tested positive for parvalbumin (the remaining 2 were not located during immunofluorescence).

One IS interneurone was identified that discharged a burst of action potentials followed by spikes emitted at an irregular frequency (see figure 5.5).

5.6 The correlation of morphology, firing characteristics and neurochemistry of layer 4 interneurones.

Table 5.1 shows the anatomical dendritic/axonal characteristics, input/output layer preferences, postsynaptic targets, firing properties and immunochemistry of all the synaptically connected layer 4 interneurones recorded onto tape from cat and rat cortex. The location, firing properties and the nature of PSPs to or from the pre and postsynaptic pyramidal cells are listed to attempt to correlate interneuronal properties of individual cell classes and with pre/postsynaptic targets and the behaviour of their synaptic potentials.

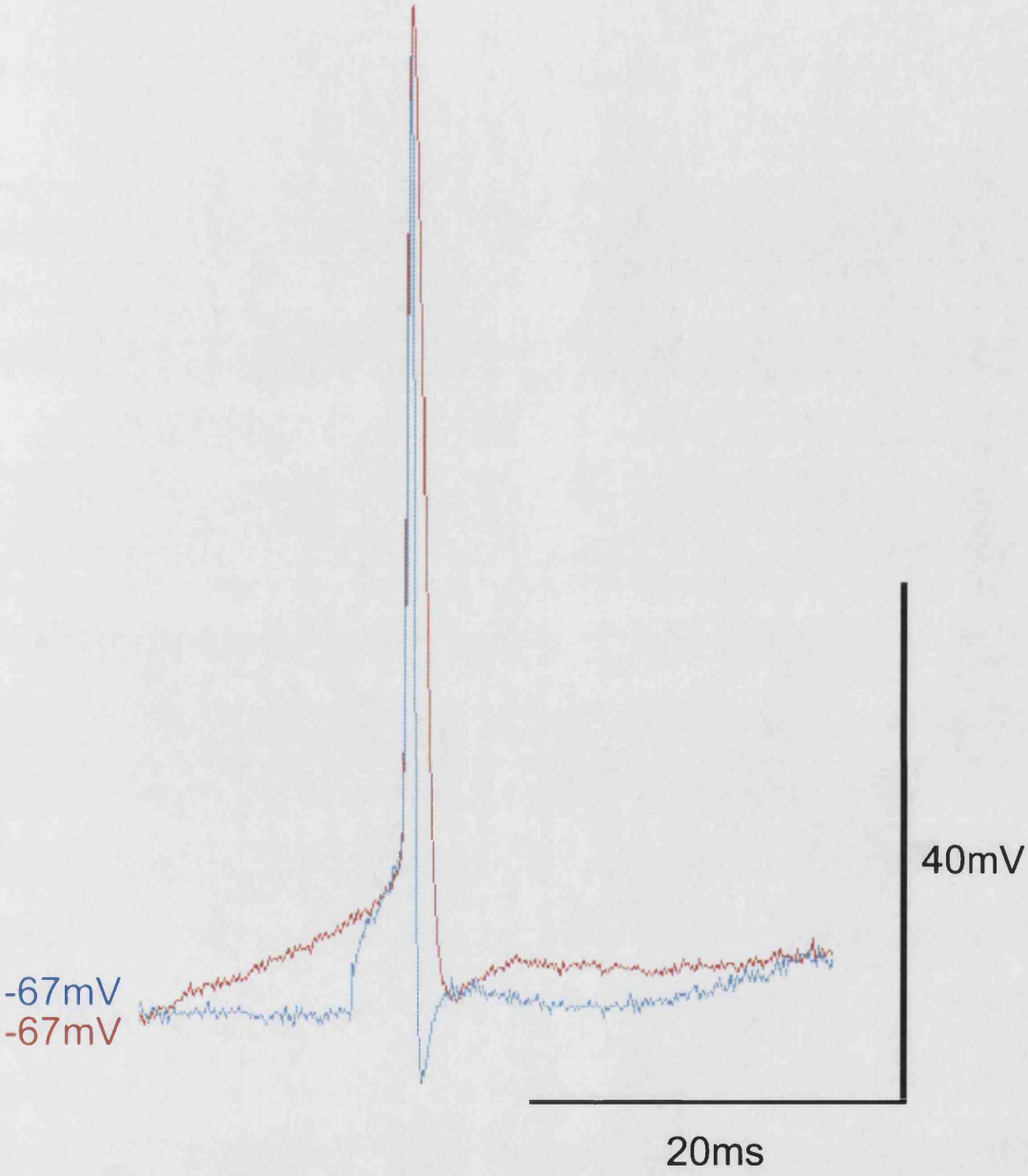

Figure 5.6. Typical spikes from a regular spiking pyramidal cell (red) and a regular spiking interneurone (blue) from cat layer 4 superimposed (raw data). The cells have similar membrane potentials and firing frequencies but the interneurone spikes repolarise in half the time taken for those of pyramidal cells. This interneurone has complex AHPs following the action potential.

Certain characteristics are apparent between all classes of interneurones recorded. Firstly, all of the cells were either pre and/or postsynaptic exclusively to regular spiking pyramidal cells with no apparent connections to or from the burst firing cells in the vicinity which represented some 37% of the layer 4 pyramidal cell population recorded throughout these studies.

All of the FS interneurones that were recorded, filled and identified during PV/CB fluorescence microscopy were immunopositive for Parvalbumin and not for Calbindin. Five of six FS interneurones were successfully labelled for biocytin and of these all were multipolar. All were pre and/or postsynaptic to RS pyramidal cells in layer 4 and where the interneurone was postsynaptic the excitatory PSPs were depressing.

Where permanent biocytin labelling was successful the RS interneurones were also multipolar. However, none of the RS interneurones identified at fluorescence microscopy (3 of 4) was immunopositive for Parvalbumin or Calbindin. All were pre and/or postsynaptic to RS layer 4 pyramidal cells (one was also presynaptic to a RS layer 3 pyramid). In the one case where the RS interneurone was postsynaptic to a layer 4 pyramid the EPSPs were facilitating. All 4 RS cells were presynaptic to pyramidal cells and where putative synaptic contacts were observed the interneurones appeared to be dendrite targeting. One RS interneurone made 3 and 6 observed axo-dendritic close appositions with 2 pyramidal cells respectively. Another RS interneurone made 4 putative contacts with the apical tuft and 2 to basal dendrites of the same postsynaptic pyramid. One reciprocally connected FS, PV immunopositive and CB negative interneurone also appeared to contact a pyramidal basal dendrite. Of all the putative contacts identified with layer 4 pyramids, all appeared to be onto basal dendrites whereas one layer 3 pyramid received both basal and dendritic tuft appositions.

Only one bipolar interneurone was identified in these studies. This cell had irregular spiking properties, was immunonegative for PV and CB and received a strongly facilitating excitatory connection from a RS layer 4 pyramidal cell.

Species	Presynaptic Interneurone Properties										Postsynaptic Pyramid Properties				
	Pair ID	Pre/ post	MP (mV)	FP	Immuno	Soma	Dendritic Span	Axon Span	Axon Preference	Target	Layer	MP (mV)	FP	IPSP Amp (mV)	Putative synapse target
Cat	20430p1b/c	pre	-50	RS	PV -ve/CB -ve	Stellate	L4	L1-L6	L4,L6,L1,L3,L5,L2	2x L4Pyramid	4P 4P	-45 -63	RS RS	-1.53 -0.53	3xBasal 6xBasal
	20501p2c	both	-57	RS	PV -ve/CB -ve	Stellate	L4-L3	L1-L4	L4,L3,L2,L1	1x L3 Pyramid	3P	-46	-	-0.42	2xBasal + 4xTuft
	20510p2b	pre	-57	RS	PV -ve/CB -ve	-	-	L4-L3	L4,L3	1x L4 Pyramid	4P	-55	-	-0.3	-
	20521p1d	both	-63	FS	PV+ve/CB -ve	Stellate	L3-L5	L2-L6	L4,L5,L6,L3,L2	1x L4 Pyramid	4P	-76	RS	-0.21	1xBasal dendrite
	20611p1	pre	-63	FS	PV+ve/CB -ve	Stellate	L3-L6	L4	L4	1x L4 Pyramid	4P	-65	RS	-1.22	-
Rat	20219p4	pre	-65	FS	-	Stellate	L4-L3	L3-L4	L3,L4	1x L4 Pyramid	4P	-51	RS	-0.54	-
	20227p1	pre	-73	S	-	-	-	-	-	1x L4 Pyramid	4P	-65	-	-1.23	-
	21031p1	pre	-50	RS	-	-	-	L4	L4	1x L4 Pyramid	4P	-64	RS	-1.51	-
	21031p2a	both	-65	IS	PV-ve/VIP-ve	Bipolar	L4	-	-	1x L4 Pyramid	4P	-57	RS	-0.7	-

Species	Postsynaptic Interneurone Properties									Presynaptic Pyramid Properties					
	Pair ID	Pre/ post	MP (mV)	FP	Immuno	Soma	Dendritic Span	Axon Span	Axon Preference	Layer	FP	EPSP 1st Amp (mV)	EPSP Fac/ Dep	EPSP PPR (interval)	Put. Syn. Target
Cat	20501p2b	both	-57	RS	PV -ve/CB -ve	Stellate	L4-L3	L1-L4	L4,L3,L2,L1	4P	RS	0.77	Fac	1.74 (35±1ms)	1x3*
	20510p1b	post	-75	FS	PV +ve/CB -ve	Stellate	L4-L2	L4-L2	L3,L4,L2	4P	RS	2.55	Dep	0.70 (51±1ms)	-
	20510p2a	post	-60	-	-	Stellate	L4	-	-	4P	RS	1.87	Dep	0.74 (35±1ms)	-
	20510p2c	post	-69	-	-	-	-	-	-	4P	RS	1.98	Dep	0.61 (47±1ms)	-
	20521p1c	both	-63	FS	PV +ve/CB -ve	Stellate	L3-L5	L2-L6	L4,L5,L6,L3,L2	4P	RS	0.77	Dep	0.88 (47±1ms)	1x1* 1x2*
Rat	20409p3a	post	-74	FS	PV+ve/CCK-ve	Stellate	L3-L6	L2-L6	L4,L3,L6,L5,L2	4P	RS	1.02	Dep	0.55 (35±1ms)	1x3*
	21031p2b	both	-65	IS	PV -ve/VIP -ve	Bipolar	L4	-	-	4P	RS	0.13	Fac	2.04 (40±1ms)	1x3*
	30520p3b	post	-55	FS	-	-	-	-	-	4P	RS	0.47	Dep	0.97 (36±1ms)	-

Table 5.1. Anatomical and neurochemical description of layer 4 interneurones recorded in cat and rat neocortex and their interaction with pyramidal cells in the vicinity. Pair IDs are the numbers given to identify each recording composed of the date, experimenter, slice number and a letter denoting the order of recordings from that slice. The axon preference field lists the cortical laminae receiving inhibitory innervation from the interneurone in order of axon density within those layers. Fac or Dep denotes facilitating or depressing EPSPs respectively and PPR refers to the paired pulse ratio at the given interval. The locations of synaptic contacts are based on the presence of close membrane appositions that could not be resolved as separate at light level microscopy.

5.7 Characteristics of EPSPs in layer 4 interneurones.

All excitatory neurones that were presynaptic to interneurones in this study were RS. The measurements of EPSP shape characteristics are given below (table 5.2) taken from averages (including apparent transmission failures) triggered by the rising phase of the presynaptic action potential in sweeps with only single spikes. All sweeps were obtained from portions of the recordings in which the membrane potential remained stable.

With this small sample of postsynaptic interneurones it is not possible to draw adequate conclusions as to differences in 1st EPSP amplitude and shape properties that could correlate with the class of interneurone innervated. However, it should be noted that the most powerful 1st excitatory inputs were onto the FS parvalbumin immunopositive interneurones in both species.

The mean EPSP amplitudes in interneurones and those in pyramidal cells described in the previous section were not significantly different at 1.82 ±0.84mV and 1.59 ±0.79mV for pyramid to pyramid or pyramid to interneurone connections respectively in cat tissue and 0.92 ±0.78mV and 0.54 ±0.45mV for pyramid to pyramid or pyramid to interneurone connections respectively in rat material. However, the EPSP shape properties at excitatory inputs onto the interneurones were different. Rise times and half widths in the interneurones were shorter than those in the pyramids. Cat pyramid to pyramid EPSP RT was 1.24 ±0.39ms and HW 11.88 ±2.81ms compared with EPSP RT 0.7 ±0.29ms and HW 5.78 ±3.33 for pyramid to interneurone connections. This trend is continued in the rat connections with EPSP RT 1.95 ±0.82ms and HW 15.38 ±7.25ms for pyramid to pyramid connections compared with EPSP RT 0.5 ±0.17ms and HW 4.37 ±2.11 for pyramid to interneurone connections. Figure 5.7 illustrates the differences in EPSP duration exhibited by pyramid to pyramid and pyramid to interneurone connections in layer 4. Numerous factors that may influence the shape of EPSPs including the positions of contacts on the dendritic tree and the properties of postsynaptic receptors will be discussed in section 8.

Species	Cell ID	Immuno-fluorescence	Pre	MP post (mV)	Mean Amp (mV)	10-90% Rise Time (ms)	Half Width (ms)	%1st failure
CAT	20501p2b	-	RS L4 Pyr	-63	0.77	0.9	10.7	44.4
	20510p1b	PV+/CB-	RS L4 Pyr	-75	2.55	0.6	4.4	0
	20510p2a	-	RS L4 Pyr	-57	1.87	1.1	7.3	0
	20510p2c	-	RS L4 Pyr	-69	0.77	0.4	2	0
	20521p1c	PV+/CB-	RS L4 Pyr	-63	1.98	0.5	4.5	2.9
	Mean	-		-65.4	1.59	0.7	5.78	-
	±SD	-		6.8	0.79	0.29	3.33	-
RAT	20409p3a	PV+/CCK-	RS L4 Pyr	-74	1.02	0.3	3.1	1.5
	21031p2b	PV-/VIP-	RS L4 Pyr	-65	0.13	0.6	6.8	74
	30520p3b	-	RS L4 Pyr	-55	0.47	0.6	3.2	6.3
	Mean	-		-64.6	0.54	0.5	4.37	-
	±SD	-		9.5	0.45	0.17	2.11	

Table 5.2. Properties of first EPSPs in layer 4 interneurones with available neurochemical properties. The largest and fastest EPSPs were observed in PV immunopositive interneurones from both species.

5.9 Paired Pulse and Brief Train EPSP properties.

5.9.1 Depression.

Four recordings of postsynaptic interneurones from cat and 2 from rat exhibited depressing EPSPs in which the average EPSP amplitude for the second and all subsequent EPSPs were depressed relative to the first. Where immunofluorescence was performed (and the interneurone identified) the depressing connections were all onto neurones immunopositive for PV and negative for CB. Where the recordings were of suitable quality to analyse the recovery from depression (with sufficient sweeps at a range of interspike intervals) the rate of recovery was similar to that observed in pyramidal cells with the strongest depression apparent at short interspike intervals and progressive recovery in amplitude occurring as the interspike interval was lengthened. Figure 5.8 illustrates the recovery from depression for a pyramid to interneurone connection with second EPSPs at progressively longer intervals from the 1st. The paired pulse ratio (PPR) for these

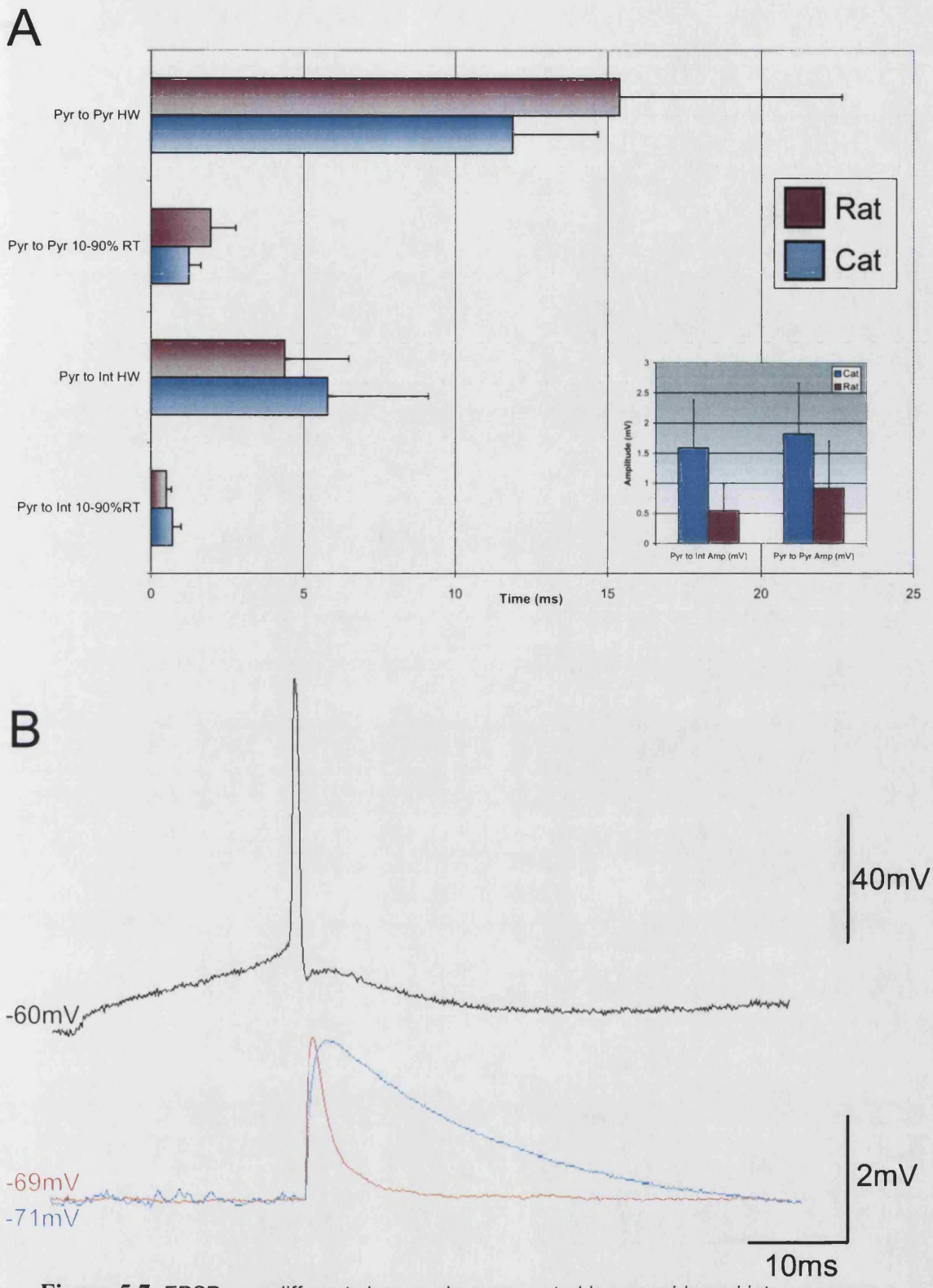

Figure 5.7. EPSPs are different shapes when generated in pyramids and interneurones. A, Bar plot comparing half width and 10-90% rise time of EPSPs generated in pyramid to pyramid and pyramid to interneurone connections throughout these studies. Note that RT and HW are larger in pyramid to pyramid connections. The EPSP amplitudes do not differ significantly. B, Examples of the averaged first EPSP (291 sweeps) in a pyramidal cell (blue) and in an interneurone (75 sweeps in red) in layer 4 of cat neocortex. Both postsynaptic cells have similar membrane potentials. Note that the EPSP in the interneurone is considerably shorter in duration than that in the pyramidal cell. In both cases the presynaptic cell was a pyramid in layer 4.

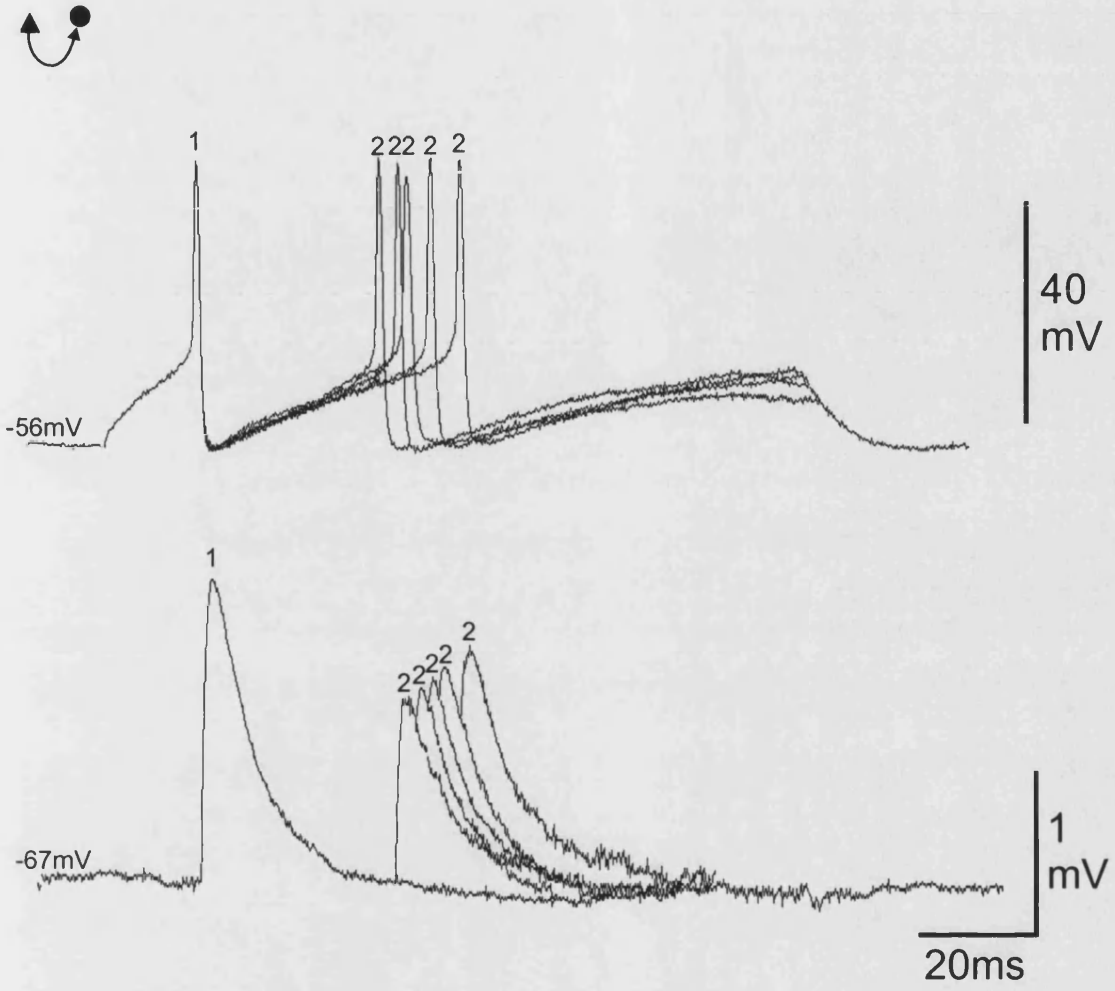

Figure 5.8. Example illustrating recovery from paired pulse depression for a cat pyramid to interneurone connection in layer 4. The average 1st EPSP was made from 79 sweeps triggered on the rising phase of the 1st spike. Average 2nd EPSPs were made from records at which the second presynaptic spike occurred 31, 34, 35, 39 and 43 ±1ms from the 1st (17,24,36,28 and 11sweeps respectively). Note that with increasing interspike interval the 2nd EPSP amplitude recovers to approach that of the average 1st.

depressing connections were calculated from averaged 1st and 2nd EPSP amplitudes where the second AP fell within a 2ms time window from the 1st at an interval with enough sweeps to allow adequate averages to be made (ie. the averaged 1st EPSP triggered on the 2nd spike should match the shape of the average triggered on the 1st). The PPRs given below were calculated from averaged 1st and 2nd EPSPs (>10 sweeps per average). The mean PPR for the depressing cat pyramid to pyramid connections was 0.73 (range 0.61 - 0.88 in 2ms windows between 35 and 51ms from the 1st AP) and for rat was 0.76 (range 0.55 - 0.97 in 2ms windows between 35 and 40ms from the 1st AP). These data indicate that the depressing EPSPs exhibited by the interneurones of layer 4 decreased in amplitude by 27% and 24% between the 1st and 2nd EPSPs at these intervals for cat and rat cells respectively.

Transmission failures at depressing connections.

For all layer 4 pyramid to layer 4 interneurone connections recorded, single sweep peak amplitude measurements were taken for each EPSP in trains of up to 10 under direct visual control. Apparent failures of transmission were entered as zero. Data sets containing >30 sweeps for each EPSP in trains for each connection were binned in 0.2mV subsets the amplitude distribution plotted to identify trends of apparent transmission failure relating to the depression observed.

Of the 4 cat and 2 rat depressing layer 4 pyramidal cell to layer 4 interneurone connections observed, 3 cat pairs showed no apparent failures of synaptic transmission in response to the 1st action potential throughout the recordings. Of the remaining 3 recordings the 1st AP failure rate was 2.87% (16 of 557 sweeps) for the cat pair and for the rat recordings 1.53% (9 of 588 sweeps) and 6.25% (3 of 48 sweeps). In all recordings (bar one cat pair that depressed only very slightly) the probability of apparent transmission failure showed a tendency to increase with each successive action potential in a train. This increased failure rate is an indication that the depression observed at these connections is (as with the pyramid to pyramid connections of the previous section) presynaptic in origin as a function of decreased probability of release or a reduction in the number of available release sites. Amplitude distribution histograms were plotted for all EPSPs for which adequate sweeps (>30) were collected and are shown in figure 5.9.

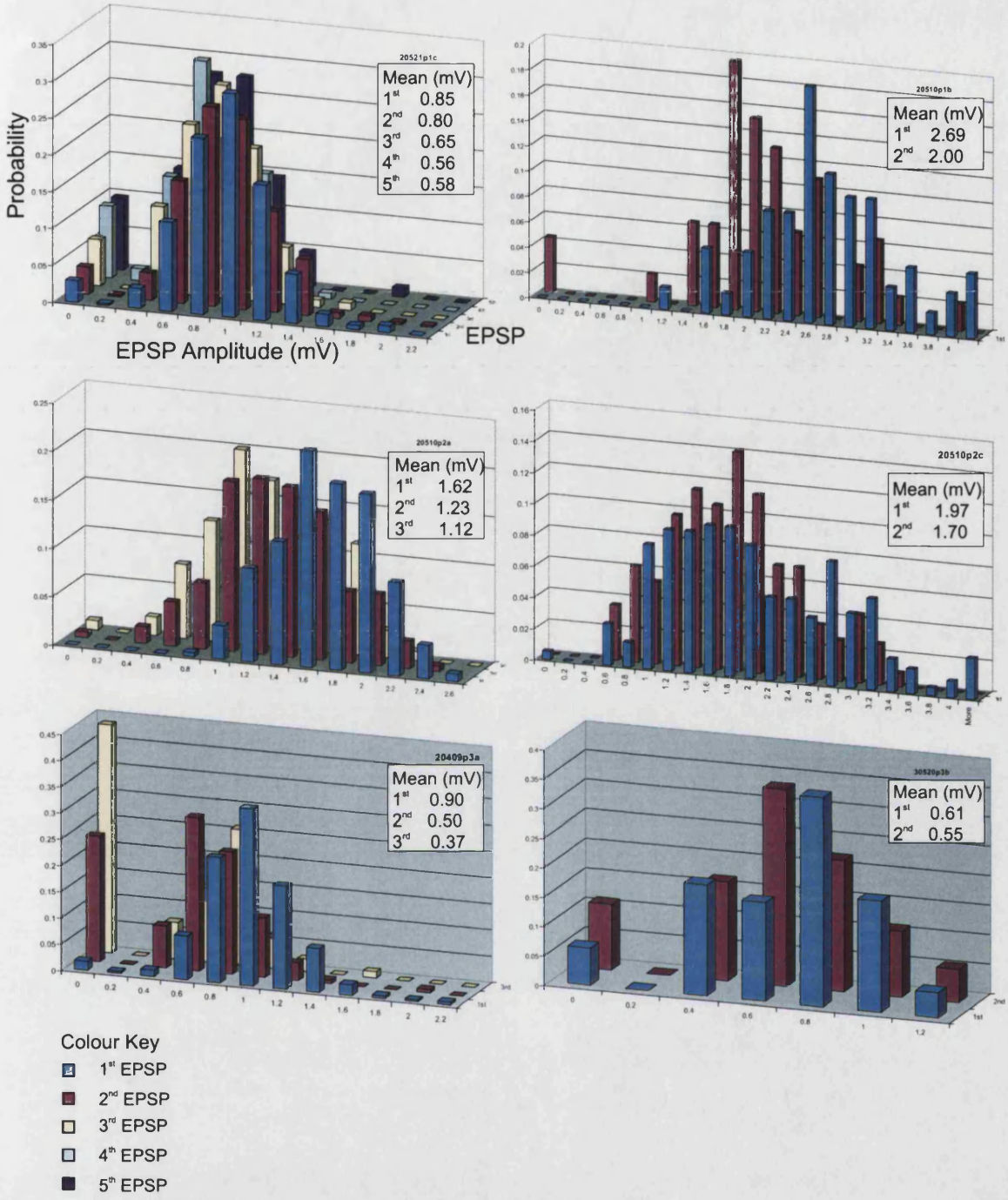

Figure 5.9. Amplitude distribution histograms for 1st, 2nd (3rd, 4th, 5th) EPSPs irrespective of interspike intervals for depressing layer 4 pyramid to layer 4 interneurone connections in cat and rat cortex. 4 cat recordings (top - white walls) and 2 rat recordings (bottom - grey walls). Data subsets were binned coarsely (0.2mV) and plotted with gaps between the subsets to aid visibility of the data for 2nd, (3rd...) EPSPs in these 3D plots. All of the connections shown here were depressing as is indicated by the progressive shifts in amplitude frequency towards the left of those for preceding EPSPs. Note that in all but one cat recording (which depressed only very slightly on average) there is a progressive increase in probability of apparent transmission failure.

5.9.2 Facilitation.

Two recordings of postsynaptic interneurones (1 rat, 1 cat) exhibited facilitating EPSPs in which the average second EPSP was larger in amplitude than the first. The cat cell was stellate and RS and the rat cell was bitufted and IS. Both cells were immunonegative for PV and CB.

As with the decay of depression, the strength of facilitation appears to decay with increasing interspike interval. However the recovery of EPSPs from facilitation with increased interspike intervals is difficult to measure and plot accurately due to the very low amplitude of EPSPs in response to early spikes in trains (the later and larger EPSPs in response to longer trains occurring at an insufficient range of interspike intervals). The PPR for these connections was 1.74 (within 34-36ms of the 1st EPSP) for the cat pair and 2.04 (within 39-41ms of the 1st EPSP) for the rat connection indicating that in these connections at these intervals the average second EPSP in trains was 174% and 204% of the mean 1st EPSP in cat and rat connections respectively.

Transmission failures at facilitating connections.

Of the 2 facilitating layer 4 pyramid to layer 4 interneurone connections recorded (1 cat and 1 rat), both had apparent failures of transmission in response to the 1st action potential in trains of up to 10. For the cat connection the 1st failure rate was 44.43% (383 of 862 sweeps) and for the rat pair 73.98% (785 of 1061 sweeps). Amplitude distribution histograms for the 1st to 6th EPSPs were plotted for the cat interneurone (figure 5.10) and the rat interneurone (figure 5.11) and both showed a progressive shift in peak EPSP amplitude to the right reflecting the increasing amplitude observed in successive averaged EPSPs. Both connections also showed a progressive decrease in failure rate compared to the preceding EPSP in the trains.

Figure 5.12 shows a plot of normalised CV^{-2} against normalised EPSP amplitude for the 2nd and 3rd EPSPs at 21 ±1ms interspike intervals normalised against the 1st EPSP for both of the facilitating layer 4 pyramid to layer 4 interneurone connections from cat and rat. The majority of points fall with a slope >1 indicating the facilitation is the result of presynaptic mechanisms (ie. increased probability of release and/or increased number of available release sites).

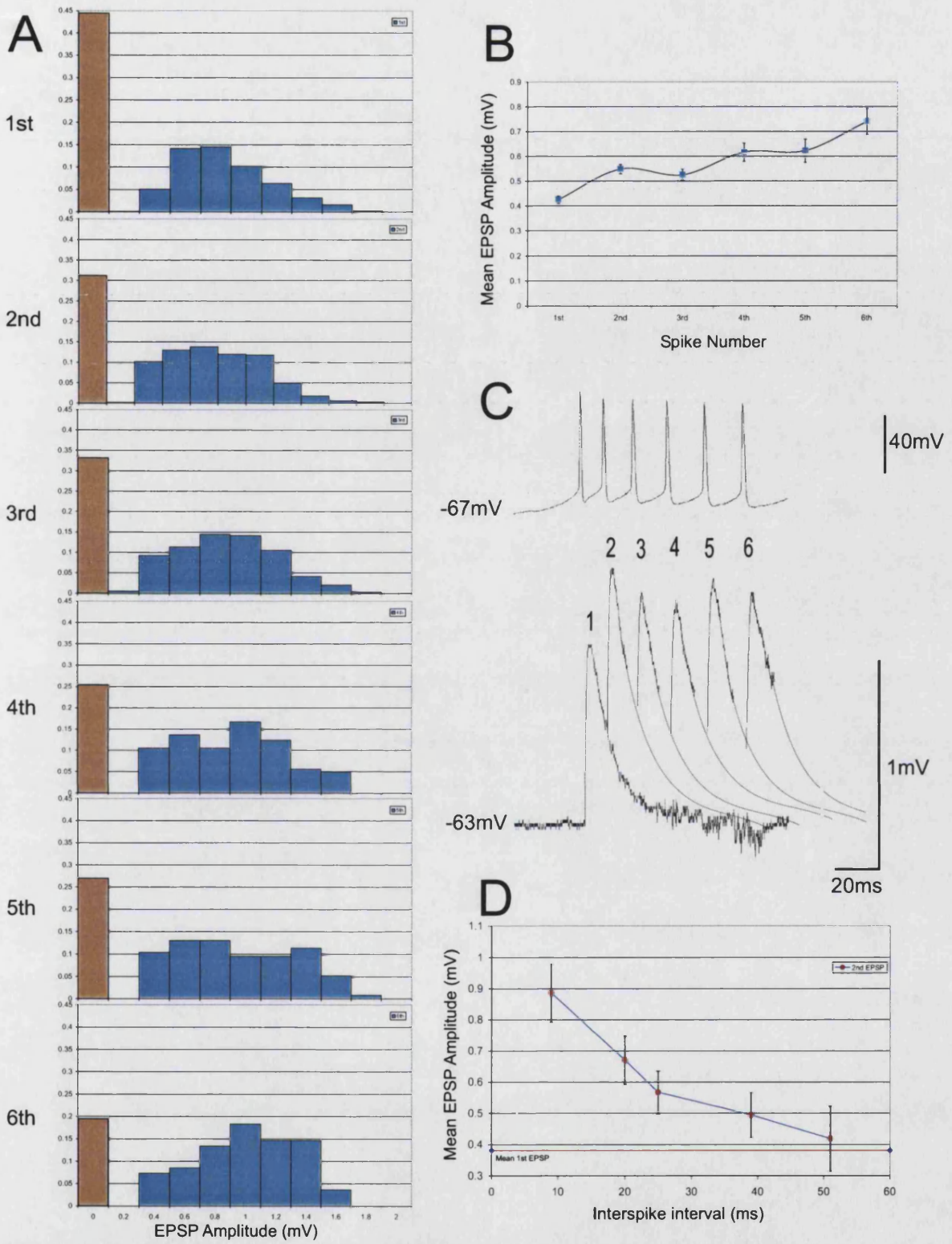

Figure 5.10. 20501p2b. A, Conventional EPSP amplitude distribution histograms for 1st, 2nd.....6th EPSPs binned coarsely (0.2mV). The EPSP amplitude tends to shift to the right with each spike indicating an increase in general amplitude and the probability of transmission failure tends to decrease with each spike indicating the mechanism for this facilitation is of presynaptic origin. B, Plot of mean EPSP amplitude in response to each spike in trains of 6 irrespective of interspike interval showing a trend towards increased mean EPSP amplitude. C, Averages of 1st, 2nd...6th EPSP amplitude made from 56 consecutive sweeps with consistent firing frequency. Dotted lines represent the shape of the EPSPs in the absence of spike artefacts and were made from the 1st EPSP scaled to match the amplitude. D, Decay of facilitation with increased 1st to 2nd interspike interval. As the interval increases the facilitation of the second EPSP decays towards the mean 1st EPSP amplitude.

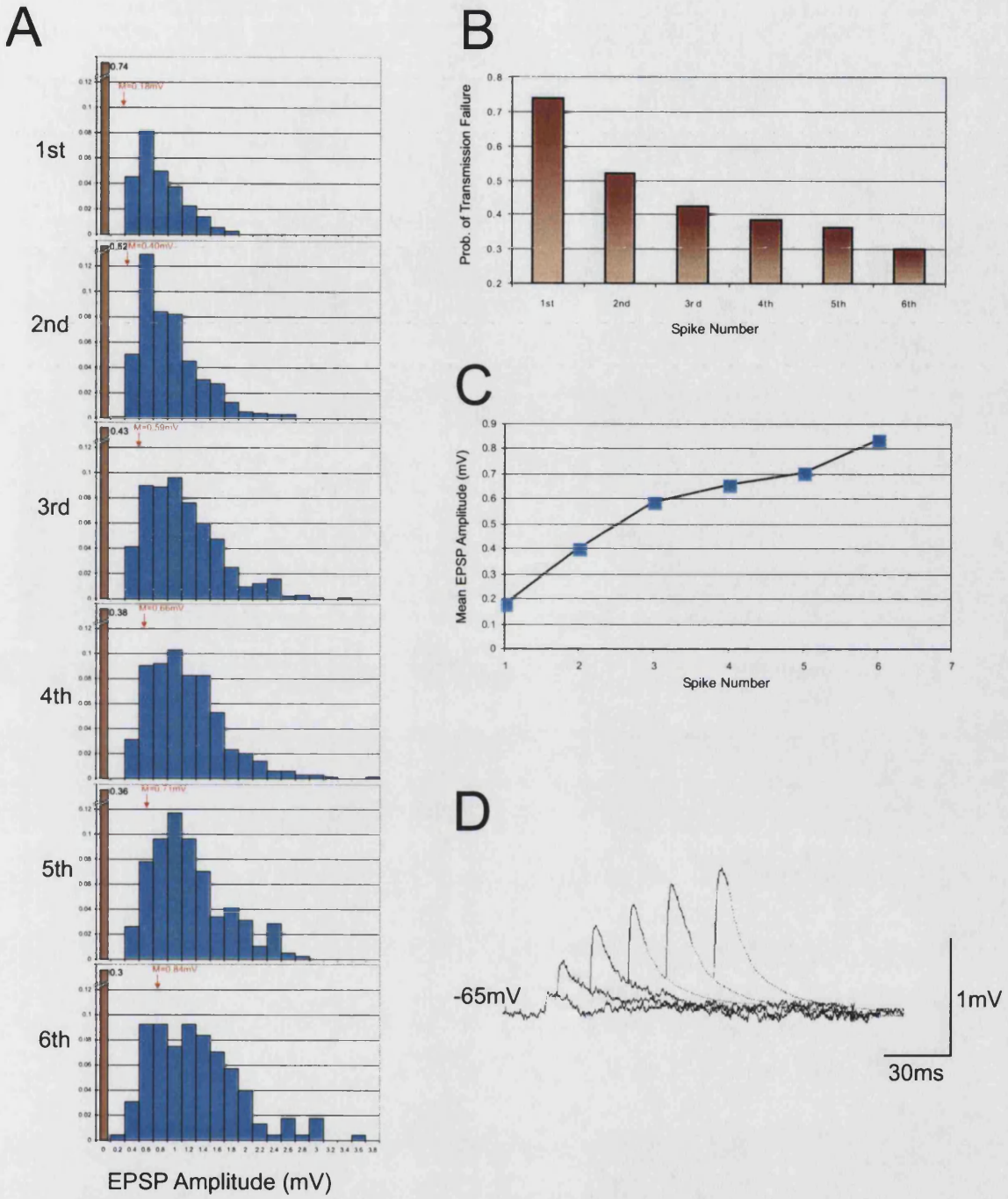

Figure 5.11. Facilitation of this pyramid to interneurone EPSP (21031p2b) appears to be due to increased probability of transmitter release. A, Histogram plots of EPSP amplitude distribution for 1st, 2nd.....6th EPSPs binned coarsely (0.2mV). The EPSP amplitude tends to shift to the right with each spike. B, Apparent transmission failures are plotted separately and show a decreased probability of failure for each spike. C, Plot of mean EPSP amplitude in response to each spike in trains of 6 irrespective of interspike interval (range: 10ms for 1st to 2nd AP increasing to 26ms for 5th to 6th AP) showing a consistent increase in mean EPSP amplitude. D, Averaged EPSPs triggered on the rising phase of the presynaptic action potential with interspike interval selection windows of ±1ms. The peak amplitudes are accurate representations of those EPSP averages, the decay phases of the 4th,5th and 6th EPSPs are distorted due to the inclusion of sweeps containing longer trains of spikes (17-59 sweeps per average), dotted lines used to represent EPSP shape for these sweeps were generated from a scaled average of the 3rd EPSP.

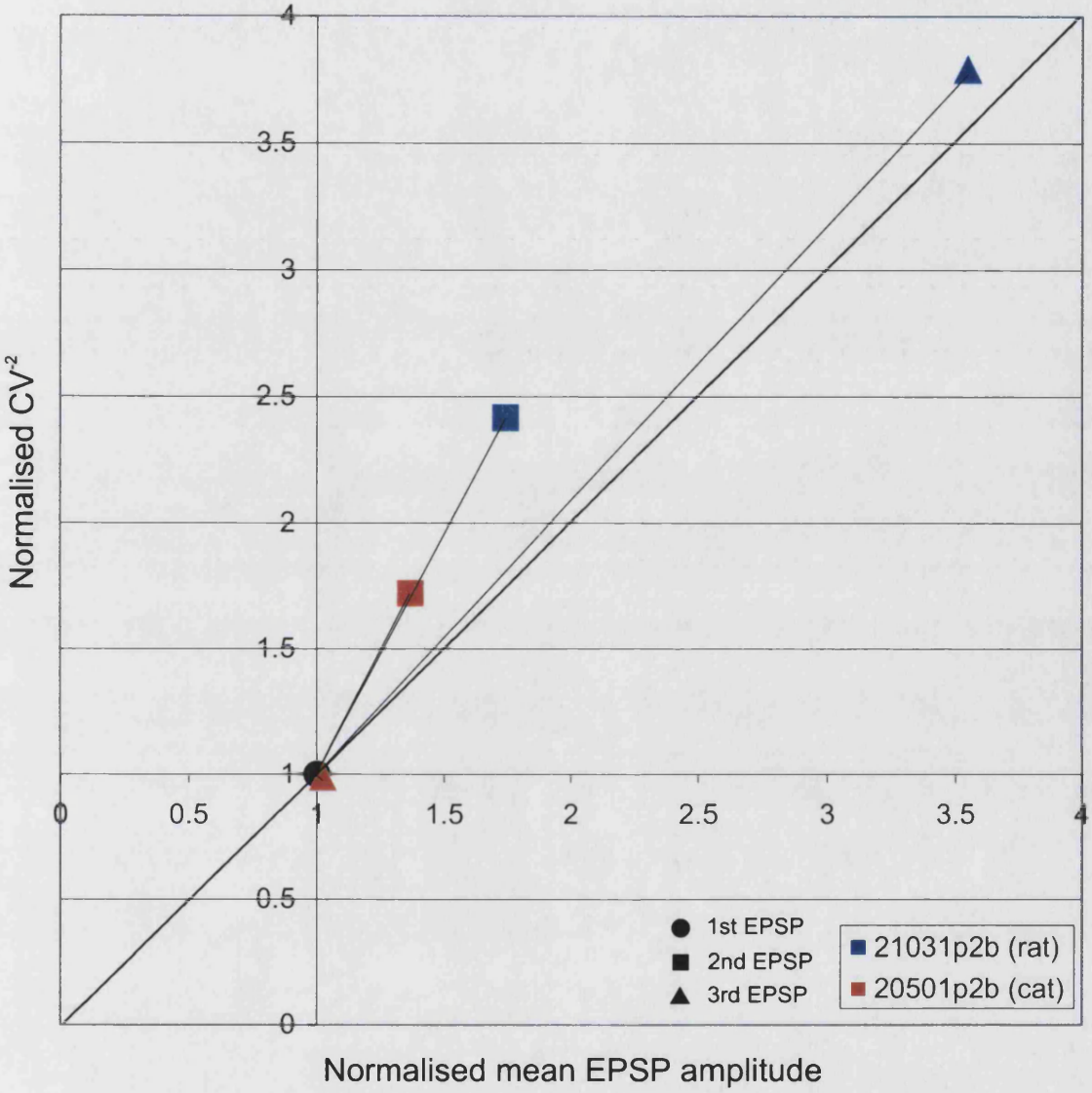

Figure 5.12. Normalised change in CV^{-2} equal to (np/(1-p)) in a binomial distribution plotted against normalised change in mean EPSP amplitude for 2nd, 3rd EPSPs in trains at interspike intervals of 21 ±1ms for two facilitating pyramid to interneurone connections in cat and rat layer 4. Most of the points fall with a slope >1 indicating that the facilitation of EPSP amplitude is presynaptic in origin corresponding with an increased probability of release (p) and/or the number of available release sites (n). The points in red correspond with the cat connection (20501p2b) and blue with the rat connection (21031p2b) with circles, squares, triangles representing 1st, 2nd and 3rd EPSPs respectively.

5.10 Feed Forward within Layer 4.

Spontaneous PSPs were apparent in all recordings of cells from all layers of the cortex in both species reflecting the activity of non-recorded cells and their influences on the recorded neurone pairs independent of any artificial driving of the cells towards action potential threshold. Indeed, the presence of spontaneous activity observed in impaled neurones at the time of the experiment was used (in part) to judge the general health of the area of each slice and therefore to aid the selection of regions likely to harbour many healthy cells and so provide a greater likelihood of impaling synaptically connected pairs.

In 24 paired recordings (out of 61) in both species, where the pre and/or postsynaptic cells were in layers 3 and 4, coincident spontaneous PSPs were exhibited and recorded in both cells of synaptically connected pairs (20 of EPSPs and 4 of IPSPs). The high incidence of coincident PSPs in both cells of recorded pairs of neurones indicated that both were receiving the same inputs from at least one other neurone. These data also indicate the high level of interconnectivity within these layers even in cortical slice preparations within which many axonal projections have been cut.

In one reciprocally connected pair of pyramidal cells from layer 4 of the cat cortex, both recordings of pre and postsynaptic membrane potentials revealed the presence of an individual, non-recorded interneurone exerting spontaneous simultaneous inhibitory PSPs in both cells. One of the two pyramids appeared to be connected to the non-recorded interneurone through which it regularly promoted disynaptic inhibition of itself and its reciprocally connected partner. When the pyramid to pyramid connection (for clarity I will call this recording P1 to P2) was recorded with spikes evoked in P1 the coincident IPSPs were scattered infrequently throughout the recordings, indicating that the interneurone was being driven by other cells (figure 5.13a). However, when pyramid P2 was driven to action potential threshold, the spontaneous IPSPs demonstrated temporal synchrony, regularly occurring in trains following the pyramidal cell action potential (figure 5.13b). The consistent timing of IPSP trains generated when P2 was driven and the absence of such synchrony when P1 was driven indicate that only cell P2 was involved in the generation of reliable disynaptic inhibition of itself and its reciprocally connected partner via a single non-recorded (and therefore unfilled) interneurone in the vicinity. The interval between each successive IPSP in the trains progressively increased suggesting that the non recorded interneurone was RS.

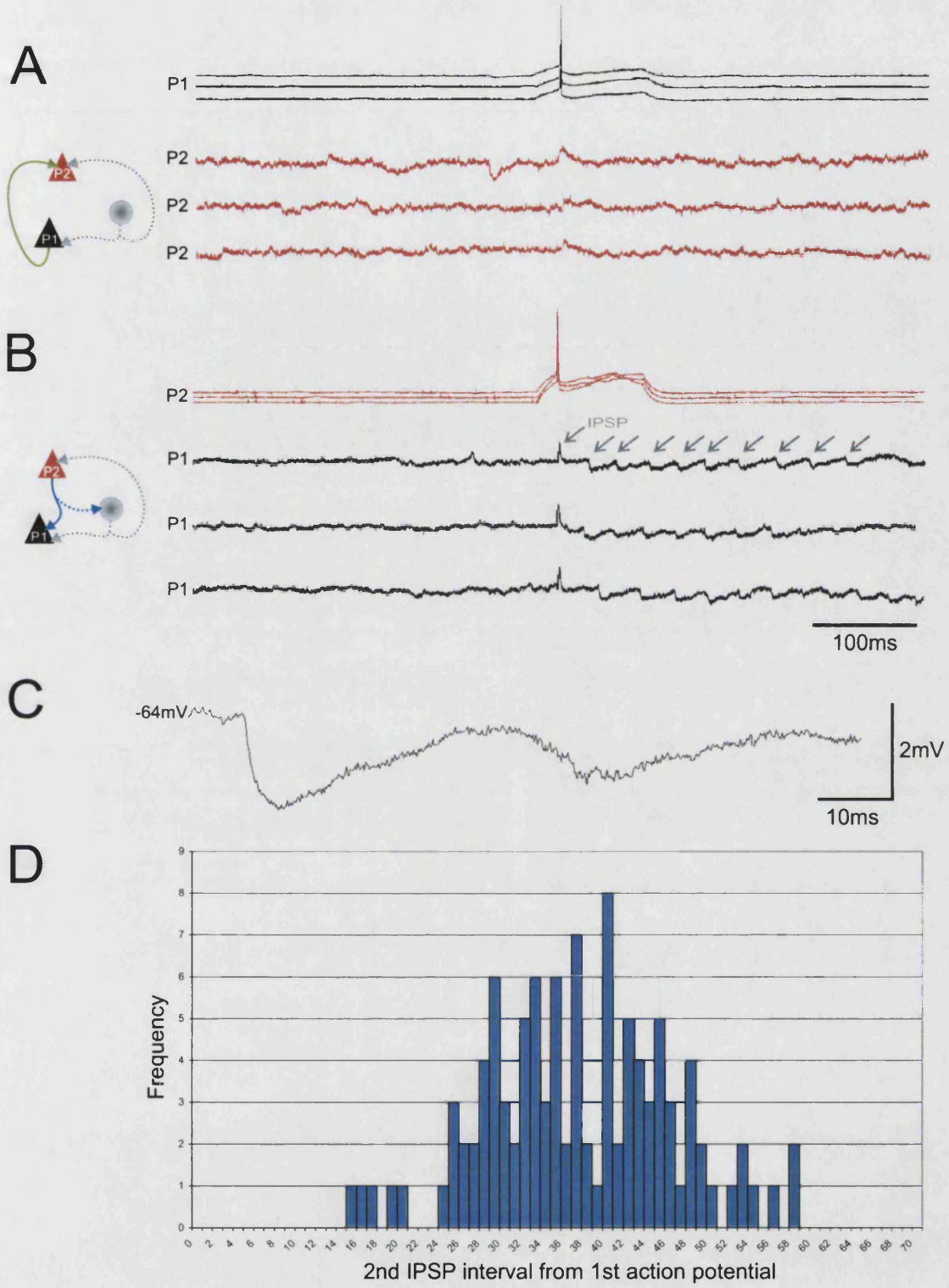

Figure 5.13. Disynaptic IPSPs are driven by one of two reciprocally connected pyramidal cells in cat layer 4. A, raw data (20521p2a) illustrating presynaptic spikes and postsynaptic EPSPs. Spontaneous IPSPs occur infrequently and are randomly distributed. B, raw data (20521p2b) of the same cells with spikes evoked in cell P2. Note that following the spikes in this recording, trains of IPSPs occur quickly with the first acting to repolarise the EPSP in cell P1. The total sweep length is 1 second with the action potential at 500ms. C, Twenty sweep average of the second IPSP in the trains generated in recording 20521p2b. D, interval histogram for second IPSPs after the pyramidal action potential in recording B (20521p2b). This distribution indicates that the IPSPs are not occurring spontaneously and are being actively driven by the pyramidal cell.

Figure 5.14a illustrates the excitatory connection between the two layer 4 pyramidal cells (P1 to P2) with simultaneous (non-disynaptic) IPSPs apparent in both the pre and postsynaptic recordings. Figure 5.14b shows recording P2 to P1 in which the interneurone was also receiving excitatory input from cell P2 and resulted in disynaptic inhibition of both pyramidal cells. The latency between the 1st pyramidal spike (P2) and the 1st IPSP was sufficiently short to repolarise 93.1% of the 1st EPSPs in P1 before they reached peak amplitude as illustrated in figure 5.14c. Averages of 1st EPSPs that were either interrupted or uninterrupted by the disynaptic IPSP were made from 197 and 31 sweeps respectively and measurements taken of peak amplitude and width at half amplitude. The average uninterrupted EPSPs had a peak amplitude of 2.19mV and HW of 14.6ms. The average interrupted EPSP peak amplitude was 1.94mV and HW 3.9ms. The difference between the uninterrupted and interrupted EPSPs was therefore -0.25mV and -10.7ms indicating that the disynaptic IPSP exerted its effects on the peak amplitude of the EPSP and profoundly upon EPSP duration potentially preventing trains of EPSPs generated by this presynaptic cell from reaching spike threshold without the intervention of other excitatory connections converging to summate within a narrow time window.

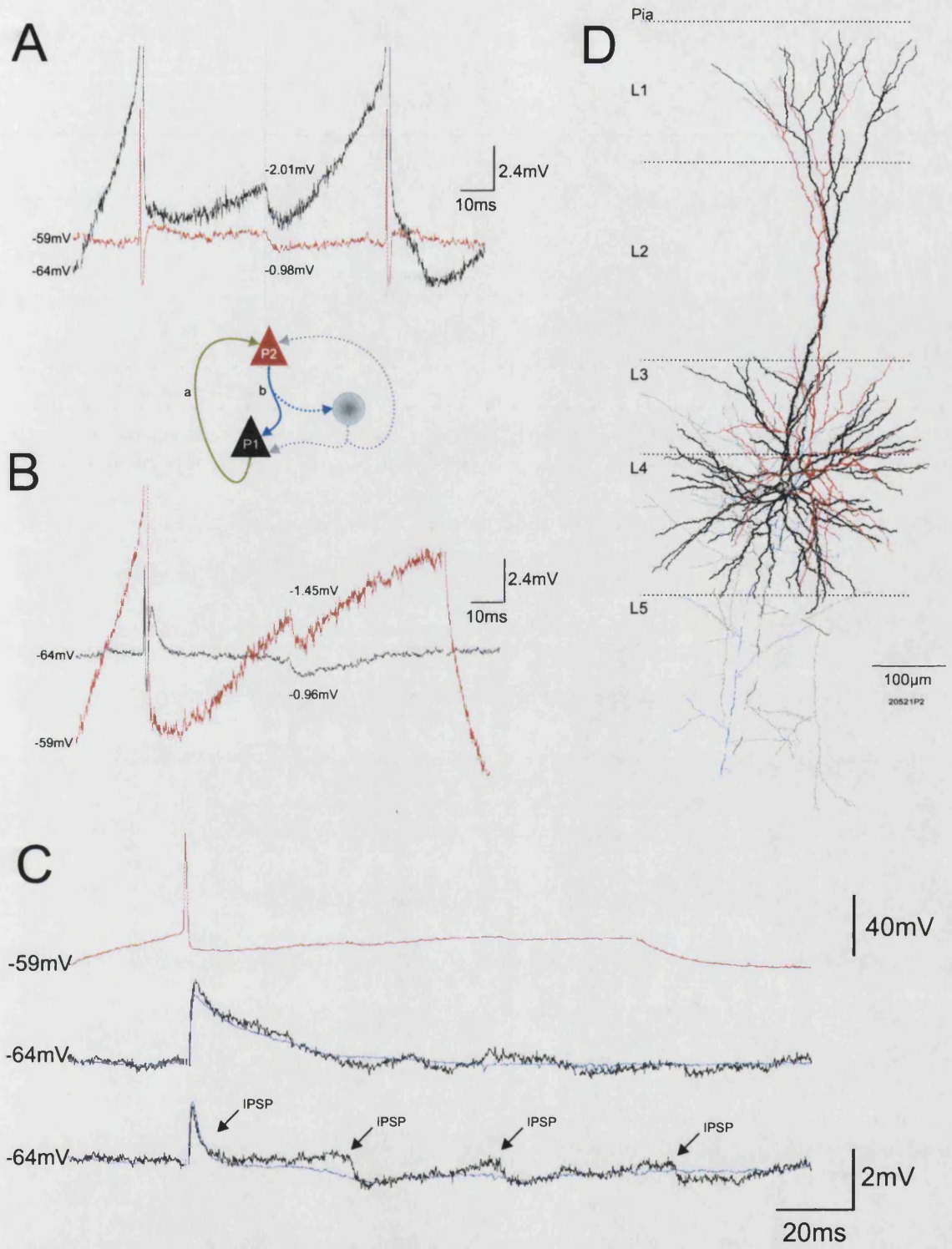

Figure 5.14. Spontaneous/disynaptic IPSPs are driven by one of two reciprocally connected pyramidal cells in cat layer 4. A, raw data (20521p2a) illustrating the presynaptic and postsynaptic recordings at the same scale. The coincident IPSP occurs spontaneously on both the pre- and post-synaptic traces. B, Raw data (20521p2b) of the reciprocal connection in reverse to that of A. The disynaptic IPSPs occurs quickly in response to an action potential in cell P2 and repolarises the EPSP in P1. The cartoon represents the directly recorded connections between the pyramidal cells (solid lines) and imagined connections with the disynaptic interneurone (dotted lines). C, Examples of EPSPs from recording B showing raw sweeps of an EPSP that is not repolarised by the IPSP and another that is repolarised before it can reach mean peak amplitude. Averages are superimposed in blue (31sweeps and 23 sweeps respectively). D, Anatomy of the recorded pyramidal cells (a larger scale image of these cells can be found in figure 4.3a).

5.13 Conclusions.

The data presented here illustrates that the classes of interneurones in layer 4 of both cat and rat neocortex do **not** form anatomically homogenous groups providing non-specific inhibition to the same areas of cortex. Instead they comprise an anatomically diverse population, exhibiting a broad range of morphologies and input/output target preferences, even within similar groups classified according to their firing patterns and neurochemistry. For example both cat and rat cortex had cells that were stellate, FS and PV immuno-positive and both also had cell that were stellate, RS and PV immuno-negative. However, even within these groups the individual cells had very different input (dendrite) and output (axonal) domains as can only be determined by the histological demonstration of their anatomy. These results indicate that even cells with similar physiological and neurochemical properties and even similar preferences for postsynaptic cell subclasses and the subcellular compartments thereof may have strikingly different roles within the circuitry of cortical columns as defined by their gross anatomy.

Within layer 4 the patterns of connectivity between the interneurones and excitatory pyramidal cells of layer 4 were similar in both species. All excitatory synapses (putatively) identified were made onto dendrites, as were the inhibitory synapses, even those originating from a neurone that was stellate, FS and PV immunopositive suggesting that even the combination of these features may not necessarily correlate with the basket cells as is often assumed in the literature. As with the excitatory to excitatory connections all of the pre- or post-synaptic pyramidal cells in layer 4 were RS and no connections were seen with BF pyramidal cells in the same layer. In both species the interneurones receiving excitatory inputs exhibited EPSPs that were faster than those observed between pyramidal cells and showed frequency dependent depression that decayed at a similar rate to the depressing connections between pyramidal cells. Facilitation of EPSP amplitude in response to trains of action potentials was observed at excitatory connections to interneurones from both species. One was IS (rat) and the other RS (cat) the first of which was immuno-negative for CB, the other for VIP and both were immuno-negative for PV suggesting that these particular neurochemical characteristics may not be used as indicators for facilitating connections. All excitatory connections to FS interneurones generated depressing EPSPs, all PV immuno-positive cells were FS and the FS PV containing interneurones received the largest excitatory inputs.

6.0 EVIDENCE FOR ELECTRICAL GAP JUNCTIONS BETWEEN PYRAMIDAL CELLS IN ADULT RAT NEOCORTEX.

Introduction:

Electrical gap junctions have been described between interneurones and between pyramidal cells in the developing rat neocortex (Peinado *et al.*, 1993) and are proposed to have an important role to play in neuronal synchrony (Perez Velazquez & Carlen, 2000) and possibly in mechanisms determining the position of neurones within the laminae as they migrate though the cortex (Peinado *et al.*, 1993). Ultrastructural studies (Fukuda & Kosaka, 2003;Simburger *et al.*, 1997;Tamas *et al.*, 2000) provide evidence for gap junctions between interneurones in the adult rat neocortex and the expression mRNA coding for connexin 43 subunits (Simburger *et al.*, 1997) suggest the junctions are also formed by pyramidal cells. The existence of gap junction connectivity between pyramidal cells in adult tissue has also been predicted by computer simulations, particularly in the hippocampus where the sub-millisecond synchrony of pyramidal cells suggests the gap junctions are located between pyramidal cell axons (Traub *et al.*, 2002) but to date little physical or physiological evidence has been available to confirm their presence in adult neocortex.

One recording of a layer III pyramid to layer V pyramid connection in the primary visual cortex area V1B (binocular area) of an adult rat 450μm cortical slice exhibited convincing evidence for the presence of an electrical gap junction between the presynaptic pyramidal cell in layer III and an unidentified cell in the vicinity (see figure 6.1). The unidentified coupled cell also appeared to be presynaptic to the recorded postsynaptic deep layer V pyramidal cell. Electrical coupling was revealed in the electrophysiological recordings by a distinct spikelet approximately 9.5mV in amplitude with a half width of 2.0ms on the presynaptic layer III pyramid trace and clear double EPSPs in the postsynaptic cell. The impaled presynaptic cell and its electrically coupled partner were driven to action potential threshold by the same square wave and ramped current pulse injections to generate EPSPs in the postsynaptic target. The double EPSPs occasionally combined to depolarise the target towards firing threshold initiating bursts of postsynaptic action potentials.

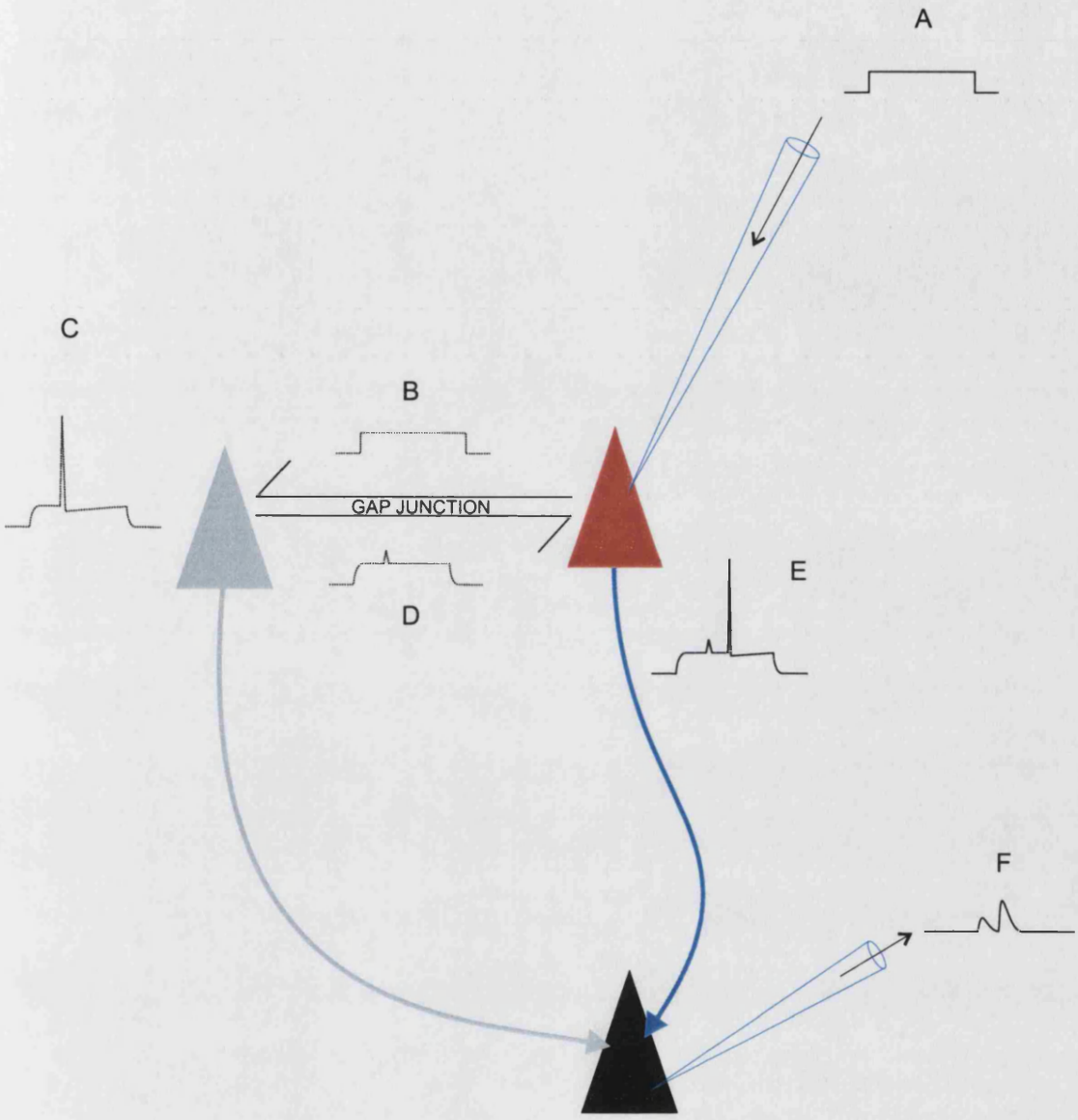

Figure 6.1. Schematic diagram of the sequence of events leading to double EPSP generation in a postsynaptic pyramidal cell by current pulse injections into a single presynaptic pyramidal cell with pulse conductance via an electrical junction. A, Square wave current pulse passed into presynaptic cell. B, Pulse is transmitted through gap junction depolarising coupled cell to action potential threshold (C). D, spikelet passes back through the gap junction to become apparent on the impaled presynaptic recording. E, Impaled presynaptic reaches spike threshold. F, both EPSPs recorded at postsynaptic electrode.

When powerful (+2.0nA) depolarising ramp and square wave current pulse injections were applied to the impaled presynaptic layer III pyramid, spikelets (transmitted through the gap junction) caused modifications to the impaled presynaptic cells' normal regular spiking firing pattern causing high frequency spike doublets. The resultant combined EPSPs consistently drove the postsynaptic cell to spike threshold.

6.1 The directly recorded presynaptic layer III pyramidal cell.

The pyramidal cells of layer III recorded throughout these studies were either burst firing or regular spiking in roughly equal proportions (45% and 55% of the population respectively). The impaled layer III pyramid from this recording that was electrically coupled to an unidentified neurone and presynaptic to layer V pyramid was RS at a membrane potential of -69mV (ie. responded to sustained depolarising current pulses with trains of spikes that exhibited frequency adaptation).

The recorded presynaptic layer III pyramidal cell dendritic arbour was well filled and was reconstructed at x1000 (figure 6.2). The cell had spiny dendrites and an apical projecting perpendicular to the pial surface. The axon initial segment projected from the base of the soma, did not show signs of myelination and ramified little in layer IV. The axon was poorly filled and so was not well stained in histological preparations with no axonal profiles identifiable in layer V. No close axo-dendritic appositions were observed.

Excitatory postsynaptic potentials that were generated by overshooting action potentials in this cell were recorded in the postsynaptic pyramid in layer V. Where these EPSPs appeared independent of those generated by the electrically coupled neurone (the spikelet being either absent or so far in advance of the first full action potential to allow complete decay of the spikelet-generated EPSP) the peak amplitude was 3.98mV, RT 2.4ms, HW 16.5ms.

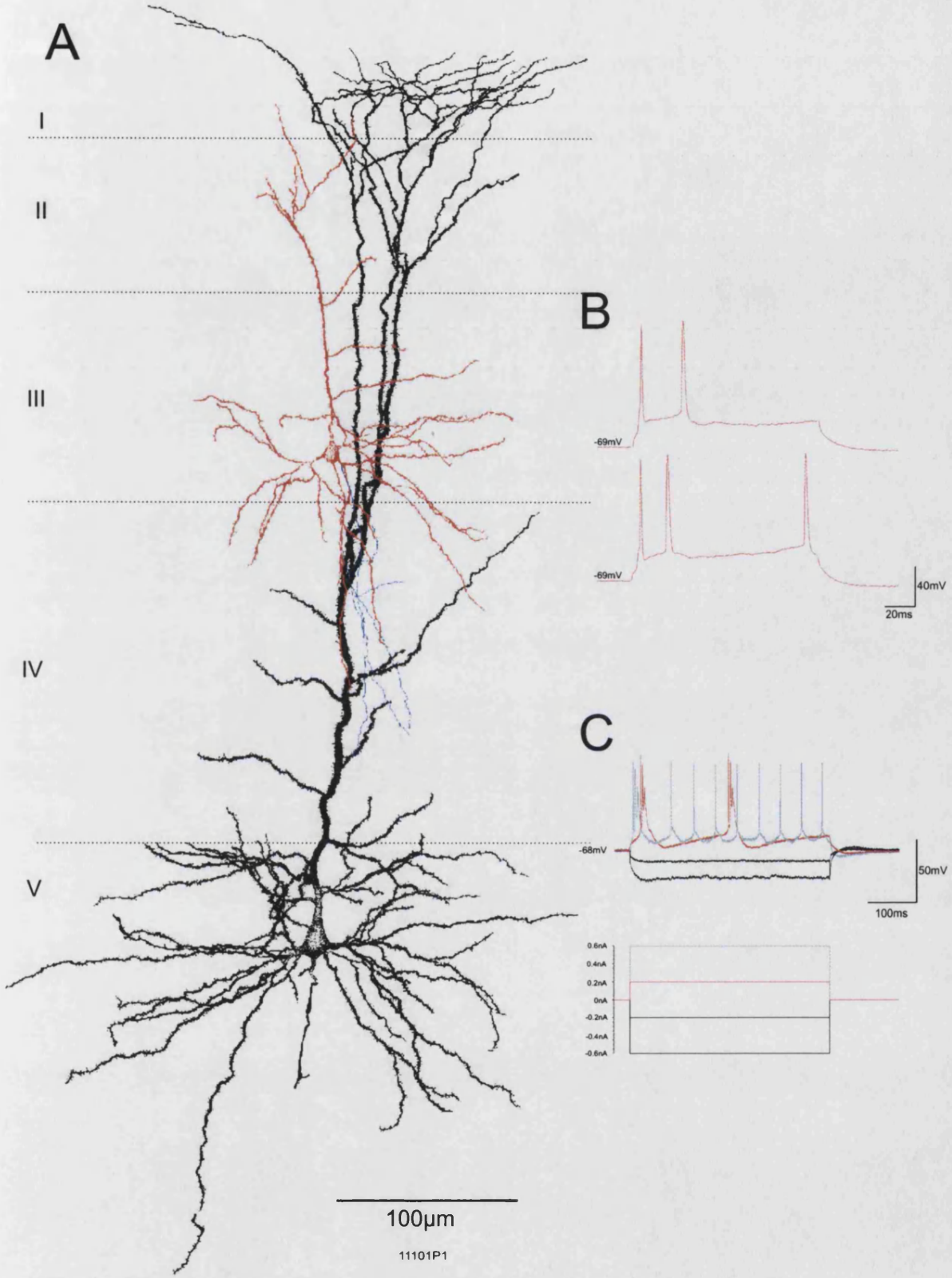

Figure 6.2. Morphology and firing patterns of the two directly recorded, synaptically connected pyramidal cells from adult rat neocortex. A, x1000 reconstruction of the presynaptic layer III cell dendrites (red) and axon (blue) and postsynaptic layer V cell dendrites (black). B, Examples of the presynaptic RS firing pattern. C, The postsynaptic responses to 400ms current pulses at -0.6nA, -0.2nA, +0.2nA and +0.4nA. The cell generates repetitive bursts of action potentials at threshold (red trace). The initial burst is followed by tonic firing when the depolarising pulse is increased (grey trace), typical of type 2 layer V pyramidal cells.

6.2 The postsynaptic layer V pyramidal cell.

The physiological and anatomical properties of the postsynaptic pyramidal cell fit the description typical of the (type 2) intrinsically burst firing pyramidal cells described previously (see Thomson & Bannister, 1998). The recorded and well filled layer V pyramid was also stained and reconstructed at x1000 (figure 6.2). All dendrites had spines and a single apical dendrite projected vertically, perpendicular to the pial surface and formed a large dendritic tuft in layer I. The axon was not reconstructed but microscopic examination revealed the initial segment projecting from the base of the soma. The main axonal trunk projected down towards the white matter and had myelinated portions between which axonal branches emerged at oblique angles.

The cell membrane potential was -68mV and responded to positive 0.2nA square wave current pulse injections with repetitive bursts of 3 action potentials at threshold that broadened and the amplitude accommodated from 73mV to 64mV to 45mV for each successive AP in the bursts. Each burst was followed by a long afterhyperpolarisation. As the depolarising current pulses were increased in strength the cell exhibited tonic firing following the initial spike burst (figure 6.2c)

6.3 The non-impaled presynaptic cell.

The presynaptic layer III pyramidal cell was impaled and recorded for 70 minutes with spikelets present throughout, indicating that the gap junction was open and active for the duration. Despite the length of time available for dye transfer through the gap junction to occur, no evidence of the coupled cell was apparent in histological preparations. As such the position of the electrically coupled cell, its morphology and the potential location of the gap junction(s) are unavailable for analysis. However information was available relating to the intrinsic firing pattern and the influences exerted upon the postsynaptic cell.

The action potentials in this cell (recorded as spikelets in the impaled layer III pyramidal cell) always occurred within the duration of the depolarising current pulse injected into the impaled presynaptic cell indicating that the cell was being driven by the same current pulse. The 1st spikelet occurred either before, during or shortly after the impaled presynaptic 1st action potential. Where the

spikelets occurred prior to the impaled presynaptic cell action potentials they would only occur as single events (Figure 6.3a) indicating that the cell was most likely to be regular spiking. The non-recorded electrically coupled neurone often appeared to reach AP threshold in response to the current pulse more quickly than the impaled layer III pyramid. The resultant spikelet appeared to depolarise the recorded neurone to spike threshold, even when ordinarily sub-threshold current pulses were injected (figure 6.3b). After the first full AP, the spikelets tended coincide with subsequent APs in trains of up to 4 spikes (figure 6.3c).

The EPSPs generated in the postsynaptic pyramidal cell by the electrically coupled neurone that were independent of those generated by the impaled presynaptic pyramid were on average 2.84 ±SD 0.36mV in amplitude, 10-90% RT 2.7ms and HW 16.9ms measured from an average of 62 sweeps triggered on the rising phase of the 1st spikelet where it preceded spikes/spike trains generated by the impaled presynaptic neurone. Where the spikelet was detected there was always a corresponding EPSP indicating a low probability of total transmission failure at this connection.

6.4 The spikelet affects the recorded neurone's firing pattern.

Of all the RS pyramidal cells recorded from all layers throughout these studies the shortest interval between the first and second spikes at all stimulus intensities used (0.1 - 2nA) was 6ms using powerful combined square wave and ramped pulse injections. The impaled presynaptic cell of this connection was driven with square wave and ramped depolarising current pulses to generate action potentials in trains of between 120 and 200ms duration. A post stimulus interval histogram of 1st to 2nd interspike interval was plotted for every pulse through the recording to reveal the preferred 2nd spike interval over the range of current pulses used (figure 6.4a). Six hundred and forty one of 759 (84.5%) second spikes clustered within a window 14-30 ms from the first spike. The preferred 1st to 2nd spike interval was 23-24ms across the range of stimulus intensities used. Under conditions of powerful current pulse injections the cell also produced second spikes at shorter intervals between 4.9ms and 5.7ms of the first spike in the train. These spikes did not appear to reach threshold as a result of the artificial stimulus alone; the short interval second action potentials were initiated following spikelet activity shortly after the 1st AP resulting in strong depolarisation of the impaled cell to reach threshold at times corresponding to the peak of the spikelet (figure 6.4b).

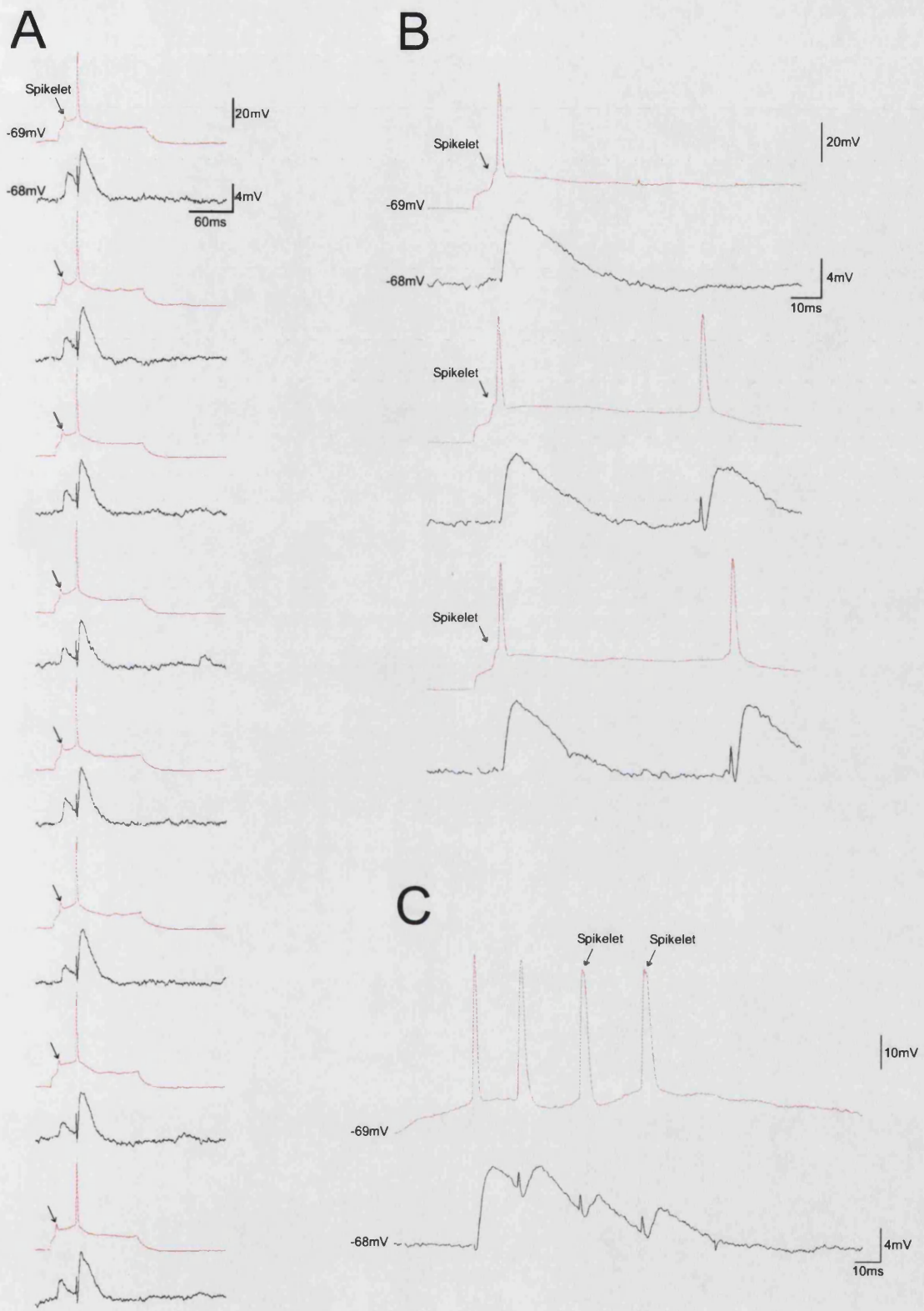

Figure 6.3. Raw data illustrating spikelet occurrence in the impaled presynaptic layer III pyramidal cell recording and double EPSPs recorded in the postsynaptic layer V pyramid. A, Panel showing 8 examples of the pre- and post-synaptic recordings with the spikelet preceding the first AP generated by the recorded presynaptic neurone. When the spikelet was apparent it always generated an EPSP throughout the recording. B, Spikelets transmitted to the impaled presynaptic cell caused it to reach spike threshold. C, Spikelets were frequently seen to coincide with the recorded presynaptic cell's APs in trains containing multiple spikes.

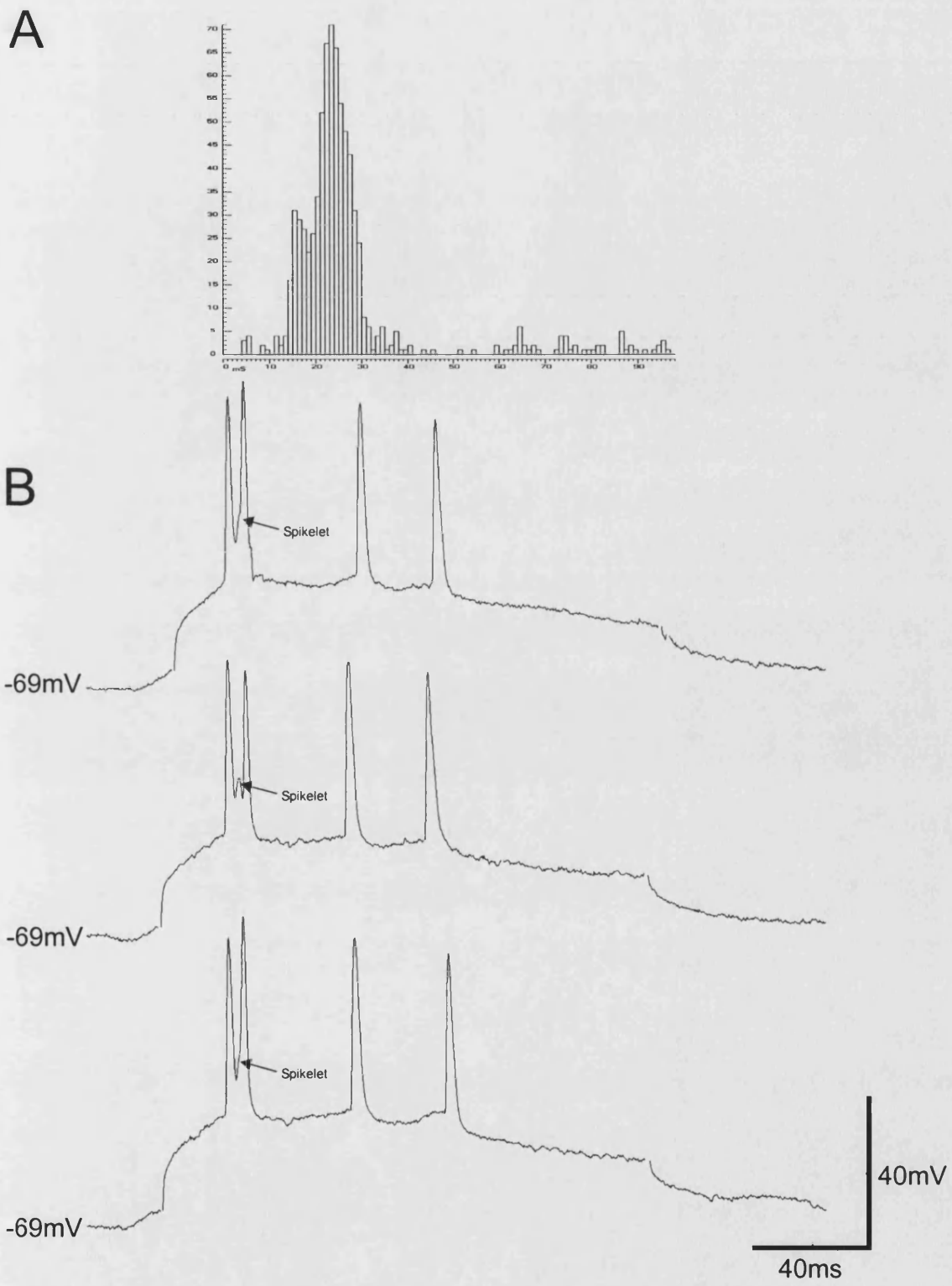

Figure 6.4. Spikelets can cause changes in the firing pattern of the impaled presynaptic layer III pyramidal cell. A, Post-stimulus interval histogram for 2nd spikes in all sweeps containing more than 1 spike at all stimulus intensities used, with zero representing the time of the 1st spike. The preferred 2nd spike interval is between 23 and 24ms. B, raw data illustrating examples of presynaptic spikes in trains of 4. The second spike occurs at very short interspike intervals of 4.9 - 5.7ms initiated by spikelets under conditions of ramp and square wave current pulse injections.

6.5 The combination of presynaptic inputs generates powerful EPSPs in the postsynaptic cells.

The combined EPSPs generated by the impaled presynaptic pyramidal cell and its electrically coupled partner provided powerful input to the postsynaptic neurone. The mean amplitude of EPSPs generated in response to the spikelet was 2.84mV. The combined EPSPs generated by spikes in the recorded presynaptic pyramid and near simultaneous spikelets from the coupled cell had a mean amplitude of 7.66mV (figure 6.5a). Insufficient sweeps were available with EPSPs generated by the recorded presynaptic cell that were independent of those generated by spikelet activity to assess whether the 2 inputs summed linearly (only 2 sweeps at the beginning of the recording with EPSP amplitudes of 3.91 and 4.03mV).

The combined strength of EPSPs generated by the electrically coupled cells in the postsynaptic pyramid was frequently powerful enough to achieve firing threshold and initiate bursts of action potentials (figure 6.5c). Where the spikelet generated second spikes in the recorded presynaptic pyramid at very short intervals as described above, the postsynaptic cell consistently generated AP bursts.

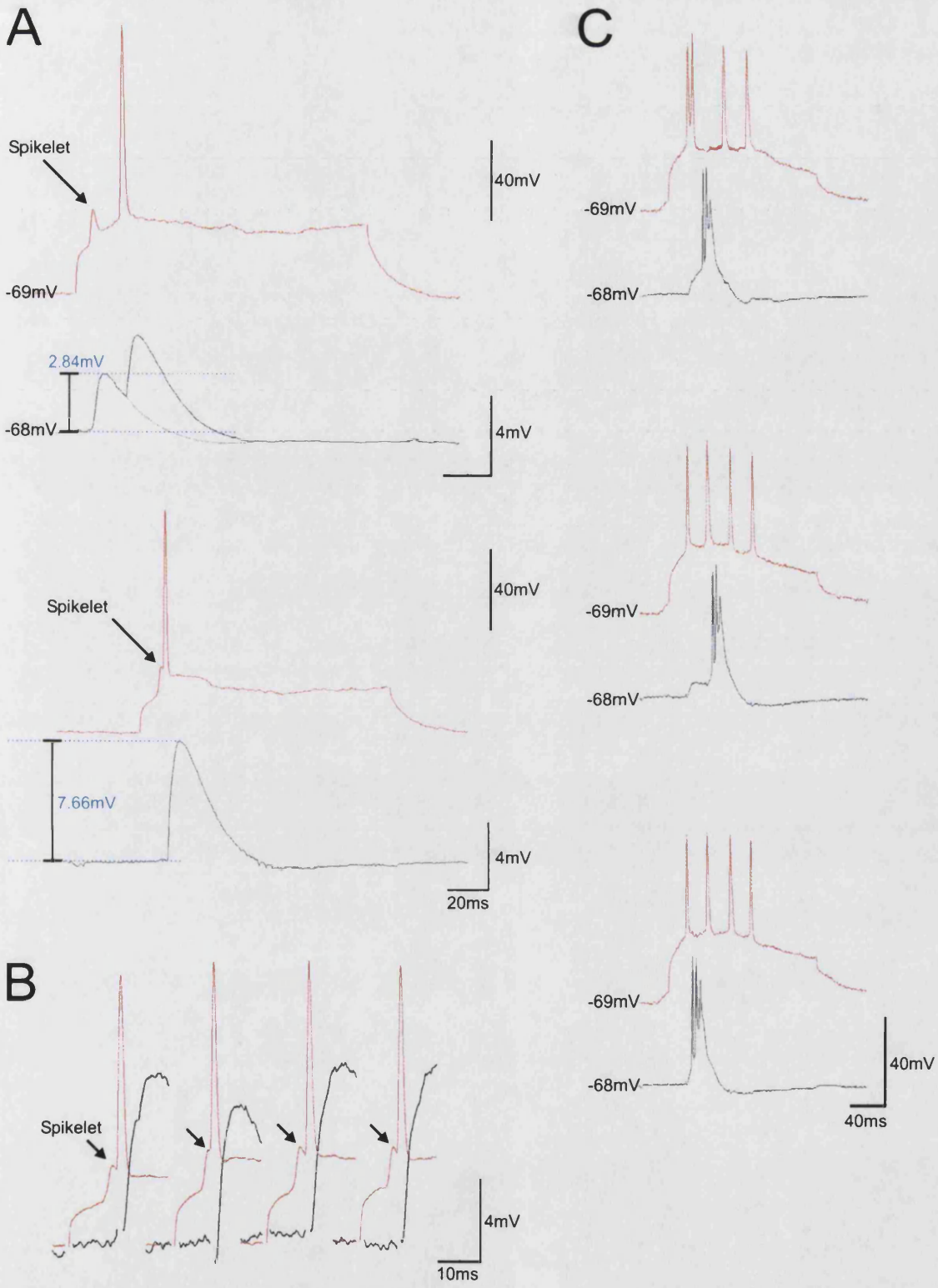

Figure 6.5. The combined effects of EPSPs recorded in a layer V pyramidal cell that were generated by the recorded presynaptic layer III pyramid and its electrically coupled partner. A, Averaged EPSPs (62 sweeps) triggered on the peak of the spikelet where it preceded the first AP (upper) and where the spikelet and AP occurred near simultaneously (lower). Insufficient sweeps were available with the recorded presynaptic cell APs and EPSPs independent of spikelet activity to assess whether they summed linearly. B, Four examples of raw data illustrating the double rising phase of the combined EPSP. Presynaptic spikes and spikelets (red) and postsynaptic EPSP rising phases (black) C, Raw data illustrating the ability of combined EPSPs generated by both presynaptic neurones to promote the postsynaptic layer V pyramid to spike threshold initiating bursts of action potentials.

6.6 Conclusions:

This dual recording provides evidence for the persistence of gap junction intercellular communication (GJIC) between pyramidal cells in adult rat neocortex. The recording also allows a number of suggestions to be made regarding the effects of gap junction mediated communication both upon the coupled neurones and upon their common synaptic targets. For example, GJIC between the two excitatory neurones appears to allow simultaneous depolarisation of both cells in response to the same excitatory stimuli. Also, the gap junction mediated transfer of depolarising current spikelets resulting from spikes in either cell may cause the coupled neurone to reach action potential threshold, thereby promoting temporal synchrony of outputs from the two cells. Spikelet conduction through the gap junctions occurring shortly after the first action potential generated by its regular spiking electrically coupled partner may also cause it to reach firing threshold and generate multiple spikes at intervals ordinarily dominated by the spike afterhyperpolarisation. Also, the shape of the spikelet suggests that the gap junction is proximally located, which may correlate with predictions made by computer simulations of cortical network activity (Traub *et al.*, 2002).

As a result, the features of electrical communication between these two excitatory neurones appear to promote synchronised outputs to the same postsynaptic target pyramidal cell in layer V. The temporal synchrony of the two excitatory outputs causes consistently suprathreshold input to the burst firing pyramid that could cause highly efficacious feedforward of information to subcortical regions.

7.0 POTENTIAL EXCITATORY CONNECTIONS FROM PYRAMIDAL CELLS TO IMMUNO-LABELLED INTERNEURONES.

Introduction:

The paired intracellular recording, biocytin filling and immunofluorescence of synaptically connected pyramidal cells and interneurones allows the subclassification of connected neurones and assessment of synaptic properties at those connections. However, the requirement for histological processing of tissue slices shortly after physiological recording curtails the search for similar connections from the same presynaptic cell, therefore limiting the estimation of connection probability and the number of similar cells contacted by the same presynaptic axon. To investigate further the extent of excitatory pyramidal cell innervation of specific populations interneurones a novel staining protocol was developed to provide permanent and differential staining of filled pyramidal neurones and immuno-labelled interneurones.

The principles of the procedure are given in methods section 2.12. In brief, the technique comprises the electrophysiological recording of pyramidal cells in layer 4 to allow broad classification of the cells by their firing pattern. Cells were filled with Biocytin by iontophoretic discharge of the dye from the recording electrode by passing positive current in a half duty cycle (0.5nA, 500ms, 1 pulse second^{-1}) prior to withdrawal of the electrode and aldehyde fixation. Double peroxidase staining was performed, first to stain the biocytin filled pyramidal cells and then to localise antibodies raised against the calcium binding protein Parvalbumin (PV), or the neuropeptides Cholecystokinin (CCK) or Vasoactive Intestinal Polypeptide (VIP). Differential staining was achieved by the omission of nickel intensification of the DAB reaction product for the second of the two peroxidase reactions.

Eight layer IV pyramidal neurones were selected for this preliminary study on the basis of the quality of immunostaining achieved, the presence of a sufficiently well stained pyramidal axonal arbour to permit detailed microscopic reconstruction, and on the basis of the pyramidal cells' general anatomy and physiological properties to allow comparison with the pyramid to interneurone connections described in section 5.

For each sample, all immunopositive somata (for each of the 3 antibodies used) were drawn at x1000 within a standard circular field with a radius of 200μm and through three 60μm thick sections giving a total volume of 22,619μm^3 of tissue with the biocytin filled pyramidal soma at its centre. The pyramidal axons and varicosities representing sites of synaptic boutons were reconstructed in detail within the same standard circular field and the locations of potential axo-dendritic synaptic contact onto immuno-labelled interneurone profiles were marked.

7.1 Properties of layer IV pyramidal neurones.

All of the layer 4 pyramidal cells selected for this study were regular spiking (2 of which were RS-2). All had somata 10-15μm in diameter from which 3 to 7 primary basal dendrites projected up to 210μm from the soma and 1 apical dendrite that projected perpendicular to the pial surface towards layer I. All dendrites were spiny 5-20μm from the cell body. Basal dendrites bifurcated up to 4 times giving between 14 and 25 last order branches. Apical dendrites had between 3 and 9 oblique branches and 4 cells had a distal apical tuft in layer I; 1 cell had an apical tuft in layer II and the remaining 3 terminated, without a tuft, in layer II.

All cells had a primary axon shaft originating from an initial segment at the base of the cell body. Six of eight had intermittently myelinated portions of their primary axon shaft and nodes from which unmyelinated collateral branches projected horizontally or at oblique angles towards the superficial layers. The pattern of axonal collateral distribution was similar for both myelinated and unmyelinated primary axons with between 4 and 6 branches forming within 200μm of the cell body. Synaptic boutons, approximately 1μm in diameter were distributed at intervals of 2-20μm along all collateral axonal branches. The sampled axons had between 141 and 656 boutons per 22.62mm^3 of tissue sampled with the pyramidal cell body at its centre.

7.2 Morphology of neurones immunopositive for Parvalbumin, VIP and CCK.

Parvalbumin labelled somata were mostly multipolar, with between 3 and 5 primary dendrites radiating in all directions from the cell body. The dendrites were smooth, infrequently bifurcated and often beaded at their distal portions. In the 3 areas of tissue sampled, between 77 and 127 PV positive somata were identified.

In contrast to the PV positive neurones, the population labelled using anti-VIP was found to be composed primarily of bipolar somata that had 2 primary dendrites projected from the two poles straight and perpendicular to the pial surface or white matter. The dendrites were smooth and rarely bifurcated within the sampled tissue. Distal dendrites were less well stained than those proximal to the soma and distal ramification of dendrites could not therefore be assessed. Between 29 and 37 VIP immunopositive cells were found (mean = 34.3 ±2.7) in the 3 tissue volumes sampled.

Two tissue samples containing 13 and 16 CCK immunopositive somata were drawn. In general these cells were multipolar with between 3 and 6 primary dendrites emerging from the cell body though a few bipolar type cells were also observed. The dendrites were aspiny, and weakly stained at their most distal portions.

Somata immunopositive for each of the three antibodies were distributed throughout all layers with the exception of layer I. In slices stained for PV a densely stained band was seen in superficial layer IV and deep layer III that may correspond with immuno-stained axon terminals that were seen to cluster around some unstained cell bodies. As yet, electron microscopy has not been performed to confirm either putative synapses from filled pyramidal axon to immuno-labelled interneurone profiles or to confirm the presence of PV labelled axonal boutons. Figure 7.1 illustrates typical labelling observed for each of the antibodies used in this preliminary study.

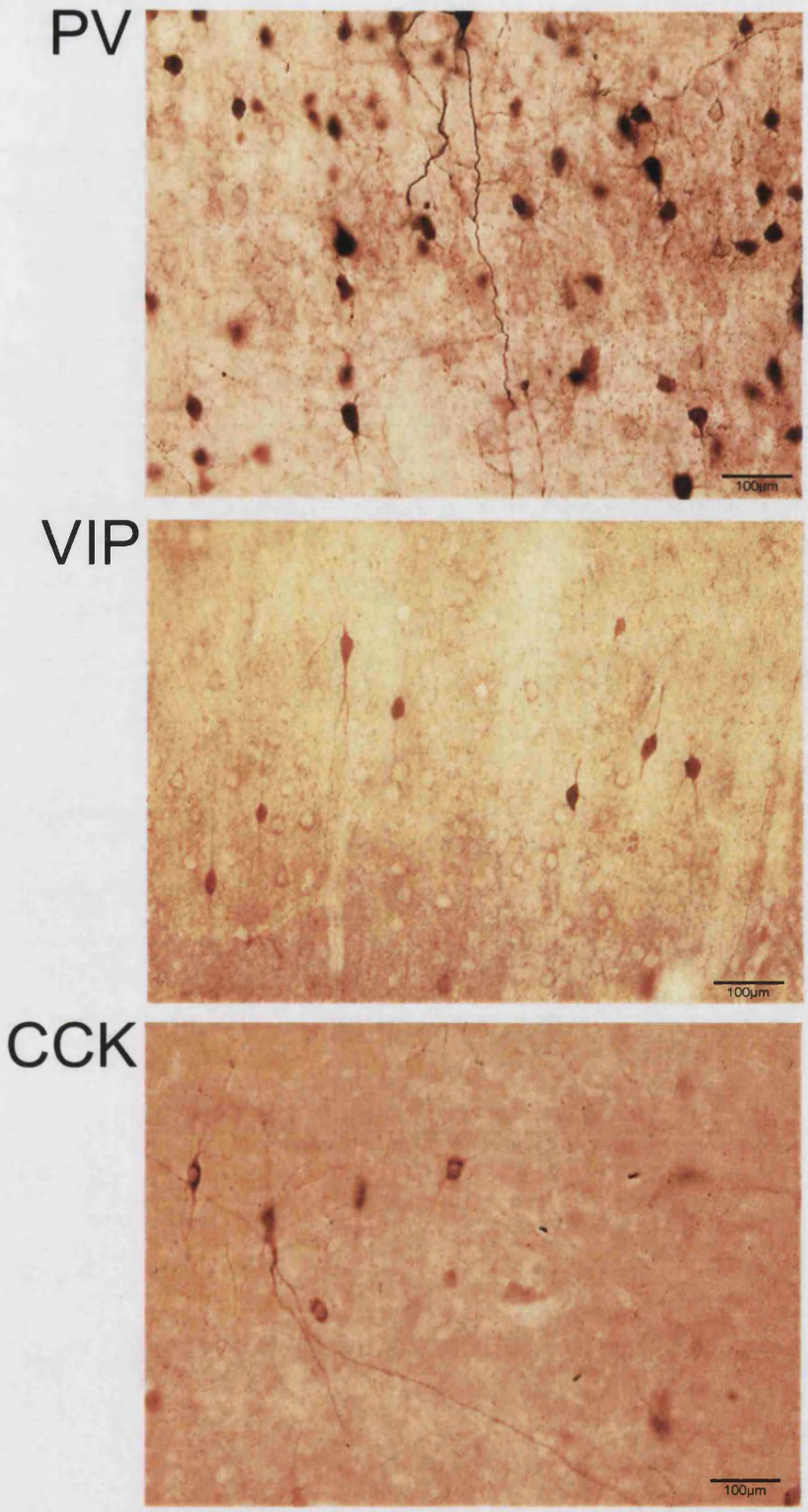

Figure 7.1. Photomicrographs of typical immunopositive staining of interneurones labelled with antibodies for PV (top), VIP (centre) and CCK (bottom) in layer IV of adult rat neocortex, observed using a x20 objective and taken at a single focal plane within one 60i m thick section for each. The picture of PV positive neurones illustrates numerous multipolar (stellate) immunopositive cells distributed evenly through layer IV and a single biocytin filled pyramidal cell axon. VIP immunopositive interneurones are typically bipolar and were sparsely distributed throughout layer IV. CCK neurones were typically multipolar with long portions of the dendrites stained. CCK immunopositive neurones were uniformly distributed in comparatively low numbers throughout layer IV.

7.3 Potential synaptic contacts by layer IV pyramidal cells onto Parvalbumin immunopositive interneurones.

Of the 3 pyramidal cells reconstructed (figures 7.2, 7.3 and 7.4), cells 1 and 2 were in the superficial portion of layer IV with their uppermost basal dendrites extending into deep layer III and cell 3 was deep with the tips of some basal dendrites reaching into layer V. Cells 1 and 3 had an apical tuft in layer I whereas cell 2 terminated without a tuft in layer II. All 3 pyramidal axons had similar RS firing characteristics, numbers of boutons within the area of tissue sampled and each made 4 close membrane appositions with individual PV immunopositive interneurones. As such, in this preliminary study, no obvious correlations between each pyramidal cell's physiology, position within layer IV, their general anatomy or their likelihood of making close axonal contact with stained interneurones could be observed. A more varied sample of pyramidal neurones in later studies may reveal differences in probability of potential connections made by different subclasses of neurones.

Ten of the twelve close appositions observed were with proximal dendrites <50µm away from the interneurone cell body. The 2 remaining contacts from cell 1 and cell 2 were 210 and 75µm from the cell body respectively. These data indicate that close appositions are made onto proximal dendritic portions and also onto more distal portions.

No selective orientation of the contacted PV dendrites or their somata relative to the pyramidal cell was observed. Each of the PV cell bodies were within 33 to 190µm (mean = 104µm) (calculated in 3 dimensions) of the pyramidal cell and the potential synapses 35 to 207µm (mean = 102µm). 9 contacts were made onto primary dendrites 2 onto secondary and 1 onto a tertiary dendrite. The ratio of boutons making contact onto PV neurones was 1 in 41.3 when the data for all 3 reconstructions are combined.

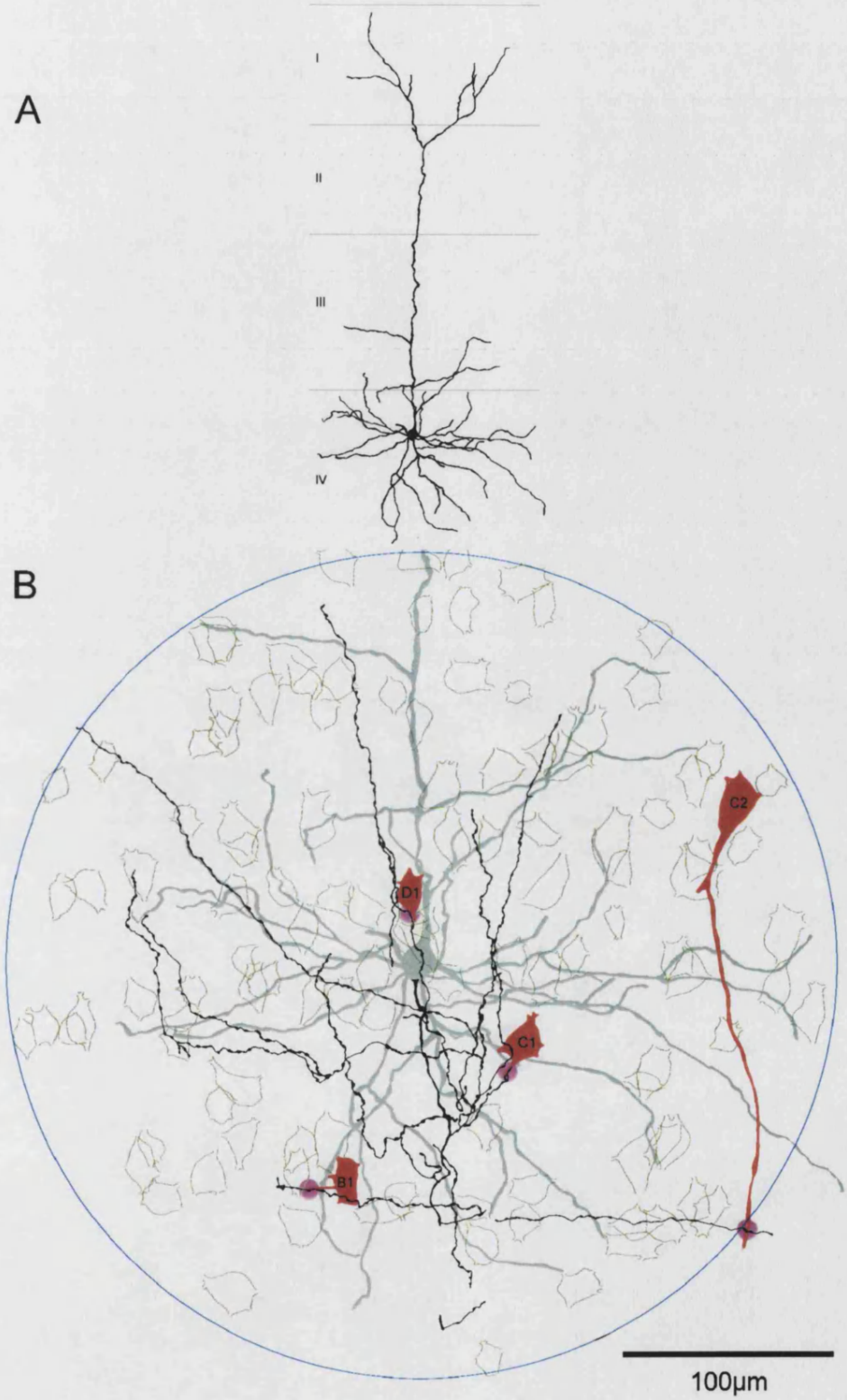

Figure 7.2. PV cell1. A, Reconstruction of dendritic morphology and position within the layers of the layer IV pyramidal neurone (x40 Objective). B, x100 reconstruction of pyramidal cell axon (black) showing 4 potential synapses onto 4 PV immunopositive neurones within a 200µm radius. Pyramidal soma and dendrites (grey), non-contacted PV cells (green outlines). Contacted PV cells are (filled red) and close appositions are indicted (filled pink circles).

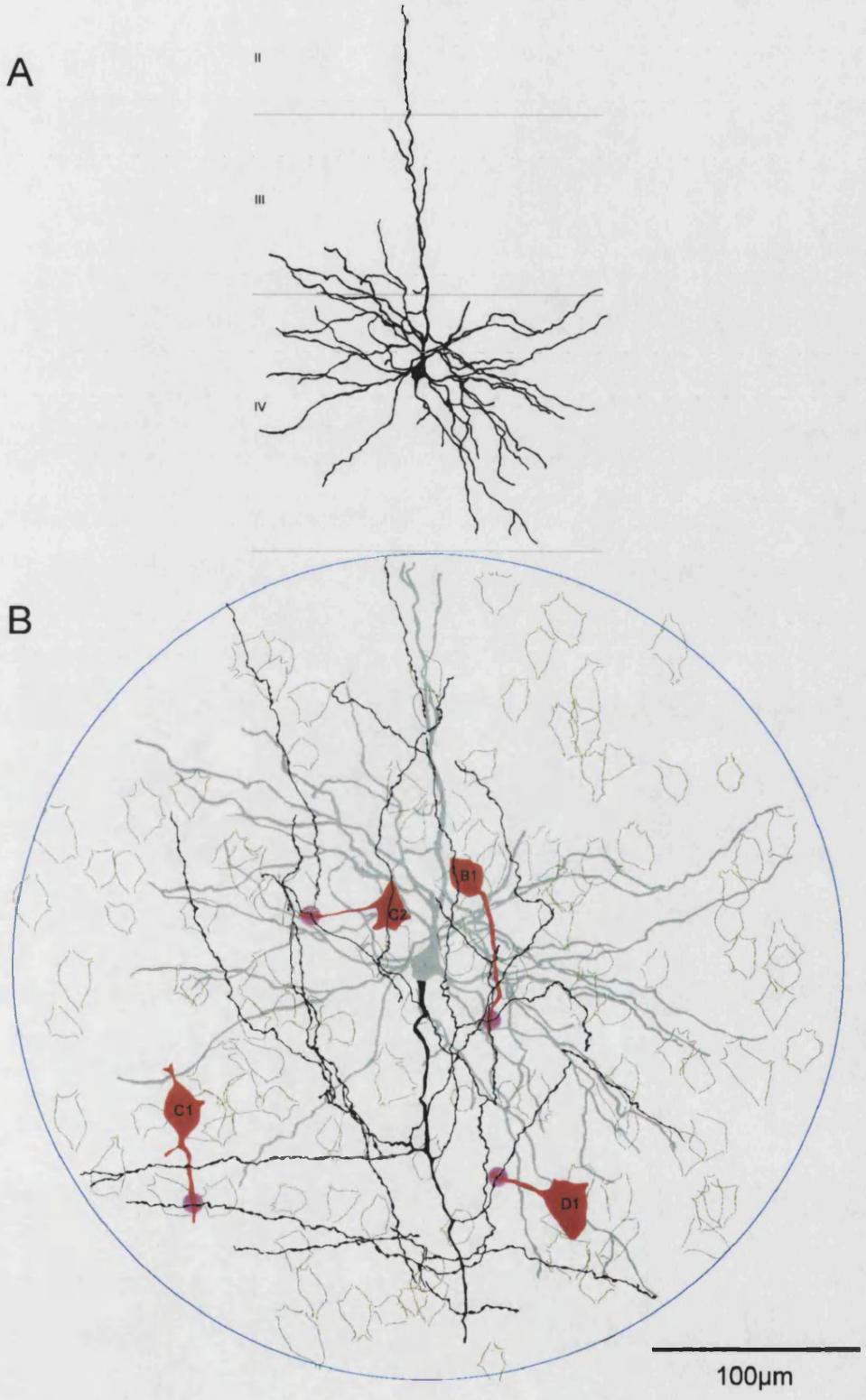

Figure 7.3. PV cell2. A, Reconstruction of dendritic morphology and position within the layers of the layer IV pyramidal neurone (x40 Objective). B, x100 reconstruction of pyramidal cell axon (black) showing 4 potential synapses onto 4 PV immunopositive neurones within a 200µm radius. Pyramidal soma and dendrites (grey), non-contacted PV cells (green outlines). Contacted PV cells are (filled red) and close appositions are indicted (filled pink circles).

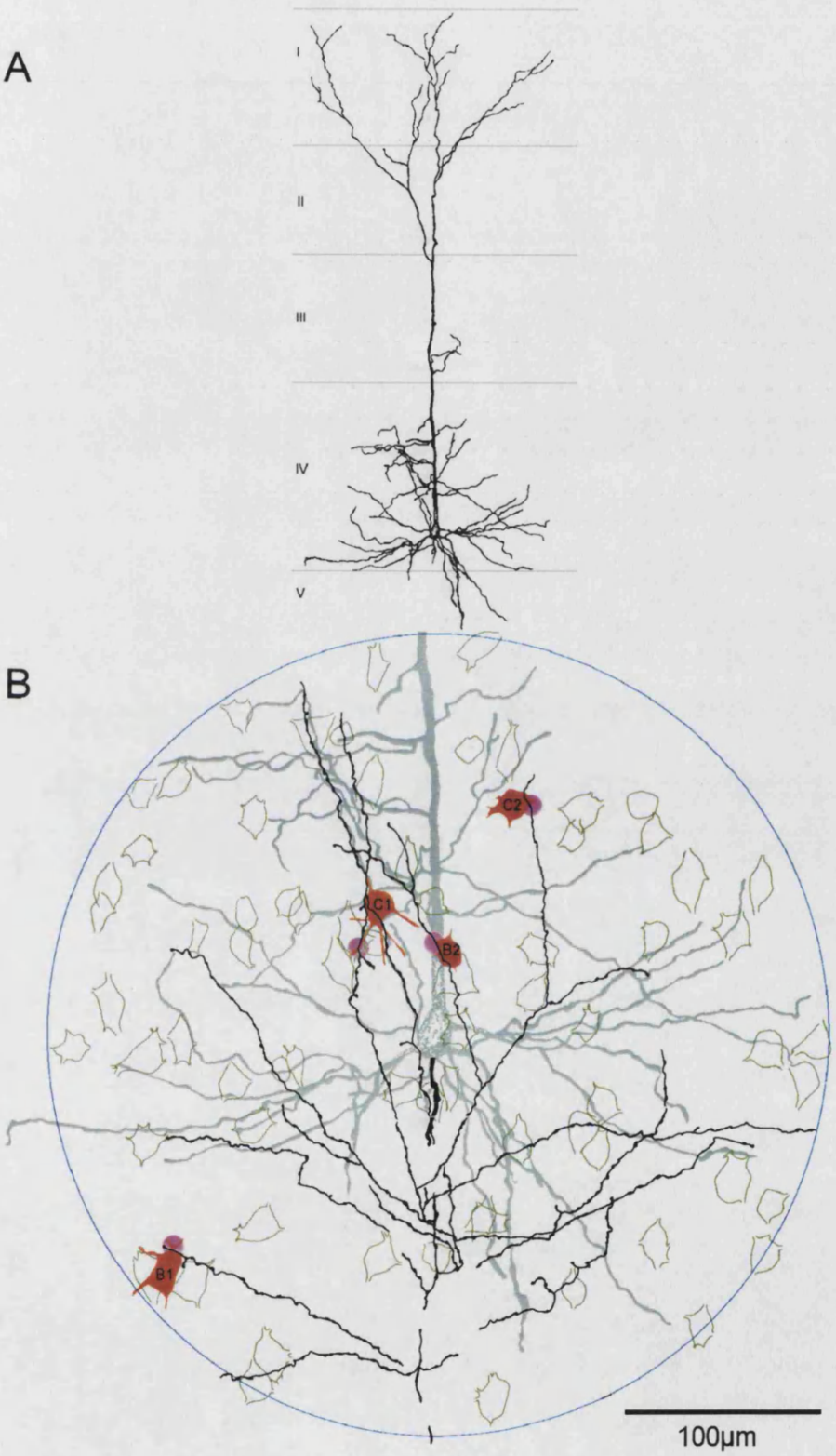

Figure 7.4. PV cell3. A, Reconstruction of dendritic morphology and position within the layers of the layer IV pyramidal neurone (x40 Objective). B, x100 reconstruction of pyramidal cell axon (black) showing 4 potential synapses onto 4 PV immunopositive neurones within a 200µm radius. Pyramidal soma and dendrites (grey), non-contacted PV cells (green outlines). Contacted PV cells are (filled red) and close appositions are indicted (filled pink circles).

7.4 Potential synaptic contacts by layer IV pyramidal axons onto VIP immunopositive interneurones.

The 3 pyramidal neurones reconstructed in tissue stained for VIP immunopositive neurones had similar RS firing characteristics and very similar somato-dendritic morphology. All had their somata situated towards the middle of layer IV with their uppermost basal dendrites reaching into deep layer III. All apical dendrites terminated without a tuft in layer II and all axons were myelinated along the primary shaft with unmyelinated collaterals distributed widely throughout the tissue sample. The amount of axon and, more specifically, the number of boutons present did vary between the cells but this did not correlate with the likelihood of close apposition with a labelled interneurone.

Cell 1 had 656 boutons within the sampled tissue volume but none was seen to make contact with the 37 VIP labelled interneurones in the vicinity (figure 7.5).

Cell 2 had 462 boutons present and made 4 close appositions with the dendrites of 3 VIP positive cells. 2 were onto primary dendrites of individual neurones and 2 onto secondary and tertiary dendrites of the same Interneurone (figure 7.6). A total of 29 VIP labelled cells were available within the sampled tissue.

The axon of Cell 3 had only 309 boutons and made contact with a primary dendrite of 1 VIP positive interneurone of 37 in the volume sampled (figure 7.7).

No obvious pattern of potential postsynaptic VIP labelled neurones was found. Of the 5 contacts seen, all were distributed with no obvious pattern within the 200μm radius reconstructed though 2 were contacting dendrites of a cell 40μm outside the sample area. The mean distances from pyramidal cell to VIP positive somata was 168.5μm and 141μm to the contacts. The ratio of boutons making contact onto VIP neurones is 1 in 118.9 when the data for all 3 reconstructions are combined. The measurements for individual reconstructions is given in table 7.1.

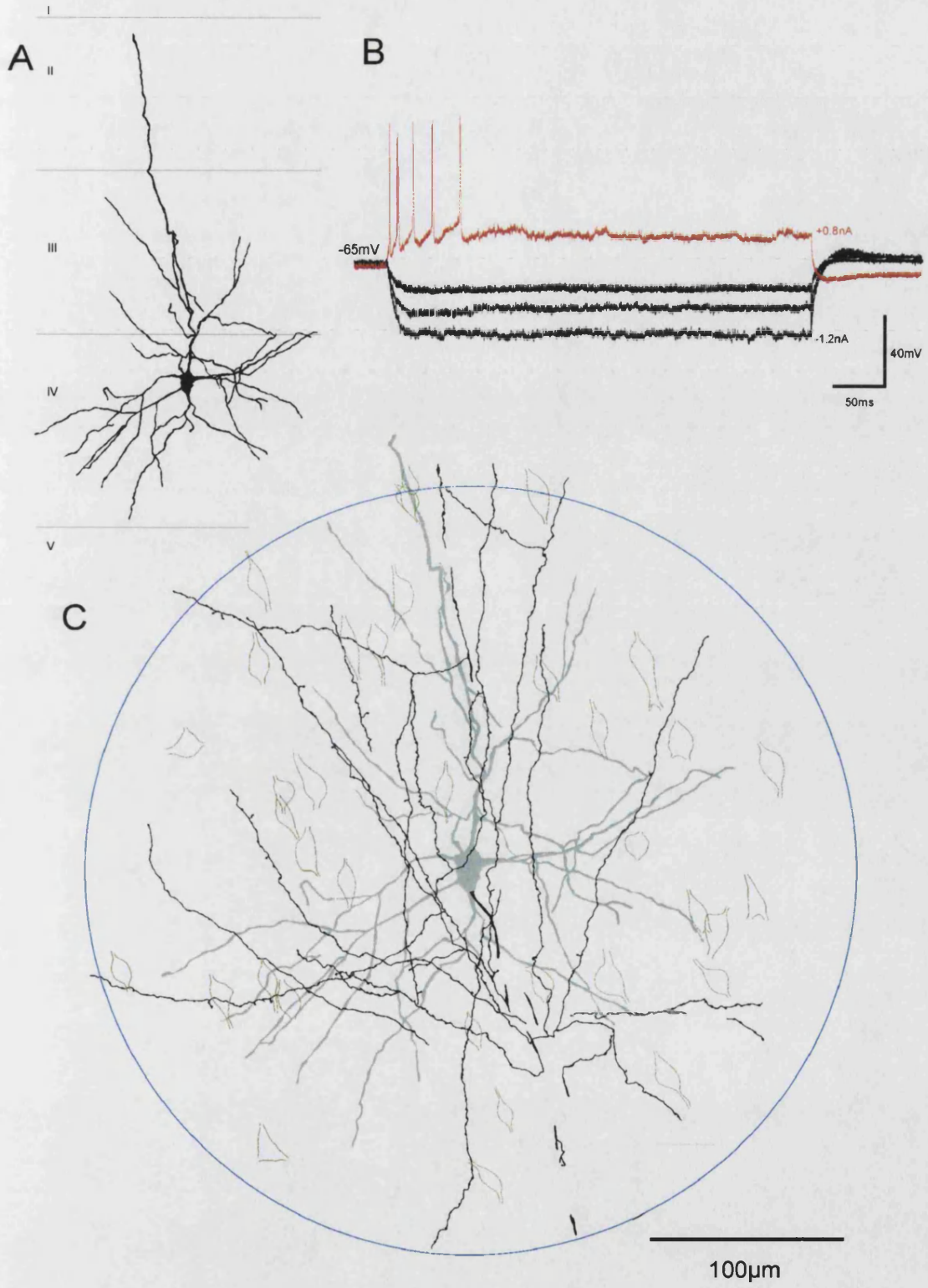

Figure 7.5. VIP cell1. A, Reconstruction of dendritic morphology and position within the layers of the layer IV pyramidal neurone (x40 Objective). B, Pyramidal cell physiological response to -1.2, -0.8,-0.4 and +0.8nA square wave current pulses. This cell shows phasic or RS-2 type firing characteristics C, x100 reconstruction of pyramidal cell axon (black) showing no potential contacts onto VIP immunopositive neurones within a 200µm radius. Pyramidal soma and dendrites (grey), non-contacted VIP cells (green outlines).

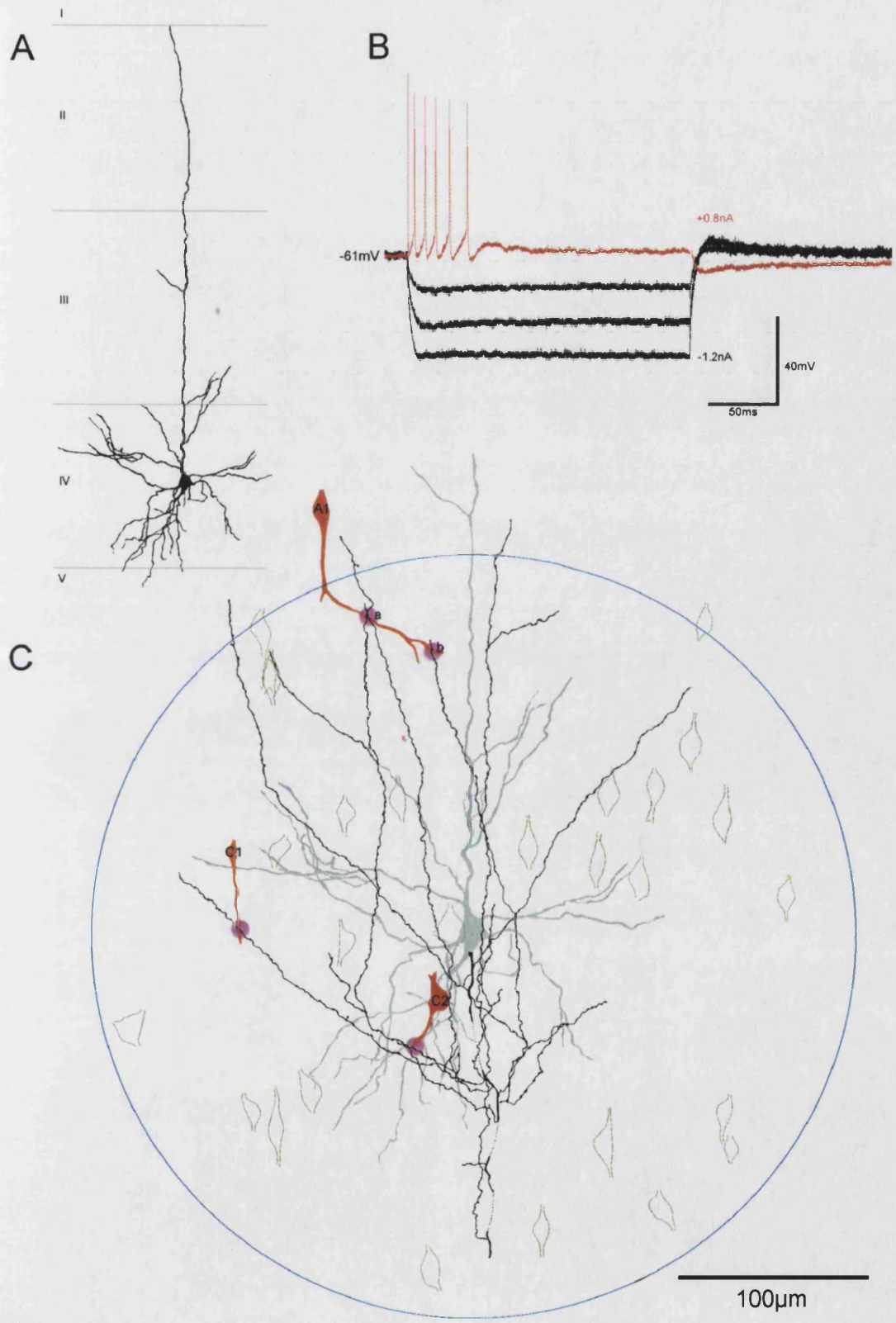

Figure 7.6. VIP cell2. A, Reconstruction of dendritic morphology and position within the layers of the layer IV pyramidal neurone (x40 Objective). B, Pyramidal cell physiological response to -1.2, -0.8,-0.4 and +0.8nA square wave current pulses. This cell shows phasic or RS-2 type firing characteristics C, x100 reconstruction of pyramidal cell axon (black) showing 4 potential contacts onto 3 VIP immunopositive neurones within a 200µm radius. Pyramidal soma and dendrites (grey), non-contacted VIP cells (green outlines). Contacted VIP cells (filled red) and close appositions are indicted (filled pink circles).

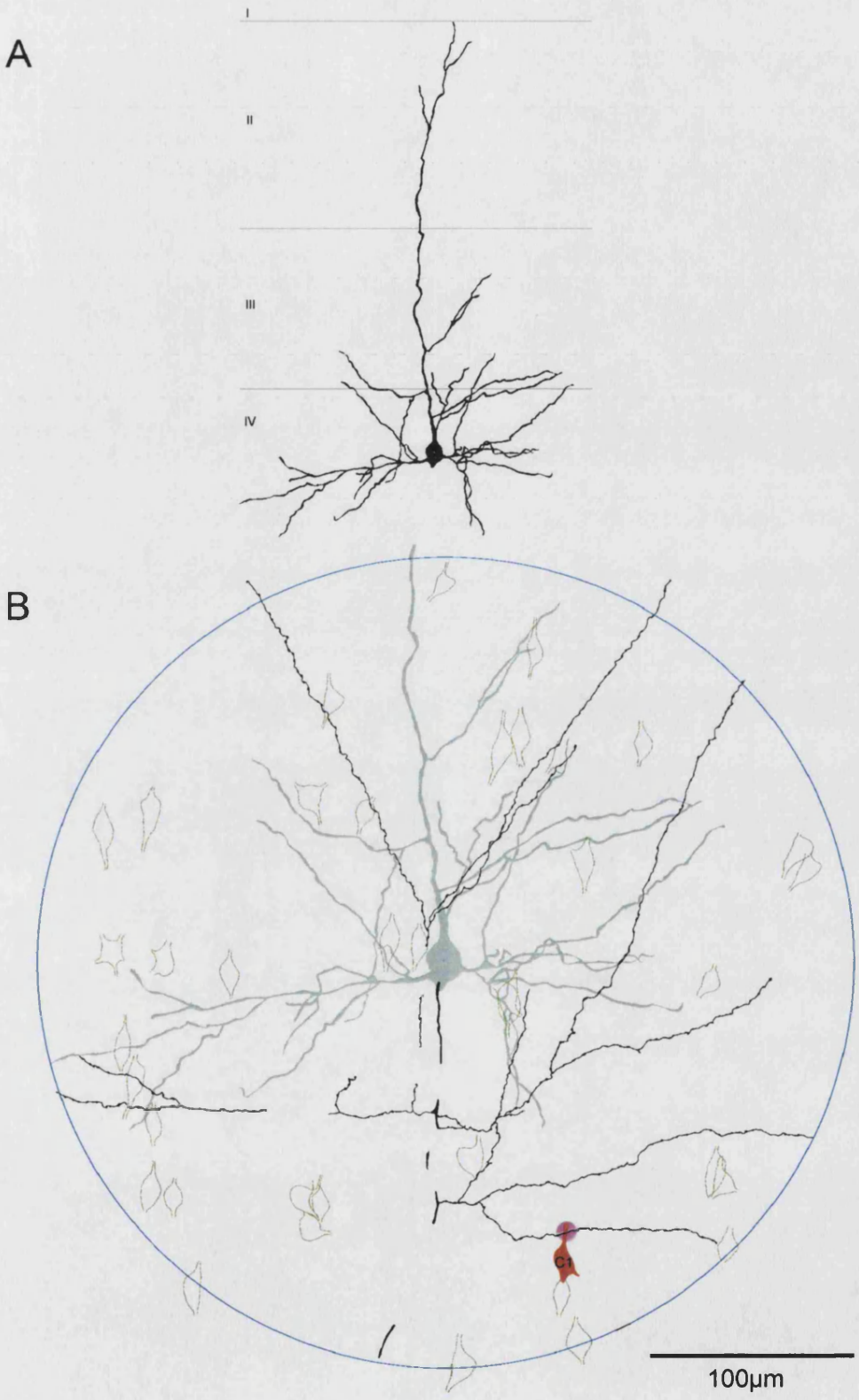

Figure 7.7. VIP cell3. A, Reconstruction of dendritic morphology and position within the layers of the layer IV pyramidal neurone (x40 Objective). B, x100 reconstruction of pyramidal cell axon (black) showing 1 potential contact onto 1 VIP immunopositive neurone within a 200µm radius. Pyramidal soma and dendrites (grey), non-contacted VIP cells (green outlines). Contacted VIP cell (filled red) and the close apposition is indicted (filled pink circle).

7.5 Potential synaptic contacts by layer IV pyramidal axons onto CCK immunopositive interneurones.

The two layer IV pyramidal neurones reconstructed from tissue stained for CCK had similar electrophysiological properties but different positions within layer IV and consequently had different morphological properties. Cell 1 was situated in upper layer IV with most basal dendrites projecting downwards though not reaching into layer V. Few apical oblique branches were seen and a small apical tuft initiated and terminated in layer I (see figure 7.8). The axon was intermittently myelinated along the primary descending branch and unmyelinated axon collaterals were distributed throughout the sampled region. Cell 2 was situated deep in layer IV close to the layer V border with 6 basal dendrites crossing into layer V. Cell 2 also had numerous apical oblique branches within layer IV and a tuft that initiated in layer II and terminated in layer I. The axon was unmyelinated within the sample area and a small amount of collateral axon was seen (see figure 7.9).

Both tissue samples had similarly scant distributions of CCK immunopositive cells with 16 and 13 respectively. Cell 1 had 398 axonal boutons and made one contact onto a primary dendrite close (15μm) to the soma of a labelled neurone 103μm from the pyramid. Cell 2 had 141 boutons, none of which was observed to make contact with any stained cells.

In this preliminary study with only 2 axonal reconstructions and very low numbers of CCK positive neurones it is, of course, not possible to identify any patterns which may correlate pyramidal cell physiology, morphology and position within the layer with the distribution of contacts. However, it is notable that despite the low numbers of neurones with this neurochemistry close pyramidal axon appositions, and therefore potential contacts may be observed.

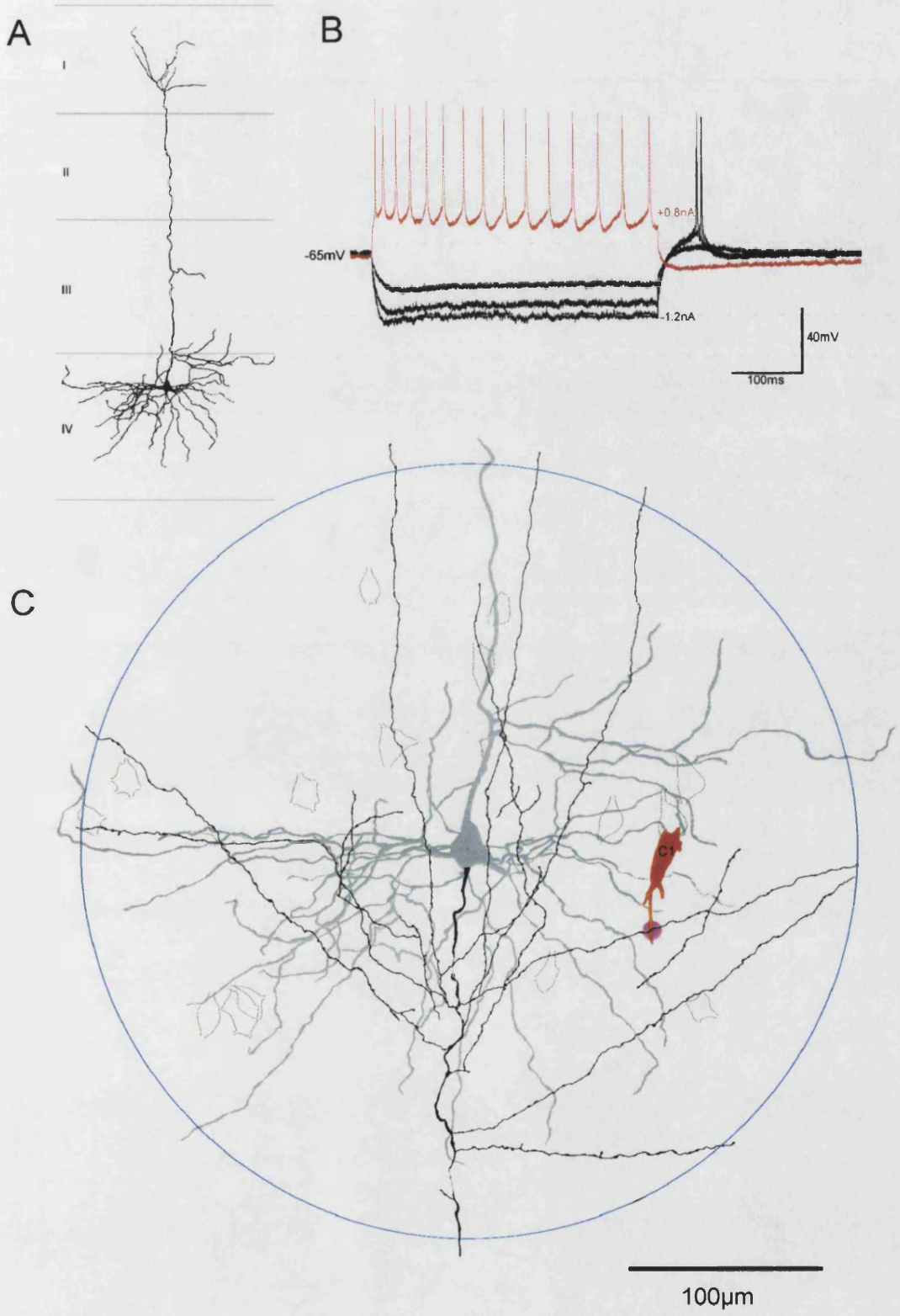

Figure 7.8. CCK cell1. A, Reconstruction of dendritic morphology and position within the layers of the layer IV pyramidal neurone (x40 Objective). B, Pyramidal cell physiological response to -1.2, -0.8,-0.4 and +0.8nA square wave current pulses. This cell shows RS type firing characteristics C, x100 reconstruction of pyramidal cell axon (black) showing 1 potential contact onto 1 CCK immunopositive neurone within a 200µm radius. Pyramidal soma and dendrites (grey), non-contacted VIP cells (green outlines). Contacted CCK cell (filled red) and the close apposition is indicted (filled pink circle).

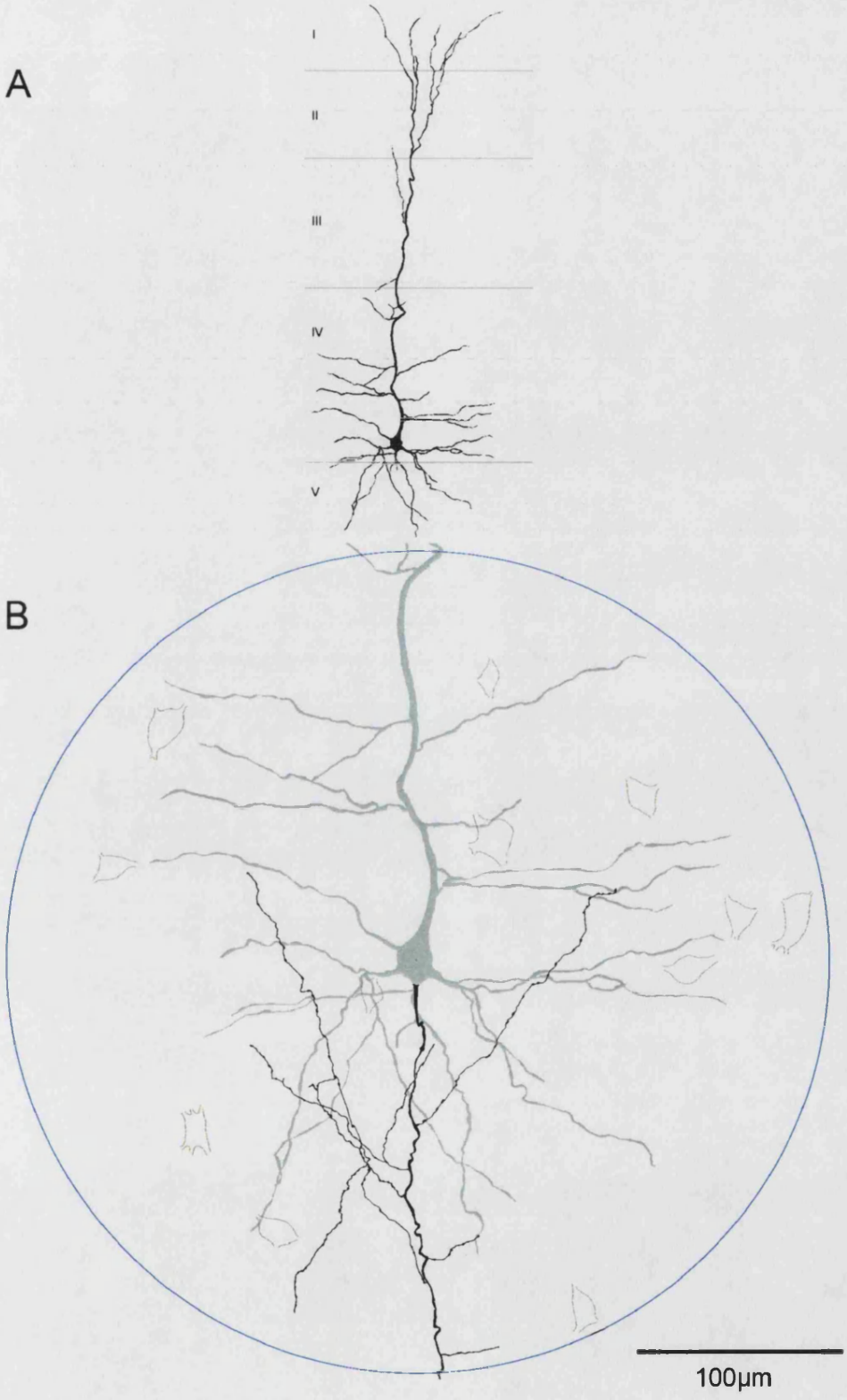

Figure 7.9. CCK cell2. A, Reconstruction of dendritic morphology and position within the layers of the layer IV pyramidal neurone (x40 Objective). B, x100 reconstruction of pyramidal cell axon (black) showing no potential contacts onto CCK immunopositive neurones within a 200µm radius. Pyramidal soma and dendrites (grey), non-contacted CCK cells (green outlines).

7.6 Summary.

The PV, VIP and CCK populations of interneurones are present at differential densities within the tissue samples from layer 4 of adult rat neocortex. Relative to each other PV immunopositive interneurones represent 68%, VIP 23% and CCK 9% of the total population of neurones stained with the three antibodies within the 8 slices sampled.

A total of 3451 synaptic boutons from all the pyramidal axon samples taken made a total of 18 putative synapses with a total of 456 of the three interneurone populations sampled giving a ratio of 7.6 boutons for each PV, VIP or CCK immunopositive neurone and 191 boutons available for every one potential contact observed. For each of the immunolabelled populations tested the ratio of boutons per immunopositive cell was 4.58:1 for PV, 8.4:1 for VIP and 18.6:1 for CCK. The ratio of boutons per potential synaptic contact to the same populations of neurones was 123.8:1 for PV, 860:1 for VIP and 539:1 for CCK indicating that the axons of the RS type layer 4 pyramidal cells selected for this study preferentially contact PV immunolabelled neurones (see table 7.1 for data from individual tests). These findings are unsurprising considering the different densities of immunopositive cells of each class within the cortex.

Putative synaptic contacts were made onto primary, secondary and tertiary dendrites. No potential axo-somatic contacts were observed.

Pyramidal Cell ID	Total		Boutons per Immuno +ve Cell	No. Immuno +ve Contacts	Boutons per contact	Dendrite Contact	Distance (μM)	
	Boutons	Immuno +ve cells					Pyr - Int Soma	Pyr - Int Contact
PV1	447	120	3.7	4	111.8	B1: 1° C1: 1° C2: 2° D1: 1°	121.5 70.6 171.3 42.1	133.5 78.5 207.2 35.1
PV2	617	127	4.9	4	154.3	B1: 3° C1: 2° C2: 1° D1: 1°	100.5 137 33.3 136.6	75.2 160 65 42
PV3	421	77	5.5	4	105.3	B1: 1° B2: 1° C1: 1° C2: 1°	190.5 55.6 71 121	181.8 62.6 59.9 123.2
Mean	495	108	4.58	4	123.8		104.3	102
VIP1	656	37	17.7	0	656	n/a	n/a	n/a
VIP2	462	29	15.9	3	154	A1a:2° A1b:3° C1: 1° C2: 2°	251.2 " 132.1 40.6	192 171.6 121.8 66.1
VIP3	309	37	8.4	1	309	C1: 1°	167.2	154.7
Mean	475.7	34.3	13.8	1.3	373		147.75	176.5
CCK1	398	16	24.8	1	398	C1: 1°	103.1	107.4
CCK2	141	13	10.8	0	141	n/a	n/a	n/a
Mean	269.5	14.5	18.6	1	269.5		103.1	107.4

Table 7.1. Total numbers of RS layer IV pyramidal cell axonal boutons counted within each sample area. Measurements of total distance in 3 dimensions from layer IV pyramidal cell body to potential contacts and somata of PV, VIP and CCK immunopositive cells.

7.7 Conclusions.

This preliminary study was performed to develop the double peroxidase technique for the permanent and differential visualisation of immunolabelled interneurones and individual neurones filled with biocytin by intracellular injection whilst also permitting the ultrastructural preservation of neuronal fine structure for electron microscopic confirmation of putative synaptic contacts. The study has indicated the potential of the method to provide a means for the assessment of the selective axonal targeting by electrophysiologically characterised pyramidal cell populations to

immunocytochemically labelled interneurone classes. The technique may be readily applied to different brain regions and may also utilise many antibodies to select specific interneuronal populations that may shed light onto the proportional excitation of specific interneurone subtypes.

The clarity of the labelling achieved by this technique may also allow similar studies to be performed to assess the immunocytochemically classified targets of biocytin filled and electrophysiologically classified interneurones. A single slice containing a filled FS interneurone was also successfully subjected to immunofluorescence to co-localise PV with injected biocytin, followed by the double peroxidase technique using the same antibody with successful differential staining indicating the possibility of identifying contacts between interneurones of the same neurochemical class.

The correlation of electrophysiological properties of a variety of neurones filled with biocytin in different layers and/or functionally defined brain regions and the assessment of their preferred immunocytochemically defined targets using this technique may provide useful circuitry information.

8.0 DISCUSSION.

Paired intracellular recording with biocytin filling in neocortical slices is a versatile technique for the examination of cellular connectivity, the properties of synaptic connections and the morphology of the recorded cell pairs with unambiguous identification of the neurones involved. The combination of physiological recordings, with antibody visualisation techniques and with anatomical analysis of synaptically connected pairs of neurones is shedding light into the distribution and specificity of connections between classified neurones within functionally identified regions of the brain.

The recordings sought in the studies described by this thesis were between the excitatory pyramidal cells and between pyramidal cells and inhibitory interneurones in the primary visual and somatosensory regions of the neocortical thalamo-recipient layer 4 of the adult cat and rat. The studies attempted to compare the neuronal morphology of synaptically connected pairs of cells between cat and rat neocortex and to identify any differences (or similarities) in the physiological properties, connection probability or synaptic dynamics for those pairs. The studies were also directed to identify clearly which of the cell subtypes in layer 4 made synaptic connections and to identify any specific target selection. In addition, paired recordings of synaptically connected excitatory cells were scrutinised for evidence of gap junction mediated intercellular communication.

8.1 METHODOLOGICAL CONSIDERATIONS.

The slice preparations, electrophysiological and histological techniques used here, whilst arguably being the most suitable protocols for the inclusive study of intercellular connectivity and synaptic dynamics with cellular morphology, by their very nature introduce artefacts and biases to the observations made, not least because the neurones under examination are displaced from their natural *in-vivo* environment. As such, experimental design (most specifically related to the use of cortical slices) has several implications with respect to the data obtained that must be addressed.

The slicing procedure may introduce several potential biases to connectivity ratio estimation

through the cutting of axonal afferents. The curtailment of axonal processes limits synaptically connected neurones to relatively closely neighbouring pairs of cells within a relatively undamaged and therefore healthy band of neurones within the depth of the slice. Slicing of the cortex may therefore introduce a potentially profound underestimation of the levels of connectivity, particularly over greater distances when compared with the natural state *in-vivo*. On the other hand, deafferentation by slicing has been found to promote artificial plasticity of dendritic spines and sprouting of axonal processes in hippocampus (Kirov *et al.*, 1999). This occurs during the first 1-2 hours after slice preparation (slices compared with perfusion fixed tissue), and the processes formed appear to support intact synapses with both pre and postsynaptic densities. This has obvious implications for the validity of all slice-based experimentation but it should be pointed out that despite the increased spine density observed in hippocampal slices, there is no evidence to date suggesting that the connections formed do not follow the patterns of connectivity expressed by the same neurones *in-vivo*.

The quality of the recordings (ie. the cells selected, the recording duration and the stimulus protocols applied to each) dictate which frequency-dependent synaptic properties may be studied at each connection. The post-hoc analytical demonstration of specific frequency- dependent synaptic properties at certain connections and not others does not necessarily preclude their existence at connections recorded under slightly different stimulus conditions. It does, however indicate which mechanisms are available to those cells at connections between groups of identified neurones at specific laminar locales relative to each other.

The search strategy of individual experimenters appears to dictate the types of neurones impaled, stabilised, recorded and filled. For example, different researchers using the same techniques, the same equipment and even in some cases slices from the same animals record connections involving differing classes of neurones. For instance, during the course of these experiments, no spiny stellate cells were observed in cat tissue (and only two in rat) despite other investigators recording and visualising them in material from the same cat.

8.2 THE NEURONES OF BOTH CAT AND RAT NEOCORTEX EXHIBIT CROSS SPECIES CONFORMITY.

The neocortical neurones comprise broad groups of functionally diverse cells that may be subclassified according to their spike discharge characteristics, neurochemistry, target preferences and anatomy. Excitatory and inhibitory neurones from both cat and rat that were recorded and adequately filled to permit total reconstruction of their dendritic and axonal arbours were compared to attempt to identify any significant differences in their anatomical characteristics, spike discharge patterns or synaptic properties between the species.

8.2.1 The Pyramidal Cells.

When comparing the morphology and neurophysiological characteristics of pyramidal cells from cat and rat neocortex a large degree of cross species conformation was observed. Cells from cat and rat cortex were similar in size, shape, axo-dendritic distribution, firing properties and in the range of dynamic properties of the synaptic connections they made and received (see section 8.6 below). The pyramidal cells of the two species were therefore easily recognisable as commensurate components in terms of anatomical characteristics including dendritic distribution, axonal morphology, the propensity for dendritic spines of similar size and shape and even the overall cell sizes did not show appreciable differences between the species in the sample analysed, despite the difference in cortical and layer depth available for them to occupy. Physiologically the pyramidal cells of both species were equally identifiable as such with action potential shapes and firing patterns of remarkable similarity.

While the pyramidal cells of layer 4 exhibit a great deal of similarity both within and across the species they may not be considered a homogenous population throughout the cortex. Cells from each layer have significantly different axo-dendritic radiations with distinct axonal layer preferences as well as different firing patterns depending on their location within the laminae, indicating different roles in the direction specific feed-forward of excitation through the cortex, and therefore the neurones (or circuits of neurones) that they may activate.

8.2.2 The Interneurones.

The family of interneurones comprise a functionally diverse population with a complex and overlapping range of properties such as spike discharge patterns of either FS, IS, RS or BF, they can have very specific target preferences for the dendrites, somata or axon initial segments of their postsynaptic partners and they can also express a variety of neurochemicals including specific calcium binding proteins or neuropeptides (see Kawaguchi & Kubota, 1997). That these properties can occur in many different combinations results in an apparent population continuum of interneurones with potentially dramatically different roles in cortical inhibition, but despite this complexity, even a relatively small sample of interneurones can reveal groups of cells that share combinations of the above properties such that peaks in the continuum become apparent. The PV containing FS cells that typically target the somata and proximal dendrites of postsynaptic neurones, for example, exhibit a combination of features that constitutes a relatively well defined peak in the wider interneuronal population - the FS, PV-containing 'basket cells'.

The layer 4 interneurones filled and stained here from both cat and rat cortex could be placed into groups with similar properties according to the above criteria. All of the PV positive cells from both species were, for example, FS and had stellate dendritic radiations, and all of the PV and CB immunonegative neurones were RS, stellate and appeared to make dendritic contacts with their postsynaptic targets. The interneurones of the sample presented here did not therefore appear to differ dramatically between the species.

8.2.2.1 Interneurones sharing many similar properties have strikingly different axonal arbours

Even the subclasses of interneurones (as determined by their spike discharge patterns, neurochemistry and target preferences) did not however comprise homogenous populations. When comparing their anatomical properties, aside from the consistent absence of dendritic spines, the shape and span of their dendritic and particularly of their axonal arbours displayed striking variability in both species such that no two layer 4 cortical interneurones recorded filled and visualised could be considered alike in gross morphology. The axonal arbours of individual interneurones that

otherwise shared similar electrophysiological and neurochemical properties ranged from a dense arbour contained entirely within layer 4 to large arbours spanning layers 1 to 6, indicating that even cells of the same broad class distribute inhibition to different targets and must therefore have dramatically different roles in the function of cortical columns.

8.2.3 Summary.

The similarity of neurons from cat and rat neocortex are perhaps surprising considering that the two species have very different physical characteristics and environmental specialisations and very different cortices in terms of size and shape, but are a little less surprising when it is understood that these similarities are exhibited by the entire family of mammals which has diverged in evolutionary terms for tens or even hundreds of millions of years. For example, the pyramidal cell, the major excitatory neurone of the neocortex and a variety of anatomically identifiable interneurones have been observed in both marsupial and primate visual cortex and their presence is often ubiquitous to many areas of the cortex sampled (Lund, 2002). It would seem that the basic building blocks of a functionally diverse cortex are governed by highly conserved genetic determinants passed down through evolutionary selection from species to species.

Continued study of the interneurones with detailed anatomical reconstruction of complete axo-dendritic arbours is required to generate both a much larger database of thoroughly classified cells, perhaps identifying additional peaks in the continuum, and to assess more accurately their functions according to the location of the neurones they innervate.

8.3 THE PROBABILITY OF SYNAPTIC CONNECTION BETWEEN THE NEURONES OF LAYER 4.

In order to assess the frequency of synaptic interactions between layer 4 neurones, the number of tests required before synaptic connection was observed between pairs of recorded neurones was noted and used to generate a 'hit rate' expressed as a ratio.

Excitatory to excitatory cell connections were observed at 1 in every 31 tests for cat and 1 in 48 for rat and reciprocal connections were observed in both species. Such estimates are of course subject to biases imposed by the search strategies employed by different experimenters and by experimental design (see methodological considerations, section 8.2) that may explain the difference between these estimates and those of a smaller previously published sample (around 1 in 6 for both species (Thomson *et al.*, 2002)) but do comply with the suggestion that the level of interconnectivity is similar between the species. The probabilities of interactions between randomly selected pyramidal cells and interneurones were also similar in both species with excitatory connections (pyramid to interneurone) observed for 1 in 20 and 1 in 23 for cat and rat respectively and inhibitory connections (interneurone to pyramid) 1 in 15 for cat and 1 in 9 for rat with reciprocal connections observed in cat as has been seen before (Tarczy-Hornoch *et al.*, 1998). These results comply with a previously published estimate from a smaller sample of 1 in 10 inhibitory to excitatory layer 4 connections observed in cat (Thomson *et al.*, 2002). No estimates of rat layer 4 excitatory and inhibitory cell connectivity are available in the literature, but these results indicate the levels do not differ dramatically from those of the cat cortex.

So, in addition to the conformity of neocortical structure and cellular content for both cat and rat the probability of finding synaptically connected pairs of neurones was also similar, indicating comparable levels of cellular interconnectivity between the sampled neurones from each species.

8.3.1 All putative intralaminar synaptic contacts from layer 4 pyramidal cells were made onto the basal dendrites of their postsynaptic targets.

The number of synaptic contacts made by a single axon is an important factor in determining the size and efficacy of EPSPs and the location of those synapses on the postsynaptic dendritic tree is thought to be an important factor in determining the shape of EPSPs elicited by individual presynaptic APs via the filtering of more distal dendritic inputs (Jack & Redman, 1971), and a variety of mechanisms that enhance the impact of distal excitatory inputs overcoming the cable properties of the dendrites (see Williams & Stuart, 2003 for review). All of these factors have important implications in the control of action potential output from postsynaptic neurones both via

the summation of inputs from a single presynaptic cell as well as via the integration of multiple inputs to the same postsynaptic neurone.

All the demonstrably synaptically connected layer 4 pyramidal cells that were adequately filled and stained to allow complete reconstruction of their dendritic and axonal arbours were studied to locate the sites of potential synaptic contact. In concurrence with previous studies of pyramidal cell connectivity, all putative excitatory synapses (observed at the light microscope) were onto the dendritic arbour of the postsynaptic pyramidal cells irrespective of subclass. Moreover, the number of contacts ranged from 1 to 7 and all were made onto the basal dendrites. Of course this is a relatively small sample of layer 4 pyramidal neurones and as their axons tend to arbourise most densely in layer 4, the basal dendrites of postsynaptic neurones in the same layer might be expected to receive the most synaptic input. Nevertheless this feature of layer 4 circuitry might be an important factor in the function of those circuits as fast local Na^+ spikes (Ariav *et al.*, 2003) and NMDA spikes (Schiller *et al.*, 2000) in basal dendrites are thought to improve the temporal precision of neuronal output.

8.3.2 Pyramidal cells frequently make putative autapses with their own dendrites.

Autapses are synapses made by a neurone's axon onto its own soma or dendrites. They have been observed on adult rat and cat neocortical inhibitory FS basket and dendrite targeting cells (Thomson *et al.*, 1996; Tamas *et al.*, 1997), and on pyramidal cells (particularly in layer 5) of the developing rat neocortex (Lubke *et al.*, 1996). In the course of these studies, where complete reconstructions of dendritic and axonal arbours were performed, no potential interneuronal autapses were found, but multiple putative autapses were observed upon adult layer 4 pyramidal cells in both species indicating that excitatory self-innervation occurs frequently in this layer. In all cases they occurred either more than once (on average 2.8 autapses per cell, range 2-4), or not at all. There were no immediately apparent morphological differences between the pyramidal cells that harboured potential autapses and those that did not and the putative targets were similar to those of their synapses (ie. the spiny dendrites).

So what might autaptic self innervation be good for? A number of potential roles have been

suggested ranging from 'self sensing' (Van der Loos & Glaser, 1972) whereby the inhibitory autapses might provide a gating mechanism though which a neurone's output controls its input, to a more probable means for regulating excitability (Bekkers & Stevens, 1991). Studies of the GABAergic basket and dendrite targeting interneurones in slices of the visual cortex have revealed abundant (up to 30) autaptic connections (Tamas *et al.*, 1997). Experiments designed to identify their roles have indicated that they do affect cellular excitability (Bacci *et al.*, 2003) by contributing to the spike afterhyperpolarisation (AHP) of fast spiking and burst/regular spiking interneurones (Pawelzik *et al.*, 2003) and hence are involved in the modulation of spike discharge characteristics. This effect is manifest by the alteration (slowing or interruption) of repetitive firing. Autaptic self-innervation of interneurones may therefore constitute an effective short term form of feedback inhibition contributing to the timing of action potential generation by interneurones.

If autaptic self innervation of pyramidal neurones has a contrasting role, the modulation of excitability by contributing in this case to the afterdepolaristation (ADP) might be expected to generate potentially undesirable positive feedback of excitation at the onset of suprathreshold excitation. However, as the pyramidal autapses that have been described in developing rat neocortex (Lubke *et al.*, 1996) and in that of the rabbit (Van der Loos & Glaser, 1972), and that are observed here in adult cat and rat layer 4 (though electron microscopic confirmation has not as yet been performed) are low in number (between 2 and 4 autapses for each cell) compared with those seen previously on the basket interneurones, and assuming that they are subject to the same levels of paired pulse depression as is observed in recordings of their synaptic connections, their effect on pyramidal firing rate can be expected to be transient.

Pyramidal cell autaptic self innervation appears to occur frequently in layer 4 and may therefore serve as an effective form of short term feedback of excitation, elevating the spike discharge rate for a short period following the onset of novel suprathreshold excitation.

8.4 ALL LAYER 4 PYRAMIDAL NEURONES THAT WERE SYNAPTICALLY CONNECTED TO OTHER NEURONES IN LAYER 4 WERE REGULAR SPIKING.

In order to identify whether layer 4 neurones targeted specific neuronal populations according to the intrinsic firing patterns of the pre and/or postsynaptic cell, all impaled and stabilised neurones were subjected to positive square wave current pulse injections to evoke trains of action potentials and their spike discharge patterns noted. Each electrophysiologically classified neurone was then tested in both directions for synaptic connection with randomly selected excitatory or inhibitory neurones in the vicinity as revealed by the generation of PSPs recorded in the postsynaptic cell in response to evoked presynaptic action potentials.

All the cat and rat layer 4 excitatory neurones reported here exhibited either RS (63%) or BF (37%) properties typical of excitatory cells reported previously (McCormick *et al.*, 1985). Of these, a total of 1598 tests for synaptic connections to other neurones located in layer 4 were performed and 32 connections were observed (of these the location of 10 cat and 12 rat somata were confirmed by light microscopy). Interestingly, all of the pyramidal cells recorded from layer 4 from both species that made or received synaptic connections within layer 4 (with both pyramidal cells and with layer 4 interneurones) exhibited RS discharge characteristics. BF pyramidal cells were never found to be connected with another layer 4 cell (240 tests) despite demonstrable connections to these cells from layer 3 in rat (1:8, not reported). The local synaptic connections of neocortical layer 4 pyramidal cells therefore appear to be highly selective, targeting RS rather than BF excitatory neurones in layer 4.

The identification of potentially specific target selection within local cortical circuits is not in itself novel. Layer and cell specific forward projections from layer 4 to 3 and for 3 to 5 that primarily involve the selective activation of pyramidal cells and back projections from layer 3 to 4 and 5 to 3 that primarily involve the activation of interneurones are examples of clear patterns of selective innervation within the neocortex as revealed by paired recordings with correlated anatomy (see Thomson & Bannister, 2003 for review). What is novel here is that the pyramidal cells of layer 4 appear to innervate other pyramidal cells selectively within the same layer, innervating those that have RS discharge characteristics and excluding connections with the BF cells. In addition, the layer

4 pyramidal cells that were pre- or post-synaptic to layer 4 interneurones were also all RS.

These data beg potentially very important questions: From which cells do the BF layer 4 pyramids receive input in layer 4, to which cells are they presynaptic and what is the purpose of such selectivity of intralaminar connectivity? The first aspect of this question requires a detailed study of extralaminar inputs to layer 4 since other layer 4 neurones (with large quantities of axon in the vicinity) appear to avoid contact with the BF cells. The second aspect of this question may in part be answered by a detailed study of the axonal distribution patterns produced by the BF cells and to compare these with those of the RS cells (unfortunately insufficient BF pyramidal cell anatomy was available to reveal any differences in axonal distribution patterns during these studies so the elucidation of differential target or layer preferences awaits further investigation). The third aspect of the question above requires an understanding of the different roles of presynaptic firing patterns upon the neurones innervated.

8.5 THE SYNAPTIC PROPERTIES OF EXCITATORY CONNECTIONS WITHIN LAYER 4.

In order to identify the properties of interactions between layer 4 neurones, pairs of synaptically connected cells were recorded, and recordings digitised and analysed offline. The excitatory connections generated postsynaptic potentials with significantly different timecourses and frequency dependent properties which were apparently dependent on the types of cells innervated. Such frequency-dependent properties included paired pulse depression at all pyramid to pyramid connections and at many pyramid to interneurone connections and frequency dependent facilitation between some pyramid to interneurone pairs. Layer 4 pyramidal synapses were capable of retaining past history of high frequency activity for periods of seconds through post tetanic potentiation and some layer 4 cells may also have the capability to modulate their outputs to other neurones via branch point failure of axonal conduction. All of these features of layer 4 excitatory connections will be discussed separately below.

8.5.1 The EPSPs generated in excitatory and inhibitory neurones had different shapes.

To assess the properties of excitatory inputs onto other excitatory neurones and onto inhibitory neurones, EPSP amplitude, time to peak and half width was measured for each intralaminar layer 4 to layer 4 connection. In both species, while the range of excitatory postsynaptic potential amplitudes recorded was similar, EPSPs generated in pyramidal cells were significantly broader and had slower rise times than those generated in the inhibitory cells (see figure 5.7) even when recorded at similar postsynaptic membrane potentials and with synaptic contacts at similar distances from the soma.

These findings in both cat and rat are in compliance with those reported previously in rat, with EPSPs generated by most pyramid to interneurone connections (Buhl *et al.*, 1997;Thomson *et al.*, 1996;Thomson, 1997) having a shorter duration than those seen at pyramid to pyramid connections (Deuchars *et al.*, 1994;Thomson, 1997) and several factors are thought to contribute to the differences. The size, shape and structure of the postsynaptic dendritic tree contributes to PSP shape via the passive cable properties of the dendrites (Stafstrom *et al.*, 1984), such that the distance of excitatory inputs relative to the soma affects the duration due to the capacitive properties of the dendrites. Pyramidal cell dendrites are densely covered in spines, which adds significantly to the amount of membrane between the point of synaptic contact and the postsynaptic soma and therefore to the capacitance of pyramidal cells compared with the interneurones (which are typically devoid of spines) resulting in increased duration of PSPs onto excitatory cells. In addition, the duration of EPSPs generated in pyramidal cells and interneurones is greatly affected by differential postsynaptic glutamate receptor composition.

Most, if not all inputs to pyramidal cells from other pyramidal cells are mediated by both N-methyl-D-aspartate (NMDA) and α-amino-3-hydroxy-5-methyl-4-isoxazole proprionic acid (AMPA) receptors. The higher affinity of NMDA receptors for glutamate and their slower activation and inactivation kinetics result in EPSPs of longer duration than those mediated by AMPA receptors alone. This is particularly the case when the postsynaptic membrane is depolarised, relieving the NMDA receptor channels of the Mg^{++} block that dramatically reduces their open duration at more negative membrane potentials. EPSPs in interneurones are more rapid in time course for two reasons. Firstly because they typically involve fewer or no NMDA receptors and secondly because

many (particularly the FS) interneurones express AMPA receptors that lack GluRB (Jonas *et al.*, 1994). AMPA receptors lacking this subunit display faster kinetics and unlike those mediated by GluRB-containing AMPA receptors are permeable to Ca^{++}.

The timecourse of EPSPs has functional implications related to the temporal summation of multiple transmitter releases onto the same postsynaptic neurone, which increases the probability that the postsynaptic neurone will reach action potential threshold. The brief duration of subthreshold interneuronal EPSPs ensures that temporal summation of the postsynaptic response requires either an extremely high frequency of presynaptic discharge or precisely coincident inputs from multiple presynaptic cells. Pyramidal EPSPs on the other hand, are more likely to sum effectively at lower frequencies (and sum coincident inputs from multiple cells over a broader range of intervals). Moreover, the non-linear voltage relation of the NMDA receptors at pyramid to pyramid synapses can result in supra-linear summation of coincident EPSPs, provided they arise in adjacent regions of the dendritic tree. The properties of pyramidal cell and interneuronal dendrites and the different composition of their postsynaptic glutamate receptors therefore appears to contribute significantly to the different shape of the EPSPs generated and so the integrative properties of those neurones in both cat and rat neocortex.

8.6 FREQUENCY DEPENDENT EPSP PROPERTIES.

The control of information flow through the cortex and in all other regions of the brain is thought to be governed not only by the patterns of action potential generation in networks of neurones but also by the modulation of the inherently 'unreliable' (a more suitable term might be 'flexible') patterns of synaptic release that manifest as stimulus frequency dependent modifications in synaptic strength (Tsodyks & Markram, 1997). The regulation of the synaptic mechanisms responsible for modifications to the probability of transmitter exocytosis is an essential requirement for the fine tuning of neural code processing and as such the study of these processes has been a major objective of research over recent decades. The mechanisms thought to contribute to differential probability of synaptic release in a wide variety of cortical circuits include the gross anatomy (in particular, the size) of synaptic boutons and the anatomy of synaptic active zones, the

regulation of transmitter vesicle release by calcium influx to the presynaptic terminal and the possible involvement of synaptic vesicle proteins with different affinities for calcium (Dodge & Rahamimoff, 1967), and calcium buffering proteins capable of attenuating transmitter release by dampening the rise in free calcium at the terminal in response to presynaptic action potentials (Adler *et al.*, 1991).

The mechanisms employed at each synapse for the modulation of presynaptic release probability are essential for determining whether a particular connection will exhibit depressing or facilitating outputs in response to repeated activity. The rates of onset and decay of these properties determine how capable a synapse is of retaining the past history of action potential activity and are differentially expressed at different neocortical connections. In order to determine which synaptic properties may be exhibited by connections between different types of neurones in layer 4 in cat and rat, synaptically connected pairs of neurones were tested with a range of interspike intervals, recorded and analysed offline.

8.6.1 All pyramid to pyramid and most pyramid to interneurone connections in both cat and rat layer 4 generated 'depressing' EPSPs.

Paired pulse and frequency dependent depression was observed at all layer 4 pyramid to pyramid connections and at some connections between pyramidal cells and interneurones from both species. Where immunocytochemistry was performed, none of the interneurones exhibiting depressing EPSPs was immunoreactive to calbindin, VIP or CCK and all were immunoreactive to parvalbumin antibodies.

The effect was manifest by a reduction of the EPSP amplitude in response to successive action potentials relative to the response to the preceding APs in trains elicited by current pulse injections to the presynaptic neurone. In all recordings where sufficient sweeps containing multiple presynaptic action potentials at a range of interspike intervals were available to analyse the frequency dependent properties of the depression, average 2^{nd} EPSP amplitudes were observed to recover towards that of the average 1^{st} EPSP as the interspike interval increased.

All depressing connections were analysed to identify the potential mechanisms involved.

Depression appeared to be due to a progressive decrease in the probability of transmitter release in response to successive action potential in the trains as revealed by plots of amplitude distributions. In all cases where the distribution plots appeared to fit a binomial, they were investigated further using the classical coefficient of variation method (Faber & Korn, 1991) to indicate whether the phenomenon was the result of pre- or post synaptic mechanisms. The resultant evidence was suggestive of presynaptic mechanism typically involving a decrease in transmitter release probability (though a postsynaptic contribution cannot be entirely ruled out).

8.6.2 EPSPs generated in some interneurones from both cat and rat exhibited paired pulse facilitation.

Powerful paired pulse facilitation was observed in two recordings of pyramid to interneurone synaptic connections (1 cat and 1 rat). Neither of the interneurones exhibiting facilitating EPSPs was immunoreactive to antibodies raised against parvalbumin, calbindin or VIP.

The effect was manifest by an increase in EPSP amplitude in the average response to 2^{nd}, 3^{rd} (4^{th}...) action potentials compared with that of the 1^{st}. In one connection (rat) the responses to each successive AP in the trains (of up to 6 spikes) was larger than the response to the preceding AP, resulting in progressively more powerful excitation in response to the longer presynaptic spike trains. In the cat connection, the second EPSP was the most powerfully facilitated although all subsequent EPSPs maintained a steady level of excitation, perhaps due to the onset of depression at the same synapses. Facilitation was observed to be frequency dependent, with the most powerful enhancement of EPSP amplitude recorded at shorter interspike intervals and progressive decrease in amplitude toward that of the average first EPSP with increasing interspike intervals.

As with the depressing connections, the amplitude distributions for both facilitating connections were plotted. The number of apparent total failures of synaptic transmission were observed to decrease with each successive AP in the trains indicating in this case a progressive increase in the probability of synaptic release. In both cases, plots of the normalised coefficient of variation versus normalised mean EPSP amplitude indicated that the mechanism for facilitation may be of presynaptic origin.

8.6.3 Functional implications of depression and facilitation.

These electrophysiological recordings of excitatory connections to pyramidal cells and interneurones in layer 4 of both cat and rat neocortex comply with the findings of previous investigations in the same and in other layers. The postsynaptic response to presynaptic action potentials is not uniform, instead the response to successive APs may be qualitatively different from those in response to preceding events depending on the firing rate and the timecourses of frequency dependent depression and facilitation. The rate dependent changes in PSP amplitude and efficacy that result from variable neurotransmitter release probability therefore further affect the coding of neuronal output patterns dependent on the recent history of synaptic activity (Tsodyks & Markram, 1997). That these phenomena are dependent on spike frequency is a given (since the most powerful effects are often observed at short interspike intervals), but the rate of onset and decay determines which aspect of the presynaptic spike train code is relayed most efficiently at individual synapses.

The output of depressing synapses which exhibit relatively high probabilities of release ensures fairly faithful transmission of low presynaptic discharge rates. They detect changes in presynaptic firing pattern as the synapses take time to adapt to a new firing frequency and convey novel activity well but report maintained activity poorly. Facilitating outputs, with relatively lower probabilities of release on the other hand, report low frequency activity poorly with little or no response whereas maintained high frequency activity results in powerful excitation. Progressive facilitation of excitatory outputs increases the probability of its postsynaptic partners reaching action potential threshold provided high frequency activity is maintained.

Depression and facilitation of EPSP amplitude in response to repeated activity is ubiquitously expressed by the excitatory synapses of layer 4 in both cat and rat neocortex. They are the result of presynaptic modulation of release probability and are expressed at synaptic connections in a manner dependent on the types of neurones innervated. That profound depression and facilitation can be expressed simultaneously at connections by the same axon onto different targets (Thomson *et al.*, 1993;Thomson, 1997) indicates that these characteristics combine to determine which circuits (or parts thereof) are activated and in response to which temporal pattern under the control of individual synapses (see Gerstner *et al.*, 1997 for review)

8.6.4 Post-tetanic potentiation may cause postsynaptic cell to fire earlier in response to potentiated input, an important mechanism of cellular retention of past activity.

Post tetanic potentiation (PTP) was studied at a rat pyramid to pyramid recording in layer 4 in which the presynaptic cell was driven to generate sequential sweeps containing trains of up to 10 action potentials for extended periods (the stimulus interval was 1 pulse every 3 seconds). The effect was manifest firstly by an increase in 1st EPSP amplitude that was dependent on the number of presynaptic action potentials in the preceding sweep. Subsequent EPSPs in the trains were depressed in amplitude relative to the first. Following potentiation, when only single action potentials were elicited the effect decayed slowly over a period of around 10 seconds.

The onset of PTP was slower than that of facilitation and it decayed more slowly. The mechanism appears to be of presynaptic origin and is thought to result from the Ca^{++} dependent liberation of vesicles from the reserve pools due to loading of the presynaptic terminals with Ca^{++} following tetanic activity (Llinas *et al.*, 1991) leading to an increased probability of release due to increased occupancy of release sites. Potentiation at the neuromuscular junction has been suggested to result from an increase in the amplitude of APs after extended periods of high frequency activity which may also underlie the increased probability of release due to increased calcium influx in response to each AP (Hubbard, 1963).

The functional significance of PTP at excitatory synapses is twofold. Firstly, as potentiation is slow to develop, periods of extended high frequency spike bursts/trains progressively increases the chances of the postsynaptic cell reaching action potential threshold from the single presynaptic input alone. In addition, the greater rate at which the postsynaptic cell is depolarised increases the probability of action potential generation. Secondly, it results in a wider window during which loosely coincident inputs may sum to reach firing threshold compared with that provided when unpotentiated (see figure 4.13b). In other words, PTP may provide a looser form of temporal filter similar to that provided by facilitation but allowing more time for the summation of inputs to promote a postsynaptic action potential.

8.6.5 Branch point failure may provide a mechanism for the unleashing of latent synaptic connections depending on the integration of convergent inputs.

One recording between two layer 4 pyramidal cells in adult rat cortex exhibited unusual properties suggesting the occurrence of branch point failure of axonal conduction. While branch point failure is not a frequency dependent property of synaptic connections, it does appear to provide a mechanism for either decreasing or enhancing synaptic output according to specific stimulus parameters.

In this single example, current pulse injections into the presynaptic pyramid that were adequate to initiate trains of up to 6 action potentials often failed to generate postsynaptic EPSPs in response to any. Occasionally, single or multiple EPSPs occurred apparently randomly in response to action potentials at any point within a train and when the strength of injected current pulses were increased activation of EPSPs became more and more likely. While the relevant data available from this connection was not sufficient to analyse the current pulse intensities required to achieve conduction in great detail, it did suggest that the power at which the presynaptic neurone was driven impacted upon the likelihood of EPSP generation in the postsynaptic cell. The EPSP was large (3.06mV) and surprisingly stable in amplitude, showing little evidence of the more conventional depression or facilitation described above. Apart from the unusual skewing of amplitude histograms of 1^{st}, 2^{nd} and 3^{rd} EPSPs resulting from the unusual occurrence of total transmission failures the distributions did fit the binomial as observed for most other excitatory to excitatory connections (see figure 4.12a).

The efficacy of impulse conduction along axons to the nerve terminals could be an important factor in determining the probability of transmitter release. The phenomenon is not considered to be common at central synapses, at least in young rats (Wang *et al.*, 1999) but has been described in pyramidal cells in hippocampal slice cultures in which the voltage dependent activation of A-type K^+ channels was revealed by the application of 4-aminopyridine (a K^+ channel blocker) to be involved in curtailing AP propagation at individual axonal branch points (Debanne *et al.*, 1997). Debanne *et al* also showed that in sequential recordings from pairs of pyramidal cells, action potential propagation failed at some but not all connections from the same axon (Debanne *et al.*, 1997). These data suggest that the physiological activation of the K^+ channels may allow the

integration of membrane potential changes at individual axonal branch points, thereby altering their ability to transmit action potentials.

The function of pyramidal branch point failure in this layer 4 pyramid to pyramid connection in rat may therefore be related to latent excitatory connections that are unveiled by integrated inputs from multiple presynaptic cells and the effect could be that of facilitating or increasing synaptic output under increased stimulus intensity.

8.6.6 Summary.

The modulatory mechanisms employed at central synapses for the modification of synaptic efficacy allow postsynaptic neuronal responses to paired pulse/brief train stimuli to be either increased or decreased in strength depending on the history of presynaptic AP activity. In layer 4, both cat and rat excitatory connections exhibited paired pulse depression and facilitation that was similar in both power and duration. Rat connections were observed that exhibited post-tetanic potentiation and apparent branch point failure of axonal conduction (these features can not however be ruled absent from excitatory connection in the cat). While the exact molecular mechanisms by which they operate are still unknown, release- and frequency-dependent depression are most probably of presynaptic origin; as are facilitation, and potentiation.

8.7 GAP JUNCTION-MEDIATED INTERCELLULAR COMMUNICATION BETWEEN ADULT PYRAMIDAL CELLS.

Electrical gap junction-mediated intercellular communication (GJIC) is characterised by fast conduction between electrically coupled neurones via complex intercellular pores. They are capable of permitting electrical communication between neurones in the absence of phase lag compared with the >0.5ms latency required for axonal conduction. The presence of gap junctions in the mammalian neocortex is most often observed between the interneurones and is thought to provide an important means for the synchronisation of neuronal populations. GJIC between excitatory pyramidal cells has been observed during development of the neocortex, is indicated by dye transfer

between intra-cellularly filled neurones and coupled neurones in the vicinity. GJIC is thought to be an important factor in the migration of neurones through the neuropil during development. The dye-coupling, readily observed at postnatal age (P1 - P4) appears to decrease with increasing postnatal age (Naus & Bani-Yaghoub, 1998) indicating that pyramidal gap junctions may be lost with increasing maturity. However, this form of communication has been predicted to persist in the adult through computer modelling of neuronal network activity by other investigators (Traub & Bibbig, 2000;Traub *et al.*, 2003), and by the observed retention of expression of connexin mRNA in layer 5 pyramidal cells (Simburger *et al.*, 1997). However, to date, no direct physiological evidence has been presented to confirm their existence in the adult mammalian neocortex.

A single recording presented here exhibited compelling evidence for the existence of two-way pyramidal cell to pyramidal cell gap junction mediated intercellular communication (GJIC) in adult rat neocortex between two excitatory pyramidal neurones in layer 3 that were both presynaptic to the same layer 5 pyramidal cell (see section 6). The presence of the electrically coupled neurone was revealed by spikelets, consistently evoked by positive current pulses injected into the impaled presynaptic pyramidal cell that always preceded, at a short invariant interval, EPSPs generated in the postsynaptic cell (see figure 6.3a). The spikelet occurred only during the current pulse injection and often preceded the first presynaptic action potential, indicating that the coupled neurone was being driven by the same stimulus. When the current pulse strength was increased to evoke trains of action potentials in the impaled neurone, spikelets were often observed to precede the first AP then coincide nearly precisely with subsequent events, indicating that the electrically coupled neurone was also being driven by the impaled cell (see figure 6.3c). Under conditions of combined square wave and ramped current pulse injections into the impaled presynaptic neurone, spikelets were observed to occur shortly after the first evoked AP and promote more rapid depolarisation of the impaled cell back to action potential threshold at a time ordinarily dominated by the spike AHP, indicating that the coupled neurone was also capable of driving the impaled cell (see figure 6.4). When the spikes and spikelets from the impaled and coupled neurones were separated in time by a very short interval or when the coupled neurones were observed to drive each other, the resultant EPSPs often drove the postsynaptic pyramidal cell to action potential threshold (see figure 6.5c), whereas their individual EPSPs did not.

8.7.1 The roles of gap junctions in adult cortex.

To date the majority of evidence for intercellular communication between neurones in the adult neocortex is focussed towards the interneuronal population. Such communication is thought to synchronise the firing of coupled interneurones which in turn modulates the output patterns of their postsynaptic pyramidal cells (Traub *et al.*, 2001). The result of such synchrony is potentially very important in the perception of multiple sensory stimuli for which phase-locking of multiple neuronal signals is proposed to be required.

But what use might GJIC between adult pyramidal neurones be? Computer simulation studies have suggested that electrotonic coupling between pyramidal cells in hippocampus may be involved in the generation of 100Hz oscillations when independent of interneurone involvement (Traub & Bibbig, 2000). When the pyramidal cell network simulations were combined with those of the interneurones, ultrafast 200Hz 'ripples' were observed which are predicted to influence or drive gamma oscillations in larger neuronal networks. These simulations predict that pyramidal cell electrical coupling is a prerequisite for the generation of gamma frequencies with the coupling of interneurones providing modulation (Traub *et al.*, 2003).

On a smaller scale (ie. between 2 cells rather than in neuronal network models) the electrical communication between pyramidal cells was observed here to have several striking effects on the properties of the cells connected and a resultant impact on their chemical synaptic outputs to postsynaptic neurones. The electrically coupled neurones were readily observed to be driving each other to action potential threshold, and promoting their near synchronous discharge. The coupling effect was powerful enough to modify the normal discharge pattern of the impaled neurone such that it could fire successive action potentials at times ordinarily dominated by the spike AHP. This indicates that the coupled neurones could be driven to AP threshold by excitatory inputs from other cells and result in the synchronous discharge of its electrically coupled partner even if that cell did not receive the same excitatory inputs. While not a bonafide change in spike discharge characteristics, this property did effectively promote burst like firing frequencies in an otherwise RS neurone. This feature is backed up by experiments performed on pyramidal cells from hippocampus that have shown a correlation between whether a cell has regular spiking or burst firing

characteristics and whether or not the cells were coupled to other neurones (Baimbridge *et al.*, 1991). In addition, theoretical computer models of neuronal firing characteristics add further weight to the possibility that cells coupled by gap junctions fire burst-like AP patterns when they would ordinarily be RS in the absence of electrical junctions (Sherman & Rinzel, 1992).

The other striking effect of GJIC between the two excitatory cell illustrated here was the effect of their combined outputs to the same postsynaptic neurone in layer 5. When the spikelet and first AP coincided precisely, and second APs and spikelets occurred at very short intervals the synchronous EPSPs generated in the postsynaptic neurone consistently achieved AP threshold whereas individual EPSPs did not. Postsynaptic threshold may have been reached due to the activation of voltage dependent currents resulting from the precisely synchronous EPSPs and/or NMDA receptors. Unfortunately however, as the spikelet was so consistently generated in response to each action potential, insufficient data (2 sweeps) were available to compare accurately the EPSPs generated both with and without spikelet activity and therefore measurement of possible non-linear summation of EPSPs was not possible. On the other hand, AP threshold may have been reached by simple arithmetic temporal summation of the common inputs with two synchronised transmitter releases from each cell at very short intervals summing as a direct result of their electrical connection.

GJIC between pyramidal cells therefore appears to be highly effective at ensuring powerful excitation of postsynaptic neurones both by modifying the spike discharge properties of coupled RS neurones and by synchronising excitatory outputs to common postsynaptic cells. In this respect the location of the postsynaptic neurone in the example presented here is of interest. Layer 5 pyramidal neurones are the primary output neurones of the neocortex and the excitatory connections between layers 3 and 5 are exceedingly common (Thomson & Bannister, 1998). Provided coupled layer 3 pyramidal cells contact the same targets in layer 5, GJIC between them in adult tissue may provide a mechanism for enhancing the probability of layer 5 output to subcortical regions.

8.8 FUTURE STUDIES/PERSONAL RESEARCH INTERESTS.

Paired intracellular recording and biocytin filling of synaptically connected neocortical neurones is providing important information relating to the specificity of cortical connectivity, the properties of those connections and the morphology of connected cells. During the course of the studies presented here, a number of novel and potentially important observations have been made for which I would like to continue gathering evidence.

Firstly, the apparent specificity of pyramidal target selection within layer 4 has indicated potentially significant differences in the roles of the RS and BF pyramidal cell populations. I would like to investigate this finding further by selecting, filling and visualising BF pyramidal cells in layer 4 to identify any differences in their axonal arbourisation patterns compared with the RS pyramidal cells from the same layer. In addition it would be interesting investigate which cells are their preferred synaptic targets.

Secondly, the identification of gap junction mediated intercellular communication between pyramidal cells in adult slice preparations is both interesting and important in relation to cortical dynamics, population firing and network properties. The recording shown here (and others made by investigators in this group) amount to compelling physiological evidence for gap junction communication of this kind. Morphological evidence for gap junctions between these cells has proved elusive to date not least because the electron microscopic scrutiny of pyramidal cells for such evidence is a daunting task since although coupling may be functionally very important, it may occur infrequently.

To achieve these aims, I propose to perform experiments directed towards selecting pyramidal gap junctions using paired intracellular recording by targeting cells in very close proximity within cortical columns, gathering further physiological evidence for this form of communication in adult tissue, and locating the junctions at the electron microscopic level. These techniques coupled with post embedding immunogold may shed light into which connexin(s) are involved and direct further study into junction kinetics.

8.9 CONCLUDING REMARKS.

The wealth of neurones that comprise the intact brain are responsible, in some way or other, for almost everything that makes its owner what it is. They are responsible for almost everything we do, every decision we make, every movement we achieve and every aspect of our personality. Perhaps, from the scientists point of view, the most striking capacity the brain furnishes us with is the desire and imagination to ask one very important question - How does it work?

The classes of neurones so far discovered, are embodied with beautifully diverse morphology and daunting arrays of interconnections in networks so intricate and wide ranging that so far it defies comprehension. The intercellular connections are governed by an ever expanding range of modulatory mechanisms which we assume are responsible for selecting and filtering the neural code. The cortical connections illustrated here express many of these information filtering mechanisms at different synapses, even those provided by the same axon. The result of these capabilities is a phenomenally complex capacity for tuning, modifying and distributing neural code by individual neurones, the implications of which present fantastically complex problems for the researcher attempting to understand complete information pathways.

The comprehension of information processing requires a multi-disciplinary approach to define the structure and function of neurones at the molecular level leading up to the understanding of small circuits between well defined cells and finally to whole systems and behaviour. Of course, an enormous wealth of knowledge and an incredible amount of detail on individual systems has already been acquired and the neural code is beginning to be understood. However, a major task for the future will be to tie these details together and establish how they cooperate to accomplish so much, so quickly and in such a consistent manner, often simultaneously.

A great deal of time, energy, imagination and skill from enthusiastic scientists far into the future is going to be required to further our understanding, and undoubtably the project will never be entirely complete. But we must try. In short - at the moment, we are only scratching the surface.

9.0 REFERENCES.

Adler, E. M., Augustine, G. J., Duffy, S. N., & Charlton, M. P. (1991). Alien intracellular calcium chelators attenuate neurotransmitter release at the squid giant synapse. *Journal of Neuroscience* **11**, 1496-1507.

Ahmed, B., Anderson, J. C., Douglas, R. J., Martin, K. A., & Nelson, J. C. (1994). Polyneuronal innervation of spiny stellate neurons in cat visual cortex. *J.Comp Neurol.* **341**, 39-49.

Ahmed, B., Anderson, J. C., Martin, K. A., & Nelson, J. C. (1997). Map of the synapses onto layer 4 basket cells of the primary visual cortex of the cat. *J.Comp Neurol.* **380**, 230-242.

Ali, A. B., Deuchars, J., Pawelzik, H., & Thomson, A. M. (1998). CA1 pyramidal to basket and bistratified cell EPSPs: dual intracellular recordings in rat hippocampal slices. *J.Physiol (Lond)* **507 (Pt 1)**, 201-217.

Ali, A. B. & Thomson, A. M. (1998). Facilitating pyramid to horizontal oriens-alveus interneurone inputs: dual intracellular recordings in slices of rat hippocampus. *J.Physiol (Lond)* **507 (Pt 1)**, 185-199.

Anderson, J. C., Douglas, R. J., Martin, K. A., & Nelson, J. C. (1994). Synaptic output of physiologically identified spiny stellate neurons in cat visual cortex. *J.Comp Neurol.* **341**, 16-24.

Ariav, G., Polsky, A., & Schiller, J. (2003). Submillisecond precision of the input-output transformation function mediated by fast sodium dendritic spikes in basal dendrites of CA1 pyramidal neurons. *J Neurosci* **23**, 7750-7758.

Bacci, A., Huguenard, J. R., & Prince, D. A. (2003). Functional autaptic neurotransmission in fast-spiking interneurons: a novel form of feedback inhibition in the neocortex. *J.Neurosci.* **23**, 859-866.

Baimbridge, K. G., Peet, M. J., McLennan, H., & Church, J. (1991). Bursting response to current-evoked depolarization in rat CA1 pyramidal neurons is correlated with lucifer yellow dye coupling but not with the presence of calbindin-D28k. *Synapse* **7**, 269-277.

Beierlein, M., Gibson, J. R., & Connors, B. W. (2003). Two Dynamically Distinct Inhibitory Networks in Layer 4 of the Neocortex. *Journal of Neurophysiology* **90**, 2987-3000.

Bekkers, J. M. & Stevens, C. F. (1991). Excitatory and inhibitory autaptic currents in isolated hippocampal neurons maintained in cell culture. *Proc.Natl.Acad.Sci.U.S.A* **88**, 7834-7838.

Benfenati, F., Onofri, F., & Giovedi, S. (1999). Protein-protein interactions and protein modules in the control of neurotransmitter release. *Philos.Trans R.Soc Lond B Biol Sci.* **354**, 243-257.

Bennett, M. V. (1997). Gap junctions as electrical synapses. *J Neurocytol* **26**, 349-366.

Benshalom, G. & White, E. L. (1986). Quantification of thalamocortical synapses with spiny stellate neurons in layer IV of mouse somatosensory cortex. *J Comp Neurol* **253**, 303-314.

Betz, W. J. & Wu, L. G. (1995). Synaptic transmission. Kinetics of synaptic-vesicle recycling. *Curr Biol* **5**, 1098-1101.

Bittner, G. D. & Kennedy, D. (1970). Quantitative aspects of transmitter release. *J Cell Biol* **47**, 585-592.

Bourassa, J. & Deschenes, M. (1995). Corticothalamic projections from the primary visual cortex in rats: a single fiber study using biocytin as an anterograde tracer. *Neuroscience* **66**, 253-263.

Budd, J. M. & Kisvarday, Z. F. (2001). Local lateral connectivity of inhibitory clutch cells in layer 4 of cat visual cortex (area 17). *Exp Brain Res* **140**, 245-250.

Buhl, E. H., Han, Z. S., Lorinczi, Z., Stezhka, V. V., Karnup, S. V., & Somogyi, P. (1994). Physiological properties of anatomically identified axo-axonic cells in the rat hippocampus. *Journal of Neurophysiology* **71**, 1289-1307.

Buhl, E. H., Szilagyi, T., Halasy, K., & Somogyi, P. (1996). Physiological properties of anatomically identified basket and bistratified cells in the CA1 area of the rat hippocampus in vitro. *Hippocampus* **6**, 294-305.

Buhl, E. H., Tamas, G., Szilagyi, T., Stricker, C., Paulsen, O., & Somogyi, P. (1997). Effect, number and location of synapses made by single pyramidal cells onto aspiny interneurones of cat visual cortex. *J.Physiol* **500 (Pt 3)**, 689-713.

Burkhalter, A. (1989). Intrinsic connections of rat primary visual cortex: laminar organization of axonal projections. *J.Comp Neurol.* **279**, 171-186.

Carlson, C. G. & Jacklet, J. W. (1986). The exponent of the calcium power function is reduced during steady-state facilitation in neuron R15 of Aplysia. *Brain Res* **376**, 204-207.

Castro-Alamancos, M. A. & Connors, B. W. (1997). Thalamocortical synapses. *Prog.Neurobiol.* **51**, 581-606.

Cauli, B., Audinat, E., Lambolez, B., Angulo, M. C., Ropert, N., Tsuzuki, K., Hestrin, S., & Rossier, J. (1997). Molecular and physiological diversity of cortical nonpyramidal cells. *J.Neurosci.* **17**, 3894-3906.

Chang, Q., Gonzalez, M., Pinter, M. J., & Balice-Gordon, R. J. (1999). Gap Junctional Coupling and Patterns of Connexin Expression among Neonatal Rat Lumbar Spinal Motor Neurons. *Journal of Neuroscience* **19**, 10813-10828.

Colino, A. & Halliwell, J. V. (1993). Carbachol potentiates Q current and activates a calcium-dependent non-specific conductance in rat hippocampus in vitro. *Eur.J Neurosci* **5**, 1198-1209.

Connors, B. W., Gutnick, M. J., & Prince, D. A. (1982). Electrophysiological properties of neocortical neurons in vitro. *Journal of Neurophysiology* **48**, 1302-1320.

Davis, A. F., Bai, J., Fasshauer, D., Wolowick, M. J., Lewis, J. L., & Chapman, E. R. (1999). Kinetics of synaptotagmin responses to Ca2+ and assembly with the core SNARE complex onto membranes. *Neuron* **24**, 363-376.

Debanne, D., Guerineau, N. C., Gahwiler, B. H., & Thompson, S. M. (1997). Action-potential propagation gated by an axonal I(A)-like K+ conductance in hippocampus. *Nature* **389**, 286-289.

DeFelipe, J. (1997). Types of neurons, synaptic connections and chemical characteristics of cells immunoreactive for calbindin-D28K, parvalbumin and calretinin in the neocortex. *J.Chem.Neuroanat.* **14**, 1-19.

DeFelipe, J., Hendry, S. H., & Jones, E. G. (1989a). Synapses of double bouquet cells in monkey cerebral cortex visualized by calbindin immunoreactivity. *Brain Res.* **503**, 49-54.

DeFelipe, J., Hendry, S. H., & Jones, E. G. (1989b). Visualization of chandelier cell axons by parvalbumin immunoreactivity in monkey cerebral cortex. *Proc.Natl.Acad.Sci.U.S.A* **86** , 2093-2097.

Deuchars, J., West, D. C., & Thomson, A. M. (1994). Relationships between morphology and physiology of pyramid-pyramid single axon connections in rat neocortex in vitro. *J Physiol* **478 Pt 3**, 423-435.

Dodge, F. A. & Rahamimoff, R. (1967). Co-operative action a calcium ions in transmitter release at the neuromuscular junction. *Journal of Physiology* **193**, 419-432.

Douglas, R. J., Koch, C., Mahowald, M., Martin, K. A., & Suarez, H. H. (1995). Recurrent excitation in neocortical circuits. *Science* **269**, 981-985.

Douglas, R. J. & Martin, K. A. (1991). A functional microcircuit for cat visual cortex. *J Physiol* **440**, 735-769.

Doussau, F. & Augustine, G. J. (2000). The actin cytoskeleton and neurotransmitter release: an overview. *Biochimie* **82**, 353-363.

Faber, D. S. & Korn, H. (1991). Applicability of the coefficient of variation method for analyzing synaptic plasticity [published erratum appears in Biophys J 1992 Mar;61(3):following 831]. *Biophysical Journal* **60**, 1288-1294.

Fatt, P. & Katz, B. (1952). Spontaneous Subthreshold Activity at Motor Nerve Endings. *J Physiol* **117**,

109-128.

Feldman, M. L. (1984). Morphology of the Neocortical Neuron. In *The Cerebral Cortex.*, eds. Peters, A. & Jones, E. G., pp. 123-200. Plenum Press, New York.

Feldmeyer, D., Egger, V., Lubke, J., & Sakmann, B. (1999). Reliable synaptic connections between pairs of excitatory layer 4 neurones within a single 'barrel' of developing rat somatosensory cortex. *J.Physiol* **521 Pt 1**, 169-190.

Freund, T. F. (2003). Interneuron Diversity series: Rhythm and mood in perisomatic inhibition. *Trends Neurosci* **26**, 489-495.

Fukuda, T. & Kosaka, T. (2003). Ultrastructural study of gap junctions between dendrites of parvalbumin-containing GABAergic neurons in various neocortical areas of the adult rat. *Neuroscience* **120**, 5-20.

Gabbott, P. L. & Somogyi, P. (1986). Quantitative distribution of GABA-immunoreactive neurons in the visual cortex (area 17) of the cat. *Exp Brain Res* **61**, 323-331.

Gerstner, W., Kreiter, A. K., Markram, H., & Herz, A. V. (1997). Neural codes: Firing rates and?beyond. *Proceedings of the National Academy of Sciences U.S.A.* **94**, 12740.

Gibson, J. R., Beierlein, M., & Connors, B. W. (1999). Two networks of electrically coupled inhibitory neurons in neocortex. *Nature* **402**, 75-79.

Gil, Z., Connors, B. W., & Amitai, Y. (1999). Efficacy of thalamocortical and intracortical synaptic connections: quanta, innervation, and reliability [see comments]. *Neuron* **23**, 385-397.

Gilbert, C. D. & Wiesel, T. N. (1979). Morphology and intracortical projections of functionally characterised neurones in the cat visual cortex. *Nature* **280**, 120-125.

Gilbert, C. D. & Wiesel, T. N. (1989). Columnar specificity of intrinsic horizontal and corticocortical connections in cat visual cortex. *J.Neurosci.* **9**, 2432-2442.

Gray, E. G. (1959). Axo-somatic and axo-dendritic synapses of the cerebral cortex: an electron microscope study. *J Anat.* **93**, 420-433.

Habeeb, A. J. & Hiramoto, R. (1968). Reaction of proteins with glutaraldehyde. *Arch.Biochem Biophys.* **126**, 16-26.

Hess, O. (1959). Osmium tetroxide as a fixative for unsaturated fatty acids and animal tissue. *Exp Cell Res* **16**, 452-455.

Hestrin, S. (1992). Activation and desensitization of glutamate-activated channels mediating fast excitatory synaptic currents in the visual cortex. *Neuron* **9**, 991-999.

Hubbard, J. I. (1963). Repetitive stimulation at the mammalian neuromuscular junction, and the mobilization of transmitter. *J Physiol* **169**, 641-662.

Hughes, D. I., Bannister, A. P., Pawelzik, H., & Thomson, A. M. (2000). Double immunofluorescence, peroxidase labelling and ultrastructural analysis of interneurones following prolonged electrophysiological recordings in vitro. *J.Neurosci.Methods* **101**, 107-116.

Jack, J. J. & Redman, S. J. (1971). The propagation of transient potentials in some linear cable structures. *J Physiol* **215**, 283-320.

Jonas, P., Racca, C., Sakmann, B., Seeburg, P. H., & Monyer, H. (1994). Differences in Ca2+ permeability of AMPA-type glutamate receptor channels in neocortical neurons caused by differential GluR-B subunit expression. *Neuron* **12**, 1281-1289.

Karunanithi, S., Marin, L., Wong, K., & Atwood, H. L. (2002). Quantal size and variation determined by vesicle size in normal and mutant Drosophila glutamatergic synapses. *J Neurosci* **22**, 10267-10276.

Katz, B. & Miledi, R. (1968). The role of calcium in neuromuscular facilitation. *J.Physiol* **195**, 481-492.

Kawaguchi, Y. (1995). Physiological subgroups of nonpyramidal cells with specific morphological characteristics in layer II/III of rat frontal cortex. *J Neurosci* **15**, 2638-2655.

Kawaguchi, Y. & Kondo, S. (2002). Parvalbumin, somatostatin and cholecystokinin as chemical markers for specific GABAergic interneuron types in the rat frontal cortex. *J Neurocytol* **31**, 277-287.

Kawaguchi, Y. & Kubota, Y. (1993). Correlation of physiological subgroupings of nonpyramidal cells with parvalbumin- and calbindinD28k-immunoreactive neurons in layer V of rat frontal cortex. *J.Neurophysiol.* **70**, 387-396.

Kawaguchi, Y. & Kubota, Y. (1996). Physiological and morphological identification of somatostatin- or vasoactive intestinal polypeptide-containing cells among GABAergic cell subtypes in rat frontal cortex. *J.Neurosci.* **16**, 2701-2715.

Kawaguchi, Y. & Kubota, Y. (1997). GABAergic cell subtypes and their synaptic connections in rat frontal cortex. *Cereb.Cortex* **7**, 476-486.

Kawaguchi, Y. & Kubota, Y. (1998). Neurochemical features and synaptic connections of large physiologically-identified GABAergic cells in the rat frontal cortex. *Neuroscience* **85**, 677-701.

Kirov, S. A., Sorra, K. E., & Harris, K. M. (1999). Slices have more synapses than perfusion-fixed

hippocampus from both young and mature rats. *J.Neurosci.* **19**, 2876-2886.

Kisvarday, Z. F. (1992). GABAergic networks of basket cells in the visual cortex. *Prog.Brain Res.* **90**, 385-405.

Kosaka, T. & Hama, K. (1985). Gap junctions between non-pyramidal cell dendrites in the rat hippocampus (CA1 and CA3 regions): a combined Golgi-electron microscopy study. *J Comp Neurol* **231**, 150-161.

Kosaka, T., Katsumaru, H., Hama, K., Wu, J. Y., & Heizmann, C. W. (1987). GABAergic neurons containing the Ca2+-binding protein parvalbumin in the rat hippocampus and dentate gyrus. *Brain Res.* **419**, 119-130.

Kumar, N. M. & Gilula, N. B. (1996). The gap junction communication channel. *Cell* **84**, 381-388.

Liu, G. & Tsien, R. W. (1995). Properties of synaptic transmission at single hippocampal synaptic boutons. *Nature* **375**, 404-408.

Llinas, R., Gruner, J. A., Sugimori, M., McGuinness, T. L., & Greengard, P. (1991). Regulation by synapsin I and Ca(2+)-calmodulin-dependent protein kinase II of the transmitter release in squid giant synapse. *J Physiol* **436**, 257-282.

Llinas, R. & Yarom, Y. (1981). Properties and distribution of ionic conductances generating electroresponsiveness of mammalian inferior olivary neurones in vitro. *J Physiol* **315**, 569-584.

Loewenstein, W. R. (1981). Junctional intercellular communication: the cell-to-cell membrane channel. *Physiological Reviews* **61**, 829-913.

Lubke, J., Egger, V., Sakmann, B., & Feldmeyer, D. (2000). Columnar organization of dendrites and axons of single and synaptically coupled excitatory spiny neurons in layer 4 of the rat barrel cortex. *J.Neurosci.* **20**, 5300-5311.

Lubke, J., Markram, H., Frotscher, M., & Sakmann, B. (1996). Frequency and dendritic distribution of autapses established by layer 5 pyramidal neurons in the developing rat neocortex: comparison with synaptic innervation of adjacent neurons of the same class. *J Neurosci* **16**, 3209-3218.

Lund, J. S. (2002). Specificity and non-specificity of synaptic connections within mammalian visual cortex. *J.Neurocytol.* **31**, 203-209.

Lundberg, J. M., Anggard, A., & Fahrenkrug, J. (1981). Complementary role of vasoactive intestinal polypeptide (VIP) and acetylcholine for cat submandibular gland blood flow and secretion. I. VIP release. *Acta Physiol Scand.* **113**, 317-327.

Markram, H. & Tsodyks, M. (1996). Redistribution of synaptic efficacy between neocortical pyramidal neurons. *Nature* **382**, 807-810.

Massengill, J. L., Smith, M. A., Son, D. I., & O'Dowd, D. K. (1997). Differential expression of K4-AP currents and Kv3.1 potassium channel transcripts in cortical neurons that develop distinct firing phenotypes. *J Neurosci* **17**, 3136-3147.

McCormick, D. A., Connors, B. W., Lighthall, J. W., & Prince, D. A. (1985). Comparative electrophysiology of pyramidal and sparsely spiny stellate neurons of the neocortex. *Journal of Neurophysiology* **54**, 782-806.

Miles, R., Toth, K., Gulyas, A. I., Hajos, N., & Freund, T. F. (1996). Differences between somatic and dendritic inhibition in the hippocampus. *Neuron* **16**, 815-823.

Nadarajah, B. & Parnavelas, J. G. (1999). Gap junction-mediated communication in the developing and adult cerebral cortex. *Novartis Found Symp* **219**, 157-170.

Naus, C. C. & Bani-Yaghoub, M. (1998). Gap junctional communication in the developing central nervous system. *Cell Biol Int.* **22**, 751-763.

Pappas, G. D. & Bennett, M. V. (1966). Specialized junctions involved in electrical transmission between neurons. *Ann.N.Y.Acad.Sci.* **137**, 495-508.

Pawelzik, H., Hughes, D. I., & Thomson, A. M. (2002). Physiological and morphological diversity of immunocytochemically defined parvalbumin- and cholecystokinin-positive interneurones in CA1 of the adult rat hippocampus. *J.Comp Neurol.* **443**, 346-367.

Pawelzik, H., Hughes, D. I., & Thomson, A. M. (2003). Modulation of inhibitory autapses and synapses on rat CA1 interneurones by GABAA receptor ligands. *Journal of Physiology* **546** , 701.

Peinado, A., Yuste, R., & Katz, L. C. (1993). Gap junctional communication and the development of local circuits in neocortex. *Cereb.Cortex* **3**, 488-498.

Perez Velazquez, J. L. & Carlen, P. L. (2000). Gap junctions, synchrony and seizures. *Trends Neurosci.* **23**, 68-74.

Petersen, C. C. (2002). Short-term dynamics of synaptic transmission within the excitatory neuronal network of rat layer 4 barrel cortex. *J.Neurophysiol.* **87**, 2904-2914.

Petersen, C. C. & Sakmann, B. (2000). The excitatory neuronal network of rat layer 4 barrel cortex. *J.Neurosci.* **20**, 7579-7586.

Porter, J. T., Cauli, B., Staiger, J. F., Lambolez, B., Rossier, J., & Audinat, E. (1998). Properties of

bipolar VIPergic interneurons and their excitation by pyramidal neurons in the rat neocortex. *Eur.J.Neurosci.* **10**, 3617-3628.

Reid, C. A., Bekkers, J. M., & Clements, J. D. (1998). N- and P/Q-type Ca2+ channels mediate transmitter release with a similar cooperativity at rat hippocampal autapses. *J Neurosci* **18**, 2849-2855.

Reyes, A., Lujan, R., Rozov, A., Burnashev, N., Somogyi, P., & Sakmann, B. (1998). Target-cell-specific facilitation and depression in neocortical circuits. *Nat.Neurosci.* **1**, 279-285.

Rockland, K. S. (1998). Complex microstructures of sensory cortical connections. *Curr Opin Neurobiol* **8**, 545-551.

Sabatini, D. D., Bensch, K., & Barrnett, R. J. (1963). Cytochemistry and electron microscopy. The preservation of cellular ultrastructure and enzymatic activity by aldehyde fixation. *J Cell Biol* **17**, 19-58.

S.Ramón Y Cajal (1911). *Histologie du système nerveux de l'homme et des vertébrés.* Maloine, Paris.

Schiller, J., Major, G., Koester, H. J., & Schiller, Y. (2000). NMDA spikes in basal dendrites of cortical pyramidal neurons. *Nature* **404**, 285-289.

Schwindt, P. C., Spain, W. J., Foehring, R. C., Stafstrom, C. E., Chubb, M. C., & Crill, W. E. (1988). Multiple potassium conductances and their functions in neurons from cat sensorimotor cortex in vitro. *Journal of Neurophysiology* **59**, 424-449.

Seagar, M., Leveque, C., Charvin, N., Marqueze, B., Martin-Moutot, N., Boudier, J. A., Boudier, J. L., Shoji-Kasai, Y., Sato, K., & Takahashi, M. (1999). Interactions between proteins implicated in exocytosis and voltage-gated calcium channels. *Philos.Trans R.Soc Lond B Biol Sci.* **354**, 289-297.

Sherman, A. & Rinzel, J. (1992). Rhythmogenic effects of weak electrotonic coupling in neuronal models. *Proc.Natl.Acad.Sci.U.S.A* **89**, 2471-2474.

Sherman, S. M. (2001). Tonic and burst firing: dual modes of thalamocortical relay. *Trends Neurosci.* **24**, 122-126.

Sillito, A. M. (1975). The contribution of inhibitory mechanisms to the receptive field properties of neurones in the striate cortex of the cat. *J Physiol* **250**, 305-329.

Simburger, E., Stang, A., Kremer, M., & Dermietzel, R. (1997). Expression of connexin43 mRNA in adult rodent brain. *Histochem Cell Biol* **107**, 127-137.

Somogyi, P. (1977). A specific 'axo-axonal' interneuron in the visual cortex of the rat. *Brain Res.* **136**, 345-350.

Somogyi, P. & Takagi, H. (1982). A note on the use of picric acid-paraformaldehyde-glutaraldehyde fixative for correlated light and electron microscopic immunocytochemistry. *Neuroscience* **7**, 1779-1783.

Stafstrom, C. E., Schwindt, P. C., & Crill, W. E. (1984). Cable properties of layer V neurons from cat sensorimotor cortex in vitro. *Journal of Neurophysiology* **52**, 278-289.

Storm-Mathisen, J., Leknes, A. K., Bore, A. T., Vaaland, J. L., Edminson, P., Haug, F. M., & Ottersen, O. P. (1983). First visualization of glutamate and GABA in neurones by immunocytochemistry. *Nature* **301**, 517-520.

Storm, J. F. (1988). Temporal integration by a slowly inactivating K+ current in hippocampal neurons. *Nature* **336**, 379-381.

Swadlow, H. A. (1994). Efferent neurons and suspected interneurons in motor cortex of the awake rabbit: axonal properties, sensory receptive fields, and subthreshold synaptic inputs. *Journal of Neurophysiology* **71**, 437-453.

Tamas, G., Buhl, E. H., Lorincz, A., & Somogyi, P. (2000). Proximally targeted GABAergic synapses and gap junctions synchronize cortical interneurons. *Nat.Neurosci.* **3**, 366-371.

Tamas, G., Buhl, E. H., & Somogyi, P. (1997). Massive autaptic self-innervation of GABAergic neurons in cat visual cortex. *J.Neurosci.* **17**, 6352-6364.

Tamas, G., Lorincz, A., Simon, A., & Szabadics, J. (2003). Identified sources and targets of slow inhibition in the neocortex. *Science* **299**, 1902-1905.

Tamas, G., Somogyi, P., & Buhl, E. H. (1998). Differentially interconnected networks of GABAergic interneurons in the visual cortex of the cat. *J.Neurosci.* **18**, 4255-4270.

Tarczy-Hornoch, K., Martin, K. A., Jack, J. J., & Stratford, K. J. (1998). Synaptic interactions between smooth and spiny neurones in layer 4 of cat visual cortex in vitro. *J.Physiol (Lond)* **508 (Pt 2)**, 351-363.

Tarczy-Hornoch, K., Martin, K. A., Stratford, K. J., & Jack, J. J. (1999). Intracortical excitation of spiny neurons in layer 4 of cat striate cortex in vitro. *Cereb.Cortex* **9**, 833-843.

Thomson, A. M. (1997). Activity-dependent properties of synaptic transmission at two classes of connections made by rat neocortical pyramidal axons in vitro. *J.Physiol (Lond)* **502 (Pt 1)**, 131-147.

Thomson, A. M. (2000). Molecular frequency filters at central synapses. *Prog.Neurobiol.* **62**, 159-196.

Thomson, A. M. (2003). Presynaptic frequency- and pattern-dependent filtering. *J Comput Neurosci* **15**, 159-202.

Thomson, A. M. & Bannister, A. P. (1998). Postsynaptic pyramidal target selection by descending layer III pyramidal axons: dual intracellular recordings and biocytin filling in slices of rat neocortex. *Neuroscience* **84**, 669-683.

Thomson, A. M. & Bannister, A. P. (2003). Interlaminar connections in the neocortex. *Cereb.Cortex* **13**, 5-14.

Thomson, A. M., Deuchars, J., & West, D. C. (1993). Large, deep layer pyramid-pyramid single axon EPSPs in slices of rat motor cortex display paired pulse and frequency-dependent depression, mediated presynaptically and self-facilitation, mediated postsynaptically. *Journal of Neurophysiology* **70**, 2354-2369.

Thomson, A. M. & Morris, O. T. (2002). Selectivity in the inter-laminar connections made by neocortical neurones. *J.Neurocytol.* **31**, 239-246.

Thomson, A. M. & West, D. C. (1993). Fluctuations in pyramid-pyramid excitatory postsynaptic potentials modified by presynaptic firing pattern and postsynaptic membrane potential using paired intracellular recordings in rat neocortex. *Neuroscience* **54**, 329-346.

Thomson, A. M., West, D. C., Hahn, J., & Deuchars, J. (1996). Single axon IPSPs elicited in pyramidal cells by three classes of interneurones in slices of rat neocortex. *J.Physiol (Lond)* **496 (Pt 1)**, 81-102.

Thomson, A. M., West, D. C., Wang, Y., & Bannister, A. P. (2002). Synaptic connections and small circuits involving excitatory and inhibitory neurons in layers 2-5 of adult rat and cat neocortex: triple intracellular recordings and biocytin labelling in vitro. *Cereb.Cortex* **12**, 936-953.

Thomson, A. M. & West, D. C. (2003). Presynaptic Frequency Filtering in the Gamma Frequency Band; Dual Intracellular Recordings in Slices of Adult Rat and Cat Neocortex. *Cerebral Cortex* **13**, 136-143.

Traub, R. D., Draguhn, A., Whittington, M. A., Baldeweg, T., Bibbig, A., Buhl, E. H., & Schmitz, D. (2002). Axonal gap junctions between principal neurons: a novel source of network oscillations, and perhaps epileptogenesis. *Rev Neurosci* **13**, 1-30.

Traub, R. D. & Bibbig, A. (2000). A Model of High-Frequency Ripples in the Hippocampus Based on Synaptic Coupling Plus Axon-Axon Gap Junctions between Pyramidal Neurons. *Journal of Neuroscience* **20**, 2086-2093.

Traub, R. D., Kopell, N., Bibbig, A., Buhl, E. H., LeBeau, F. E. N., & Whittington, M. A. (2001). Gap Junctions between Interneuron Dendrites Can Enhance Synchrony of Gamma Oscillations in Distributed Networks. *Journal of Neuroscience* **21**, 9478-9486.

Traub, R. D., Pais, I., Bibbig, A., LeBeau, F. E. N., Buhl, E. H., Hormuzdi, S. G., Monyer, H., & Whittington, M. A. (2003). Contrasting roles of axonal (pyramidal cell) and dendritic (interneuron) electrical coupling in the generation of neuronal network oscillations. *Proceedings of the National Academy of Sciences U.S.A.* **100**, 1370-1374.

Tsodyks, M. V. & Markram, H. (1997). The neural code between neocortical pyramidal neurons depends on neurotransmitter release probability. *Proc.Natl.Acad.Sci.U.S.A* **94**, 719-723.

Van der Loos, H. & Glaser, E. M. (1972). Autapses in neocortex cerebri: synapses between a pyramidal cell's axon and its own dendrites. *Brain Res* **48**, 355-360.

Wahle, P. (1993). Differential regulation of substance P and somatostatin in Martinotti cells of the developing cat visual cortex. *J Comp Neurol* **329**, 519-538.

Wang, Y., Gupta, A., & Markram, H. (1999). Anatomical and functional differentiation of glutamatergic synaptic innervation in the neocortex. *J Physiol Paris* **93**, 305-317.

Wang, Y. & Ramage, A. G. (2001). The role of central 5-HT1A receptors in the control of B-fibre cardiac and bronchoconstrictor vagal preganglionic neurones in anaesthetized cats. *Journal of Physiology* **536**, 753.

Williams, S. M., Goldman-Rakic, P. S., & Leranth, C. (1992). The synaptology of parvalbumin-immunoreactive neurons in the primate prefrontal cortex. *J.Comp Neurol.* **320**, 353-369.

Williams, S. R. & Stuart, G. J. (2003). Role of dendritic synapse location in the control of action potential output. *Trends Neurosci.* **26**, 147-154.